Copyright

by

Cem Akgüner

2007

The Dissertation Committee for Cem Akgüner Certifies that this is the approved version of the following dissertation:

ELASTIC ANALYSIS OF AXIAL LOAD-DISPLACEMENT BEHAVIOR OF SINGLE DRIVEN PILES

Committee:

Robert B. Gilbert, Supervisor

Roy E. Olson, Co-Supervisor

Michael D. Engelhardt

John M. Sharp, Jr.

Kenneth H. Stokoe II

ELASTIC ANALYSIS OF AXIAL LOAD-DISPLACEMENT BEHAVIOR OF SINGLE DRIVEN PILES

by

Cem Akgüner, B.S.; M.S.C.E

Dissertation

Presented to the Faculty of the Graduate School of

The University of Texas at Austin

in Partial Fulfillment

of the Requirements

for the Degree of

Doctor of Philosophy

The University of Texas at Austin

December 2007

Dedication

To my dearest family

that I love and care for
who suffered through this process,
made so many sacrifices,
stood by me at all times,
supported me in all possible ways...

you are all one can wish for and dream about...

Life is nothing but a tiresome journey. For a man, it consists of false starts, snail-like advances, nasty setbacks, and lost collar buttons.
Jean Giraudoux - The Enchanted

Happiness is someone to love, something to do, and something to hope for.
-Chinese Proverb

We know accurately only when we know little, with knowledge doubt increases.
Johann Wolfgang von Goethe, who completed his masterpiece Faust in over 60 years.

Acknowledgements

It has truly been a drawn-out process which was followed its own course. This dissertation could not have been possible without the influence of many individuals who smoothed the way. Dr. Robert B. Gilbert was the voice of reason and a constant source of optimism and encouragement as my co-supervisor. He always pointed to the full half of the cup whenever I focused on the empty portion. His knowledge, keen understanding and problem-solving skills, generously shared throughout, have been instrumental toward my completing this dissertation.

My other co-advisor Dr. Roy E. Olson offered me my first and last jobs. Things have not always been rosy between us, but one thing I could always count on was his unwavering dedication to engineering, inspiring in-depth knowledge and sense of perspective at times when my mind and interests would wander. He was always available and willing to discuss a wide range of topics and to bluntly express his point-of-view. I sincerely appreciate his support and guidance in my successfully concluding this dissertation. I will always cherish having worked alongside Dr. Olson.

I would be remiss if I did not thank the other members of my dissertation committee: Drs. Michael D. Engelhardt, John M. Sharp, Jr., and Kenneth H. Stokoe II. I am truly grateful for the support they have given to my research using their extensive knowledge, experience, and wisdom.

Dr. Glen R. Andersen, who was formerly at Texas A&M University and was my very first advisor, also deserves credit for offering me a chance to work with him. I learned many important lessons about where one’s priority should lie. Dr. Alan Rauch also served as my co-supervisor and helped me formulate a rational approach to my research questions.

I want to thank the warm and helpful UT staff who have had a positive impact on me and my work: Teresa Tice-Boggs, Vittoria Esile, Evelyn Porter, D.D. Berry, Chris Treviño, Maximo Treviño, Alicia and Gonzalo Zapata, and Wayne Fontenot. I feel privileged to have known each and every one of them.

I can not even phantom how my life as a graduate student would have been without the super, special members of the Engineering Library and Interlibrary Services. They contributed greatly to my excitement and eagerness to learn and explore new ideas and approaches.

I must acknowledge some of my amazing fellow geotechies: Mike Myers, Mike Duffy, Cynthia Finley, Rollins Brown, Elliott Mecham, Celestino Valle, and Beatriz Camacho. I sincerely benefited from being in an environment where almost everyone is friendly and genuinely nice to each other. My Korean friends and officemates Dr. Jeong-Yun Won, Heejung Youn, Boohyun Nam, and Kyu-Seok Woo made me a part of their close-knit gang and played a very important role for me during the last stages of writing/correcting/reviewing process of my dissertation. I could not possibly have asked for a better environment to be in.

I have been extremely lucky and blessed with friends during my stay in Austin, each of whom has a special place in my heart and mind: Nalan-Ahmet Yakut, Aysu-Mehmet Darendeli, Rüya-Murat Küçükkaya, Tarkan Yüksel, Cengiz Vural, Cem Topkaya, Murat Argun, Selim Sakaoğlu, and Tanju Yurtsever. I promise to show my appreciation to each every time I see them. I want to thank them for letting me be a part of their lives. I also wronged some people I cared for and I am truly sorry for it.

Over the last five years, there is nobody that I have been closer to than Umut Beşpınar-Ekici and Özgür Ekici. We have spent much of our free time together, sharing our thoughts, joys, concerns, walks, frustrations, opinions, movies, prayers, stories, news,

food, and coffee. Özgür has had a refreshing and calming effect on me, although we both are Gemini. Umut has always found a way to lift my spirits and been first in line to support me whenever I felt lost or wanted to just give up.

I can not say enough of my family. I would not be where I am right now without the sacrifices they have made throughout my studies. I am forever indebted to them. My mother Mary must be canonized as a saint and/or angel with her never-ending optimism, sunny disposition and intellectual capacity. She has been and will continue to be an inspiration and a role model for me. I will always remember her yelling, “Adalante! To İzmir,” every morning trying to encourage me and keep me going. My father Tayfun has been a tornado-like driving force, making me strive to continually do my best no matter what the circumstances are. He is a problem-solver and a go-getter, or, in other words, the engine that could. My sister Perim has served as the resident child of our family while I have been gone and done an admirable job. She worked full time while taking a full load of classes to earn her masters degree, and begin her doctorate, feats which are simply awe-inspiring to me.

So far so good! Last one to leave should turn-off the lights.

Elastic Analysis of Axial Load-Displacement Behavior of Single Driven Piles

Publication No._____

Cem Akgüner, Ph.D.

The University of Texas at Austin, 2007

Co-Supervisors: Robert B. Gilbert and Roy E. Olson

Deep foundations are commonly recommended when large displacements are expected. Typically, though, their design involves only checking and providing for sufficient capacity to carry the applied loads. Load-displacement behavior of piles is considered secondary to the axial capacity; displacements are ordinarily overlooked or not calculated if and when the estimated pile capacity is two to three times the design or expected loading. However, in cases, such as long piles or piles in dense cohesionless soils, displacements can be the critical factor in design or it could be a structural requirement to limit the displacements.

In this dissertation, the displacements of axially loaded single piles are investigated by conducting analyses with the aid of an approach based on elasticity. The original solution predicting displacements due to a vertical load within a semi-infinite soil mass has been modified for varying soil conditions and layering, and assumptions of stresses and displacements acting on the soil-pile interface. Aside from the available/known factors of the pile (length, diameter, cross-sectional area, etc.) and the

layering of the surrounding soil, Young's modulus and Poisson's ratio of the soil encompassing a pile are the unknowns required as input to obtain predictions based on the elastic method. In this study, attention is directed towards determining Young's modulus because the range and variability of Poisson's ratio is not significant in displacement calculations.

Axial pile load testing data were provided by the California Department of Transportation as part of a project to improve its general approach to pile design. All of the tested piles were driven into the ground. Measurements of displacements and loads were made only at the top of the pile. Supplementary in-situ testing involving cone penetration (CPT) and standard penetration (SPT), drilling, and sample collection, were conducted in addition to laboratory testing to enhance the available information.

In this research, predicted displacements are compared with those deduced from pile load tests. Two sets of predictions based on elastic method are conducted for comparing displacements. First, various correlations for Young's modulus are employed to determine how accurately each predicts the actual measured displacement. The chosen correlations utilize laboratory triaxial undrained shear strength and standard penetration test blowcount for cohesive and cohesionless soils, respectively. Secondly, the same data are also utilized to obtain back-calculated values of Young's moduli for analyses involving the elastic method. The measured displacements at loads of a third, a half, two-thirds, and equal to the failure load were matched iteratively.

Results from this research are deemed to have an impact on engineering practice by improving the determination of Young's modulus for displacement analyses involving the elastic method. A unique approach that has potential is the reconciliation of load ratios (percentage of failure load) with displacement calculations to provide a better overview of the range of load ratios for which these newly formulated correlations may

be employed. Through this research, it is anticipated that better determination of soil parameters for elastic analysis of axial pile displacements can be made by researchers and engineers alike.

Table of Contents

Table of Contents xi

List of Tables xvi

List of Figures xix

Chapter 1: Introduction 1

1.1 Motivation 1

1.2 Pile Load Database 2

1.3 Research Approach 3

1.4 Dissertation Outline 5

Chapter 2: Pile Load Database 7

2.1 Introduction 7

2.2 Pile Load Database 7

2.2.2 Limitations of Both Pile Load Test Databases 11

2.3 Field Investigation 14

2.3.1 Field Exploration Segments 15

2.3.1.2 Drilling and Sampling Methods 20

2.3.1.3 Water Levels 21

2.4 Laboratory Testing and Results 22

2.4.1 Specimen Preparation Procedures 23

2.4.1.2 Data Acquisition System 24

2.4.1.3 Completed Laboratory Tests 25

2.4.2 Measurements of Undrained Shear Strength, c_u 26

2.4.2.1 Effects of Trimming on UU Triaxial Undrained Shear Strength 26

2.5 Summary 33

Chapter 3: Elastic Method – Concept and Measurement of Parameters 34

3.1 Introduction 34

3.2 Formulation of Elastic Method 34

3.2.2 Mindlin's Solution for Concentrated Loading....36
3.2.3 Displacements along Pile Shaft, ρ_s....38
3.2.4 Displacement of Pile Shaft, ρ_p....38
3.2.5 Pile Tip Displacement, ρ_{tip}....38
3.2.6 Pile Head Displacement....39
3.3 Modifications to Elastic Method....39
3.3.1 Shear Stresses on Pile....40
3.3.2 Non-Homogeneous Soil....41
3.3.3 Finite Depth of Soil Layers....44
3.3.4 Piles Founded on a Rigid Base....45
3.3.5 Pile-Soil Relative Displacement....46
3.3.6 Residual Stresses....47
3.4 Parameters of Elastic Method....49
3.4.1 Drained versus Undrained Parameters....49
3.4.2 Poisson's Ratio, ν_s....50
3.4.3 Young's Modulus of Pile, E_p....50
3.4.4 Young's (Elastic) Modulus, E_s....51
3.4.5 Importance of Poisson's Ratio versus Young's Modulus....55
3.5 Limits and Justification of using the Elastic Method....56
3.6 Determination of Young's Modulus....60
3.6.2 Young's Modulus Based on Laboratory Testing....62
3.6.3 Young's Modulus Correlations Based on In-Situ Tests....63
3.6.3.1 Standard Penetration Test (SPT)....63
3.6.3.2 Cone Penetration Test (CPT)....65
3.6.3.3 Pressuremeter Test (PMT)....67
3.6.3.4 Plate Loading Tests (PLT)....69
3.6.3.5 Flat Plate Dilatometer (DMT)....70
3.6.3.6 Geophysical Methods....71
3.6.4 Limits of Empirical Correlations....73
3.7 Variability of Parameters....73
3.7.1 Undrained Shear Strength Variability....74

3.7.2 Standard Penetration Test (SPT) Variability 74
3.8 Summary 75

Chapter 4: Database Classification and Evaluation of Displacements 76
4.1 Introduction 76
4.2 Definitions of Soil Types 76
4.2.1 Cohesive Soils 77
4.2.2 Cohesionless Soils 77
4.2.3 Mixed Profiles 78
4.3 Definitions of Terms Used for Comparison 78
4.4 Analytical Procedure Using Modified Tapile 79
4.5 List of Pile Load Tests 81
4.5.1 Cohesive Soils 82
4.5.2 Cohesionless Soils 83
4.5.3 Pile Load Tests in Mixed Profiles 85
4.6 Research Approach 91
4.6.1 Failure Load Determination 91
4.6.2 Investigation 95
4.6.3 Graphical Evaluation 96
4.6.4 Statistical Evaluations 97
4.7 Summary 98

Chapter 5: Evaluation of Methods to Predict Axial Displacements 99
5.1 Introduction 99
5.1.1 Direct Prediction of Displacement 99
5.2 Cohesive Soils 101
5.2.1 Magnitude of Displacements 101
5.2.2 Correlations 103
5.2.3 Measurements versus Predictions 105
5.2.4 Displacement Ratio, s_c/s_m 106
5.2.5 Displacement Difference, s_c-s_m 108
5.2.6 Outliers 110

5.3 Cohesionless Soils 114
5.3.1 Magnitude of Displacements 114
5.3.2 Correlations 115
5.3.3 Predictions versus Measurement 117
5.3.4 Displacement Ratio, s_c/s_m 118
5.3.5 Displacement Difference, s_c-s_m 120
5.3.6 Outliers 121
5.4 Mixed Profiles 128
5.4.1 Magnitude of Displacements 129
5.4.2 Measured versus Predicted Displacements 130
5.4.3 Displacement Ratio, s_c/s_m 133
5.4.4 Displacement Difference, s_c-s_m 136
5.4.5 Outliers 137
5.5 Conclusions 137
5.5.1 Piles in Cohesive Soils (N = 26) 137
5.5.2 Piles in Cohesionless Soils (N = 34) 139
5.5.3 Piles in Mixed Profiles (N = 83) 140
5.6 Summary 141

Chapter 6: Proposed Method of Predicting Displacements 143
6.1 Introduction 143
6.2 Cohesive Soils 143
6.3 Cohesionless Soils 149
6.4 Proposed Method Applied to Piles in Mixed Profiles 159
6.5 Summary 161

Chapter 7: Conclusions 162
7.1 Published Methods to Predict Axial Displacements 163
7.1.1 Cohesive Soils 163
7.1.2 Cohesionless Soils 164
7.1.3 Mixed Profiles 164
7.1.4 Recommendations for Future Work 164

7.2 Suggested Correlations 165
7.2.1 Conclusions on Methodology 165
7.2.1.1 Cohesive Soils.....166
7.2.1.2 Cohesionless Soils 167
7.2.1.3 Suggested Correlations Applied to Piles in Mixed Profiles 168
7.2.2 Recommendations for Future Work.....168
7.3 Other Recommendations.....169
Appendix A: Pile Load Test Information 170
Appendix B: Correlations for Young's Modulus.....180
Appendix C: Tapile Input and Output Files.....192
Appendix C.1 Example Input File 192
Appendix C.2 Example Output File.....195
References.....212
Vita.....223

List of Tables

Table 2.1 List of soil borings. 15

Table 2.2 Cone Penetration Test (CPT) soundings..... 17

Table 2.3 Laboratory tests and applicable standards. 23

Table 2.4 Summary of completed laboratory tests. 25

Table 2.5 Summary of UU compression tests conducted to investigate the effects of trimming. 31

Table 3.1 Pile Young's modulus values applied for analyses. 51

Table 3.2 Typical elastic constants of various soils (HB-17: AASHTO Standard Specifications for Highway Bridges, 17th ed., 2002). 52

Table 4.1 Summary of pile load tests used in analyzing clayey profiles. 82

Table 4.2 Details of pile load tests with clayey profiles (N = 26). 82

Table 4.3 Summary list of pile load tests analyzed (sandy soils). 83

Table 4.4 List of pile load tests in sandy profiles (N = 34). 84

Table 4.5 Summary list of pile load tests driven into mixed profiles. 85

Table 4.6 Details of piles founded in mixed soils (N = 68). 85

Table 5.1 Correlations of Young's modulus with undrained shear strength, c_u. 103

Table 5.2 The statistics of displacement ratio (s_c/s_m) (N = 26). 107

Table 5.3 Ranking of correlations based on displacement ratio (s_c/s_m). 108

Table 5.4 The statistics for displacement differences (s_c-s_m) (inch) (N = 26). 109

Table 5.5 Comparison of predicted and measured displacements for outliers. 111

Table 5.6 Details of pile load tests that have been investigated further. 112

Table 5.7 Range of parameters for all pile load tests in clay compared to those for outliers. 113

Table 5.8 Correlations for Young's modulus, E_s with SPT blow count (N in bpf). 116

Table 5.9 Mean and standard deviation for correlations (N = 34). 119

Table 5.10 Rankings corresponding to each correlation. 120

Table 5.11 The statistics of displacement difference (s_c-s_m) for comparison with correlations in cohesionless soils (N = 34). 121

Table 5.12 Displacement ratio and difference for outliers. 122

Table 5.13 Properties and soil layering for outlying pile load tests. 123

Table 5.14 Range of parameters for all pile load tests in sand versus that for outliers. . 127

Table 5.15 Mean and standard deviation of displacement ratio (s_c/s_m) for correlations. 134

Table 5.16 Rankings for correlations based on the statistics of s_c/s_m. 135

Table 5.17 Summary of the mean and standard deviation for displacement differences (all in inches). 136

Table 5.18 The statistics for the displacement ratios (s_c/s_m) in cohesive soils. 138

Table 5.19 Mean and standard deviation of displacement differences (s_c-s_m). 138

Table 5.20 Mean and standard deviation of the displacement ratio for predictive methods in cohesionless soils. 139

Table 5.21 The statistics of displacement difference (s_c-s_m) for predictive methods in cohesionless soils. 139

Table 5.22 Statistics of displacement ratio (s_c/s_m) for predictions in mixed profiles. 141

Table 5.23 Summary of mean and standard deviation for displacement differences of predictions with measurements. 141

Table 6.1 Summary statistics for (s_c/s_m) and (s_c-s_m) employing the proposed method (N=26). 146

Table 6.2 Statistical values for displacement ratios and differences in cohesionless soils (N=34). 155

Table 6.3 Statistics for settlement ratio (s_c/s_m) and displacement difference (s_c-s_m) (N=83). 161

Table 7.1 Multiplication factors at loading increments ($^{\dagger}K_1 = E_s/c_u$). 166

Table 7.2 Values for logarithmic fitting conducted for piles in cohesionless soils. 167

Table 7.3 Statistics for settlement ratio (s_c/s_m) and displacement difference (s_c-s_m) (N=83). 168

List of Figures

Figure 2.1 Sites in Northern California. 10

Figure 2.2 Sites in Southern California. 10

Figure 2.3 Trailer-mounted drill rig in operation. 20

Figure 2.4 a) Triaxial sample cutting lathe and miter box, b) Consolidation sample cutter. 24

Figure 2.5 Comparison of undrained shear strength values for trimmed versus untrimmed specimens. 29

Figure 2.6 Relative error for the effect of trimming on UU test results. 30

Figure 2.7 Changes in water content of trimmed and untrimmed samples. 30

Figure 2.8 The effect of water content on undrained shear strength. 30

Figure 3.1 a) Displacements and b) loads for a pile in compression (*i* and *j* refer to soil elements). 35

Figure 3.2 Geometry and assumptions for Mindlin's equations (Mindlin, 1936; Poulos and Davis, 1974). 37

Figure 3.3 Shear stress distribution along the side of pile segments. 41

Figure 3.4 Problem definition by Lee et al. (1987) a) Axially loaded pile in a layered soil, b) Extended soil layers, c) fictitious pile. 43

Figure 3.5 Mirror-image approach for a pile on a rigid base. 47

Figure 3.6 Various definitions of elastic of elastic modulus: E_i: Initial tangent modulus; E_s: Secant modulus; E_t: Tangent modulus (defined at a given stress level). 53

Figure 3.7 A schematic for the normalized shear modulus – shear strain relationship. 55

Figure 3.8 Displacements with varying Young's modulus and Poisson's ratio. 56

Figure 3.9 An example for the effect of varying ultimate capacity on the load-displacement curve. 59

Figure 3.10 Conceptual variation of shear modulus with strain level under static monotonic loading; relevance to in-situ tests (Mayne et al., 2001). (PMT: pressuremeter; DMT: dilatometer). 61

Figure 3.11 Strain dependence of measurement and analysis of soil properties (Yoshida and Iai, 1998)..... 61

Figure 3.12 A comparison of typical strains applied in laboratory tests versus in-situ strains around structures (Clayton et al., 1995)..... 63

Figure 3.13 Parts and pore pressure sensors of a piezocone penetrometer (CPTU)..... 66

Figure 3.14 Example of a pressuremeter test result (Baguelin et al., 1978)..... 69

Figure 4.1 View of the pre-processing interface for Tapile program. 90

Figure 4.2 Tapile final screen in command window after execution..... 91

Figure 4.3 An example of the collected pile load test data in cohesive soil..... 92

Figure 4.4 Flow chart depicting the steps in Tapile analyses (adapted from Poulos, 1979)..... 93

Figure 4.5 Failure load determination (pile weight not considered): a) peak applied load corresponding to pile capacity in a tension test, b) failure load for a prematurely terminated pile load test in compression..... 94

Figure 4.6 Load-displacement envelope..... 95

Figure 5.1 The magnitude of measured displacements, s_m..... 102

Figure 5.2 Measured displacements over pile diameter. 102

Figure 5.3 Young's modulus correlations with undrained shear strength. 104

Figure 5.4 Difference between calculated pile capacities: Davisson (167 kips) versus peak applied load (173 kips). 105

Figure 5.5 Comparison of measured and predicted displacements. 106

Figure 5.6 Comparison of correlations based on mean and standard deviation of displacement ratio (s_c/s_m). 107

Figure 5.7 Comparison of correlations based on mean and standard deviation of displacement differences (s_c-s_m) (both in inches)..... 110

Figure 5.8 Pile diameter versus displacement ratio for outliers. 113

Figure 5.9 The magnitude of measured displacements for load ratios up to a half. ... 114

Figure 5.10 Measured displacements over pile diameter for piles in cohesionless soils..... 115
Figure 5.11 Correlations of SPT blow count with Young's modulus of soil. 117
Figure 5.12 Measured and predicted displacements for piles in sandy soils. 118
Figure 5.13 Comparison of correlations based on mean and standard deviation of displacement ratio (s_c/s_m). 119
Figure 5.14 Comparison of predictions based on mean and standard deviation of displacement difference (s_c-s_m). 121
Figure 5.15 Pile diameter and displacement ratio for all tests and outliers. 126
Figure 5.16 The pile stiffness and displacement ratio for all tests and outliers..... 127
Figure 5.17 Magnitudes of measured displacements. 129
Figure 5.18 Absolute value of measured displacements, s_m, divided by pile diameter, D. 130
Figure 5.19 Comparison of displacements for piles driven into mixed profiles (N = 83). 131
Figure 5.20 Comparison of displacements predicted using Frank's correlation. 132
Figure 5.21 Predictions utilizing the elastic column approach in mixed profiles..... 133
Figure 6.1 Young's modulus versus undrained shear strength for each load ratio (N=26). 144
Figure 6.2 Change of Young's modulus with undrained shear strength and fitted correlations. 145
Figure 6.3 Calculated and measured displacements using suggested correlations..... 146
Figure 6.4 Comparison of proposed E_s correlations with others from literature. 147
Figure 6.5 Suggested correlations and data for concrete piles (N=6)..... 148
Figure 6.6 Suggested correlations and available data for closed-ended pipe piles (N=3). 148

Figure 6.7 Calculated Young's moduli from pile load tests and suggested correlations for open-ended pipe piles (N=17). 149
Figure 6.8 Variations of Young's modulus with SPT blow count (N=34). 150
Figure 6.9 Young's modulus versus blow count in logarithmic axes given along with fitted curves (N=31). 151
Figure 6.10 The effect of varying displacements on the values of Young's modulus. 153
Figure 6.11 Comparison of fitted curves to Young's modulus versus blow count results at each load ratio. 154
Figure 6.12 Fitted curves in relation to other recommended correlations for cohesionless soils. 155
Figure 6.13 Displacements calculated for piles in cohesionless soils using correlations derived from Caltrans database. 156
Figure 6.14 Values of Young's modulus obtained for the closed-ended pipe pile (N=1). 157
Figure 6.15 Calculated Young's modulus for concrete-filled pipe piles (N=2). 157
Figure 6.16 Young's modulus values calculated from H-piles in Caltrans pile load tests (N=4). 158
Figure 6.17 Variation of E_s and N for concrete piles (N=6). 158
Figure 6.18 Young's modulus versus SPT N for open-ended pipe piles (N=18). 159
Figure 6.19 Predicted and measured displacements of piles in mixed profiles (N=83). 160

Chapter 1: Introduction

1.1 MOTIVATION

Limits must be placed on displacements of structures, especially differential displacements, to minimize damage. These limits can vary based on the type and importance of the structure. For example, the limit for heavy multi-storied structures is much less than that for a steel-framed warehouse. Drilled or driven piles are generally utilized in cases where shallow foundations do not provide a satisfactory outcome. However, once the decision for piles is made, the typical design approach is to ensure that the estimated capacity is greater than the expected loading multiplied by a safety factor to include uncertainties. Such an approach implicitly assumes that the displacements will remain within tolerable amounts. A recent trend considers serviceability limits to apply the LRFD (load and resistance factor design) approach (Barker et al., 1991; CFEM, 2006; Eurocode 7, 1997; NCHRP Report No. 507, 2004). Nevertheless, limitations of budget, time, available resources in terms of personnel and computing, and the provided site/soil information are all reasons for overlooking pile displacement.

Usually the displacements of individual piles are small and most are complete during or shortly after the loads are applied without adverse effects to the structures. Nevertheless, displacements may be an important factor for various conditions; for example when long and compressible piles are considered, when piles are driven in dense cohesionless soils and large loads are involved, when static loads represent a large fraction of the total load and soil is susceptible to increased displacements with time, or when live loads are applied and removed cyclically due to wind or wave. Stricter

structural requirements for some facilities may also call for the evaluation of displacements.

1.2 PILE LOAD DATABASE

Axial pile load tests are conducted to have a better understanding of pile capacity and load-displacement behavior, reducing the uncertainty involved with the design and implementation. The costs of performing a pile load test may lead to savings due to the reduced safety factors and increased reliability of the results. However, it may not be feasible to carry out tests during the initial phases of a design or if the piles are proposed at a location where the designers already have a significant amount of experience and knowledge. Pile load test databases combine such collected experience at different locations in a convenient manner. Databases can be beneficially utilized to find piles and site conditions similar as to type, length, diameter, and soil layering as to those that are under consideration.

A database comprised of axial pile load tests conducted at multiple locations throughout California has been employed to predict load-displacement behavior. The pile load tests have been provided by the California Department of Transportation (Caltrans). Additional in-situ testing involving cone soundings and standard penetration tests, and soil borings have been completed at or near the location of the pile load tests to supplement the furnished information. Various laboratory tests conducted on the soil samples collected from borings are also included to augment the parameters for the evaluation and development of predictive methods. The author supervised the fieldwork and actively participated in all phases of laboratory testing.

The database initially contained 337 pile load tests on 239 piles at eighty-three Californian bridges and abutments. However, the database used for this dissertation

(FinalCT.dat dated May 29, 2005) has been reduced to 143 pile load tests due to various complications and restrictions with the initial information. All of the tested piles were driven into the ground. Measurements of displacements and loads were made only at the top of the pile.

Although the data incorporated into the study were based on pile load tests conducted in California, this dissertation is expected to have broader implications to predict pile displacements in other regions because multiple types of soils and piles are considered.

1.3 RESEARCH APPROACH

Prediction of the response of a single friction pile to axial loading involves an analysis of soil-pile interaction. Under ideal circumstances, the design engineer would like to predict the entire load-displacement curve, along with the rate of load transfer from the pile to the soil as a function of depth. Practically, though, failure load is estimated along with a prediction of the displacements under working loads, which is defined as a factor of safety between two to three applied to the failure load. Practical rules of thumb have been suggested for estimating displacements for such cases based on pile diameter (Vesic, 1970; Briaud and Tucker, 1985; Frank, 1985, 1995). However, a more accurate analytical approach should undoubtedly involve other relevant parameters such as pile length and soil layering.

For determining displacements, the empirical elastic or load transfer (t-z) methods are usually favored over more sophisticated, yet complicated and costly approaches such as finite elements methods. They are simpler to set-up and can rapidly be conducted with the aid of computer codes. Although potentially more universal, sophisticated and accurate, finite element or boundary element methods have not been widely accepted as

part of routine geotechnical engineering practice for pile design. Costs involved due to the complexity of models and the difficulty of obtaining relevant parameters can be listed as reasons for the lack of implementation. Some suggested soil models require a significant number of parameters (up to fifteen) to be determined with specialized laboratory and/or field testing (Whittle, 1993; Barbour and Krahn, 2004).

In this dissertation, the displacements of axially loaded single piles are explored using a modification of Mindlin's solution (1936) based on elasticity, which provides a solution to predict displacements within a semi-infinite soil mass induced by a vertical load. Changes are made to the original solution to account for:

- varying soil conditions and layering (Poulos and Davis, 1968; Poulos, 1979),
- assumptions of stresses and displacements acting on the soil-pile interface (D'Appolonia and Romualdi, 1963; Salas, 1965; and Poulos and Davis, 1968), and
- residual stresses (Poulos; 1987).

Young's modulus or modulus of elasticity, E_s, and Poisson's ratio, ν_s, of the soil along the periphery and below the tip of a pile are the two parameters that influence the predictions in this approach. However, the effect of Young's modulus on the predicted displacements is much more pronounced than Poisson's ratio; therefore, the focus in this study is towards establishing an approach to determine appropriate values of E_s.

Many researchers have suggested Young's modulus correlations with a multitude of parameters. Most of the correlations involve simple, readily available laboratory and/or in-situ information. These Young's modulus correlations can be utilized to predict displacements with the elastic method. A few of these relationships are evaluated in this

dissertation to investigate the accuracy of the predictions when compared to the measurements from pile load tests within the compiled database. While the laboratory triaxial undrained shear strength, c_u, is employed for cohesive soils, the standard penetration test blow count, N, is used for cohesionless soils.

In addition to evaluating existing correlations, the same pile load test data are utilized to obtain back-calculated values of Young's moduli in order to improve the predictions of load-displacement behavior. The measured displacements at loads of a third, a half, and two-thirds of the failure load (or determined pile capacity) are iteratively matched by a trial-and-error process. Separate Young's modulus correlations are obtained for cohesive and cohesionless soils. The correlation factors thus derived are then used to predict the displacements of piles driven in mixed profiles. The displacements at increasing load increments can be used to construct a complete load-settlement curve.

1.4 DISSERTATION OUTLINE

This dissertation contains seven chapters and two appendices. An outline for each chapter is given below.

The database used for analyses in this dissertation is described in Chapter 2, with an emphasis given to the field and laboratory testing conducted in support of the information provided by the California Department of Transportation.

The theory behind the elastic method and its modifications suggested by other researchers to better simulate load-displacement behavior of single axially loaded piles are described in Chapter 3.

In Chapter 4, the database is broken into three main classifications according to the type of soil in which the piles are founded. Definitions are given for cohesive, cohesionless and mixed soil profiles. Relevant information regarding the pile load test

database is summarized in tables. The graphical and statistical evaluations in the following chapters are explained.

In Chapter 5, analyses of pile load tests based on recommended correlations obtained from the literature are shown. Results are compared to the measurements from actual pile load tests. Suggested correlations are ranked in terms of the ratio of calculated to measured displacements ("displacement ratio") as well as the difference between the two displacement values ("displacement difference").

Attempts to obtain improved correlations for Young's modulus with widely available parameters for cohesive and cohesionless soils are described and evaluated in Chapter 6. The outcome is placed in context with correlations employed in the previous chapter.

Conclusions of this research, shortcomings and recommendations for extending the findings are given in the last chapter.

Appendix A contains a listing of site names, bridge numbers, pile load test numbers, and other descriptive terms used in tables in Chapters 2 and 4.

Correlations collected from literature relating a wide range of parameters to Young's modulus are given in Appendix B.

Appendix C includes an example of the input and output files used in estimating displacements with Tapile computer code.

Chapter 2: Pile Load Database

2.1 INTRODUCTION

An axial pile load test database from locations throughout California was compiled and utilized as part of this dissertation. The information was furnished by the California Department of Transportation. Fifty-six cone soundings, numerous standard penetration tests and forty-six soil borings were conducted to supplement the furnished information. Laboratory tests are also conducted on the soil samples collected from borings.

In this chapter the establishment of the pile load test database is described along with various aspects of laboratory and in-situ tests conducted as part of an effort to increase the available information. Limitations observed in the compiled data are discussed.

2.2 PILE LOAD DATABASE

Typical California Department of Transportation (Caltrans) practice is to install driven piles to support structures such as abutments, overpasses, and bridges within the state. The design of such piles commonly relies on general site investigations providing sample descriptions along with measures of undrained shear strength for cohesive soils and standard penetration resistance for cohesionless soils without any further laboratory and/or in-situ tests. The importance of improved understanding of soil properties and proficient design approaches to pile foundations were underscored following major structural failures and financial ramifications of earthquakes in California, such as Loma Prieta in 1989 and Northridge in 1994. The retrofit efforts following these earthquakes

have resulted in “overdesign” of foundations, i.e., an approach that is conservative and costly (DiMillio, 1999).

Since 1957, Caltrans has conducted a large number of pile load tests (approximately 450 by July 1994 at a cost reaching $30,000 per test, Liebich 2003) as part of an intense effort to estimate the capacity of their piles. Unfortunately, the accumulated experience has not yet translated into improved design approaches. Typically basic general site investigations were conducted as part of designing piles for Caltrans. Common pile design methods could not be used because generally no laboratory testing was conducted. The pile load tests were mainly conducted to verify capacity and were not an integral part of a standard pile design. Piles were often driven essentially to refusal. Pile design estimates of load capacity were commonly compared to those obtained from dynamic formulas (Engineering News, Hiley, etc.) based on pile driving records. Furthermore, the capacity was determined using a half-inch failure criterion, in which the load measured at half an inch of displacement is considered as the pile capacity based on recommendations of structural engineers. Results from load tests on instrumented piles found in the literature indicate that side and tip capacities develop at different displacements. Shaft capacity reaches its peak value at a lower displacement than the tip capacity. Thus, a constant displacement value having a constant value as a failure criterion may lead to uneconomical designs if sufficient displacement is not allowed to mobilize tip capacity. Despite these shortcomings, a half-inch displacement continues to be Caltrans’ preference for defining pile capacity and remains as a critical parameter for design (Caltrans California Foundation Manual, 1997).

In the summer of 1998, Caltrans funded a project at The University of Texas at Austin entitled “Improvement of Caltrans Pile Design Methods through Synthesis of

Load Test Results" to evaluate years of accumulated pile load test data and ultimately to develop updated design methodologies. This dissertation focuses on the load-displacement behavior of piles based on the information supplied by Caltrans and on additional testing conducted in the field and in the laboratory as part of this project.

Initially, Caltrans provided an archive of pile test reports that contained measurements of pile head load-displacements along with site characterization information, which were entered in the "Geotechnical Measurements Database" (GMD) established by Brown (2001). The GMD includes 319 static load tests on 227 untapered (no changes in the cross-section) driven piles in 161 pile groups at 75 bridge locations throughout California. Additional laboratory and field investigations were conducted, which likewise contributed to the GMD. Further details of the GMD can be found in Brown (2001). Two tables coupling the bridge numbers, site names and locations, load test numbers and other descriptive terms for all of the pile load tests are provided in Appendix A. Designation from these tables was also used to provide details for project borings and soundings (Tables 2.1 and 2.2). A general overview of pile load test locations sorted by counties is shown in Figures 2.1 and 2.2. The majority of the Caltrans data is concentrated in areas near California's largest metropolitan centers: Los Angeles, San Diego and the Bay Area. A few other tests were conducted at remote bridge locations.

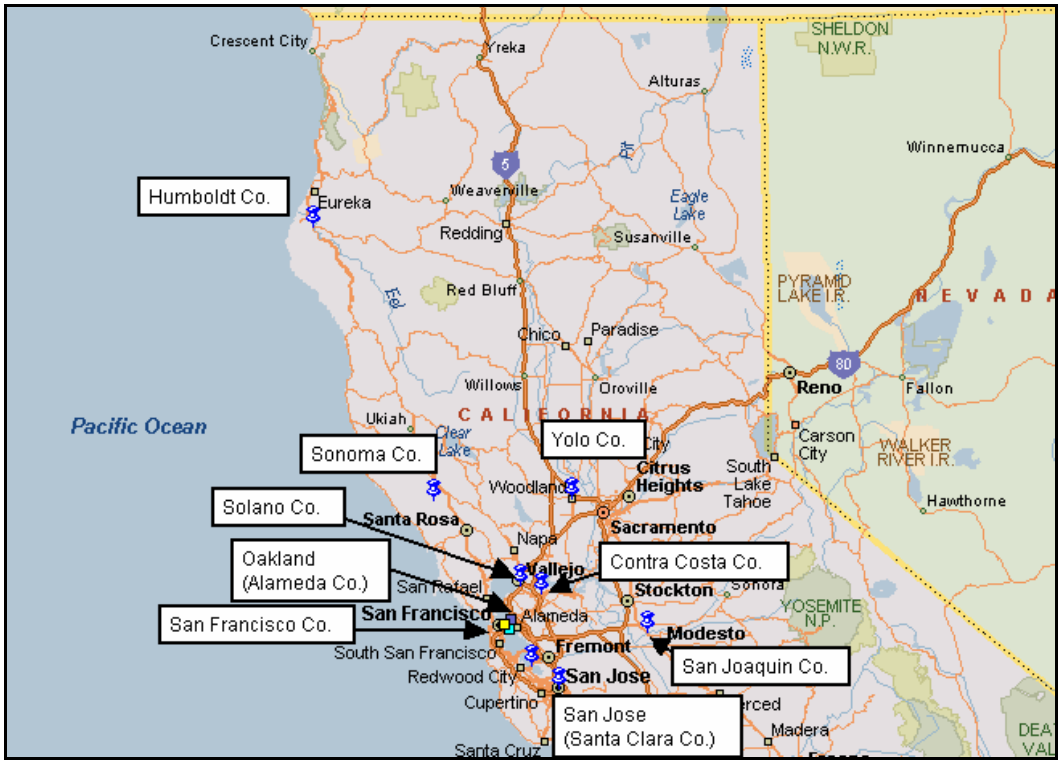

Figure 2.1 Sites in Northern California.

Figure 2.2 Sites in Southern California.

At the beginning of the project, the aim was to enter essentially all available data into the GMD and then to utilize those tests which were deemed useful in developing design methods. In some cases, inadequacies in data were not apparent until analyses were attempted. Since 2001, analysis and checking of the interpreted soil profiles included in the GMD have resulted in modifications (Olson, 2005). The main reasons for such changes are the reevaluation of pile load test reports, additional field/laboratory investigations provided by Caltrans, incorporation of pile driving records into the site characterization, and an increased emphasis on soil borings that were conducted as part of this project.

Therefore, a database called FinalCT (Olson, 2005) was created as a text file, which is similar to that established for the American Petroleum Institute by Olson and Dennis (1982). The number of load tests in FinalCT was reduced to 143 from 337 in the GMD.

In this dissertation, the load-displacement behavior is investigated utilizing the pile load tests listed in the FinalCT database.

2.2.2 Limitations of Both Pile Load Test Databases

Despite frequent revisions, neither database can be considered ideal. Obviously a database is only as good as the data included in it. In some cases, the locations of the pile load tests were not readily accessible due to restrictions from owners, and the presence of utilities that restricted access. Among the other most evident limitations of both databases are the following:

1. There is no instrumentation along the length of any pile; i.e., only pile-head load and displacement measurements are available. Therefore, the distributions of loads

and displacements along the sides and on the tip have not been properly assessed. They may at best be estimated from previous experience.

2. Some of the pile load tests were not carried to failure or had very few data points. The goal in most of these cases was to evaluate the performance of a pile within working loads, but unplanned situations such as equipment malfunction, failure of support piles, etc., also occurred. Piles tested within working loads may be useful in analyzing displacements up to that load but they do not provide pile capacities.

3. Setup time (the time between driving the pile into the ground and load testing) is either not known or was not sufficient for some pile load tests (less than a week in clayey profiles and a day for piles in coarser materials). Setup time may increase the load carrying capacity of piles due to pore-pressure changes or stress distributions in the soil.

4. In some of the older tests, there is no clear indication of the loading direction. However, in most such cases, an estimate has been made based on further evaluation of the load test report.

5. When a pile was tested in both compression and tension, one following the other, the properties of the soil surrounding the pile might have been affected by the first load test and thus the second load test might not produce capacities that would have been achieved in the absence of a previous load test.

6. It was not always clearly stated whether steel pipe piles were open-ended or closed-ended. The size of the cover plate might be missing even if there was a note that the steel pipe pile was closed-ended.

7. Soil borings were sometimes not close to the pile because of restricted site access. In other cases, it was difficult to determine the precise location and top

elevation of a test pile due to site regrading. This may have significantly affected soil characterization, considering the heterogeneous nature of soil properties.

8. The soil profiles and SPT blow counts were estimated from pile driving records if there were no borings at or near the location of a pile load test (FinalCT only). Notes were made to indicate which blow counts were estimated.

9. Most of the piles are in interstratified profiles, which complicate analyses and make it more difficult to separate pile behavior in a specific material within the strata.

10. All of the piles in this study were used for supporting bridges and all were in significant earthquake zones. These conditions restricted the type and size of the piles. Predominantly, steel pipe piles were used.

11. The project boring and sounding elevations do not necessarily correspond to the tested pile elevations. Many of the piles were driven at the bottom of excavations below the surface elevation where soil explorations were made.

12. For storage purposes, original Caltrans soil boring and sounding logs were reduced greatly in size by Caltrans through photocopying, which made them difficult to read. In older reports, the quality of the report reproduction was low.

In-spite of the limitations listed above, any approach based on the established databases is expected to improve future Caltrans' design methods for foundations constructed in soil profiles typically encountered in California. It can also reduce construction costs by eliminating overly-conservative designs and provide design engineers with site-specific information. Additionally, a database provides a basis for any future improvements of aspects not considered within the University of Texas at Austin (UT) project.

The Federal Highway Administration (FHWA) has pooled pile load tests from a multitude of state highway departments and established a pile load test database containing a broad range of information. FHWA has recently updated its deep foundations design guidelines and manuals, which are widely used (Design and Construction of Driven Pile Foundations Reference Manual – Volumes I and II, 2006). Caltrans, under the umbrella of FHWA, similarly sponsored the project at UT with the aim of being a part of the occurring changes. Results from this dissertation are aimed towards providing additional insight into the load-displacement aspect of designing pile foundations.

2.3 FIELD INVESTIGATION

Additional borings and in-situ tests beyond those which existed in Caltrans files were conducted at selected sites where subsurface information was deemed inadequate. The main reasons for this evaluation are the following:

1. For a pile design relying on empirical correlations, it is reasonable that all relevant parameters be obtained in a consistent manner to avoid any uncertainties regarding the test method or equipment. Relatively undisturbed soil samples were obtained to re-evaluate visual classification and perform laboratory tests. This is the most important reason for conducting additional soil borings.

2. In some cases the original Caltrans soil borings were too far from the site of the load test to characterize the subsurface conditions adequately.

3. Standard penetration test (SPT) hammers vary in the energy that they transfer to the rods resulting in uncertainty in terms of the blow counts being measured. A calibrated hammer with an 80% efficiency was used for most of the borings. A cathead

and rope system was utilized for some borings which was assumed to provide a 60% efficiency.

4. Cone penetration testing (CPT) was expected to be utilized for designing pile foundations because of its increased reliability.

5. In some cases the groundwater level was not well defined either because no measurements were noted on the original boring log or because the water level in a boring was measured with a drilling fluid containing bentonite, which has a very low hydraulic conductivity. Its presence impedes the flow of water essential for correct determination of the water table.

2.3.1 Field Exploration Segments

Field investigation was performed in five task orders over approximately fifteen months. Each task order covered work in a single geographic region, thus simplifying mobilization of drilling rigs. Generally task orders were based on soil borings because CPTu soundings were mostly conducted independent of UT supervision.

Forty-six borings and fifty-six cone soundings with pore pressure measurements were conducted. Starting and completion dates of borings and soundings along with target and actual depths are given in Tables 2.1 and 2.2. Details of each bridge and bent number location can be found in Appendix A.

Table 2.1 List of soil borings.

Boring Number	Site[1]	Bent Number	Bridge Number	Date Started	Date Completed	Target Depth (ft)	Actual Depth (ft)	Water Table (ft)
UTB-1	Oak-03-2	17R	33-0611R	7/7/1999	7/7/1999	75	63.5	5
UTB-1A[2]	Oak-03-2	17R	33-0611R	7/8/1999	7/8/1999	75	78	5
UTB-2	Oak-03-3	29R	33-0611R	7/8/1999	7/21/1999	85	87	4.5
UTB-3	Oak-04-4	31NC(LT)	33-0612E	7/21/1999	7/23/1999	100	101.5	5.5
UTB-4	Oak-02	3F(LT)	33-0393	7/26/1999	7/26/1999	90	92	5.5

Boring Number	Site[1]	Bent Number	Bridge Number	Date Started	Date Completed	Target Depth (ft)	Actual Depth (ft)	Water Table (ft)
UTB-5	Oak-04-3	27NC(RT)	33-0612E	7/27/1999	7/28/1999	115	115.5	7.5
UTB-6	Oak-04-1	10NCI	33-0612E	7/28/1999	7/29/1999	110	110	6
UTB-7	Oak-01-1	E28L	33-0025	7/30/1999	7/30/1999	60	62	4
UTB-8	Oak-04-2	17NC1	33-0612E	8/23/1999	8/25/1999	110	112.5	6
UTB-9	Oak-05-3	Site 3	I880 IPTP	8/25/1999	8/27/1999	115	119	5
UTB-10	Oak-05-1	Site 1	I880 IPTP	8/30/1999	8/30/1999	45	46.5	14
UTB-11	Oak-05-2	Site 2	I880 IPTP	8/30/1999	8/30/1999	65	22	4.5
UTB-11A	Oak-05-2	Site 2	I880 IPTP	8/31/1999	8/31/1999	65	65.5	4.5
UTB-12	Oak-05-4	Site 4	I880 IPTP	9/1/1999	9/2/1999	85	87.5	4
UTB-13	SJ-01	4	37-0011	9/8/1999	9/9/1999	75	77	15
UTB-14	SJ-02-2	GD-2, 6	37-0270H	9/10/1999	9/13/1999	60	61.5	25
UTB-15	SJ-03-3	6L-2	37-0279L	9/14/1999	9/14/1999	75	77	14.5
UTB-16	SJ-02-3	GD-2, 14	37-0270H	9/15/1999	9/15/1999	80	83.5	20.5
UTB-17	SJ-04	DC-4, 8	37-0353	9/16/1999	9/16/1999	85	89	7.5
UTB-18	SF-03-3	Site C	34-0088	3/27/2000	3/27/2000	75	75.5	N/A
UTB-19	SF-03-4	Site D	34-0088	3/28/2000	3/28/2000	70	70	11.5
UTB-20	SF-03-6	Site F	34-0088	3/29/2000	3/29/2000	80	80	9
UTB-21	SF-03-5	Site E	34-0088	3/30/2000	3/31/2000	105	106.5	6.5
UTB-22	SF-03-7	Site G	34-0088	3/31/2000	4/3/2000	90	90.5	7.5
UTB-23	Oak-04-4	31NC(LT)	33-0612E	4/4/2000	4/4/2000	100	102	5
UTB-24	Oak-04-2	17 NC1	33-0612E	4/5/2000	4/5/2000	110	7.25	2.5
UTB-24A	Oak-04-2	17NC1	33-0612E	4/5/2000	4/5/2000	110	110	2.5
UTB-25	LA-03	5	53-1181S	5/31/2000	5/31/2000	50	50	18
UTB-26	LA-01-1	10	53-0527L	6/1/2000	6/1/2000	60	60	39.5
UTB-27	LA-13-1	2	53-2733	6/2/2000	6/2/2000	45	45	26
UTB-28	LA-14	5	53-2791S	6/3/2000	6/3/2000	70	70	22.5
UTB-29	LA-09	21 Foot. A	53-1851	6/5/2000	6/5/2000	50	50	20
UTB-30	LA-22	8	55-0794F	6/6/2000	6/6/2000	65	65	28
UTB-31	LA-20	4	55-0682F	6/7/2000	6/7/2000	65	65	N/A
UTB-32	LA-17	6	55-0642	6/8/2000	6/8/2000	70	70	N/A
UTB-33	LA-21-2	16	55-689E	6/8/2000	6/8/2000	70	70	N/A
UTB-34	LA-15	2	55-0422G	6/13/2000	6/13/2000	60	60	17
UTB-35	LA-02	5	53-0114	6/14/2000	6/14/2000	60	60	42
UTB-36	SD-07-2	2L	57-1017R/L	6/15/2000	6/15/2000	40	40	15.5
UTB-37	SD-07-1	Abutm. 7R	57-1017R/L	6/15/2000	6/15/2000	30	30	15.5

Boring Number	Site[1]	Bent Number	Bridge Number	Date Started	Date Completed	Target Depth (ft)	Actual Depth (ft)	Water Table (ft)
UTB-38	SD-08-2	Site 2	I-5/I-8 IPTP	6/16/2000	6/16/2000	120	118.5	23
UTB-39	SD-03	5	57-0783F	6/17/2000	6/17/2000	60	60	19
UTB-40	Oak-05-2	Site 2	I880 IPTP	9/12/2000	9/12/2000	60	61.5	4
UTB-41	Oak-05-4	Site 4	I880 IPTP	9/13/2000	9/13/2000	90	92.5	4
UTB-42	SM-02	8B	35-0284	9/14/2000	9/15/2000	115	115	12.5
UTB-43	CC-02	5L	28-0056L	9/18/2000	9/18/2000	75	75	8.5
UTB-44	Mon-03	Test Group	44-0216R/L	9/19/2000	9/20/2000	140	141.5	8
UTB-45	Son-01	3	20-0172	9/21/2000	9/22/2000	60	60.5	10
UTB-46	Son-02	Abutm. 2R	20-0251R	9/22/2000	9/23/2000	60	60	9

[1] The corresponding load test numbers, cities and counties are given in Appendix A.

[2] A subsequent boring or sounding attempt was made at the same location due to an obstruction at some depth or a difficulty in reaching target depth.

Table 2.2 Cone Penetration Test (CPT) soundings.

CPT Number	Site	Bent Number	Bridge Number	Date	Target Depth (ft)	Actual Depth (ft)	Depth Ratio (%)	Predrill Depth (ft)
UTC-1	Oak-03-1	13L	33-0611L	7/8/1999	90	68	76	10
UTC-1A	Oak-03-1	13L	33-0611L	7/8/1999	90	69	77	5
UTC-2	Oak-03-2	17R	33-0611R	7/9/1999	75	66	88	5.5
UTC-3	Oak-03-3	29R	33-0611R	7/9/1999	85	85	100	7.5
UTC-4	Oak-02	3F(LT)	33-0393	7/21/1999	90	90	100	0
UTC-5	Oak-04-4	31NC(LT)	33-0612E	7/23/1999	100	100	100	9
UTC-6	Oak-04-3	27NC(RT)	33-0612E	7/22/1999	115	115	100	0
UTC-7	Oak-04-2	17NCI	33-0612E	7/22/1999	110	110	100	0
UTC-8	Oak-01-1	E28L	33-0025	7/26/1999	60	60	100	10
UTC-9	Oak-01-2	E31R	33-0025	7/22/1999	65	65	100	0
UTC-10	Oak-05-1	Site 1	I-880 IPTP	7/23/1999	45	34	76	4.5
UTC-11	Oak-04-1	10NCI	33-0612E	7/23/1999	110	110	100	8
UTC-12	Oak-05-3	Site 3	I-880 IPTP	7/26/1999	115	115	100	0

CPT Number	Site	Bent Number	Bridge Number	Date	Target Depth (ft)	Actual Depth (ft)	Depth Ratio (%)	Predrill Depth (ft)
UTC-13	Oak-05-2	Site 2	I-880 IPTP	9/14/1999	60	42.5	71	16
UTC-14	Oak-05-4	Site 4	I-880 IPTP	9/14/1999	85	74	87	12
UTC-15	SJ-02-2	GD-2, 6	37-0270H	9/8/1999	60	55	92	6
UTC-16	SJ-02-4	GD-4, 3	37-0270H	9/8/1999	60	60	100	5.5
UTC-17	SJ-02-3	GD-2, 14	37-0270H	9/9/1999	80	80	100	7
UTC-18	SJ-02-5	GD-4, 11	37-0270H	9/9/1999	60	60	100	5.5
UTC-20	SJ-01	4	37-0011	9/13/1999	75	75	100	7
UTC-21	SJ-03-1	2L-2	37-0279L	9/9/1999	75	75	100	5
UTC-22	SJ-03-3	6L-2	37-0279L	9/13/1999	70	70	100	5
UTC-23	SJ-03-2	3R-2	37-0279R	9/9/1999	70	70	100	0
UTC-24	SJ-04	DC-4, 8	37-0353	9/13/1999	85	85	100	6
UTC-25	SF-03-3	Site C	34-0088	3/27/2000	75	50.2	67	25
UTC-25A	SF-03-3	Site C	34-0088	3/27/2000	75	15.6	21	0
UTC-26	SF-03-5	Site E	34-0088	3/30/2000	105	89.2	85	3.5
UTC-26A	SF-03-5	Site E	34-0088	3/30/2000	105	120	114	3.5
UTC-27	LA-01-1	10	53-0527L	6/13/2000	55	35	64	0
UTC-28	LA-14	5	53-2791S	6/13/2000	70	40	57	0
UTC-29	LA-09	21 Foot. A	53-1851	6/13/2000	50	36.3	73	0
UTC-30	LA-02	5	53-0114	6/14/2000	60	60.5	101	0
UTC-31	LA-13-1	2	53-2733	6/14/2000	45	50.5	112	0
UTC-32	LA-04	6	53-1193S	6/14/2000	60	60.5	101	0
UTC-33	LA-20	4	55-0682F	6/14/2000	65	52.2	80	0
UTC-34	LA-21-2	16	55-689E	6/14/2000	70	70.5	101	0
UTC-35	LA-17	6	55-0642	6/14/2000	70	70.5	101	0
UTC-36	LA-15	2	55-0422G	6/14/2000	60	60.5	101	0
UTC-37	SD-07-2	2L	57-1017R/L	6/15/2000	40	41.3	103	0
UTC-38	SD-07-1	Abutm. 7R	57-1017R/L	6/15/2000	30	35.6	119	0
UTC-39	SD-08-2	Site 2	I-5/I-8 IPTP	6/15/2000	120	11.3	9	0
UTC-40	SD-03	5	57-0783F	6/15/2000	60	57.7	96	0
UTC-41	SF-03-1	Site A	34-0088	5/18/2000	70	40	57	0
UTC-42	SF-03-2	Site B	34-0088	5/18/2000	80	57	71	0
UTC-43	SF-03-7	Site G	34-0088	5/18/2000	90	91	101	0
UTC-44	SF-03-6	Site F	34-0088	5/18/2000	80	52	65	0
UTC-45	SF-03-4	Site D	34-0088	5/19/2000	70	53	76	0
UTC-46[1]	SF-01-8	52R	34-0046	5/19/2000		62.5		0

CPT Number	Site	Bent Number	Bridge Number	Date	Target Depth (ft)	Actual Depth (ft)	Depth Ratio (%)	Predrill Depth (ft)
UTC-50	Oak-05-4	Site 4	I-880 IPTP	10/19/2000	85	68	80	0
UTC-51B	Oak-05-4	Site 4	I-880 IPTP	10/19/2000	85	90	106	0
UTC-52	Oak-05-4	Site 4	I-880 IPTP	10/20/2000	85	93	109	0
UTC-53	Oak-05-4	Site 4	I-880 IPTP	10/23/2000	85	90	106	0
UTC-54	Oak-05-2	Site 2	I-880 IPTP	10/23/2000	60	44	73	0
UTC-55	Oak-05-2	Site 2	I-880 IPTP	10/19/2000	60	43	72	0
UTC-56[1]	CC-04	Abutm. 3	28-0292	10/24/2000	75	75	100	0
UTC-59	SF-03-3	Site C	34-0088	3/28/2000	75	50	66	0
UTC-60	SF-03-3	Site C	34-0088	3/28/2000	75	15	21	0

[1] The number(s) that follow have not been used.

The first and second field exploration segments were conducted in July, August and September, 1999, for sites in Oakland and San Jose (borings UTB-1 through UTB-17). The third field exploration segment (UTB-18 through UTB-24A) was conducted in March, 2000, after a reconnaissance of San Francisco sites by Caltrans. Unfortunately, two major San Francisco sites, SF-01 and SF-04, had to be eliminated because of access problems. In exchange, one large San Francisco site (SF-03) was added. More detailed plans were drawn up, including scheduling of the third, fourth and fifth field exploration segments. At this point, funding became available for additional field work. Several sites, which had been excluded from the original plan because of the presence of dense gravel, cobbles or boulders were added to the fourth segment (UTB-25 through UTB-39), which was conducted in May and June, 2000. The fifth field exploration segment (UTB-40 through UTB-46), completed in September, 2000, was the last one at which the author was on site and in which UT was directly involved.

2.3.1.2 *Drilling and Sampling Methods*

Boreholes were usually drilled with a 5-inch diameter solid-flight auger until groundwater was reached (Figure 2.3). Casings were set following the determination of the water table. Drilling was then continued with a 5-inch diameter wet rotary until the desired borehole depth was reached. An exception to this practice was during the fourth segment in Southern California, where an NX-type (approximately 3-inch OD) hollow-stem rod with a drill bit attached was utilized. This is a wet rotary system with rods that provide a continuous casing throughout the borehole length, and, thereby, help keep boreholes clean so as to penetrate more easily through sands and gravels. For these cases, standard penetration tests were conducted through the end of the hollow-stem rod. It was necessary to pull the rods out before Shelby tube samples could be obtained. Therefore, the use of these NX-type hollow-stem rods was not desirable for "undisturbed" sampling.

Figure 2.3 Trailer-mounted drill rig in operation.

Undisturbed or standard penetration test (SPT) samples were taken every five feet starting at a depth of five feet below the ground surface. A standard split-spoon sampler with a driving shoe inside diameter of 1.375 inches was used without any liners for sands

and gravels. Thin-walled tubes (area ratio = 9%) of 30-inch nominal length and 3-inch nominal diameter were utilized for sampling silts and clays.

Standard penetration tests employed an automatic hammer except those that were subcontracted in some locations in Northern California, where a falling weight safety hammer was used. The automatic hammers used in the project were calibrated by the manufacturer using energy measurements with a pile driving analyzer (PDA). The PDA utilizes strain gauges and accelerometers to derive the energy transferred from the hammer to the sampling rods.

2.3.1.3 *Water Levels*

Water table determination is essential to evaluate the effective stresses at any depth, which is particularly important information when the design is based on effective stresses.

Generally, the depth of the water level in the borehole was measured using a "water level indicator" (an electric sounder which is a calibrated tape measure with an electrical sensor at the tip that makes an audible sound upon entering water and completing the circuit; also called "watermeter"). At the beginning of the project and at some other times when a watermeter was not available, measurements were taken by lowering a regular tape measure down the borehole. Occasionally the boring failed to reach the water table or the sides of the borehole collapsed, thus preventing readings.

Water table measurements may be susceptible to errors due to fluctuation from the drilling operation. A dissipation test during a CPT sounding can provide a better evaluation of the water table, but requires a longer time to complete. Therefore, a comparison of water table measurements obtained from drilling and cone soundings was made at one of the sites (boring UTB-36 and corresponding sounding UTC-37). Drilling

and CPTu rigs were operating 14 feet apart at the same time. A water level measurement was made with the water meter during drilling and with a dissipation test during the CPTu operation. The watermeter detected water at a depth of 15.7 feet whereas the dissipation test indicated the water table to be at 18 feet. The ground surface was essentially horizontal between the two locations.

The writer is not aware of any studies comparing water table measurement in a borehole as opposed to through a CPT dissipation test. A single measurement is not sufficient to reach any conclusions as to the accuracy of each method, particularly when the exact water levels are not known. While a difference of 2.3 feet can be significant for load tests on shallow foundations, its effect will be less important for piles extending to deep soil layers.

2.4 LABORATORY TESTING AND RESULTS

Laboratory tests on samples obtained during the field investigation phase were performed at the University of Texas at Austin or subcontracted to Fugro geotechnical testing laboratory in Houston, Texas. The testing program was geared towards collecting data that might be readily obtained by pile-designing engineers. Laboratory testing included the following: index tests (sieve analysis, Atterberg limits), unconsolidated-undrained (UU) triaxial compression, and one-dimensional consolidation (oedometer).

Most of the tests on samples from borings UTB-18 through UTB-46 and some of the remaining Atterberg limit tests and all of the sieve analyses from the first seventeen borings were performed by the geotechnical testing laboratories of Fugro Consultants in Houston, TX.

2.4.1 Specimen Preparation Procedures

Tests were performed according to the applicable ASTM methods and procedures listed in Table 2.3. Shelby tubes were cut into approximately five-inch segments using a band saw. The first four to five inches from the top and bottom sections of the tube, where the soil is more likely to have been disturbed, were removed. The segment lengths were selected to provide the maximum number of "good quality" four-inch long triaxial test specimens from each tube. Samples were extruded vertically using a hydraulic jack.

Table 2.3 Laboratory tests and applicable standards.

PROCEDURE	ASTM STANDARD
Description and Identification of Soils (Visual-Manual Procedure)	D 2488
Classification of Soils for Engineering Purposes (Unified Soil Classification System)	D 2487
Laboratory Determination of Water (Moisture) Content of Soil and Rock by Mass	D 2216
Liquid Limit, Plastic Limit and Plasticity Index of Soils	D 4318, Procedure B
Particle-Size Analysis of Soils	D 422
Specific Gravity of Soils	D 854
Unconsolidated-Undrained Triaxial Compression Test on Cohesive Soils	D 2850
Consolidated-Undrained Triaxial Compression Test for Cohesive Soils	D 4767
One-Dimensional Consolidation Properties of Soils	D 2435, Method B

For triaxial testing at the UT geotechnical laboratory, specimens were trimmed to a two-inch diameter using a vertical soil lathe and then cut to the appropriate four-inch height in a miter box (Figure 2.4a). The estimated in-situ vertical total stress of the specimen was used as the applied cell pressure during unconsolidated-undrained compression testing. Consolidation samples were trimmed by hand to fit into a circular

testing ring of 2.5 inches in diameter and 0.75-inch in height with the ring attached to a vertically translating table, acting as a cutter (Figure 2.4b).

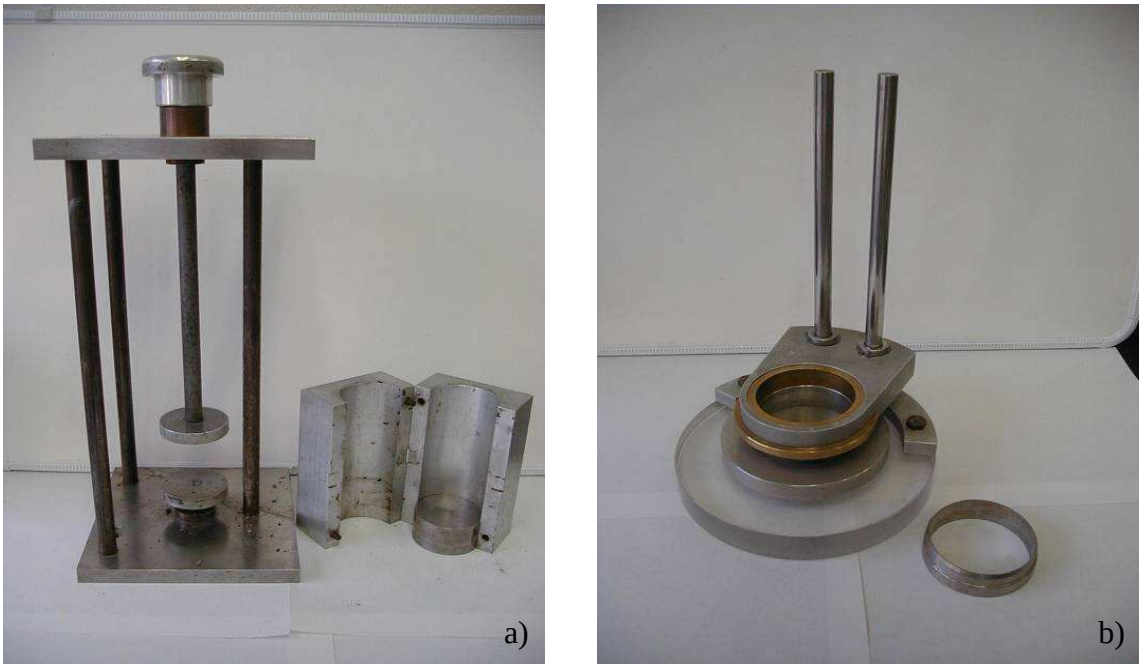

Figure 2.4 a) Triaxial sample cutting lathe and miter box, b) Consolidation sample cutter.

2.4.1.2 *Data Acquisition System*

A computerized data acquisition system was used for triaxial and consolidation testing. This system uses small analog-to-digital (A-to-D) modules that can be mounted next to the load frame, close to the transducers. The previous system, in which A-to-D boards were placed in the computers and analog signals sent from the transducers to the computer, had resulted in frequent difficulties because of interference to these analog signals.

Two independent networks were set up for data acquisition. The first network was for triaxial testing. The sensors of three load frames were connected to this network with

one analog-to-digital/input-output (AD-IO) module located next to each frame. The three AD-IO modules provided twelve channels to accommodate one linear-variable displacement transducer (LVDT), one 500-pound load cell, and two pressure transducers from each frame. The second network was for consolidation testing. One four-channel AD-IO module was located next to three consolidation frames with a LVDT on each frame connected to the module. Each network of AD-IO modules was connected to a separate network module, power supply, and computer.

2.4.1.3 *Completed Laboratory Tests*

The number of tests completed on samples obtained from borings at various locations in California is shown in Table 2.4. Further details of test results and calculated parameters can be found in the Geotechnical Measurements Database (GMD) (Brown, 2001).

Table 2.4 Summary of completed laboratory tests.

Boring		No. of Completed Laboratory Tests (UT and Fugro)					
No. (UTB-)	Depth (ft)	Atterberg Limits	Sieve Test	1-D Consolidation	UU	CD	CU
1, 1A	78	13	2	3	13	6	-
2	87	16	3	6	16	-	-
3	101.5	12	7	6	10	2	-
4	92	13	4	9	12	-	3
5	115.5	17	6	8	17	3	-
6	110	12	7	6	12	-	-
7	62	5	5	2	4	3	-
8	112.5	12	5	5	11	-	-
9	119	13	10	5	14	-	-
10	46.5	-	11	-	-	-	-
11, 11A	65.5	5	7	3	5	-	-
12	87.5	8	4	5	8	-	-
13	77	6	4	3	6	-	-
14	61	5	5	4	6	-	-
15	77	15	5	4	15	-	-

Boring		No. of Completed Laboratory Tests (UT and Fugro)					
No. (UTB-)	Depth (ft)	Atterberg Limits	Sieve Test	1-D Consolidation	UU	CD	CU
16	84	11	7	5	11	-	-
17	89	14	3	7	13	-	-
18	75.5	4	13	-	4	-	-
19	70	4	9	-	6	-	-
20	80	7	7	-	9	-	-
21	106.5	19	1	-	19	-	-
22	90.5	12	5	-	11	-	-
23	102	10	5	-	18	-	-
24, 24A	110	8	6	-	19	-	-
25	50	-	3	-	-	-	-
26	60	-	5	-	-	-	-
27	45	-	5	-	-	-	-
28	70	1	9	-	1	-	-
29	50	-	5	-	1	-	-
30	65	-	7	-	-	-	-
31	65	2	2	-	2	-	-
32	70	2	1	-	2	-	-
33	70	-	2	-	-	-	-
34	60	1	6	-	1	-	-
35	60	1	6	-	1	-	-
36	40	-	7	-	-	-	-
37	30	-	6	-	-	-	-
38	118.5	-	20	-	-	-	-
39	60	2	8	-	2	-	-
40	61.5	4	5	-	9	-	-
41	92.5	7	7	-	22	-	-
42	115	18	3	-	18	-	-
43	75	12	-	-	13	-	-
44	141.5	12	15	-	15	-	-
45	60.5	3	2	-	3	-	-
46	60	2	4	-	2	-	-
Total	3618.5	308	269	83	351	14	3

2.4.2 Measurements of Undrained Shear Strength, c_u

2.4.2.1 *Effects of Trimming on UU Triaxial Undrained Shear Strength*

Unconsolidated-undrained triaxial compression tests can be performed on untrimmed samples, i.e. as they come out of the tubes, or on trimmed samples.

Commercial geotechnical testing laboratories in the USA routinely conduct UU tests on untrimmed specimens to save on technician time and expense. Since it was felt that UU strengths should be based on procedures expected in practice, laboratory testing was performed to clarify and possibly quantify the effects of sample trimming on undrained shear strength.

Arman and McManis (1976) performed radiography on samples taken with a 2.8-inch thin-walled Shelby tube after the sample was extruded. They reported a gradual bending of horizontal planes of stratification, especially at the ends and with the maximum bending occurring on the surface of the sample. It would be reasonable to assume that the more the layers bend, the more disturbance they would create, thereby reducing undrained shear strength. Therefore, trimming a sample could increase the measured strength by removing a substantial portion of the disturbance. Brown and Paterson (1964) and Nordland and Deere (1970), while investigating failures of storage tanks, have likewise measured increased values of undrained shear strength for trimmed samples (approximately 50%).

Undisturbed samples were available from four repeated borings in the Oakland area, which provided a unique opportunity to evaluate the effects of trimming on undrained shear strength. Thirteen unconsolidated-undrained (UU) triaxial tests had already been completed on samples from the same locations. With the additional borings, there were essentially duplicates of these samples for testing. Thirty-five new UU tests were conducted. Geotechnical testing laboratories of Fugro in Houston, which was subcontracted for additional testing, provided UU test results on ten untrimmed and ten trimmed samples confined at a constant cell pressure (29 psi). The number of tests included in the analyses of the effect of trimming, thus, equaled sixty-eight. A

comparison of laboratory test results to determine the effects of trimming on undrained shear strength are shown in Figure 2.5 and are summarized in Table 2.5. Undrained strengths of trimmed and untrimmed specimens agree well at strengths less than 1000 psf with more scatter for samples of higher UU strengths.

Undrained shear strength of trimmed specimens divided by the UU strength of untrimmed specimens for all of the samples was 1.03 with a standard deviation of 0.29. The average of the same ratio for samples that had been subjected to a constant cell pressure was 0.97, with a standard deviation of 0.40. The average values compare well with the UU tests performed at the University of Texas, which have an average ratio of 1.04. However, the standard deviation is higher than those obtained from UT testing, which was 0.26.

The effect of trimming may be better seen using the "relative error":

$$\frac{c_{u(trimmed)} - c_{u(untrimmed)}}{c_{u,trimmed}} \quad \text{.....(2.1)}$$

This ratio is plotted against $c_{u(trimmed)}$ in Figure 2.6 for all of the tests conducted. The ratios seem to vary more or less equally about the x-axis with no obvious effect of trimming.

Water contents and densities may vary substantially within short distances in a soil deposit, which could have an effect on the shear strength. Although the water contents of trimmed samples, in general, were higher than those for the untrimmed specimens (Figure 2.7), there seems to be no obvious effect on the measured undrained shear strength (Figure 2.8).

Part of the problem is the relatively small number of tests conducted using untrimmed samples. In addition, the second series of borings were done because of suspect sample quality in the first set; presumably early (trimmed specimens) tests may

have been performed on more disturbed samples, thus explaining why some trimmed samples showed lower strengths than untrimmed ones. For the first set of UU tests by Fugro, a constant cell pressure was applied to the samples instead of the estimated total stresses in the field. For samples with actual total stresses below this value, the UU strength could be lower.

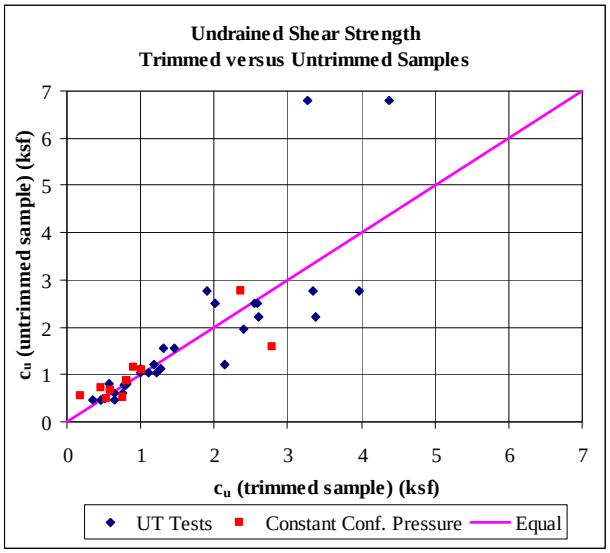

Figure 2.5 Comparison of undrained shear strength values for trimmed versus untrimmed specimens.

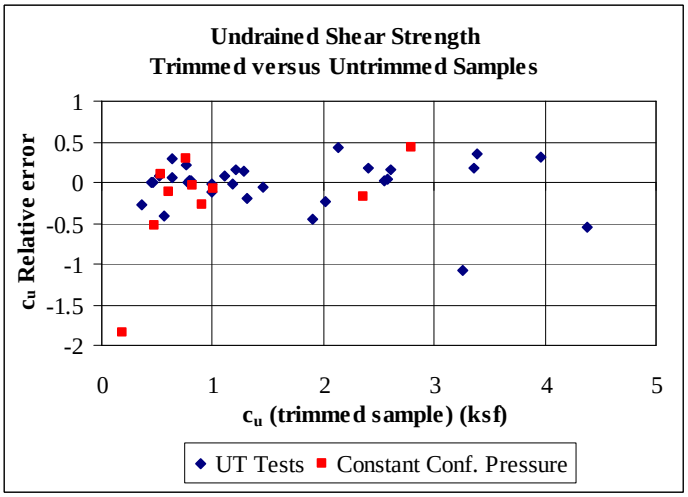

Figure 2.6 Relative error for the effect of trimming on UU test results.

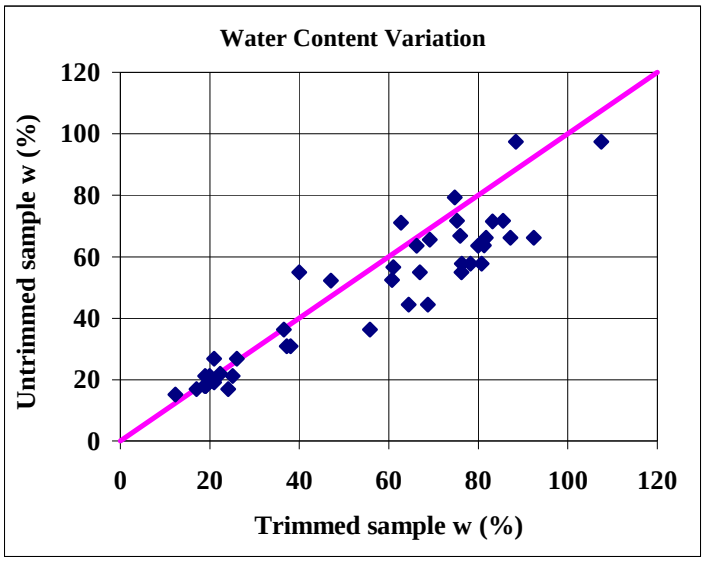

Figure 2.7 Changes in water content of trimmed and untrimmed samples.

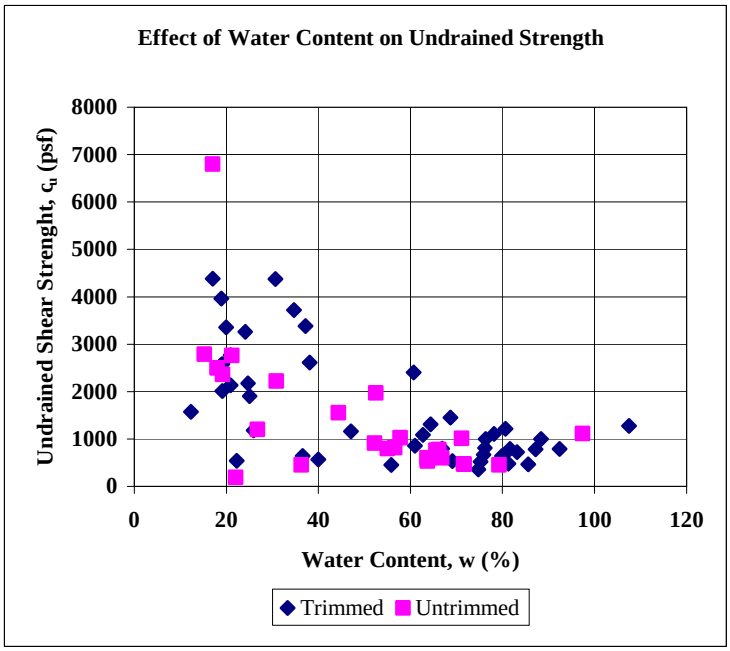

Figure 2.8 The effect of water content on undrained shear strength.

Table 2.5 Summary of UU compression tests conducted to investigate the effects of trimming.

Boring UTB-	Samp. Num.	Spec. Num.	Tip Depth (ft)	UW (psf)	WC (%)	σ_3 (psf)	UU c_u (psf)	c/p	Failure Strain (%)	U/T	Pocket Penetr. c_u Top - Bott. (psf)	Lab. USCS
18	7		34.5	138	15	4176	1570		4.2	U		CL
18	7	a	34.5	140	12		2790		2.4	T		CL
19	7		33.5	100	71	4176	1090		4.9	U		CH
19	7	a	33.5	100	63		1010		3.0	T		CH
19	16		67.5	130	22	4176	540		2.8	U		
19	16	a	67.5	120	22		190		1.8	T		
20	6		27.5	100	72	4176	720		5.6	U		CH
20	6	a	27.5	100	83		470		3.3	T		CH
20	13		57.5	130	19	4176	2770		11.1	U		
20	13	a	57.5	130	21		2360		5.5	T		
21	7		35.0	90	64	4176	480		8.1	U		OHc
21	7	a	35.0	100	81		530		4.0	T		OHc
21	12		59.5	100	67	4176	670		3.8	U		CH
21	12	a	59.5	100	76		600		4.4	T		CH
21	17		85.0	110	57	4176	860		4.8	U		CH
21	17	a	84.0	100	61		820		6.6	T		CH
22	10		50.0	100	66	4176	530		6.0	U		CH
22	10	a	50.0	100	69		760		3.0	T		CH
22	13		65.0	110	52	4176	1160		3.6	U		CH
22	13	a	65.0	110	47		910		4.4	T		CH
23	4	A	21.4	90	97	1232	1112	0.9	4.4	U	1000 – 1100	OL
23	4	B	21.8	90	108		1276	1.0	4.0	T	1000 - 1100	OL
3	4	B	21.5	90	88	1272	999	0.8	5.1	T	1000 - 1800	CH
23	8	A	40.9	120	27	2664	1200	0.5		U	900 – 2200	ML
23	8	B	41.3	120	21		2135	0.8	9.0	T	2200 - 2600	ML
3	7	A	41.0	130	26	2705	1179	0.4	17.7	T	2200	CL
23	9	A	45.9	130	19	2734	2578	0.9	1.5	T	2300 - 2800	ML
23	9	B	46.5	130	18		2500	0.9		U	2800 - 2200	ML
23	9	C	46.9	130	19		2011	0.7	16.0	T	2800 - 2200	ML
3	8	C	46.6	130	19	2774	2557	0.9	3.6	T	2900 - 3300	CL
24A	4	A	21.8	110	37	1168	642	0.5	13.6	T	1000- 400	OL
24A	4	B	22.4	130	36		454	0.4	19.5	U	1000 - 400	OL
8	4	C	21.6	110	56	1408	453	0.3	3.7	T	300 - 500	OH
24A	6	A	31.3	100	76	1500	807	0.5	4.0	T	900 – 1000	OH
24A	6	B	31.7	100	67		795	0.5	2.8	T	900 - 1000	OH
24A	6	C	32.3	100	55		796	0.5	3.3	U	900 – 1000	OH

Boring UTB-	Samp. Num.	Spec. Num.	Tip Depth (ft)	UW (psf)	WC (%)	σ_3 (psf)	UU c_u (psf)	c/p	Failure Strain (%)	U/T	Pocket Penetr. c_u Top - Bott. (psf)	Lab. USCS
8	6	C	31.6	110	40	1740	566	0.3	15.3	T	1100 - 1000	CL
24A	9	A	45.9	90	78	2076	1107	0.5	4.0	T	1200 – 1100	OH
24A	9	B	46.4	90	58		1028	0.5	3.7	U	1200 - 1100	OH
24A	9	C	46.8	90	81		1214	0.6	3.2	T	1200 - 1100	CH
8	9	B	46.2	100	76	2304	1000	0.4	3.8	T	1000 - 1000	CH
40	9	Head2	38.1	110	17	2357	4379	1.9	17.5	T	3000 - 5400	ML
40	9	A	38.7	120	17		6800	2.9	15.0	U	5400 – 1900	ML
11A	10	A	36.9	120	24	2264	3261	1.4	18.2	T	3600 – 3800	CL
40	13	A	51.0	140	20	3109	3352	1.1	17.2	T	4300 – 5200	ML
41	13	B	51.4	140	19		3966	1.3	15.2	T	4300 – 5200	ML
40	13	C	52.0	120	21		2760	0.9	6.6	U	3700 – 2100	ML
11A	13	B	51.3	130	25		1903	0.6	13.3	T	3000 – 5600	CL
41	5	A	22.9	130	75	1245	356	0.3	10.5	T	600 – 600	OH
41	5	B	23.4	130	79		455	0.4	4.6	U	500 – 600	OH
41	5	C	23.9	120	86		465	0.4	3.2	T	600 – 600	OH
41	5	D	24.4	99	72		467	0.4	4.2	U	500 – 500	CH
12	5	B	23.2	90	75	1294	520	0.4	3.5	T	600 – 500	CH
41	6	A	28.4	100	66	1439	761	0.5	3.2	T	1300 – 600	OH
41	6	C	29.4	100	64		601	0.4	4.6	U	700 – 700	OH
12	7	C	29.1	100	80	1457	639	0.4	3.1	T	500 – 700	OH
41	7	A	33.4	90	92	1541	792	0.5	?	T	90 – 900	OH
41	7	B	33.9	90	66		776	0.5	3.3	U	900 – 1000	OH
41	7	C	34.3	90	82		792	0.5	2.8	T	900 – 900	OH
12	8	A	32.9	90	87	1590	782	0.5	4.4	T	800 – 900	OH
41	12	A	56.2	110	31	2693	2220	0.8	18.2	U	2600 - 2900	CL
41	12	B	56.6	110	38		2613	1.0	1.6	T	3400 - 2100	CL
12	17	C	57.8	110	37	2630	3385	1.3	3.6	T	3500 – 3900	CH
41	18	A	80.6	100	61	4014	2402	0.6	1.6	T	1900 - 1900	CH
41	18	B	81.1	100	53		1969	0.5	1.7	U	1900 - 1700	CH
41	18	C	81.6	100	64		1308	0.3	0.9	T	1900 - 1900	CH
41	18	D	82.1	100	44		1552	0.4	3.3	U	1800 - 1800	CH
12	23	B	81.2	100	69	4045	1453	0.4	1.1	T	2700 - 1700	CH

UW: unit weight; WC: water content; U: untrimmed sample, T: trimmed sample.
c/p: c_u/σ_v', where σ_v' is the effective stress.

2.5 SUMMARY

In this chapter, an overview of the Caltrans project, upon which this dissertation was based, is provided. A database established within this project (FinalCT) is introduced and evaluated in terms of its limitations and strengths. Various aspects of the site investigation efforts are presented which were conducted to enhance/supplement the information included in the database. Laboratory testing equipment and its calibration is explained. Laboratory tests conducted within the project are tabulated. Special emphasis is given to unconsolidated-undrained (UU) triaxial tests because they were used in estimating pile capacities. Differences between the UU strength between trimmed and untrimmed samples are shown.

Chapter 3: Elastic Method – Concept and Measurement of Parameters

3.1 INTRODUCTION

The "Elastic Method" is a frequently used approach, based on the theory of elasticity for predicting the load-displacement behavior of a single pile. Mindlin's closed-form solution (1936) is used to calculate elastic displacements due to a vertical load within a semi-infinite soil mass. The method is generally applied with the help of a computer program.

In the elastic method, the utilized soil properties are Young's modulus, E_s, and Poisson's ratio, ν_s. It is usually acceptable to assume any value within the range of possible Poisson's ratios found in the literature (Poulos, 1989; Tatsuoka et al., 1994). However, the effect and variability of Young's modulus on the displacement of piles is much more pronounced than Poisson's ratio. Therefore, research efforts have primarily focused on obtaining Young's modulus through laboratory and/or in-situ measurements, which can also be utilized to correlate with simple or commonly encountered parameters, such as undrained shear strength, c_u, and standard penetration test blow count, N. for cohesive and cohesionless soils, respectively.

In the following sections, multiple aspects of applying the elastic method to estimations of pile displacements will be presented and discussed.

3.2 FORMULATION OF ELASTIC METHOD

Conceptually, pile head displacement, s, can be divided into three components, each calculated separately (Vesic, 1977):

a) Displacement of soil due to the load transmitted along the side of the pile, ρ_s,

b) Displacement due to axial deformation of the pile shaft, ρ_p, and

c) Displacement at the pile tip caused by the load transmitted at the tip, ρ_{tip} (Figure 3.1a), which is typically ignored for piles in tension.

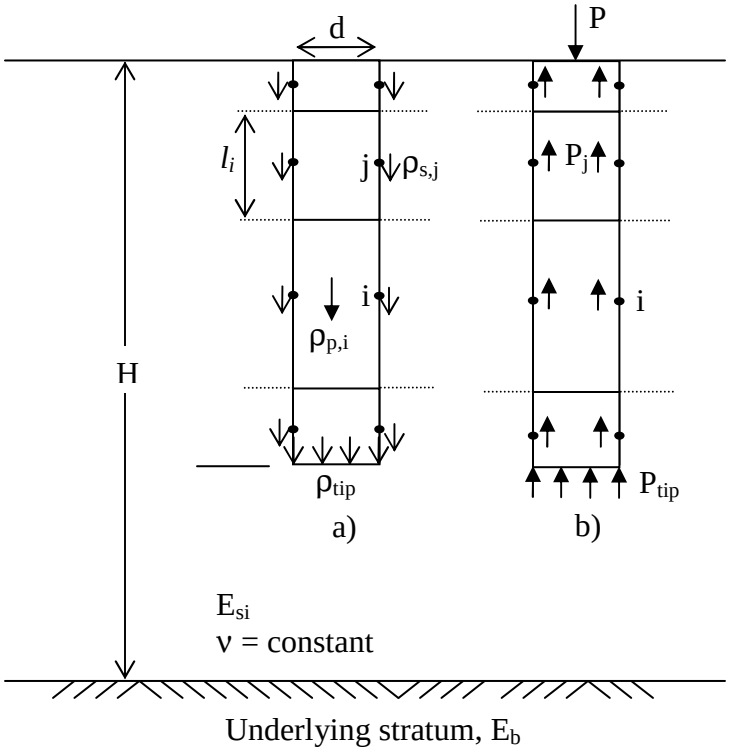

Figure 3.1 a) Displacements and b) loads for a pile in compression (*i* and *j* refer to soil elements).

The theory behind the elastic method and differing approaches for the distribution of load along the pile, pile tip condition, soil/pile properties, and pile-soil interaction are explained in many publications, e.g., Basile (1999), Butterfield and Banerjee (1971), D'Appolonia and Romualdi (1963), Mattes (1968), Mandolini (1999), Nair (1967), Poulos and Davis (1968, 1974, 1980), Poulos (1972, 1979, 1987, 1994, 2001), Randolph and Wroth (1978), Salas and Belzunce (1965), Thurman and D'Appolonia (1965), Vesic (1977), and Yamashita et al. (1987).

3.2.2 Mindlin's Solution for Concentrated Loading

Mindlin (1936) provided a solution for the stresses and displacements beneath the surface of a semi-infinite, isotropic, weightless, linearly elastic (Hookean) mass resulting from a single vertical point load of a given magnitude, *P*, located at a depth *c* below the ground surface. The vertical movement, ρ_z, at a radial distance, *r*, (Figure 3.2) can be calculated as:

$$\rho_z = \frac{P(1+\upsilon)}{8\pi E(1-\upsilon)}\left[\frac{3-4\upsilon}{R_1} + \frac{8(1-\upsilon)^2-(3-4\upsilon)}{R_2} + \ldots \right.$$
$$\left. \ldots + \frac{(z-c)^2}{R_1^3} + \frac{(3-4\upsilon)(z+c)^2-2cz}{R_2^3} + \frac{6cz(z+c)^2}{R_2^5}\right] \quad \ldots\ldots(3.1),$$

where,

$$r = \sqrt{x^2+y^2} \quad \ldots\ldots(3.2),$$

$$R_1 = \sqrt{r^2+(z-c)^2} \quad \ldots\ldots(3.3),$$

$$R_2 = \sqrt{r^2+(z+c)^2} \quad \ldots\ldots(3.4),$$

E: Young's modulus from slope of stress-strain curve $= \left[\frac{\sigma_{xx}}{\varepsilon_{xx}}\right]$ .....(3.5),

ν: Poisson's ratio, ratio of lateral to axial strains $= -\left[\frac{\varepsilon_{yy}}{\varepsilon_{xx}}\right]$ .....(3.6).

The solution, thus, requires only two elastic soil properties besides geometrical information: Young's modulus, *E*, and Poisson's ratio, ν (Section 3.4 for detailed discussion). Both Young's modulus and the modulus of elasticity are used interchangeably to refer to the same elastic constant.

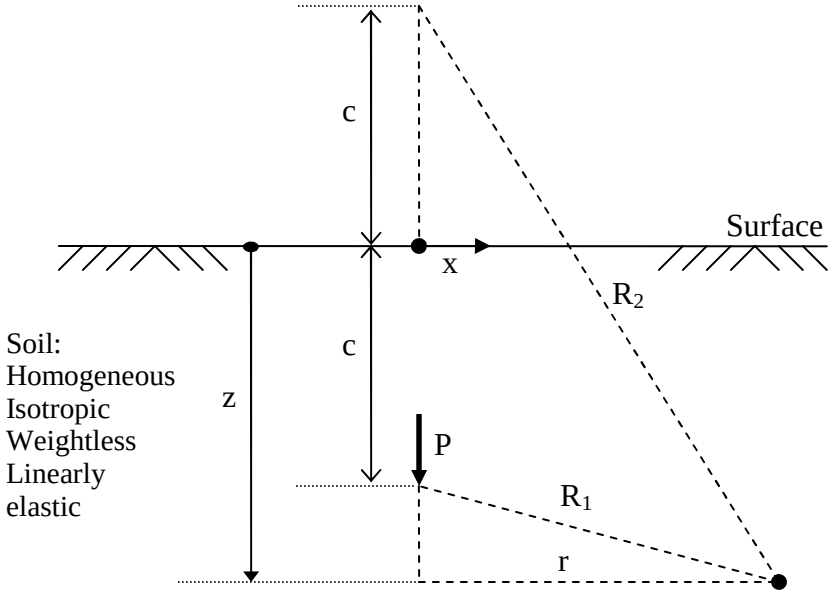

Figure 3.2 Geometry and assumptions for Mindlin's equations (Mindlin, 1936; Poulos and Davis, 1974).

The stresses and displacements acting on the pile-soil interfaces in response to a surface load applied to the pile are shown schematically in Figure 3.1. In reality such a separation is an over-simplification of the pile-soil interaction problem; however, it is helpful in establishing a framework for analysis and better understanding the factors involved in the load-displacement behavior of piles.

Constant values can be utilized for the Young's modulus and Poisson's ratio of an isotropic and homogeneous soil. Then a "displacement influence factor, I_z" (Poulos and Davis, 1980) may be introduced for conveniently simplifying Equation (3.1) to:

$$\rho_z = PI_z \quad \text{.....(3.7).}$$

The equations for the elements that combine the pile head displacement, displacement due to the load transmitted along the side of the pile, ρ_s, axial deformation of the pile shaft, ρ_p, and pile tip displacement, ρ_{tip}, are given below using Eq. (3.7).

3.2.3 Displacements along Pile Shaft, ρ_s

The elastic method takes into account the effect of a soil layer on the other layers that the pile is in contact with (Figure 3.1b). Thus, the displacement $\rho_{s,ij}$ at an arbitrary soil element *i* due to loads acting on the side of pile, P_j and the pile tip, P_{tip} can be calculated as:

$$\rho_{s,i} = \sum_{j=1}^{n} \left[P_j I_{ij} + P_{tip} I_{it} \right] \quad \text{.....(3.8).}$$

3.2.4 Displacement of Pile Shaft, ρ_p

In order to calculate the displacement of the pile shaft at each pile segment, two assumptions are made: 1) a pile segment can be considered as a free-standing elastic column compressed under applied vertical loads, and 2) there is displacement compatibility between the pile and the adjacent soil, which means that the pile and the adjacent soil displace by an equal amount when loaded. The displacement caused by the deformation of the pile shaft due to the load that is being transferred from the pile head (Figure 3.1b) can be calculated as:

$$\rho_{p,i} = \frac{P_j \; l_i}{A_p E_p} = \rho_{s,i} \quad \text{.....(3.9),}$$

where,

l_i: length of pile element i,

A_p: pile cross-sectional area,

E_p: pile modulus of elasticity.

3.2.5 Pile Tip Displacement, ρ_{tip}

Multiple recommendations have been made to incorporate the pile tip load and displacement in the analyses of the total pile head load-displacement. D'Appolonia and

Romualdi (1963) and Poulos and Mattes (1969) analyzed piles allowing for no tip displacement or load, i.e., the pile resting on a rigid base.

Poulos and Davis (1968), as well as Poulos and Mattes (1969), assumed pile tips to be in elastic soils. The displacement at the pile tip is due to the cumulative effects of the entire load transferred from other pile shaft elements, P_j and the load distributed along the cross-sectional area at the pile tip, P_{tip}:

$$\rho_{tip} = \sum_{j=1}^{n} P_j I_{tj} + P_{tip} I_{tt} \quad \text{.....(3.10).}$$

3.2.6 Pile Head Displacement

There are ($2n+2$) unknowns for calculating the pile head displacement based on the elasticity:

- (n) values of pile shaft displacements, $\sum_{i=1}^{n} \rho_{s,i}$
- (n) values of loads displacing the pile shaft, $\sum_{i=1}^{n} P_i$
- pile tip load, P_{tip} and pile tip displacement, ρ_{tip}.

Equations (3.8) through (3.10) provide ($2n+1$) equations. The additional equation is for the total load within the pile:

$$P = \sum_{i=1}^{n} P_i + P_{tip} \quad \text{.....(3.11).}$$

With the equations above, displacement can be calculated for a given load applied to the top of the pile. Moreover, a theoretical distribution of loads along the pile length and tip, and displacement occurring at each pile element can be investigated.

3.3 MODIFICATIONS TO ELASTIC METHOD

There are many simplifying aspects and assumptions in Mindlin's original solution: the vertically applied pile loads are assumed to be acting as point loads (1)

within a soil that is homogeneous (2), isotropic (3), initially stress-free (4), linearly elastic (5) and a infinite half-space (6). Additionally, no slip between the pile and adjacent soil is allowed when the solution is applied to piles (7).

Methods and recommendations to modify the elastic method for distribution of stresses on the sides of the pile, variations in soil properties (heterogeneity), finite-depth of soil layers, pile-soil relative displacement, rigid base for "end-bearing" piles, and residual stresses are considered below.

3.3.1 Shear Stresses on Pile

Although all suggestions for the elastic method are based on the same principles, there are variations proposed for handling loads transmitted to pile segments (Figure 3.3):

a) A single point load acting on the axis at the center of each pile element affects other points along the pile (D'Appolonia and Romualdi, 1963; Salace and Belzunce, 1965; Thurman and D'Appolonia, 1965; Basile, 1999),

b) In the disk approximation, point loads are distributed along the periphery at the middle of the pile element (Nair, 1967), and

c) Uniform stresses are distributed along the surface of the pile element (Poulos and Davis, 1968; Mattes and Poulos, 1969; Poulos and Mattes, 1969).

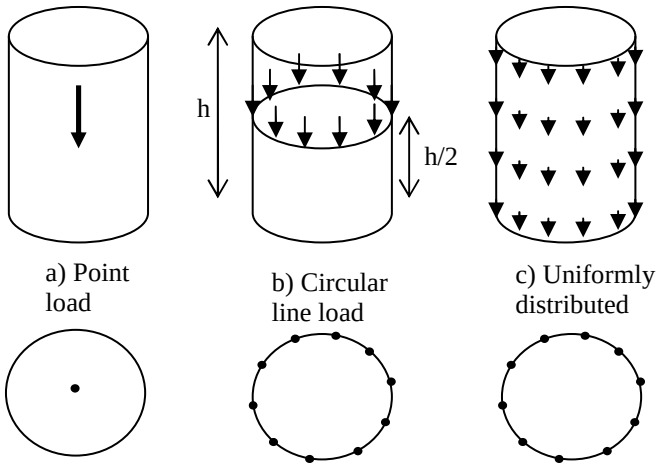

Figure 3.3 Shear stress distribution along the side of pile segments.

Aschenbrener and Olson (1984) have investigated the first two distributions of shear stresses along the pile and found them to be too crude to be useful, a finding also supported by Poulos and Davis (1980). In this dissertation, stresses are, therefore, assumed to be uniformly distributed along the pile shaft (Figure 3.3c).

3.3.2 Non-Homogeneous Soil

Soils in nature are rarely, if ever, homogeneous. Approximations are suggested by Poulos (1979), Lee et al. (1986), Yamashita et al. (1987), Lee and Small (1991), Vallabhan and Mustafa (1996), and Lee and Xiao (1999) to improve the solutions obtained through the elastic method and bring the theoretical approach closer to cases encountered in practice. Overall, they all involve some form of a modification to Young's modulus incorporated into Eq. (3.1).

The effects of a pile element on other pile elements are taken into consideration in the elastic method. When a pile element is deforming, other pile elements are also affected to some degree by the same loading. This interaction can be represented in the

form of a modified Young's modulus which incorporates the varying soil properties and layering.

Poulos (1979) compared three such options with results from more rigorous finite elements and boundary elements approaches. He recommended an average of the soil modulus next to the loaded element and the element for which displacement is being calculated. Poulos identified analyses of piles founded on a layer softer than the overlying layers as potentially erroneous when using his approach.

Lee et al. (1986) separated the system of a pile in a non-homogeneous soil into two sections (Figure 3.4): 1) "extended" soil layers which are treated as a three-dimensional elastic continuum with elastic properties of the layered soil, 2) a fictitious pile with Young's modulus equal to the difference between Young's modulus of the actual pile and the respective Young's modulus of the surrounding soil layers ($E'=E_p-E_{s,i}$). The forces interacting from the fictitious pile to the extended soil layers are considered to be uniformly distributed over the top of each "extended" soil layer. The forces and displacements on the fictitious pile are then calculated by imposing compatibility between the vertical displacement of the fictitious pile and the displacements calculated along the center axis of the real pile within the soil layers. This condition leads to the following equation for the load on top of the fictitious pile (Figure 3.4):

$$N_*(0)=\frac{E_{*1}}{E_p}P \quad \text{.....(3.12),}$$

where,

E_{*1}: Young's modulus of the soil layer directly beneath the pile head,

E_p: Young's modulus of the actual pile, and

P: Applied load on the fictitious pile.

Lee et al. (1986) provided a solution with design charts for a system which requires transforming a multilayered soil into a two-layer system depending on the contribution from each layer based on its thickness. This approach appears rather cumbersome and impractical since most piles are driven in soil layers with multiple thicknesses and properties.

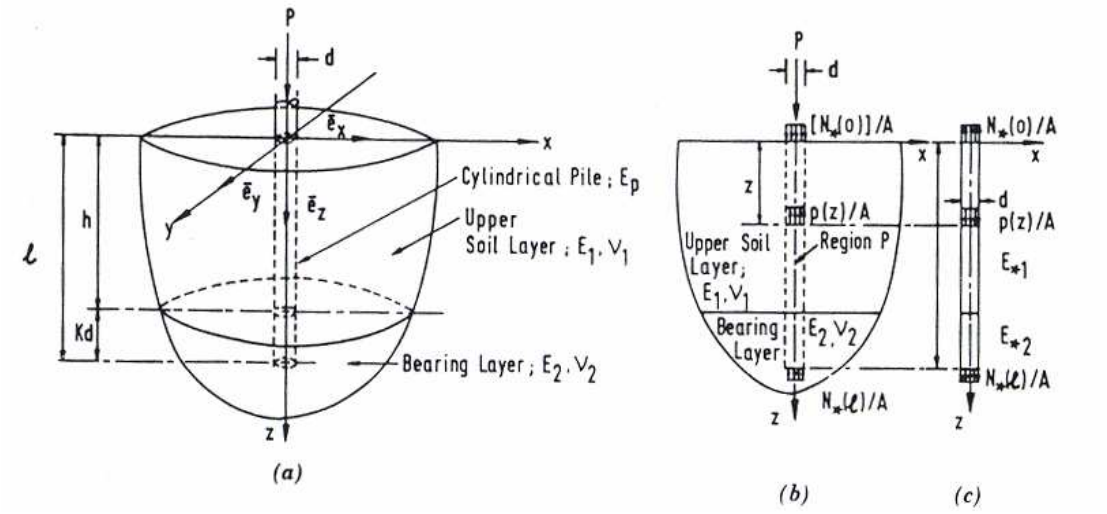

Figure 3.4 Problem definition by Lee et al. (1987) a) Axially loaded pile in a layered soil, b) Extended soil layers, c) fictitious pile.

Yamashita et al. (1987) argued that ignoring the soil elastic modulus of strata other than those two interacting, as Poulos (1979) had suggested, gives results that are in error when the soil modulus of layers differ significantly from each other. Therefore, they proposed including weighted averages of Young's modulus for other layers based on layer thickness, when calculating the equivalent Young's modulus. Their analyses result in displacement estimations about 10% closer to those obtained from finite element analyses than what would be found by using Poulos' recommendation.

A method based on finite-layer analysis was proposed by Lee and Small (1991) as a simplified alternative to other more elaborate elastic continuum methods. They considered the soil as a series of horizontal, isotropic or cross-anisotropic elastic layers of infinite lateral extent, imposing compatibility between the displacement of the pile and soil. They assumed circular concentrated circumferential stresses acting at the middle of each pile element similar to Nair (1967). The suggested method, compared to other elastic continuum methods, provides similar results with less computing time.

Vallabhan and Mustafa (1996) developed a closed-form solution based on minimizing a potential energy function using a variational approach. In this model both soil and pile are assumed to be linearly displaced by an equal amount (compatibility). The model distributes the work done by the applied load as compressive strain energy in the pile and as shear energy in the soil, as well as compressive strain energy in the soil surrounding the pile and at the bottom of the pile. The pile is assumed to be compressible and the magnitude of the load transferred to the soil on the pile interface is calculated based on the movement of the pile relative to the surrounding soil. Closed-form solutions are provided by Vallabhan and Mustafa for a two-layer soil, which consists of a uniform soil with a hard bearing stratum, a method which ignores radial displacement.

Lee and Xiao (1999) extended the method of Vallabhan and Mustafa to include multiple sub-layers along the pile based on the actual soil profile and to incorporate the displacement of soil mass horizontally, which can be important for designing pile groups.

3.3.3 Finite Depth of Soil Layers

Mindlin's solution requires the soil to extend to a semi-infinite depth. In contrast, piles sometimes have a tip on a stiff or "rigid" bearing strata. An estimate of the effects of a finite layer on the shear and displacement of a pile is obtained by using Steinbrenner's

(1934) approximation. In this approach, the displacement of a pile in a soil with a given depth *H* is calculated by subtracting the pile displacement below this height from the displacement of the same pile in a semi-infinite layer.

Poulos and Davis (1968) suggested a modification to account for stiff, but not rigid, soil layers. In general, the displacement influence factor $I_{ij(H)}$ for a point within a finite layer of depth, *H* can be approximated as:

$$I_{ij(H)} \cong I_{ij(\infty)} - I_{Hj(\infty)} \quad \text{.....(3.13),}$$

where,

$I_{ij(\infty)}$: displacement influence factor for a pile element, *i* in a semi-infinite soil mass,

$I_{Hj(\infty)}$: displacement influence factor for a point within the semi-infinite soil mass directly beneath *i*, at a depth *H* below the surface.

The above approach can also be used to calculate displacement for a pile on a stiff base. However, it is still an approximation. A more reliable approach for piles resting on rigid bases is to use a "mirror-image" pile, as discussed below.

3.3.4 Piles Founded on a Rigid Base

The displacement of a pile founded on a rigid base is less than that on an elastic base. D'Appolonia and Romualdi (1963) suggested using a "mirror-image" approximation for piles founded on rock. The same method can be applied to other stiff or rigid soils beneath a pile. A mirror-image pile is assumed below the actual pile at the soil-end bearing stratum interface in which the forces equal those in the real pile but in the opposite direction (Figure 3.5). Mindlin's formulation is then used with additional, opposite mirror-image forces; thus, the displacement of the actual pile is effectively reduced to reflect the rigid base.

This approach produces the erroneous result that the horizontal (mirror) plane is smooth because vertical radial displacements are the same whether arriving at the plane from above or below, and thus there are no shearing stresses in the plane. However, frictional forces would actually be causing shear stresses to develop in the rigid layer. Mattes (1972) investigated radial displacement compatibility and found its effects to be minor.

It can be argued that a very high value of Young's modulus for the rigid layer at the tip should be used. However, errors are likely to occur in the estimation of displacements when there is a large variation in Young's modulus. An averaging similar to that recommended by Yamashita (1987) may be utilized to overcome this problem.

3.3.5 Pile-Soil Relative Displacement

The no-slip condition (displacement compatibility) at the soil-pile interface is an essential part of calculating pile displacements using Mindlin's solution. The pile side capacity is limited by the soil-to-pile adhesion. It is, therefore, reasonable to allow for a relative displacement (slip or local yielding) between the pile and soil. D'Appolonia and Romualdi (1963), Salas (1965) and Poulos and Davis (1968) proposed a method to incorporate a limiting stress, which can develop in the pile-soil interface. If the average calculated shear stress on any pile element exceeds the adhesion, then local slip occurs and the calculated shear stress is equal to the adhesion. The excess stress will be transferred to other elements whose side shears are still less than the adhesion. The capacity of the pile tip depends on the bearing capacity of the soil beneath the pile tip. When all of the soil elements reach their limits, plunging will occur; i.e., pile capacity is reached.

The effect of soil softening, i.e., the reduction of soil shear strength to lower residual values following the peak value, which may lead to load shedding within pile elements, is not taken into account using the elastic analyses discussed here. Methods have been proposed which incorporate a reduction factor to the pile side capacity (Murff, 1980; Randolph, 1983, and Guo, 2001).

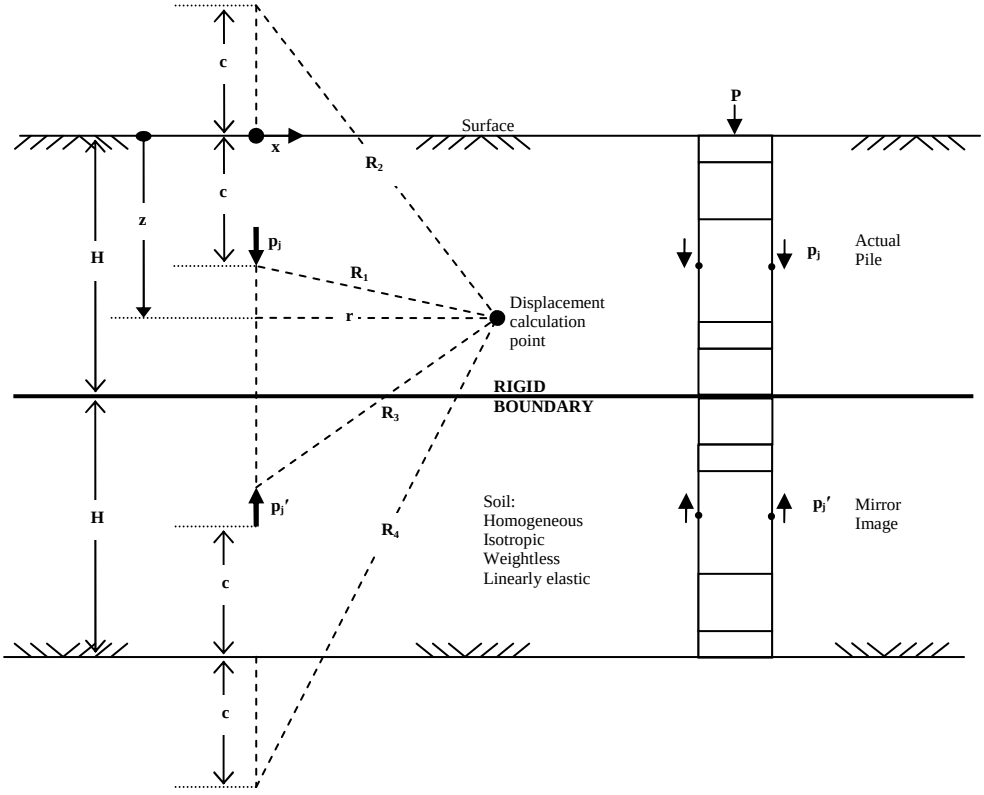

Figure 3.5 Mirror-image approach for a pile on a rigid base.

3.3.6 Residual Stresses

Load-displacement analyses are usually done assuming that no stresses due to installation effects develop either in the pile or in the surrounding soil. However, the

function of pile driving is, in fact, to continually cause the soil surrounding the pile to fail, so the pile can advance into the ground to the desired depth. Thus, in actual field conditions, the soil against the pile, as well as a certain horizontal distance away from the pile, is sheared to large displacements and may conveniently be considered as remolded. Some of the final driving energy (residual stresses) is locked up in the shaft as well as at the tip of the pile. The effect of this energy for pile capacity is mainly on the distribution of loads along the pile once loading is resumed. However, residual stresses influence the observed displacements during a pile load test. For a pile in tension, the recorded displacements will be smaller than the "actual, correct" values if residual stresses are not considered. In turn, the observed displacements for a pile in compression will be in excess of the "true" values. The residual stresses can be important mainly when displacements are predicted for compressible piles, piles driven in sands, or piles that derive a significant portion of their capacity from the tip (Fellenius, 2006; Maiorano et al., 1996; Poulos, 1987; Vesic, 1977).

Methods have been proposed to estimate the residual loads and their effects on the measured displacements (Alawneh and Husein Malkawi, 2000; Briaud and Tucker, 1984; da Costa et al, 2001; Goble and Hery, 1984; Holloway et al., 1978; Hunter and Davisson, 1969). Another procedure to consider residual stresses due to installation effects with the elastic method was discussed by Poulos (1987). He suggested estimating stresses by loading the simulated pile to failure in compression and then unloading it. This cyclic loading pattern mimics the advancement and installation of a pile. The stresses computed in the simulated pile at the end of this cycle are then taken as the residual stresses and represent the starting point for the subsequent analysis.

3.4 PARAMETERS OF ELASTIC METHOD

3.4.1 Drained versus Undrained Parameters

It may be important to distinguish between undrained and drained soil parameters utilized for elastic method: E_u, ν_u or E_d, ν_d for undrained and drained conditions, respectively.

For an elastic soil, the value of shear modulus is unaffected by the drainage condition, because the water within the soil skeleton can not bear any shear stresses. Therefore, the following can be written for the shear modulus:

$$\frac{E_u}{2(1+\nu_u)} = G_u = G = \frac{E}{2(1+\nu)} \quad \text{.....(3.14).}$$

Poisson's ratio, ν_u, for the undrained condition is equal to 0.5. Thus,

$$\frac{E_u}{E} = \frac{3}{2(1+\nu)} \quad \text{.....(3.15).}$$

A constant Poisson's ratio of 0.4 is used throughout this study. Then E_u/E is $3/2.8 = 1.07$, which is not very significant given the uncertainty of other factors involved in elastic method.

Most of the pile load tests conducted by Caltrans follow the ASTM "quick load method" (ASTM D-1143 1994 for compression and ASTM D-3689 1995 for tension) using reaction piles to apply the load (California Foundation Manual, 1997). In this method each loading increment is held for five minutes during loading and one minute during unloading without any measurements or consideration of generated or dissipated pore pressures. The soil is likely partially drained during pile load tests, although the percentage of drainage is not known. Therefore in this dissertation, the Young's modulus

and Poisson's ratio adopted for all load tests correspond to soils that are partially drained although the amount is unknown.

3.4.2 Poisson's Ratio, ν_s

Poisson's ratio is defined as the ratio of lateral strain to axial strain, i.e. $\nu = -\frac{\varepsilon_r}{\varepsilon_a}$. Under fully drained conditions, the value selected for Poisson's ratio will depend on the overconsolidation ratio (OCR) of clays or the relative density of sands. Poisson's ratio varies from nearly zero for collapsing clays and silts and for very loose sands, to more than 0.5 for dilative soils like highly overconsolidated clays and silts and very dense sands. Typical values of Poisson's ratio are presented in Table 3.2. It can be selected as (0.35±0.05) for clays under drained conditions, (0.30±0.10) for silica sands and 0.5 for saturated clays under undrained conditions (Poulos, 1989).

Within the expected strain ranges for a pile that constitute the "working range", i.e. less than 0.5 % strain, the recommended drained value of Poisson's ratio for all types of soil is between 0.1 and 0.2 (Tatsuoka et al., 1994; Jamiolkowski et al., 1995; LoPresti et al., 1995).

In this study, however, a constant Poisson's ratio of 0.4 is used for all soil layers regardless of the soil type. This approach does not conform to the recommendations of other researchers, but the induced error is deemed to be minor.

3.4.3 Young's Modulus of Pile, E_p

The elastic method requires only a single input for the Young's modulus of the pile (steel or concrete). Piles, as manufactured components, have less variability and uncertainty in their properties than soils, for which there is usually no control over the composition, deposition, and layering. Therefore, for elastic analyses, it seems reasonable

to assign a constant Young's modulus for each type of pile. Constant Young's modulus values used for each pile type are given in Table 3.1.

There are several concrete-filled pipe piles within the Caltrans database. Regardless of the loading direction, the equivalent Young's modulus for a concrete-filled composite steel pipe pile is calculated using the following equation, which assumes no effect of confinement on $E_{concrete}$:

$$E_{eq} = \frac{E_{steel} \times A_{steel} + E_{conctrete} \times A_{concrete}}{A_{steel} + A_{concrete}} \quad \text{.....(3.16),}$$

where,

E_{steel} and $E_{concrete}$: Young's modulus of steel and concrete,

A_{steel} and $A_{concrete}$: cross-sectional area.

Table 3.1 Pile Young's modulus values applied for analyses.

Pile material	Steel	Reinforced concrete	Unreinforced concrete	Cast-in-place concrete
E_p (kips/sq.inch)	29,000	4,500	3,000	3,000

3.4.4 Young's (Elastic) Modulus, E_s

Young's modulus, *E* is defined as the slope of the stress-strain curve for a one-dimensional, unconstrained loading:

$$E = \frac{\Delta\sigma}{\Delta\varepsilon} \quad \text{.....(3.17),}$$

where, $\Delta\sigma$: stress change in soil layer, and $\Delta\varepsilon$: strains within a soil.

Young's modulus is typically taken as the value appropriate to the strain conditions that will occur; i.e., a value of *E* from seismic tests might be appropriate for very small strains whereas values from plate bearing tests or laboratory tests could be

conducted on "undisturbed" samples for larger strains. Typical values of E and ν are given in Table 3.2.

Table 3.2 Typical elastic constants of various soils (HB-17: AASHTO Standard Specifications for Highway Bridges, 17th ed., 2002).

		Typical Range of Values	
Soil Type/Condition		**Young's Modulus, E_s (kips/sq.inch)**	**Poisson's Ratio, ν_s**
Clay	Soft sensitive	0.4-2.1	0.4-0.5(undrained)
	Medium stiff to stiff	2.1-6.9	
	Very stiff	6.9-13.9	
Loess	All	2.1-8.3	0.1-0.3
Silt	All	0.3-2.8	0.3-0.35
Fine Sand	Loose	1.1-1.7	0.25
	Medium dense	1.7-2.8	
	Dense	2.8-4.2	
Sand	Loose	1.4-4.2	0.2-0.35
	Medium dense	4.2-6.9	
	Dense	6.9-11.1	0.3-0.4
Gravel	Loose	4.2-1600	0.2-0.35
	Medium dense	11.1-13.9	
	Dense	13.9-27.8	0.3-0.4

Young's modulus can be found in three different ways, as shown schematically in Figure 3.6 by a non-linear stress-strain curve typical for a soil. The laboratory and/or in-situ methods to determine Young's modulus also vary. The initial tangent modulus, in particular, requires the ability to measure stresses accurately at very small strains. The equation for each type of modulus is given below:

$$E_{secant} = \frac{(\sigma_i - \sigma_0)}{\varepsilon_i} \quad \text{.....(3.18),}$$

$$E_{tangent} = \frac{d(\sigma)}{d(\varepsilon_i)} \quad \text{.....(3.19),}$$

$$E_{initial} = \lim_{\sigma,\varepsilon_i \to 0} \frac{d(\sigma)}{d(\varepsilon_i)} \quad \text{.....(3.20).}$$

Tangent, secant and initial moduli are the same at very small strains, where the stress-strain curve can be considered linear.

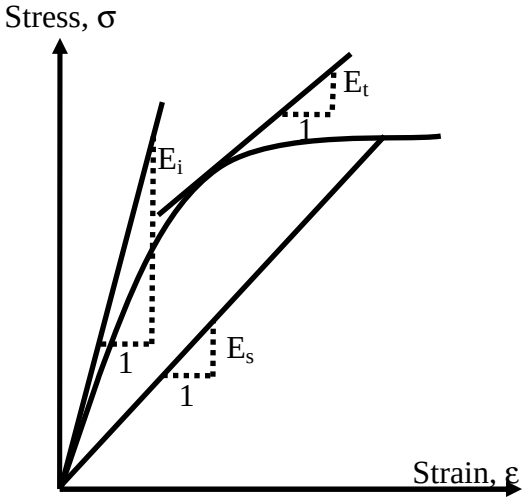

Figure 3.6 Various definitions of elastic of elastic modulus: E_i: Initial tangent modulus; E_s: Secant modulus; E_t: Tangent modulus (defined at a given stress level).

It is, however, usually preferred in practice to use empirical correlations from simple and/or easily obtained parameters to estimate Young's modulus. In the case of displacements of pile foundations, these correlations for simplicity are obtained through back-calculations from pile load tests, relating their results to soil parameters such as SPT blow count, cone penetration resistance, plasticity index, grain size, density, undrained shear strength, etc.

If one can assume elasticity, then Young's modulus, *E*, and axial strain, ε, can directly be calculated from shear modulus, *G*, and shear strain, γ, with the following equations:

$$G=\frac{E}{2(1+\nu)} \quad \text{.....(3.21),}$$

$$\gamma=(1+\nu)\varepsilon \quad \text{.....(3.22),}$$

where, ν, is Poisson's ratio. Thus, according to the theory of elasticity, any variation of shear modulus with shear strain also corresponds to changes in Young's modulus and axial strain. If the shear modulus is known, then Young's modulus can also be calculated by assuming a Poisson's ratio.

Shear modulus can also be calculated as the initial small strain shear modulus using shear wave velocity, v_s, and soil density, ρ (or unit weight, γ and gravitational acceleration, g), as:

$$G=\rho v_s^2 = \frac{\gamma}{g} v_s^2 \quad \text{.....(3.23).}$$

Shear modulus has traditionally been used for analyzing the dynamic behavior of soils at small strains, such as investigating foundation vibrations or seismic conditions. However, estimating pile displacements usually involves larger strains at the affected zones. The tangent shear modulus at small shear strains (up to about 10^{-3} %) is referred to as the maximum shear modulus or small-strain modulus G_{max} (or G_o). Soils behave in a linearly elastic manner within these strains. Maximum shear modulus is a unique property of a soil regardless of drainage (drained or undrained), loading direction, saturation, and static or dynamic conditions.

Similar to Young's modulus, secant shear modulus decreases with increasing shear strain. The relationship between shear modulus and strain is generally normalized by the ratio of shear modulus to G_{max} (Figure 3.7).

Geophysical methods are used to predict small-strain shear modulus of soils. Their limitations are discussed further in Section 3.6.3.6. The most important aspect of the conversion from shear modulus to Young's modulus for displacement calculations of pile foundations is the difference in the corresponding strains. While the shear modulus reflects the elastic stress-strain behavior at small to very small strains (in the range of 10^{-3}

%), the strain corresponding to pile foundation displacements at working loads is approximately ten to a hundred times larger (about 0.1 %). Therefore, it is crucial that the shear modulus be reduced by utilizing a corresponding modulus reduction curve.

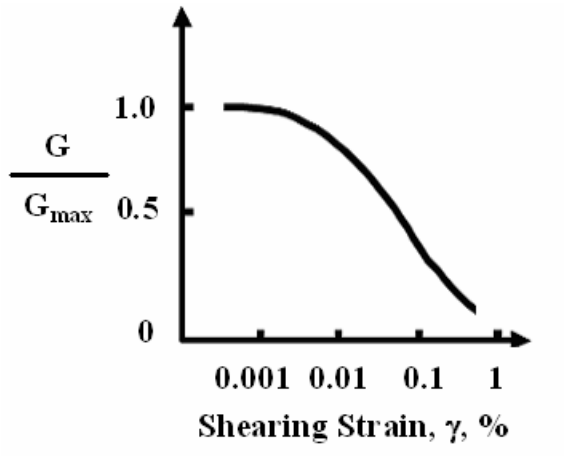

Figure 3.7 A schematic for the normalized shear modulus – shear strain relationship.

3.4.5 Importance of Poisson's Ratio versus Young's Modulus

How varying Poisson's ratio and Young's modulus affects the predicted displacements is presented in Figure 3.8 to depict the relative importance of each parameter. A pile load test driven in soils with soft, clayey layers (0.5 ksf $\leq c_u \leq$ 0.9 ksf) was selected (LTN: 447) to emphasize the changes in displacements. Poisson's ratios were varied from 0.05 to 0.5 while Young's modulus was also changed tenfold for each layer (35 to 626 psf). If the same Young's modulus is used, the difference between the two calculated displacements is not significant, approximately 5-7%. On the other hand, the differences are significantly larger when Young's modulus is varied for a given value of Poisson's ratio. A tenfold increase of Young's modulus reduces the calculated displacements by eighty-seven percent, when a constant Poisson's ratio is utilized.

Therefore, the focus of this dissertation has been on determining the Young's modulus of the soil for displacement predictions of piles.

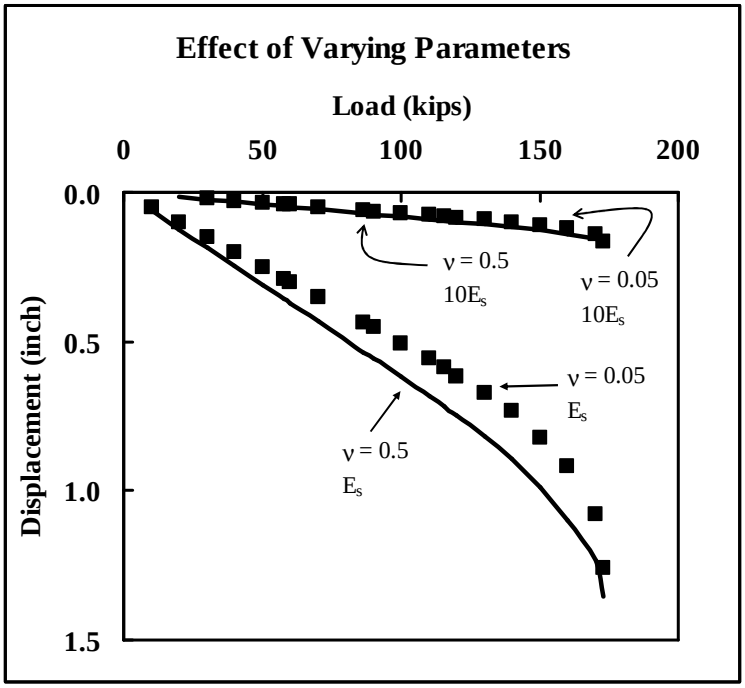

Figure 3.8 Displacements with varying Young's modulus and Poisson's ratio.

3.5 LIMITS AND JUSTIFICATION OF USING THE ELASTIC METHOD

Criticism of the elastic method centers on its assumption that the soil stress-strain relationship is linear. Indeed, soils behave in a highly non-linear manner, especially at strain levels in excess of 0.1%. It is an approximation or an overall averaging approach to model a non-linear behavior using a linear model. Young's modulus obtained from the initial linear part of the stress-strain curve results in a higher value than one from the non-linear section of the curve. Therefore, an accurate estimation of displacements needs to take the correct section of the stress-strain relationship into consideration.

Another criticism is the fact that the effects of pile installation, such as soil disturbance in an unspecified zone around the pile and sustained residual stresses following the completion of pile driving, are not considered. In other words, the pile is "wished-into-place" without any soil disturbance or locked-in residual stresses. Residual stresses, in general, do not have a significant effect on the ultimate capacity. The main concern with ignoring the residual stresses in analyses is due to the distribution of loads along the pile shaft and the errors associated with displacements especially for compressible piles in sand. The residual stresses are ordinarily not measured during a pile load test. Piles are generally instrumented only at the top (head of pile) following the installation of the test pile and data recording is started just before the application of the load although the pile is under the influence of residual stresses.

Strain softening or load shedding is a phenomenon, in which soils exhibit a loss of their overall shear strength towards a residual value with increasing deformation, after a peak strength level has been reached (Murff, 1980; Sterpi, 1999). In elastic analyses, displacements after the peak load may be underestimated, when no provision is made for load-shedding or strain-softening behavior of soils such as overconsolidated clays, dense sands or rocks (Randolph, 1983). The shear strength included in calculating displacements following the peak value will be too high resulting in reduced displacements, and, hence underestimation of actual displacements.

The analytical method involves the assumption of "no slip" between the pile and the soil, up to the shear strength of each soil layer (elastoplastic behavior). Even after a relative movement between pile and surrounding soil ("slippage") occurs, the zone affected by the pile movement can not accurately be estimated using elastic analysis (Johnston, 1983; Poulos, 1989; 1994).

Similarly, Young's modulus and Poisson's ratio back-calculated from pile load tests may not match values from laboratory tests because of factors such as remolding/densification of soil next to the pile during installation, sample disturbances, scaling, differences in the stress-strain condition, etc. (Jardine et al., 1984, 1985; Tatsuoka and Shibuya, 1992).

In spite of all the shortcomings of the elastic method, it is still widely used due to its relative simplicity. Modifications addressing some of the limitations are available. Based on load tests conducted on instrumented piles (model/full-scale) supported by numerical analyses, strains associated with most geotechnical applications and soils within the working range are not very large: conventionally about 0.1% near the top of the pile and less with increasing depth (Butterfield and Abdrabbo, 1983; Poulos, 2001). Linear displacements up to about a third or half of failure load are observed from load-displacement curves of pile load tests conducted to failure. Therefore, an "axial working load" can be identified, under which the displacements of a pile can reasonably be calculated with the assumption of linear elasticity. Elastic methods have been shown to provide displacement predictions that are in satisfactory agreement with more rigorous solutions, such as finite element or finite difference methods and do not require so many parameters to be determined (Burland, 1989; Callanan and Kulhawy, 1985; Cooke et al., 1979; Poulos and Davis, 1980; Poulos, 1989). This simplified approach corresponds to the commonly available amount and sophistication of data available for most geotechnical designs emphasized by Barbour and Krahn (2004).

An example for the linearity of load-displacement estimations within half of the peak applied load, i.e., load ratio of a half, is presented in Figure 3.9 along with the measured displacements. The peak load applied on the pile is varied by ±25% of the

measured peak load. The load-displacement curves are obtained when the load ratio is a half. The curve for all of the utilized loads remains linear for a load up to 100 kips. This value is 77%, 58%, and 46% of the reduced, actual, and increased peak loads, respectively. The fit between estimations and the measured load-displacements curve is considered excellent. Thus, even if the determined peak load is in error of 25%, the estimated displacements are within the linear zone, which can be represented with the elastic method.

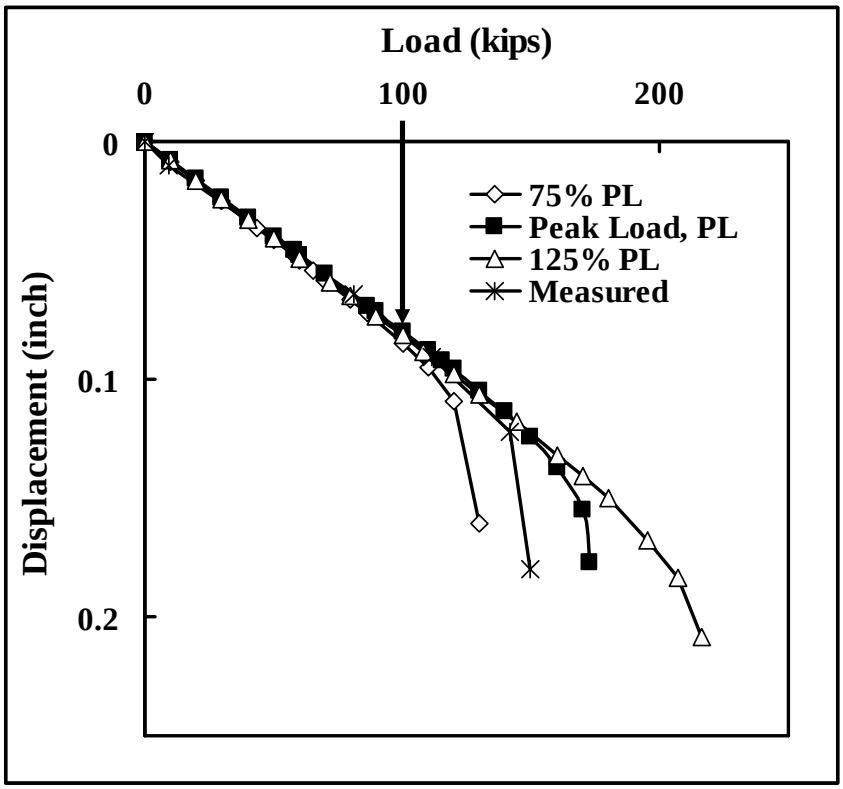

Figure 3.9 An example for the effect of varying ultimate capacity on the load-displacement curve.

In the following section, a general overview of laboratory and in-situ tests to determine Young's modulus, as well as several empirical correlations suggested in the literature, will be presented.

3.6 DETERMINATION OF YOUNG'S MODULUS

Advantages of full-scale pile load tests can be listed as: testing under actual soil conditions at the location of interest, the possibility of controlling and updating design parameters and estimations of capacity and displacements, gaining experience in the area, etc. On the other hand, the boundary conditions in a pile test are ill-defined so that they cannot be controlled efficiently or conveniently. Pile load tests are not conducted as part of the routine design process, especially in the preliminary stages, due to the time and relative expense involved. Even if they are performed, piles are generally not loaded to failure and often little information on soil properties is collected as part of the testing process. Other means of predicting pile displacements, such as empirical correlations to in-situ measurements and/or laboratory testing (Figure 3.10) may be preferred for small projects or preliminary evaluations. The predicted displacements based on various correlations, the range of strains they impose, and the ease with which they are applied varies widely (Figure 3.11).

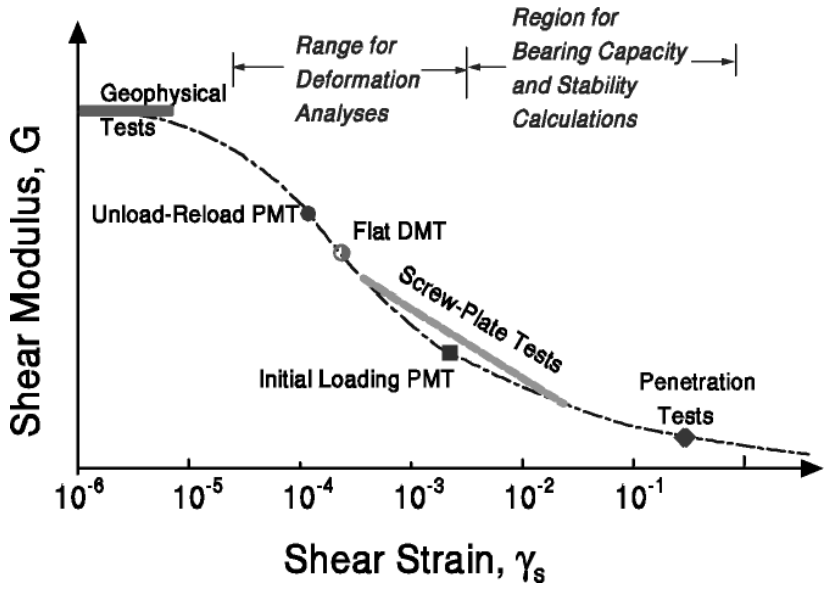

Figure 3.10 Conceptual variation of shear modulus with strain level under static monotonic loading; relevance to in-situ tests (Mayne et al., 2001). (PMT: pressuremeter; DMT: dilatometer).

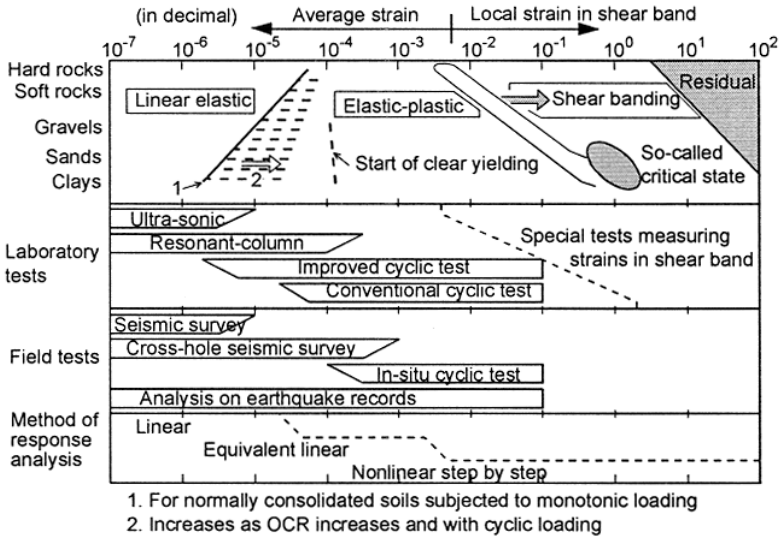

Figure 3.11 Strain dependence of measurement and analysis of soil properties (Yoshida and Iai, 1998).

3.6.2 Young's Modulus Based on Laboratory Testing

Laboratory tests, such as triaxial (ASTM D 3999-03), resonant column (ASTM 4015-00), torsional ring shear (ASTM D 6467-06a), bender elements (Shirley, 1978; Viggiani and Atkinson, 2000; Valle-Molina, 2006) and one-dimensional consolidation tests (ASTM D 2435-04) (Brown and Vinson, 1998; Burland and Burbidge, 1985; Davis and Poulos, 1963 and 1968; Hardin and Richart, 1963; Hicher, 1996; Krizek and Corotis, 1975; Tatsuoka and Shibuya, 1992; Viggiani and Atkinson, 1995) are conducted to measure Young's modulus, E_s or constrained modulus, M_s of soils.

During routine laboratory testing**,** higher average deformations and stresses of the whole specimen are measured through external gages. Young's modulus values are thus underestimated as compared to the small strains (down to about 10^{-3} %) to which the soil are actually subjected in the field. A comparison of strains for various tests and observed in-situ are presented in Figure 3.12.

Advances in technology within the last few decades and the need for improved ways of characterizing the stress-strain relationship of soils have led to changes in laboratory testing. Consequently, the practice of measuring applied loads and displacements of samples internally (either as a whole or locally) has become increasingly popular, especially in Italy, Japan and the United Kingdom (Burland and Symes, 1982; Costa-Filho, 1980; Da Re et al., 2001; Goto et al., 1991; Ibraim and Benedetto, 2005; Jardine et al., 1984, Scholey et al., 1995; Tatsuoka et al., 1997). Such equipment enable accuracy at small strains (less than 10^{-3} %) and elimination of major sources of error, such as signal noise and imprecision. Various devices including electro-level displacement gages, Hall Effect semiconductors, miniature LVDT's, proximity

sensors, and local deformation transducers have been successfully utilized in triaxial testing.

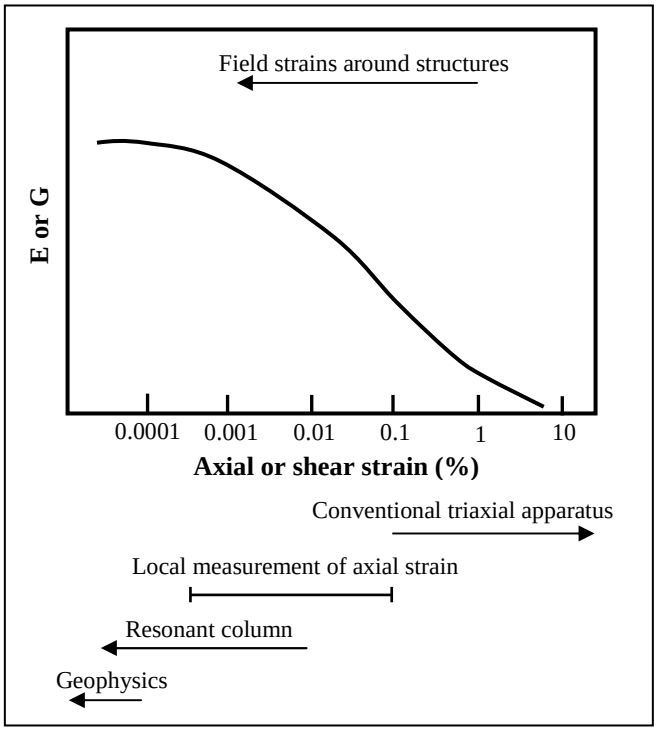

Figure 3.12 A comparison of typical strains applied in laboratory tests versus in-situ strains around structures (Clayton et al., 1995).

3.6.3 Young's Modulus Correlations Based on In-Situ Tests

3.6.3.1 *Standard Penetration Test (SPT)*

The standard penetration test (SPT), which uses a split-barrel sampler, is by far the preferred method for site investigations of cohesionless soils in situ. The test was developed by the Gow Construction Co. in 1902. The split-barrel sampler and procedure for the standard penetration test are described in detail in ISSMFE (1989), BS 1377: 1990, ASTM D1586 (1999) and AASHTO T-206. The test involves advancing a split

spoon sampler into the base of a borehole by blows from a hammer with a standard weight of 140 pounds falling from a height of 30 inches. The number of blows under dynamic penetration for a distance of eighteen inches is recorded; however, only the number of blows for the last twelve inches is included in the blow count number, *N*. The first six inches are regarded as seating for the equipment. Disturbed samples can be taken for observation and basic index testing in the laboratory.

Many factors affect the outcome of standard penetration tests. These can be summarized as:

- differences in the diameter of the borehole and drilling,
- variations in the driving energy due to different equipment and testing procedures and the resistance of the sampler to penetration,
- the in-situ horizontal effective stress with frictional materials, this varying with the overconsolidation ratio (OCR) of the soil,
- the extent of pore pressure generation during penetration,
- the relative proportion of end resistance versus shearing forces along the inner and outer sides of the sampler (Ladd et al., 1977).

Standard penetration testing is a simple and quick method for obtaining an estimate of relative density, strength, and friction of cohesionless soils. It may also be conducted in weathered rocks as a guide to the strength of such materials. However, it is generally not recommended for cohesive soils. A large number of procedural errors affecting SPT's and their consequences are listed in the Canadian Foundation Engineering Manual (1992).

Many correction factors are suggested to take into account the influences of overburden, mineral content, water table location, pore pressure development, grading,

particle size, and horizontal effective stresses. Arguably the most important correction is for the efficiency of the SPT hammer (donut, safety, or automatic), which typically is adjusted to 60% (Skempton, 1986; Clayton, 1990).

A list of correlations relating SPT N to soil Young's modulus is given in Appendix B.

Standard penetration testing in soils coarser than sand poses a problem because the driving shoe can get clogged and cause elevated N values. Therefore, larger driving devices have been suggested to overcome this shortcoming, e.g., the Large Penetration Test (LPT) and Becker Penetration Test (BPT). Correlations of these tests with the SPT have been proposed by Daniel et al. (2003) and Sy (1997). The application of these modified SPT's is not yet widespread, however.

3.6.3.2 *Cone Penetration Test (CPT)*

The basic principle of cone penetration testing (CPT) is to push a cylindrical steel instrumented conical tip and rods into the soil at a constant rate of 0.8 inch/sec (2 cm/sec). The main purpose of cone penetration test measurements is to record the resistance to penetration mobilized in the soil. The method, developed by Collin in France in 1846, has also been known as the static penetration test, quasi-static penetration test, and Dutch sounding test. Current designs were mainly developed in the 1930's. The test is performed in accordance with ASTM D 3441 (2005) for mechanical systems and ASTM D 5778 (2000) for electric and electronic systems. The diameter of the base of the standard cone is 1.4 inches (35.7 mm) with a friction sleeve of 23.3 inch^2 (150 cm^2) and the tip at an apex angle of 60°. The measured tip/point resistance is, q_c, calculated by dividing the total force acting on the cone tip to the area of the cone base. The side/sleeve resistance, f_s, is the total force on the friction sleeve divided by the surface area of the

sleeve. The friction ratio, *FR* (%) is defined as the ratio of f_s to q_c and is a useful indicator of soil type. However, pore water pressures influence the total stresses measured on the shoulder behind the cone and the ends of the friction sleeve. These effects are taken into consideration in the form of a correction factor based on the cross-sectional area of the shaft and the projected area of the tip. The cone penetration test can be conducted in most soils with the exception of very dense sands, gravels, and rocks. The CPT is ideal for fine-grained soils, providing a fast, economic, and continuous profile of soil stratification, although no samples can be obtained for further testing.

Data acquisition systems and sensors have been added to many cone penetrometers currently in use, such as the piezocone, resistivity cone, acoustic cone, seismic cone, vibrocone, cone pressuremeter, and lateral stress cone (Campanella and Robertson, 1988; Lunne et al., 1997; Meigh, 1987). Each penetrometer combines readings of other basic measurements to the features of CPT. For example; piezocone provides pore pressure values in addition to q_c and f_s. It should be noted that piezocone provides reliable pore pressure readings for most soils if the pore pressure sensor is located at the shoulder of the cone as shown with u_2 in Figure 3.13 (Mayne et al., 1995). Fissured, overconsolidated clays and dense, dilatant sands are exceptions, for which the corrected sensor on the mid-face of the cone is preferred (u_1).

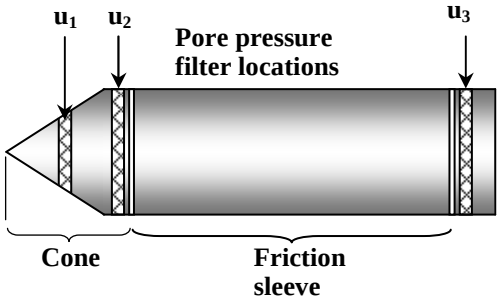

Figure 3.13 Parts and pore pressure sensors of a piezocone penetrometer (CPTU).

Cone penetrometer testing resembles the geometrical and vertical penetration process of the pile; therefore, its results are frequently used to estimate pile capacity. The CPT point resistance, q_c, is usually associated with the pile tip capacity, q_{tip}, and CPT sleeve capacity, f_s, is linked with the pile side capacity, q_{side}. CPT measurements may also be employed in correlating Young's modulus of the soil. Several correlations are listed in Appendix B.

Cone penetration testing, until recently, was not part of the Caltrans "standard" soil investigation practice and is, therefore, not available for most of the sites considered. Some CPT conducted as part of this project could not reach the target depth due to the presence of concrete blocks and other obstructions in shallow fills or strong clays, dense sands, or rock at greater depths. Essentially no CPT could be completed in Southern California where the prevalent soils are sands, gravels, and cobbles. Predrilling, i.e., drilling with an auger to some depth, was also attempted in many cases to pass through the top layers; lower layers still proved too difficult to penetrate in most cases. Therefore, CPT test results were not included in the displacement analyses of this dissertation.

3.6.3.3 *Pressuremeter Test (PMT)*

The pressuremeter (PMT) was first described by Ménard (1957). The PMT device consists of two parts: a read-out unit at the ground surface and a long cylindrical probe combining three independent cells (rubber membranes) that are inflated using a pressurized fluid, such as water, gas or oil, after being lowered into a borehole. The top and bottom cells protect the middle measuring cell applying pressure to the sidewalls of the borehole. The probe can be installed by pre-drilling a hole using a hollow stem auger or a hand auger, or forcing the probe into the ground and displacing the soil by driving, jacking, or vibrating. Self-boring probes, generally used for research, are also available.

Soil disturbance occurs during the insertion of the pressuremeter device. Pressuremeter testing and evaluation of its results are described in ASTM D 4719 (2000) and by Mair and Wood (1987).

Once the probe is at the desired depth for testing, the top and bottom cells are inflated to secure the probe in place. Then the measuring cell is pressurized to inflate its flexible rubber bladder, which in turn transfers the pressure to the borehole walls. As the pressure in the measuring cell increases, the borehole walls deform. The pressure within the measuring cell is held constant for approximately sixty seconds, during which time the increase of volume is recorded.

Due to the dimensions of the measuring cell (diameter between 1.25 and 3 inches, L/D between 3 and 10, typically 6) a large soil mass can be tested vertically with the pressuremeter to obtain parameters, which can also be a disadvantage due to the uncertainties of averaging over a zone of disturbed soil. Entire stress-strain-strength curves can be derived, as well as in-situ total horizontal stress, P_0, shear modulus, G, shear strength, s_u, or Φ, and limit pressure, p_L. Types of pressuremeters include the pre-bored (Ménard), push-in device, self-boring pressuremeter, and full-displacement type (cone pressuremeter or pressiocone).

A pressuremeter deformation modulus, E_{PMT}, can be calculated from the pseudo-elastic or straight-line portion of the load-volume change diagram. The E_{PMT} is a function of Poisson's ratio, the slope of the straight line and the cavity volume in the pseudo-elastic range (part B in Figure 3.14). Martin (1977) and Gambin and Rousseau (1988) concluded that E_{PMT}, and soil Young's modulus, E_s, are approximately equal. Martin (1987) has proposed three similar correlations between E_{PMT} and SPT N.

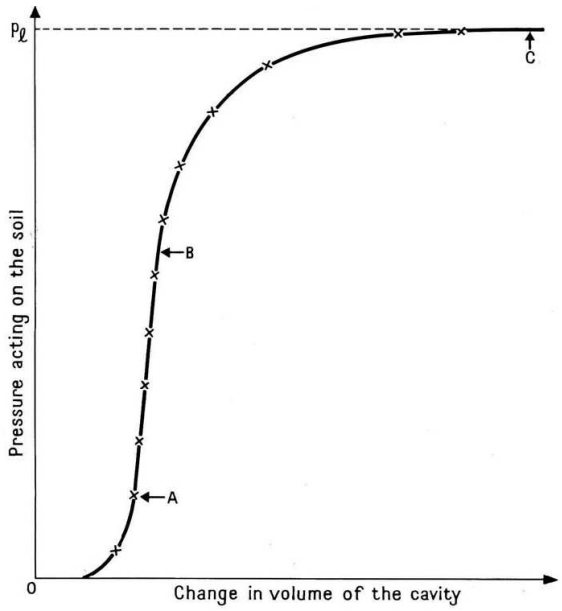

Figure 3.14 Example of a pressuremeter test result (Baguelin et al., 1978).

Based on pressuremeter readings, Frank (1985) and Frank et al. (1991) have suggested an empirical correlation which relates the pile displacements within working loads to the pile diameter (discussed in Chapter 4).

3.6.3.4 ***Plate Loading Tests (PLT)***

The plate loading test can be thought of as a scaled-down model of a shallow foundation. The PLT is commonly used for cohesionless soils although it can also be applied to cohesive soils. Furthermore, it can prove useful in assessing the properties of weak rocks. A single or a series of steel bearing plates (to increase rigidity when large bases are loaded) are used with a hydraulic loading jack against a truck or trailer or a combination of both, an anchored frame, or any other structure loaded with sufficient weight to produce the desired reaction on the surface. Extensometers are used to measure the deflection under the load applied by jack or deadweight. The equipment and testing procedure for PLT is described in ASTM D 1195 (1997). An equivalent soil Young's

modulus, E_s, can be calculated by plotting the load-displacement curve and applying the elastic method for a uniformly loaded rigid plate on a semi-infinite elastic isotropic solid as follows:

$$E_s = \frac{\left(1-\upsilon_s^{\,2}\right)}{\left[\Delta\rho/\Delta q_p\right]} B_p I_w \quad \text{.....(3.24)}$$

where,

ν_s : Poisson's ratio, typically 0.4,

$\frac{\Delta\rho}{\Delta q_p}$: the slope of displacement versus plate pressure (inches/psi),

B_p : diameter of the plate, (inches) and

I_w : influence factor, $\pi/4$ for circular plates.

The estimated Young's modulus is representative of soil within a depth of $2B_p$ beneath the plate.

A reasonable objection can be raised that the shallow foundation elastic modulus is different from that of deep foundations in that it overlooks such factors as confinement and porewater pressure, soil layering, etc. A variation of the PLT, the screw-plate loading test, can then be employed (Schmertmann, 1970). In a screw-plate test, an auger with an instrumented circular plate for controlling loads and displacements is inserted into the soil and loaded vertically. The evaluation is similar to that for PLT.

3.6.3.5 ***Flat Plate Dilatometer (DMT)***

The flat plate dilatometer (DMT), also called Marchetti dilatometer, was first introduced by Marchetti in 1975. It consists of a stainless steel blade with a flat, approximately one-inch diameter circular steel membrane mounted flush on one side, which is commonly pushed vertically into the soil. The blade is connected to a control unit on the ground, used to record pressure changes in the diaphragm. Insertion of the

blade with the help of CPT or regular drill rods is followed by the inflation of the membrane. Two readings are taken within approximately one minute of each other:

1) The “A-pressure” to push the membrane into contact with the surrounding soil (“lift-off”)

2) The “B-pressure” to move the center of the membrane 0.04 inches (1.1 mm) against the soil.

These readings can then be repeated by pushing or driving to further depths so that a soil profile can be obtained. Collected data need to be corrected by calibration factors involving membrane stiffness and local geology. Correlations are utilized for estimating design parameters, such as soil Young’s modulus or maximum shear modulus, G_{max}.

The flat plate dilatometer can be used for a wide range of soils, but not for dense or hard materials (such as gravels) due to risk of damage to the steel membrane. ASTM D 6635 (2001) and ISSMGE Committee TC16 Report on DMT (2001) further explain the equipment, calibration process, data collection and reduction as well as comparisons with other in-situ tests. A geophone can be added to the dilatometer to obtain shear wave velocity measurements alongside typical DMT parameters.

3.6.3.6 *Geophysical Methods*

All of the above testing methods involve the drilling of boreholes, sampling at a few points, and laboratory or in-situ testing of soil samples. The process is typically restricted by time and budget. The common site investigation is limited to a small portion of the volume of soil and rock that could be sampled and tested. For this purpose, geophysical methods, cost-effective ways of characterizing the soil, are increasingly

being used in conjunction with improved interpretative models. Geophysical methods can be applied to most soils and rock.

The available geophysical methods for determining the small strain modulus of soils can be divided into two groups (Campanella, 1994):

1) non-intrusive surface geophysics (seismic reflection/refraction/ resistivity and spectral analysis of surface waves (SASW)), and

2) conventional borehole geophysics (downhole, crosshole, crosshole impulse, downhole nuclear and resistivity, suspension logger).

Non-intrusive geophysical surface tests have the further advantages of not affecting the natural soil fabric during implementation and of being able to be conducted on limited access and/or difficult test sites. The difficulty with surface tests is that no sample is obtained as part of the method, which may lead to errors in interpreting the results. On the other hand, borehole tests provide a sample to be evaluated but may cause disturbance to the very surface the test is being conducted on, which could be significant especially for measurements of small strains.

In general, the deformation modulus is determined directly or indirectly by measuring S-waves (shear). The propagating shear wave velocities, v_s, are evaluated to determine the respective small-strain elastic shear modulus, G_{max}. Water has no effect on the measured shear wave velocities; therefore, the saturation of the tested material is not relevant (Stokoe and Santamarina, 2000). Typical S-wave velocities of soils are between 350 fps to 2000 fps.

Shear modulus can then be converted to Young's modulus utilizing Poisson's ratio and assuming elastic behavior (Section 3.4.4). However, it is necessary to apply an appropriate reduction factor if the strains in the wave propagation do not match the

strains in the prototype. The shear modulus is calculated from strains that are of the order of 10^{-3} %, whereas Young's modulus appropriate for displacements of pile foundations is within approximately 0.1 %. As shown previously, Young's modulus values decrease rapidly as the strains increase, thus making the adjustment critical.

A comprehensive collection of laboratory as well as in-situ correlations (mostly for SPT blow count in sandy soils) for shear wave velocities and shear modulus have been compiled by Sykora and Stokoe (1983).

3.6.4 Limits of Empirical Correlations

An important consideration for most methods from which empirical correlations for soil Young's modulus are derived is that they are almost entirely empirical and based on a knowledge-base of local/on-site experiences and conditions over the years. It is not unusual that the outcomes based on these correlations vary significantly from one another, or that they are specific to only one location. Therefore, a critical approach combined with engineering judgment, as with other real life geotechnical problems, is very important. One might find that certain correlations do not apply to their cases or that the usefulness of some of these equations could prove limited. Nevertheless, correlations provide an economical and quick alternative for initial design conditions and projects with a limited budget for site investigation, as is typical of most projects.

3.7 VARIABILITY OF PARAMETERS

In this study, empirical correlations for Young's modulus are utilized and new ones are suggested based on the findings from Caltrans database. The variability of undrained shear strength, c_u, and standard penetration test blow count has a direct effect on the predicted displacements because they are correlated with Young's modulus of the soil.

3.7.1 Undrained Shear Strength Variability

Many factors affect the results of laboratory undrained shear strength, c_u, testing conducted with triaxial equipment. Aside from natural soil non-uniformity, a large variability arises due to various disturbances that the soil sample may be subjected to during drilling, sampling, transportation, storage and sample preparation (Kulhawy and Mayne, 1990; Mayne et al., 2001; Ladd and DeGroot, 2003). The type of equipment used and the experience/practices of the workers affect test results as well.

Other variability in undrained shear strength values stems from different testing methods and their application techniques. Undrained shear strength can be measured in the laboratory using unconfined compression tests (UC), unconsolidated undrained (UU or Q for quick) triaxial tests, pocket penetrometer tests, and drop cone tests, or in the field by vane tests, pressuremeter, and dilatometer. In these tests, many factors may influence the measured c_u, such as the direction of loading, boundary conditions, strain rate, overconsolidation, degree of fissuring, etc. Many correlations exist as well to indirectly estimate undrained shear strength from water content, Atterberg limits, SPT, CPT, pressuremeter or dilatometer measurements, geophysical tests, etc. All these reflect the uncertainty involved in estimating a consistent value of undrained shear strength.

Within the context of this dissertation, undrained shear strength is measured using the unconsolidated undrained (UU or Q) triaxial compression test in accordance with ASTM 2850 (2003).

3.7.2 Standard Penetration Test (SPT) Variability

Skempton (1986) concluded that the most important variability in SPT blow counts is due to the energy applied to the rods. The penetration resistance is inversely proportional to the energy transmitted down the drill rods to the split spoon sampler

(Schmertmann and Palacios, 1979; Skempton, 1986). Due to lack of standardization of equipment, many types of SPT hammers are in use around the world, each transferring a different energy to the rods. The efficiency is then defined as the ratio of the measured energy passing through the rods over the theoretical free-fall energy (4200 pound-inch) of a standard hammer. Commonly the standard penetration test blow counts are adjusted to an energy efficiency of 60% as suggested by Seed et al. (1985) and Skempton (1986). Energy losses may occur in several ways depending upon the type of hammer being employed (Clayton, 1990).

A calibrated automatic hammer with 80% efficiency was used to conduct standard penetration tests included in this study (Abe & Teferra, 1998; Frost, 1992). No correction for the change in overburden pressure with depth was made.

3.8 SUMMARY

In this chapter, assumptions, modifications, and parameters required for the elastic method are introduced along with the steps followed to estimate pile displacements. Laboratory and in-situ methods to measure Young's modulus are presented. The shortcomings of approaches are highlighted.

Chapter 4: Database Classification and Evaluation of Displacements

4.1 INTRODUCTION

Pile load tests investigated in this study are broadly separated into three groups based on the associated soil:

1) Piles in cohesive soils, i.e., clays and/or silts.

2) Piles in cohesionless soils: sands, gravel, cobbles and rock

3) Piles in mixed profiles, i.e., where the profiles consist of multiple layers of various types of cohesive as well as cohesionless soils.

It should be noted here that an implicit assumption is made that each layer can be defined by a single soil type. The main reason for this grouping is to analyze piles in a single soil profile so as to obtain empirical multiplication factors for Young's modulus of the soil, E_s.

All of the analyses are conducted with the help of a modified version of Tapile computer code (Poulos, 1978; Aschenbrener and Olson, 1984).

4.2 DEFINITIONS OF SOIL TYPES

Throughout this dissertation, the term "clay" is used synonymously for "cohesive soil" and "sand" for "cohesionless soil".

Piles in cohesive (clayey) soils behave differently from piles in cohesionless (sandy) soils; thus, their respective design approaches differ as well. As suggested by Dennis and Olson (1983) for their API database, the terms cohesive and cohesionless are used to reflect the engineering behavior and not to indicate the standard classification of clays and sands according to the Unified Soil Classification System (USCS).

4.2.1 Cohesive Soils

Within the context of this dissertation, clay is defined as a soil that has the following characteristics:

1. Clays are essentially undrained during pile driving.

2. Clays have a consolidation stage after pile driving that typically lasts for at least a month (Caltrans data suggest that after a week the changes are not significant, Brown (2001)).

3. In clays, relatively undisturbed samples can be obtained, which enables laboratory strength tests on undisturbed samples to be conducted. Field tests, such as geophysical methods, field vane, and CPT, can also be used.

4. Clays have low hydraulic conductivity; therefore, excess pore pressures can be assumed not to have sufficient time to dissipate during quick load tests, such as those employed for testing most of the Caltrans piles. Therefore, clayey soils are assumed to be undrained during a load test.

4.2.2 Cohesionless Soils

Conversely, sand is defined as having the following properties:

1. Excess pore water pressures developed during driving undergo significant dissipation during the driving process and are likely to be fully dissipated within about 24 hours.

2. It is expensive to conduct laboratory studies on undisturbed specimens in sands, which require special sampling techniques as well as testing and preservation conditions. Reconstituting samples in the laboratory is also difficult, because important properties depend on density, which is difficult to measure in-situ.

Consequently, it is preferable to design piles in sandy soils based on in-situ testing, e.g., standard penetration test, cone penetration test, etc.

3. Sands can be assumed to be drained during a pile load test.

The term *sand* also encompasses materials classified as non-plastic silts, gravels, and cobbles.

4.2.3 Mixed Profiles

Most of the soil deposits encountered in practice are heterogeneous in composition. The properties and behavior of these soil layers may vary both vertically and horizontally based on natural processes, such as deposition, weathering, aging, cementation, chemical and mineralogical composition, etc., and on human effects, such as pre-loading, dewatering, excavating, and various improvement techniques.

"Mixed profiles" describes heterogeneous soils with any combination and number of cohesive and cohesionless soil layers. An important assumption is that each layer can be depicted as either cohesive or cohesionless. Eighty-three out of 144 (58%) pile load tests analyzed within the FinalCT database are driven into mixed soil profiles.

4.3 DEFINITIONS OF TERMS USED FOR COMPARISON

The ratio of any given pile load to the peak load is defined as the "mobilized load ratio" or, in short, the "load ratio". Correlations are utilized to obtain Young's modulus which is used to calculate pile head displacements with the elastic method (s_c). The term "displacement ratio" denotes the ratio of calculated displacement, s_c to the measured displacement, s_m, obtained from the pile load test (s_c/s_m). The subtraction of s_m from s_c (s_c-s_m) is referred to as the "displacement difference" in this dissertation and negative values for displacements in tension tests are used directly, i.e., the actual values not the absolute ones. Correlations are evaluated independently from one another in order to

establish a range of loading ratios for which Young's modulus values may be used successfully.

4.4 ANALYTICAL PROCEDURE USING MODIFIED TAPILE

In the following paragraphs, loads applied to a pile are shown with the symbol *Q* and displacements are given as *S* (positive for downwards movement). The loads at various percentages of applied peak load, Q_{max}, are symbolized as Q_i, with *i* equal to a third, a half and two-thirds. Displacements experienced when Q_i are applied are shown as S_i.

The following steps are used in the analysis of pile load test data based on the elastic method:

1. The displacement at a third, a half, and two-thirds of peak measured load is obtained from pile load tests. These loading ratios (Q_i/Q_{max}) correspond to the inverse of safety factors, FS, i.e. $[Q_i/Q_{max}] = [1/FS]$.
2. Pile weight is included in analyses.
3. The shear strength of the soil on the side of the pile as well as at the tip of the pile is adjusted iteratively until the calculated pile capacity matches the measured capacity. The tip capacity in tension is assumed to be zero. Pile capacity is calculated using the α method (Dennis and Olson, 1983) for clayey soils and using Brown's (2001) modification of Fleming's (1992) method for sands/gravels. Brown's method was derived directly from the same Caltrans database used in this dissertation.
4. Suggested correlations found in the literature are employed to predict displacements to assess their applicability.
5. As a simplified approach to estimating displacements, Young's modulus can be assumed to be a linear function of the undrained shearing strength (c_u) in cohesive

soils (clays and silts) and the standard penetration resistance (N) in cohesionless soils (sands, gravel, cobbles).

The linear relationships are expressed as:

$E_s = K_1 \times c_u$ *(cohesive soils)* ..... (4.1),

or

$E_s = K_2 \times N_{60}$ *(cohesionless soils)* .....(4.2),

where,

c_u : undrained shear strength of the soil,

N_{60} : standard penetration test blow count adjusted to an applied energy of 60% (blows/foot, also given as bpf),

K_1 and K_2 : empirical *multiplication factors* for cohesive (dimensionless) and cohesionless soils (ksf/bpf), respectively.

6. The subset of data for a single soil type is analyzed first for developing an independent correlation for Young's modulus, i.e. piles driven in only cohesive or cohesionless soils. The displacements at a third, a half, and two-thirds of peak load are matched using a trial-and-error approach by changing the multiplication factors for Young's modulus. Multiplication factors for each test are collected to obtain a reasonable value for cohesive as well as cohesionless soils.
7. Piles driven into mixed soil profiles are analyzed with the multiplication factors obtained from the previous step up to half of the peak applied load.

Predrilled or cased piles are considered to have no soil side shear strength along the length of the predrilling or casing.

Tapile was written to accept piles that are cylindrical in shape. The diameter of piles other than pipe piles were adjusted to an equivalent pipe pile diameter to calculate

the circumference and cross-sectional area correctly, as shown in Eq.s (4.3) through (4.6).

$$D_{eq} = \frac{4D_{sq}}{\pi} \quad \text{(square pile, for circumference)} \quad (4.3),$$

$$D_{eq} = \frac{2D_{sq}}{\sqrt{\pi}} \quad \text{(square pile, for tip area)} \quad (4.4),$$

$$D_{eq} = \frac{12A_{s,H}}{\pi} \quad \text{(H-pile, for circumference)} \quad (4.5),$$

$$D_{eq} = 2 \times \sqrt{\frac{A_{c,H}}{\pi}} \quad \text{(H-pile, for tip area)} \quad (4.6),$$

where,

D_{eq} : equivalent circular diameter (inch),

D_{sq} : square pile width (inch),

$A_{s,H}$: steel-to-soil surface area of H-pile (ft^2/ft),

$A_{c,H}$: cross-sectional area of H-pile ($inch^2$).

The steel-to-soil contact area is used to calculate the circumference for H-piles. The circumference is used for the calculation of side capacity whereas the solid pile tip area is used for the tip capacity.

4.5 LIST OF PILE LOAD TESTS

In this section, tests utilized for displacement analyses using the elastic method are listed for each soil type with further details provided in Appendix A. The analyses include fine grained (cohesive clays/silts), coarse grained (sands, gravels, boulders, non-cohesive silts/clays) and mixed (a combination of fine- grained and coarse-grained soils).

4.5.1 Cohesive Soils

Twenty-six pile load tests in cohesive soils were analyzed with seventeen of them being open-ended pipe piles (about two-thirds). A summary of the number of tests and sites with type of piles is shown in Table 4.1 and details are given in Table 4.2.

Table 4.1 Summary of pile load tests used in analyzing clayey profiles.

Pile Type	# of Tests	Compression		Tension	
		# of Tests	Sites	# of Tests	Sites
Concrete	6	4	3	2	1
Closed-ended pipe	3	1	1	2	2
Open-ended pipe	17	10	4	7	4
TOTAL	26	15	8	11	7

Table 4.2 Details of pile load tests with clayey profiles (N = 26).

CTID[1]	Bridge No.	Type[2]	Size (inch)[3]	Emb. Length (ft)[4]	L/D[5]	C/T[6]	Setup[7] (days)	Aver. c_u[8] (ksf)
009-05	33-0611	CP	24x0.75	66.5	33	C	14	2.72
009-06	33-0611	CP	24x0.75	66.5	33	T	14	2.72
031-08	I880 IPTP	CP	24x0.5	56	28	T	49	1.11
078-11	34-0046	Conc.	14	106	91	C	N/A	1.2
078-12	34-0046	Conc.	14	106	91	T	N/A	1.2
078-13	34-0046	Conc.	14	105.5	90	C	N/A	1.2
078-14	34-0046	Conc.	14	105.5	90	T	N/A	1.2
079-01	34-0046	OP	16x0.5	85.7	64	T	170	0.38
079-02	34-0046	OP	16x0.5	85.7	64	C	181	0.38
079-03	34-0046	OP	16x0.5	110.8	83	C	233	1.24
079-04	34-0046	OP	16x0.5	110.8	83	C	239	1.24
079-05	34-0046	OP	16x0.5	110.8	83	C	1550	1.24
079-06	34-0046	OP	16x0.5	85.7	64	T	1550	0.38
079-07	34-0046	OP	16x0.5	110.2	83	C	168	1.24
079-08	34-0046	OP	16x0.5	110.2	83	T	169	1.24
079-09	34-0046	OP	16x0.5	110.2	83	T	1553	1.24
079-10	34-0046	OP	16x0.5	110.2	83	C	1553	1.24
079-11	34-0046	OP	16x0.5	110.2	83	C	1553	1.24

CTID[1]	Bridge No.	Type[2]	Size (inch)[3]	Emb. Length (ft)[4]	L/D[5]	C/T[6]	Setup[7] (days)	Aver. c_u[8] (ksf)
098-01	34-0088	OP	24x0.75	79	40	C	35	0.703
098-02	34-0088	OP	24x0.75	79	40	T	35	0.703
098-03	34-0088	OP	24x0.75	78	39	C	33	0.703
098-04	34-0088	OP	24x0.75	78	39	T	33	0.703
100-01	34-0088	OP	24x0.75	81	41	C	14	0.76
100-02	34-0088	OP	24x0.75	81	41	T	14	0.76
118L-01	28-0056	Conc.	12	64	64	C	4	1.5
122L-01	22-0062	Conc.	12	49.3	49	C	19	2.54

[1] A unique number given to each test based on the order the Caltrans reports were delivered.
[2] Pile type: Conc. = Concrete; CP = closed-ended pipe pile; OP = open-ended pipe pile HP = H-pile (or I-pile); Comp. = composite pile (combining two or more pile types).
[3] Pile diameter for solid piles or outside diameter and wall thickness for pipe piles.
[4] Embedment length, portion of pile below ground. (equal to pile length when stick-up is added).
[5] Pile length to diameter ratio.
[6] The direction of loading, compression or tension.
[7] The time between the installation of the test pile and load testing. N/A for unknown times.
[8] Average undrained shear strength along the shaft of the pile.

4.5.2 Cohesionless Soils

The list of pile load tests included in analyses for cohesionless soils is summarized in Table 4.3 and given in Table 4.4. Open-ended pipe piles again constitute more than half of the 34 pile load tests investigated.

Table 4.3 Summary list of pile load tests analyzed (sandy soils).

Pile Type	# of Tests	Compression		Tension	
		# of Tests	Sites	# of Tests	Sites
Composite	2	2	2	---	---
Concrete	8	3	1	5	5
Closed-ended pipe	1	1	1	---	---
Open-ended pipe	19	10	6	9	4
H-pile	4	1	1	3	3
TOTAL	34	17	11	17	12

Table 4.4 List of pile load tests in sandy profiles (N = 34).

CTID	Bridge No.	Type	Size (inch)	Emb. Length (ft)	L/D	C/T	Aver. N_{60}[1] (bpf)
026-01	49-0133	Conc.	14	20	17	T	40
035-01	57-0488	OP	14x0.375	26.6	23	C	31
035-02	57-0488	OP	14x0.375	26.6	23	T	31
040-05	I880 IPTP	OP	24x0.75	28	14	C	83
040-11	I880 IPTP	OP	24x0.75	28	14	T	73
041-01	I5/I8 IPTP	OP	16x0.5	43.2	32	C	25
041-02	I5/I8 IPTP	OP	16x0.5	43.2	32	T	25
041-03	I5/I8 IPTP	OP	16x0.5	91.1	68	T	20
041-04	I5/I8 IPTP	OP	14x0.438	85	73	T	17
041-05	I5/I8 IPTP	OP	14x0.438	37	32	C	20
041-06	I5/I8 IPTP	OP	14x0.438	37	32	T	20
041-07	I5/I8 IPTP	OP	16x0.5	95.5	72	C	17
041-08	I5/I8 IPTP	OP	16x0.5	95.5	72	T	17
041-09	I5/I8 IPTP	OP	16x0.5	92.5	69	T	26
041-11	I5/I8 IPTP	OP	14x0.438	89.5	77	C	15
041-12	I5/I8 IPTP	OP	14x0.438	89.5	77	T	15
042-03	54-0967	HP	14x89	39	81	C	57
042-04	54-0967	HP	14x89	39	81	T	57
042-06	54-0967	HP	14x89	56	117	T	35
057-01	53-1181	HP	10x57	32	78	T	63
060-03	55-0794	Conc.	14	42.5	36	T	49
083-01	34-0046	OP	18x0.5	33	22	C	19
087-01	57-1017	Conc.	14	31	27	C	16
087-02	57-1017	Conc.	14	31	27	T	16
087-03	57-1017	Conc.	14	24	21	C	15
087-04	57-1017	Conc.	14	17	15	C	13
102L-01	51-0273	Conc.	12	24	24	T	12
109L-01	52-0271	CP	10.75x0.5	40.1	45	C	14
111-01	46-0255	Comp.	15	43	34	C	20
112-01	46-0252	Comp.	15	25	20	C	30
114L-01	52-0178	OP	12x0.5	44.9	45	C	11
114L-02	52-0179	OP	12x0.5	44.1	44	C	11
114L-04	52-0180	OP	12x0.5	34.9	35	C	15
115L-02	51-0276	Conc.	12	23	17	T	17

[1] The 60% energy corrected value of standard penetration test blow count for the whole profile averaged over depth.

4.5.3 Pile Load Tests in Mixed Profiles

Soil profiles typically consist of multiple layers of varying soil types. Many of the pile load tests conducted in California were driven into mixed profiles. Out of 83 pile load tests, 39 were tested in compression and 44 in tension (Table 4.5). About half of these tests were conducted on open-ended pipe piles. Details of piles in mixed profiles are presented in Table 4.6.

Table 4.5 Summary list of pile load tests driven into mixed profiles.

Pile Type	**# of Tests**	**Compression**		**Tension**	
		# of Tests	**Sites**	**# of Tests**	**Sites**
Concrete	10	8	8	2	2
Closed-ended pipe	29	11	7	18	9
Open-ended pipe	41	18	7	23	9
H-pile	3	2	2	1	1
TOTAL	83	39	24	44	21

Table 4.6 Details of piles founded in mixed soils (N = 68).

CTID	Bridge No.	Type	Size (inch)	Emb. Length (ft)	C/T	Setup (days)
004-01	20-0251	Conc.	12	52.5	C	2
009-03	33-0611	CP	24x0.5	64	C	14
009-04	33-0611	CP	24x0.5	64	C	14
009-05	33-0611	CP	24x0.5	66.5	C	14
009-06	33-0611	CP	24x0.5	66.5	T	14
010-01	33-0612	OP	42x0.625	73.3	C	27
010-02	33-0612	OP	42x0.625	73.3	T	32
011-01	33-0393	CP	24x0.5	69.5	C	14
011-02	33-0393	CP	24x0.5	69.5	T	14
012-01	33-0612	OP	42x0.625	83	C	29

CTID	Bridge No.	Type	Size (inch)	Emb. Length (ft)	C/T	Setup (days)
012-02	33-0612	OP	42x0.625	10	T	30
012-03	33-0612	OP	42x0.75	91	C	32
012-04	33-0612	OP	42x0.75	91	T	33
012-05	33-0612	OP	42x0.75	86	C	28
012-06	33-0612	OP	42x0.75	86	T	29
022-03	37-0270	CP	14x0.5	55.3	C	6
022-04	37-0270	CP	14x0.5	55.3	T	6
022-05	37-0270	CP	14x0.5	55	C	8
022-06	37-0270	CP	14x0.5	56	T	10
022-07	37-0270	CP	14x0.5	56	T	11
022-08	37-0270	CP	14x0.5	60	C	5
022-09	37-0270	CP	14x0.5	60	T	6
022-10	37-0270	CP	14x0.5	68	T	19
022-11	37-0270	CP	14x0.5	61	T	23
023-02	37-0279	CP	14x0.25	60	T	44
029-01	I880 IPTP	OP	24x0.75	40	C	30
029-02	I880 IPTP	OP	24x0.75	40	T	31
029-03	I880 IPTP	CP	24x0.75	43	C	28
029-04	I880 IPTP	CP	24x0.75	43	T	29
029-05	I880 IPTP	CP	24x0.75	40	C	24
029-06	I880 IPTP	CP	24x0.75	40	T	25
029-08	I880 IPTP	CP	24x0.75	35	T	20
029-09	I880 IPTP	CP	24x0.75	40	C	20
029-10	I880 IPTP	CP	24x0.75	40	T	21
030-01	I880 IPTP	OP	42x0.75	100.5	C	26
030-02	I880 IPTP	OP	42x0.75	100.5	T	28
030-03	I880 IPTP	OP	42x0.75	100.5	C	55
030-04	I880 IPTP	OP	42x0.75	100.5	T	60
031-01	I880 IPTP	OP	24x0.5	60	T	56
031-02	I880 IPTP	OP	24x0.5	60	T	62
031-03	I880 IPTP	OP	24x0.5	69	C	40
031-04	I880 IPTP	OP	24x0.5	69	T	43
031-05	I880 IPTP	OP	24x0.5	73	C	42

CTID	Bridge No.	Type	Size (inch)	Emb. Length (ft)	C/T	Setup (days)
031-06	I880 IPTP	CP	24x0.5	64	T	43
031-07	I880 IPTP	CP	24x0.5	56	C	49
031-09	I880 IPTP	OP	24x0.5	69	C	38
031-10	I880 IPTP	OP	24x0.5	69	T	41
031-11	I880 IPTP	CP	24x0.5	69	C	41
031-12	I880 IPTP	CP	24x0.5	69	T	42
038-01	57-0783	OP	16x0.5	50	T	1
050-01	53-1851	OP	16	41	T	13
056-01	53-1193	OP	14x0.44	55	T	2
058-01	53-1144	Conc.	12	46	C	8
058-02	53-1144	Conc.	12	46	T	15
077-01	34-0046	OP	24x0.5	42.6	C	22
077-02	34-0046	OP	24x0.5	42.6	C	21
081-02	34-0046	CP	20	58.6	C	6
082-01	34-0046	CP	20	58.6	T	8
085-01	33-0025	OP	24x0.75	49	C	10
085-02	33-0025	OP	24x0.75	49	T	11
086-01	33-0025	OP	24x0.75	56.5	C	85
086-02	33-0025	OP	24x0.75	56.5	T	85
088-01	53-2791	HP	14x89	62	T	1
093-02	44-0216	OP	72x0.75	114	T	23
094-04	34-0088	OP	24x0.75	52.5	T	33
094-06	34-0088	OP	24x0.75	42	T	26
095-04	34-0088	OP	24x0.75	63.5	T	14
096-01	34-0088	OP	16x0.5	59.5	C	50
096-03	34-0088	OP	16x0.5	59	C	51
096-04	34-0088	OP	16x0.5	59	T	51
099-01	34-0088	OP	24x0.75	68.1	C	30
099-02	34-0088	OP	24x0.75	68.1	T	31
116L-01	51-0273	CONC	12	25	C	9
117L-01	51-0066	HP	10x57	59	C	1
119L-01	35-0284	CONC	12	108.4	C	4
124L-01	22-0032	CONC	12	80.5	C	5

CTID	Bridge No.	Type	Size (inch)	Emb. Length (ft)	C/T	Setup (days)
125L-03	55-0681	HP	14x89	83	C	4
125L-05	55-0681	CONC	14	47	T	16
127L-01	37-0011	CONC	12	66.4	C	7
128L-01	37-0410	CONC	12	44.3	C	6
129L-01	37-0279	CONC	10	68	C	8

Caltrans pile load test data was fed through a computer code called TAPILE (Load-Settlement Analysis of Axially Loaded Pile) to predict displacements. The code was originally written in Fortran IV by Poulos in 1978, and then modified by Aschenbrener (1984) and later by Aschenbrener and Olson (1984). Tapile uses a modification of the original solution by Mindlin (1936) as detailed in Chapter 3 and the steps followed are summarized below.

The pile can be divided into elements of varying lengths, diameter and stiffness. In general, the number and length of the shaft elements was the same as the soil layers next to the pile. For example, if there were three soil layers of eight, twelve, and ten feet along the pile, then the number of shaft elements were also three with eight, twelve and ten feet lengths. Smaller lengths can be selected for the elements within the limit for the number of elements which is twenty. In utilizing Tapile, the tip of the pile may be separated into a number of annular elements, each having a uniform normal stress acting on it. For this dissertation, a single tip element was used because the accuracy obtained by considering multiple ones was negligible.

Stresses interacting on the pile shaft are assumed to be uniformly distributed around the peripheral surface of the element.

Tapile uses an approximation for the heterogeneity of soils. The average soil modulus is obtained by averaging the values next to the loaded element and the element for which the displacement is being calculated.

Pile-soil slippage is allowed for by specifying limiting values of interface shear stress at various elements along the pile. Different values of the limiting stresses for compression and tension loading can be specified. Poisson's ratio is assumed to remain constant throughout the whole soil mass. Tapile conducts its analyses incrementally, in which the specified increment of load is applied to the pile head and the resulting stress and displacement increment at each element is evaluated and added to the corresponding value at the previous load level. The program checks the computed pile-soil interface stresses against the specified limiting values of soil shear strength. If the computed value exceeds the limiting shear strength at any element, the side shear in for that element is set equal to the shear strength of the soil. Then the soil-pile displacement compatibility requirement is no longer valid and the soil can displace independently of the pile that it is next to ("slippage"). The next load increment is applied and the procedure is repeated until the specified number of load increments has been analyzed or all of the pile elements reach their corresponding limiting values (pile capacity). For each load increment, Tapile computes the stress and displacement at each element, the displacement at the top of the pile and the distribution of axial load with depth along the pile. The ultimate axial load capacity in compression and tension are also calculated (Poulos, 1978).

A Visual Basic interface was used to create Tapile data files and to execute the program for conducting analyses. The initial screen for input of data and subsequent editing, and the summary table following an analysis (using the Run command in the

interface) are shown in Figures 4.1 and 4.2. An example of the data collected as part of the Caltrans database is given in Figure 4.3, which also includes the matched soil properties of layers along the pile length to obtain the measured pile capacity. Input and output data files are included in Appendix C. A flow diagram of the steps involved in Tapile calculations is presented in Figure 4.4.

Details of the displacement analyses based on the elastic method involving Mindlin's solution, laboratory and in-situ determination of input parameters, typical recommended values given in literature, and further details of the pile load test database used for analyses were provided in Chapter 3.

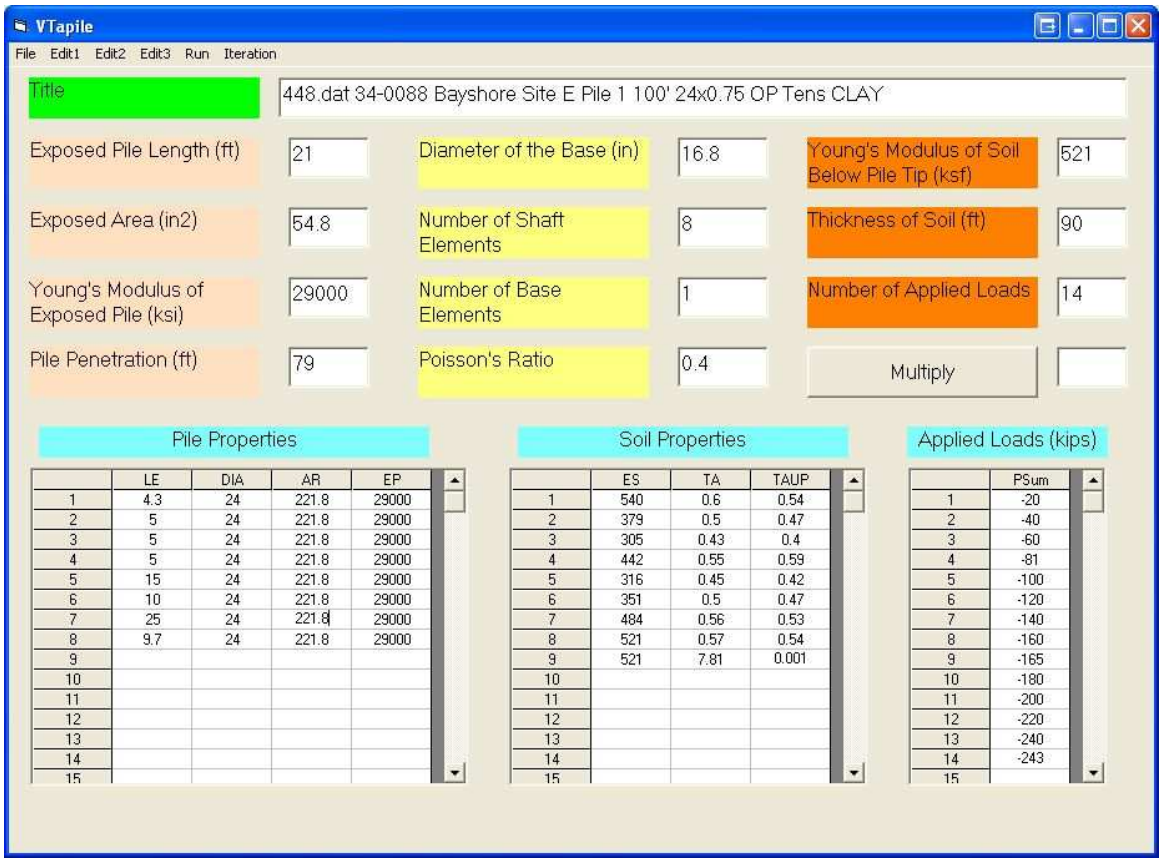

	LE	DIA	AR	EP
1	4.3	24	221.8	29000
2	5	24	221.8	29000
3	5	24	221.8	29000
4	5	24	221.8	29000
5	15	24	221.8	29000
6	10	24	221.8	29000
7	25	24	221.8	29000
8	9.7	24	221.8	29000
9				
10				
11				
12				
13				
14				
15				

	ES	TA	TAUP
1	540	0.6	0.54
2	379	0.5	0.47
3	305	0.43	0.4
4	442	0.55	0.59
5	316	0.45	0.42
6	351	0.5	0.47
7	484	0.56	0.53
8	521	0.57	0.54
9	521	7.81	0.001
10			
11			
12			
13			
14			
15			

	PSum
1	-20
2	-40
3	-60
4	-81
5	-100
6	-120
7	-140
8	-160
9	-165
10	-180
11	-200
12	-220
13	-240
14	-243
15	

Figure 4.1 View of the pre-processing interface for Tapile program.

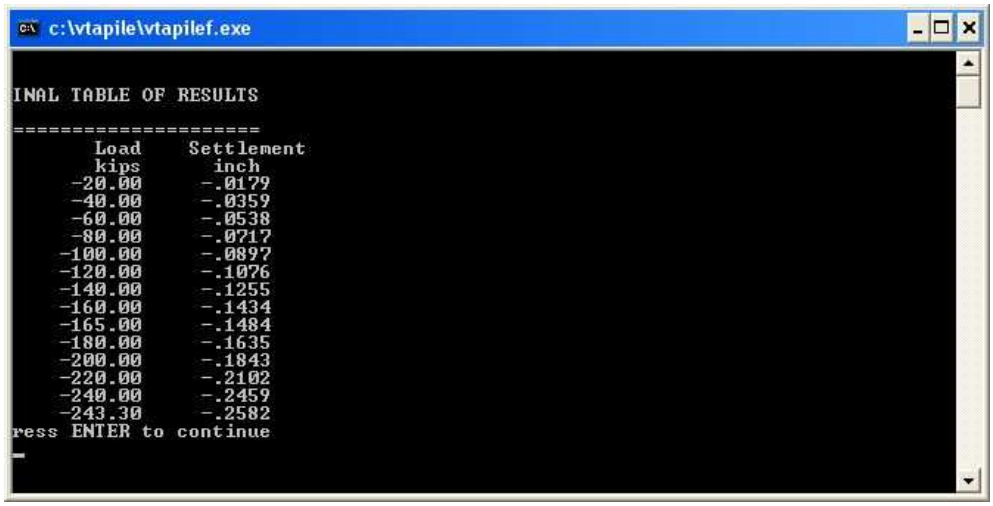

Figure 4.2 Tapile final screen in command window after execution.

In the following sections, results of analyses conducted using correlations recommended in the literature are presented. Comparisons of calculated to measured displacements are made graphically as well as statistically.

4.6 RESEARCH APPROACH

4.6.1 Failure Load Determination

It is imperative to estimate the ultimate pile capacity (failure load) as best as possible in order to achieve success in determining the expected displacements. An error in pile capacity will be reflected as an error in calculated displacements. Ideal pile analysis thus would involve a concurrent investigation of capacity and displacement. However, for an empirical study utilizing pile load tests, focus can be shifted from one to the other because both the displacement and the capacity are known from pile load tests. In this study, pile capacity is defined as the peak applied load as determined by pile load testing (Figure 4.5a). The peak load is also employed in a single case where the pile is not loaded to failure or there is no discernable failure load (Figure 4.5b).

Figure 4.3 An example of the collected pile load test data in cohesive soil.

PILE LOAD TEST INFORMATION

CTID	Bridge No.	Bridge Name	Bent No.	Pile Number	Pile Length	Stick-up	Pile Penetr.	Loading	SLTID
122L-01	22-0062	Mullen Overhead	Bent 2R	21	51.20	0.00	51.20	Compression	736

Pile Diameter, D:	12	inch	Pile Weight:	7.4	kips	
Wall Thickness, t:	6	inch	Qm,comp:	392.6	kips	
Vibrated?	N	Y or N	Qm,tens:		kips	
Fvs:	1		Setup Time:	19	days	
Fvt:	1		DQF=	2	4REO	
Pile Type:	Concrete					
Pile Shape:	Square					
Fp:	1		Equiv. Tip D:		inch	when round
Tip Unit Capacity:	30.6	ksf	Equiv. Tip D:	13.54	inch	when square for area
Pile X Area:	144	sq. inch	Equiv. Shaft D:	15.28	inch	when square for circumference
Plug Area:	0.00	sq. inch	Equiv. Tip D:		inch	when H for area
Tip Area:	144	sq. inch	Equiv. Shaft D:		inch	when H for circumference
Epile (ksi):	4500		H-Pile Surf. A:		sq.ft/ft	

Casing Depth (ft)	Predrill Depth (ft)	Relief Drill Depth (ft)	Jetted	Vibrated
1.9				

CAUTIONS 1

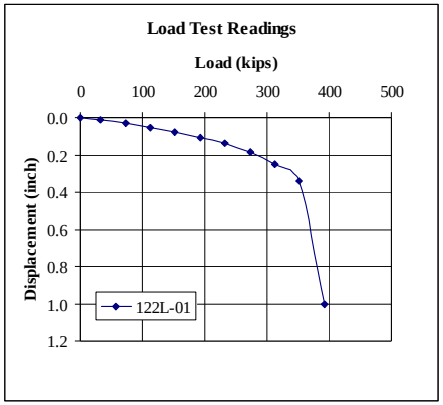

PILE CAPACITY

SOIL PROFILE

							For fs=(25+K*N60), K=		Adjust Side Shear	Rside = Tens/Comp	K1 for E=K1*Su	K3 for ft=K3*Su			$E_{s,t}/E_{s,s}$		
							1.8		1.70	0.94	804	9.0			1		
	feet	blows/foot	ksf			Fine/Coarse?	Equiv. N_{60}/c_u		compression	tension	K2 for E=K2*N		compr.	compr.		compression	tension
						F	2.82	kPa	ksf	ksf	ksf	kPa	ksf	ksf	kips	kips	
LayerNo	**Layer H**	**N_{60}**	**c_u**	**α**	**Soil Type**		**(N_{60} or c_u)*L**	**Side Shear**			**Side $E_{s,s}$**	**Tip Unit Capacity**		**Tip $E_{s,t}$**	**Total Side Capacity**		
1	1.9	0.01			sand		0.02	0.0	0.00	0.00	0				0.00	0.00	
2	3.3	19			sand		62.7	0.0	0.00	0.00	0				0.00	0.00	
3	26		2.42	0.44	clay		62.9	50.5	1.79	1.68	1946				186.2	175.1	
4	1		2.42	0.44	clay		2.4	50.5	1.79	1.68	1946				7.2	6.7	
5	19		3.4	0.38	clay		64.6	62.5	2.22	2.09	2734	1465.9	30.6	2734	168.6	158.5	
											2734						
	51.20																
	OK																
														TOTAL	**392.6**	**340.3**	
															compression	tension	

Notes:
All dimensions in feet if not stated otherwise.
Profile from FinalCT.dat (05/29/2005).
First layer cased. Second layer is given as sand, but its contribution is not significant.
The general soil classification in FinalCT is clay.
Assumed compression test.
Minimum spacing unknown. Installed with Delmag D30 (54,250 ft-lb).

Fine SUM(c_uL) 129.9
Coarse SUM(N_{60}L) 62.7

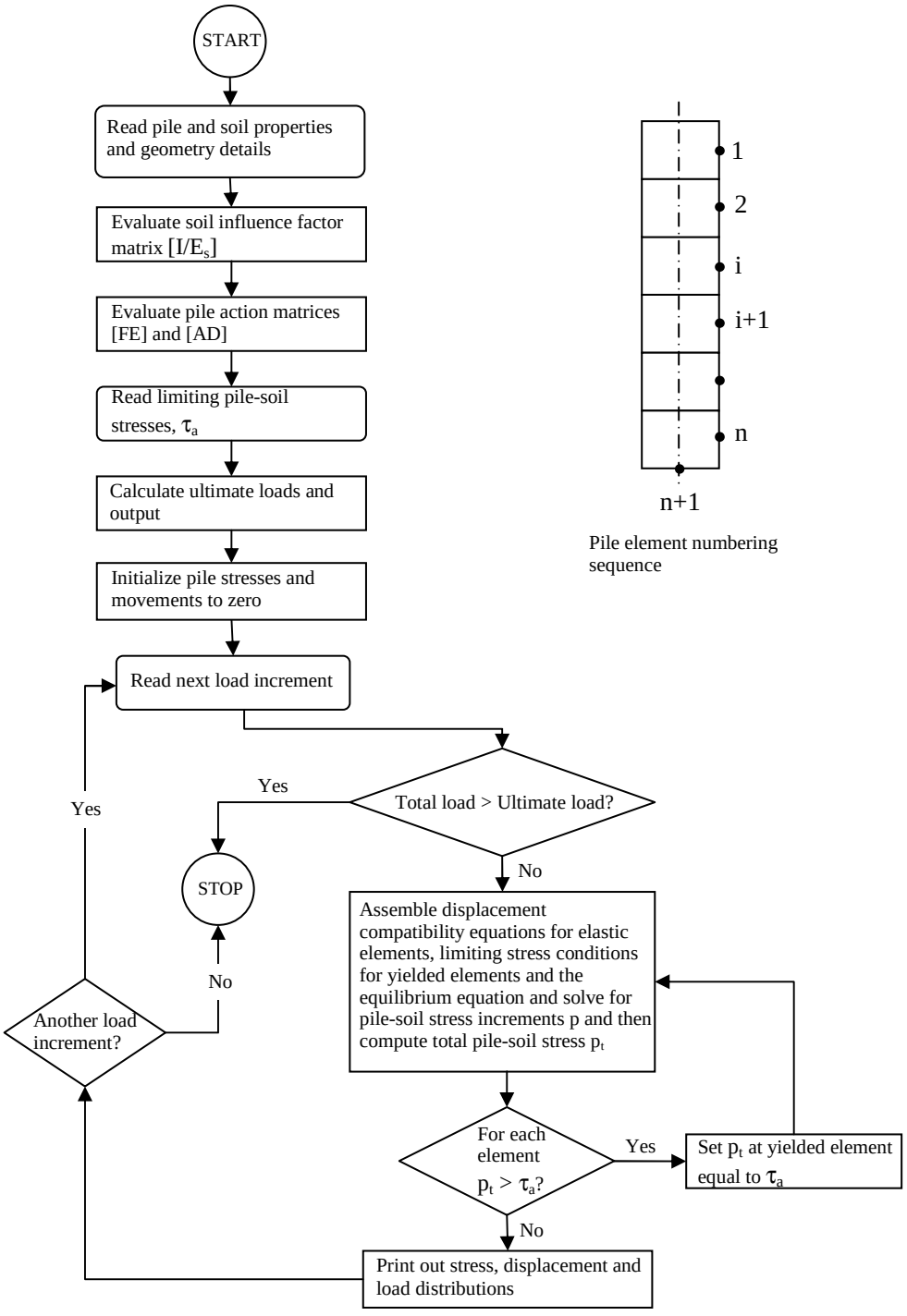

Figure 4.4 Flow chart depicting the steps in Tapile analyses (adapted from Poulos, 1979).

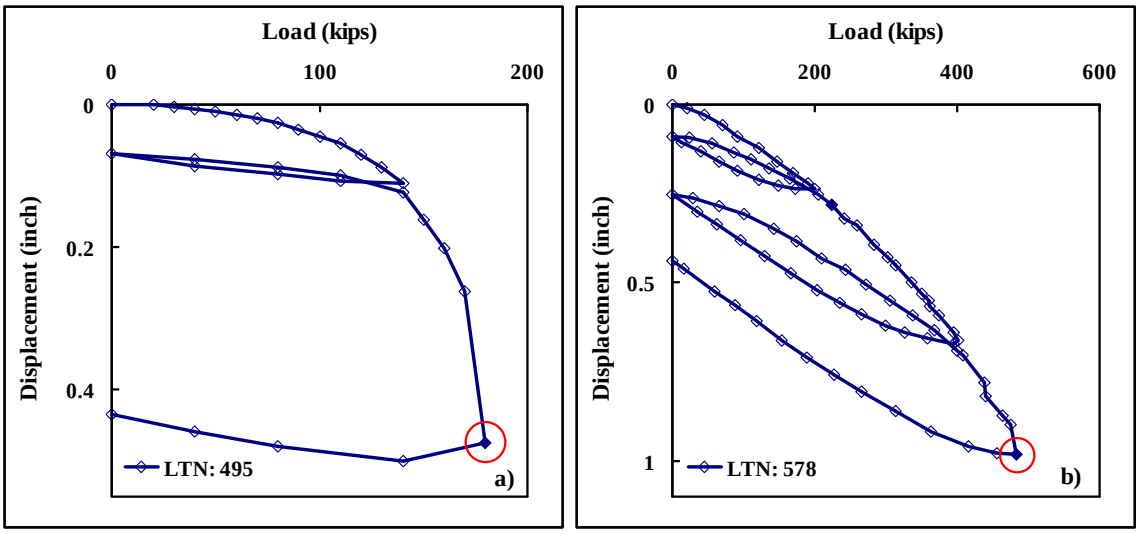

Figure 4.5 Failure load determination (pile weight not considered): a) peak applied load corresponding to pile capacity in a tension test, b) failure load for a prematurely terminated pile load test in compression.

There are multiple ways of conducting pile load tests. For example during the quick-load method adopted by Caltrans (Foundation Testing Manual, 1997), loads are held for five minutes during loading and one minute during unloading, while readings are continuously taken. Therefore, multiple displacement values are obtained. Load-displacement curves did not have a time component other than the statement that the test method complied with a standard, mostly ASTM D-1143 for compression and ASTM D-3689 for tension. The displacement increase under a constant load is probably not due to consolidation because the time of loading is about five minutes. Nevertheless, consolidation may be possible if the stressed zones on the sides of the pile are sufficiently thin to allow for excess pore pressure to dissipate or the soil has a high radial consolidation coefficient, c_r. The measured displacements might be increasing because the applied load is at or near the pile capacity. Inadequate control of the applied load may

also lead to increased displacements. Creep due to viscous aspect of the soil strength can increase displacements while the applied load is held constant.

Determination of displacement pairs at various loads from pile load test measurements is shown in Figure 4.6. The load-displacement curve becomes increasingly non-linear when loads in excess of two-thirds of the failure load are considered.

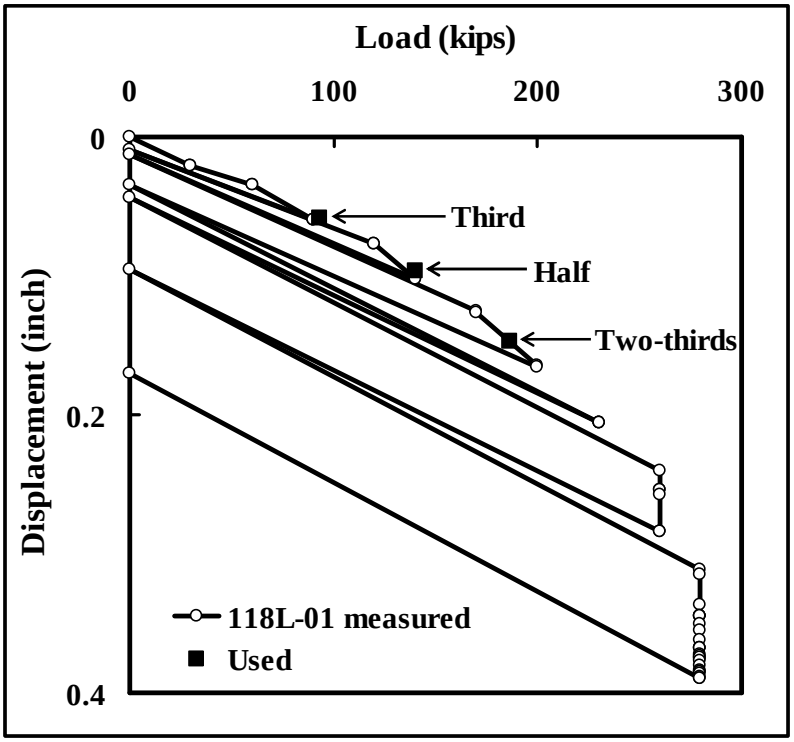

Figure 4.6 Load-displacement envelope.

4.6.2 Investigation

Two sets of elastic analyses have been conducted based on pile load tests collected from Caltrans archives:

1. The first series of analyses was aimed at evaluating a few select Young's modulus correlations out of the many available from recommendations

found in literature to determine their relevance to pile displacement calculations (Chapter 5).

2. The second set of analyses was an attempt towards establishing a correlation for Young's modulus that would improve the accuracy and reliability of elastic analyses (Chapter 6).

The calculated and measured displacements have been compared graphically as well as numerically to determine the "accuracy" of the suggested methods.

4.6.3 Graphical Evaluation

Calculated and measured displacements are compared graphically to observe general trends and characteristics of the estimates employing recommended correlations of Young's modulus in the literature. The ratio of calculated displacements to the measured displacements, (s_c/s_m), as well as the difference between displacements, (s_c-s_m), is taken into consideration.

Separate plots are provided for each Young's modulus correlation that has been studied:

- cohesive soils: Aschenbrener (1984), Callanan and Kulhawy (1985), Johnson (1986), and Poulos (1989) and (1972),
- cohesionless soils: Christoulas (1988), D'Appolonia et al. (1970), Decourt et al. (1989), Denver (1982), Komornik (1974), Kurkur (1986), Shioi and Fukui (1982), and Yamashita et al. (1987).
- mixed profiles (combination of cohesionless and cohesive soils): Aschenbrener (1984), Poulos (1989), D'Appolonia et al. (1970), Komornik (1974), Kurkur (1986), Shioi and Fukui (1982), and Yamashita et al. (1987).

Direct estimations of pile displacements using the elastic compression/tension of a free-standing column and Frank's correlations with pile diameter are also shown in graphs.

Negative values of displacements represent the displacements in a tension test and positive numbers are for pile load tests in compression. These displacements are presented on opposite axes in order to identify any possible differences due to loading direction. A straight line depicting equality between calculated and measured displacements is also plotted.

4.6.4 Statistical Evaluations

For analyses, the sample mean, ($\bar{x}$), and the standard deviation, (s_x), are used to compare the estimated displacements utilizing the suggested correlations against those observed in pile test results.

The accuracy of a method refers to how closely the calculated values can be used to predict the measured values, which can be given by the arithmetic mean (average), of the displacement ratio or displacement difference. The closer the estimated and measured displacements match, the closer is the mean value of ($x = s_c / s_m$) to unity (=1). Similarly, the better a measured displacement can be estimated, the closer will the mean value of ($x = s_c - s_m$) be to zero. All of the equations below are given for the displacement ratio. However, equations are valid for the displacement difference as well when appropriate parameters are replaced.

The mean value of the displacement ratio is calculated as:

$$\bar{x} = \frac{1}{n}\sum_{i=1}^{n}[x_i] \quad \text{.....(4.7),}$$

where, n is the number of pile load tests and i is a given pile load test.

Precision is the ability of a measurement to be reproduced consistently. The standard deviation, σ indicates the plus-minus (±) scatter around the mean values. The smaller the standard deviation, the greater is the reliability or precision of the estimation method. The standard deviation of the displacement ratio is:

$$s_x = \sqrt{\frac{1}{n-1}\sum_{i=1}^{n}\left[\left(x_i\right)^2 - \bar{x}^2\right]} \quad \text{.....(4.8).}$$

In summary, a comparison can be made between correlations using the following criteria: the better one would have a mean displacement ratio closer to one or a displacement difference near zero, and a smaller standard deviation. These parameters can then be ranked accordingly from most satisfactory to least or from best to worst. A cumulative value can then be obtained to cross-evaluate the suggested correlations.

4.7 SUMMARY

In this chapter, the definitions of cohesive, cohesionless and mixed soil profiles are given, as they are used throughout this dissertation. Caltrans database was divided into three categories based on these descriptions. All of the analyses in the following chapters rely on these subsets of data.

Various comparisons of calculated and measured displacements are made in the next two chapters. Graphical and statistical evaluations of these comparisons are explained in this chapter.

Chapter 5: Evaluation of Methods to Predict Axial Displacements

5.1 INTRODUCTION

In the literature, a large number of correlations for Young's modulus have been proposed, which are tied to various soil parameters obtained from laboratory or in-situ measurements. In this chapter, a select few of these are introduced and used as part of the elastic method to estimate displacements within the range of load ratios for which they are recommended. The calculated and measured displacements are then compared. Estimations that vary significantly from others in terms of displacement ratio (s_c/s_m) and displacement difference (s_c-s_m) are identified. Factors are examined to determine their respective effect on the outliers.

5.1.1 Direct Prediction of Displacement

An approximate prediction for displacements can be made with correlations which are obtained empirically from past experience, relating a few parameters to pile displacements via simple equations.

Frank (1985) suggested a correlation to estimate displacements based on his experience with pressuremeter tests in France. He proposed the following range and average value of displacements for piles under "working" loads, which he limited to half of the determined maximum pile capacity:

$$0.008D \leq \rho \leq 0.012D \quad \text{.....(5.1)},$$

with an average displacement of

$$\rho_{average} \approx 0.009D \quad \text{.....(5.2)},$$

where, ρ: displacement and D: pile diameter.

Briaud and Tucker (1988) determined with a 95% probability that at a load ratio of a half:

$$\rho \leq 0.0125D \quad \text{.....(5.3).}$$

Meyerhof (1959) earlier suggested a similar correlation for piles loaded up to a third of their maximum capacity without regard to loading direction:

$$\rho = \frac{D_{base}}{30(FS)} \quad \text{.....(5.4),}$$

where, D_{base} is the pile tip diameter and (FS) is the factor of safety, which he recommended to be higher than three. The correlations proposed by Briaud and Tucker, Frank, and Meyerhof are essentially the same for a factor of safety between three and four. Poulos (1994) found that displacements calculated using Frank's correlation to be consistent with the displacements predicted by elastic method when "suitable" parameters for stiffness of the soil are employed.

For convenience in this dissertation, 0.01D was employed in estimating displacements of piles driven in all types of soils.

Another correlation commonly used for approximating displacements relies on the elastic compression/tension of a free-standing column and ignores the effects of the type of soil and the embedment on the distribution of the applied load along the pile:

$$\rho_{pile,elastic} = \frac{PL_{pile}}{A_{pile}E_{pile}} \quad \text{.....(5.5),}$$

where, P: applied vertical load (kips), L_{pile}: length, A_{pile}: cross-sectional area, and E_{pile}: modulus of elasticity of the pile. For a pile of known length, the value of $\frac{L_{pile}}{A_{pile}E_{pile}}$ (inch/kips) is a constant for all applied loads, which is sometimes referred to as the "compressibility of the pile".

In the next sections, the magnitude of the measured and predicted displacements will be presented for each soil type, followed by comparisons of the predictions obtained from direct and indirect correlations.

5.2 COHESIVE SOILS

The 26 load tests within the FinalCT database driven entirely in cohesive profiles are listed in Chapter 4.

5.2.1 Magnitude of Displacements

The absolute values of almost all of the displacements measured in pile load tests are less than 0.25 inches at load ratios of a third and a half (Figure 5.1).

The ratio of the absolute values of the measured displacements, s_m, to the diameter, D, are shown in Figure 5.2. Similar to the findings by Frank (1985), Briaud and Tucker (1988), and Meyerhof (1959), approximately 90% of s_m/D ratios are equal to or less than 0.6% for a load ratio of a third with a peak value of 1.5%. Likewise, 85% of the displacements are less than 1% of the pile diameter, with a peak of 2% for the load ratio of a half. Based on these findings, it can be concluded that s_m/D=1.5% can be a reasonable upper limit of displacements for loads up to a half of capacity.

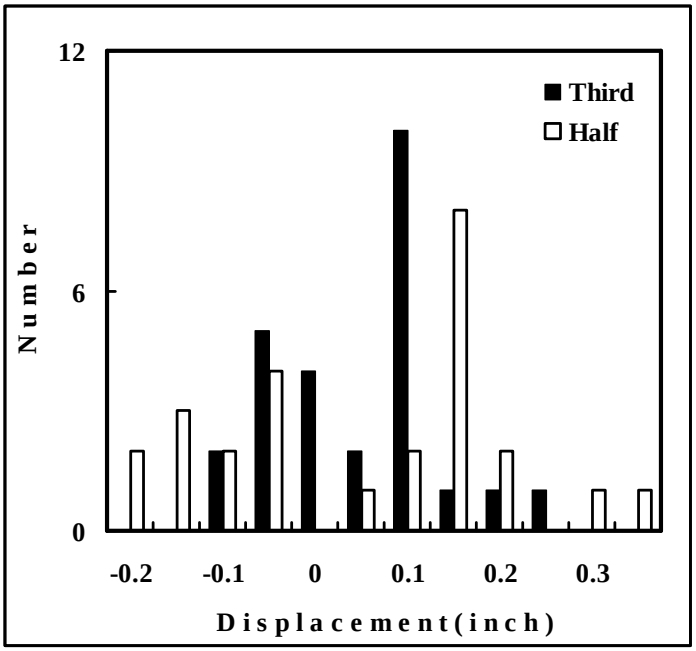

Figure 5.1 The magnitude of measured displacements, s_m.

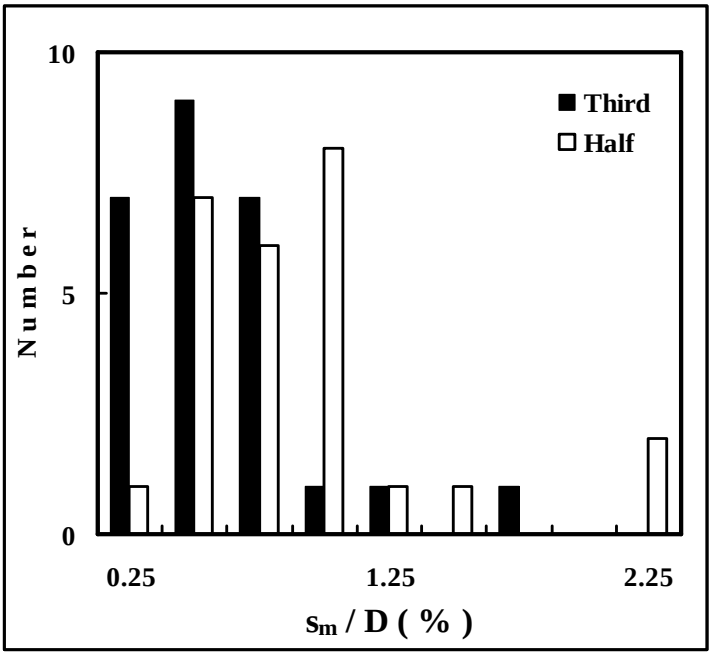

Figure 5.2 Measured displacements over pile diameter.

5.2.2 Correlations

Correlations of Young's modulus selected from the literature with undrained shear strength, c_u, are listed in Table 5.1 and compared in Figure 5.3.

Table 5.1 Correlations of Young's modulus with undrained shear strength, c_u.

Pile Install.	E_s (ksf)	Reference	Notes/Method
Driven	$(300\pm100)c_u$	Poulos (1989)*	Back-calculated from pile load tests. Valid for third to half pile ultimate capacity.
Driven	See below	Poulos (1972)	Equation derived by fitting the scanned graph. Valid for third to half ultimate capacity.
Bored	See below	Poulos (1972)	Equation derived by fitting the scanned graph. Valid for third to half ultimate capacity.
Driven	$800c_u$	Aschenbrener (1984)/Aschenbrener and Olson (1984)*	Pile load test database (APC). Derived for half peak load applied to pile.
Driven	$200c_u$	Callanan & Kulhawy (1985), Johnson (1986)	Back-analysis of bored piles at half peak load(1985); matched laboratory strength to pressuremeter, CPT and plate bearing tests (1986)

Poulos (1972) (equations derived from fitting to scanned plots, c_u in ksf)

$E_s=-15.519c_u^4+167.99c_u^3-207.11c_u^2+257.37c_u+58.374$ (870 ksf max.) (driven piles)
$E_s=140.54c_u^4-610.45c_u^3+1024.8c_u^2-623.88c_u+196.75$ (1750 ksf max.) (bored piles)

* Used for piles in mixed profiles.

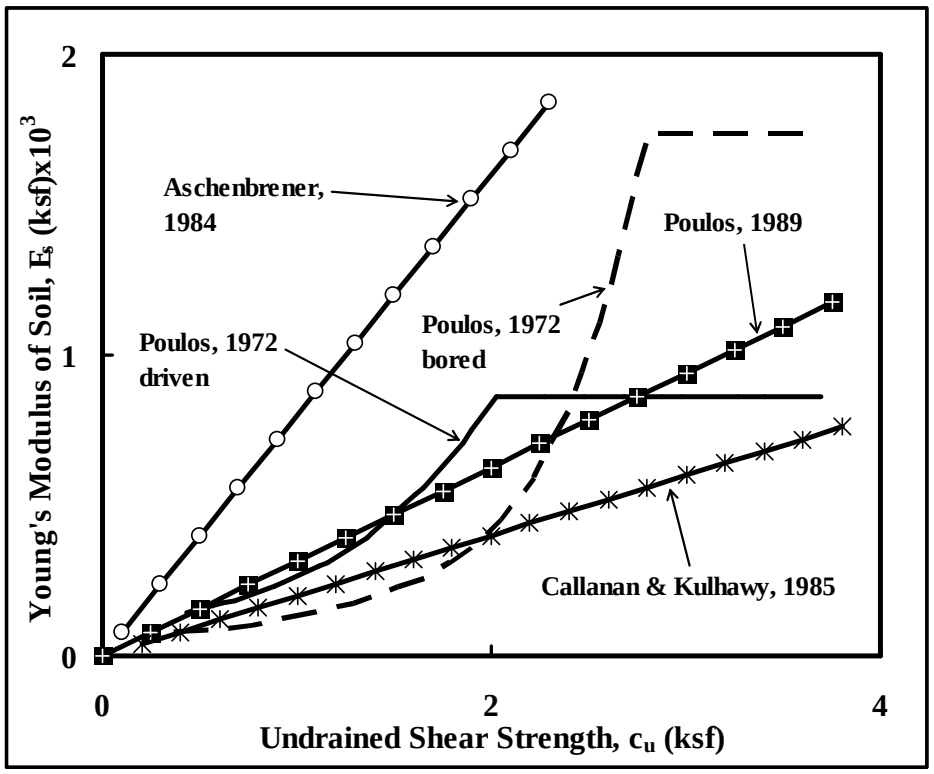

Figure 5.3 Young's modulus correlations with undrained shear strength.

Although all of the correlations are suggested for working loads, there is a noticeable divergence among the calculated values for Young's modulus. The variability of undrained shear strength was discussed in Chapter 3. Aschenbrener (1984) and Aschenbrener and Olson (1984) utilized Davisson's (1972) formula for determining pile capacity from a load-displacement curve, which corresponds to the load on the curve intersected at the following displacement value (Figure 5.4):

$$S_f = \frac{QL}{A_p E_p} + 0.15" + 0.01D_b \quad \text{(pile loaded in compression)} \quad (5.6)$$

$$S_f = -\frac{QL}{A_p E_p} - 0.15" \quad \text{(pile loaded in tension)} \quad (5.7)$$

where, Q is applied load, L is the total length, A_p is the cross-sectional area, E_p is Young's modulus, and D_b is the base diameter of the pile. Such a determination of failure load may lead to lower peak loads than those which other researchers utilized for their correlations. The smaller displacements predicted from Aschenbrener's suggestion may be explained by matching smaller displacements at lower loads (Figure 5.4).

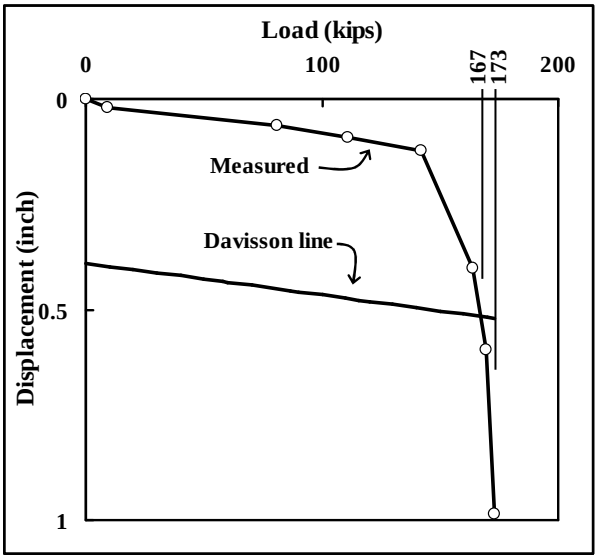

Figure 5.4 Difference between calculated pile capacities: Davisson (167 kips) versus peak applied load (173 kips).

5.2.3 Measurements versus Predictions

A comparison of the measured displacements versus predicted displacements using the correlation suggested by Poulos (1989) indicates good overall agreement and is representative of the outcome from other correlations (Figure 5.5) for a load ratio up to a half. All of absolute values of the measured and predicted displacements are less than the 0.5 inches. There is a tendency to predict larger displacements than those measured for all but one (Aschenbrener, 1984) of the correlations. A larger dispersion of the

displacements can be seen at a load ratio of a half. For all of the predictions, the loading direction, i.e., tension versus compression, does not appear to have an effect on the magnitude or error of predicted displacements.

Outliers, marked with their respective load test numbers (LTNs) in Table 5.5, are discussed in section 5.2.6.

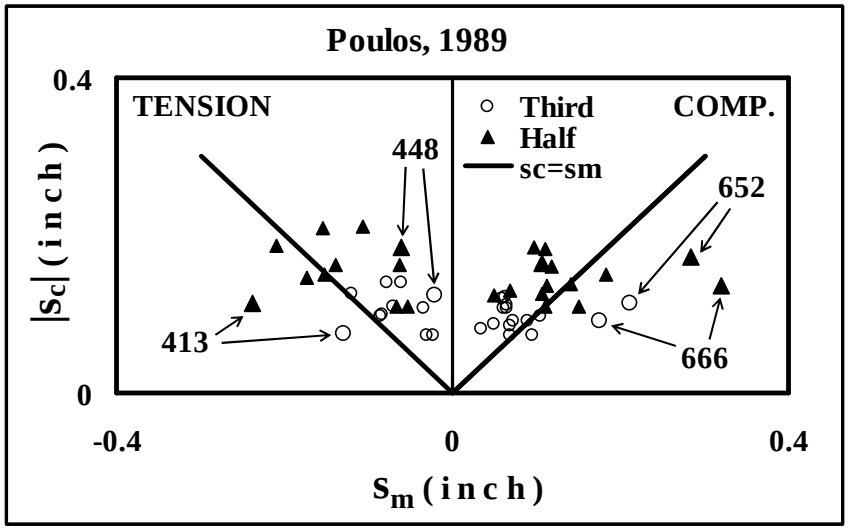

Figure 5.5 Comparison of measured and predicted displacements.

5.2.4 Displacement Ratio, s_c/s_m

The average and standard deviation of the displacement ratio for all investigated correlations at load ratios up to a half are given in Table 5.2 and shown in Figure 5.6.

Predictions can be ranked from one (best) to seven (worst) based on their relative performances (Table 5.3). An overall conclusion on the best correlation may be obtained by looking at rankings from both load ratios. The absolute difference of the displacement ratios from $s_c/s_m = 1$ is calculated to rank the mean values.

The top four predictive methods based on the rankings at both load ratios are as follows: elastic column, Aschenbrener (1984), Poulos (1989), and Poulos (1972, driven piles). These findings coincide with conclusions reached by a visual inspection of the displacements.

Table 5.2 The statistics of displacement ratio (s_c/s_m) (N = 26).

Load Ratio	Value	Poulos (1989)	Poulos (1972) (driven)	Poulos (1972) (bored)	Aschenbrener (1984)	Callanan/ Kulhawy 1985; Johnson 1986	Frank 1985	Elastic column
⅓	Mean, $\bar{x}$	1.76	1.81	3.09	1.15	2.44	3.25	1.63
	Stand. Dev., s_x	1.14	1.33	2.70	1.18	1.68	2.54	0.64
½	Mean, $\bar{x}$	1.42	1.46	2.49	0.89	1.97	1.77	1.36
	Stand. Dev., s_x	0.67	0.80	1.69	0.61	1.00	1.22	0.41

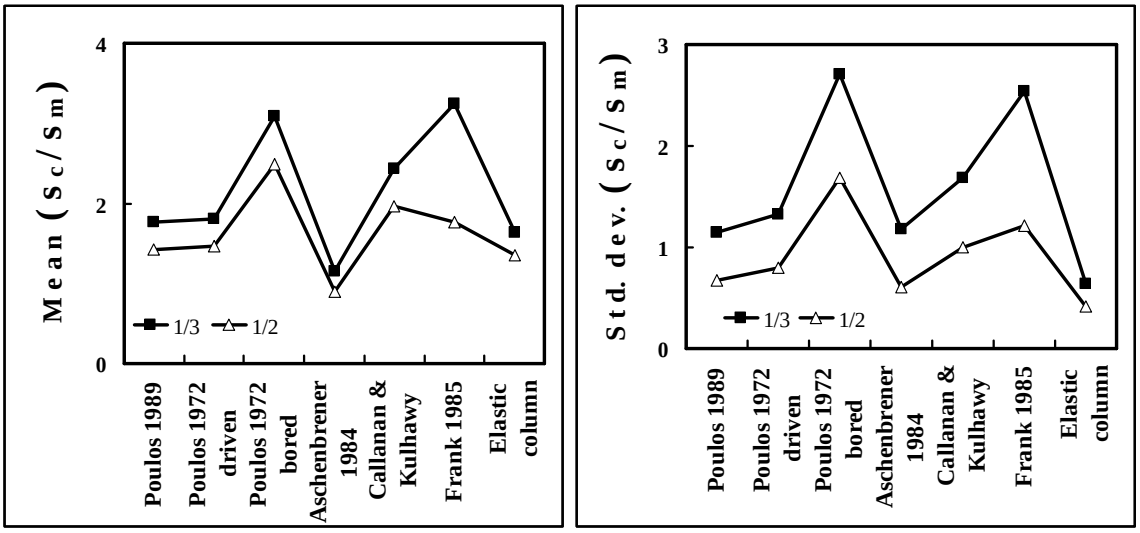

Figure 5.6 Comparison of correlations based on mean and standard deviation of displacement ratio (s_c/s_m).

Table 5.3 Ranking of correlations based on displacement ratio (s_c/s_m).

Load Ratio	Value	Poulos (1989)	Poulos (1972) (driven)	Poulos (1972) (bored)	Aschenbrener (1984)	Callanan/ Kulhawy 1985; Johnson 1986	Frank 1985	Elastic column
⅓	Mean[1], $\bar{x}$	3	4	6	1	5	7	2
	Stand. Dev., s_x	2	4	7	3	5	6	1
½	Mean, $\bar{x}$	3	4	7	1	6	5	2
	Stand. Dev., s_x	3	4	7	2	5	6	1

[1] Absolute difference from (s_c/s_m) = 1 used for ranking mean values.

Three correlations of Young's modulus result in much larger errors in terms of displacement ratios: Callanan and Kulhawy (1985)/Johnson (1986), Poulos (1972, bored pile) and Frank (1985) (Figure 5.6). Poulos (1972) especially leads to higher predicted displacements than those measured in pile load tests. The correlation of Callanan and Kulhawy and Poulos are derived from the results of load tests on bored piles, which typically require larger displacements than driven piles to mobilize their full side and tip capacity. Thus, both tend to overestimate displacements for driven piles. Frank's method, on the other hand, takes only the diameter of the pile into consideration and has a large variability when compared against measured displacements.

5.2.5 Displacement Difference, s_c-s_m

Differences in displacements are useful in evaluating a method, especially when small displacements are considered. Even a minor error in prediction may cause a large displacement ratio to be calculated although the differences may actually be trivial.

Average and standard deviation of the displacement differences are tabulated in Table 5.4 and shown in Figure 5.7. The mean values of displacement differences for each prediction are not large and the standard deviation does not change significantly for

increased loading. Based on the averages of displacement differences, all of the correlations perform reasonably well and close to each other in terms of average values and standard deviations. Hence, rankings would not necessarily reflect actual superiority of any correlation, and therefore, are not presented. However, it should be noted that the three correlations (Poulos, 1972 bored; Callanan and Kulhawy, 1985/Johnson, 1986; and Frank, 1985) that resulted in high displacement ratios do not have high displacement differences on an average; however their standard deviations the three highest among all of the correlations that were considered. The reason for average differences that are close to zero is the existence of similarly high positive and negative values.

Table 5.4 The statistics for displacement differences (s_c-s_m) (inch) (N = 26).

Load Ratio	Parameter	Poulos, (1989)	Poulos, (1972) (driven)	Poulos, (1972) (bored)	Aschenbrener, (1984)	Callanan/ Kulhawy, 1985; Johnson, 1986	Frank, 1985	Elastic column
⅓	Mean, $\bar{x}$	-0.01	-0.01	-0.01	-0.02	-0.01	0.00	0.00
	Stand. Dev., s_x	0.05	0.06	0.12	0.05	0.08	0.13	0.05
½	Mean, $\bar{x}$	0.02	0.02	0.06	0.02	0.04	0.06	0.03
	Stand. Dev., s_x	0.04	0.05	0.09	0.05	0.06	0.09	0.04

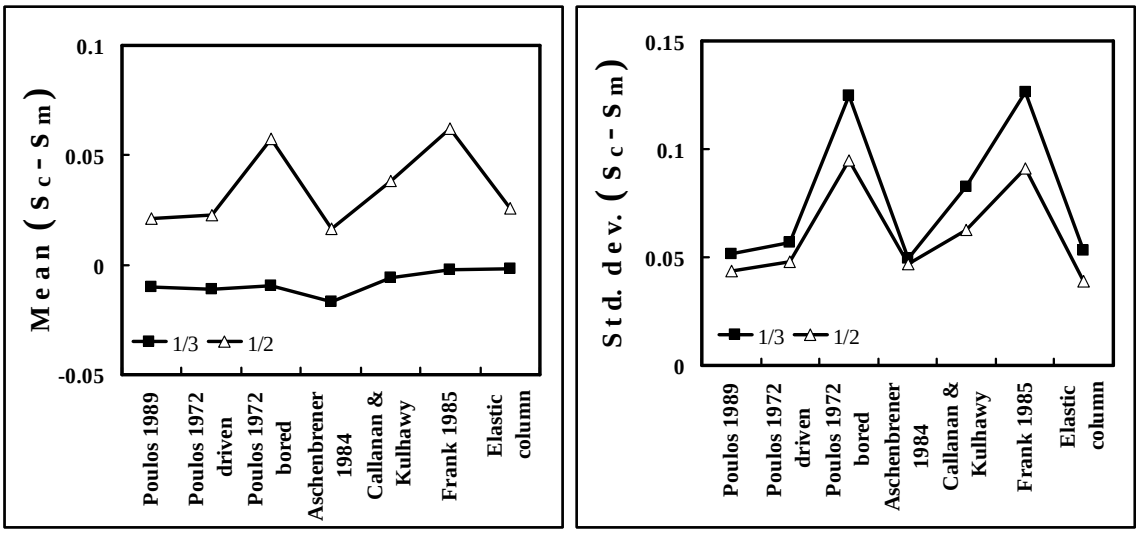

Figure 5.7 Comparison of correlations based on mean and standard deviation of displacement differences (s_c-s_m) (both in inches).

5.2.6 Outliers

Within the context of this dissertation, an outlier is defined as a prediction that deviates significantly from the displacement equality line ($s_c = s_m$) and can be ascertained by having both of the following properties:

1) a displacement ratio (s_c/s_m) that has an absolute error in excess of 20%, i.e., $0.80s_m \geq s_c$ or $s_c \geq 1.2s_m$; as well as

2) an absolute displacement difference $\left|(s_c - s_m)\right|$ larger than 0.1 inches.

Of these two criteria, the displacement difference is more influential than the displacement ratio in determining outliers.

Four tests (one high and three low in terms of s_c/s_m) consistently produce outliers for most, if not all, of the correlations and load ratios of up to a half (Table 5.5 and shown with larger symbols in Figure 5.5). They are investigated in further detail to identify properties which may explain the larger discrepancy.

Table 5.5 Comparison of predicted and measured displacements for outliers.

Load Test Number (LTN)	Load Ratio	Displ. Ratio or Diff. (inch)	Poulos (1989)	Poulos (1972) (driven)	Poulos (1972) (bored)	Aschenbrener (1984)	Callanan/ Kulhawy 1985; Johnson 1986	Frank 1985	Elastic column
413	⅓	s_c/s_m	***0.58***†	***0.68***	***0.46***	***0.32***	***0.80***	***1.85***	1.01
		$\|s_c-s_m\|$	0.05	0.04	0.07	0.09	0.03	***0.11***	0
	½	s_c/s_m	***0.48***	***0.56***	***0.38***	***0.26***	***0.66***	1.01	0.83
		$\|s_c-s_m\|$	***0.12***	***0.10***	***0.15***	***0.18***	0.08	0	0.04
448	⅓	s_c/s_m	***5.69***	***6.49***	***12.94***	***6.01***	***8.46***	***11.09***	***2.83***
		$\|s_c-s_m\|$	***0.10***	***0.12***	***0.26***	***0.11***	***0.16***	***0.22***	0.04
	½	s_c/s_m	***3.05***	***3.48***	***6.93***	***3.22***	***4.54***	***3.96***	***1.52***
		$\|s_c-s_m\|$	***0.12***	***0.15***	***0.36***	***0.13***	***0.21***	***0.18***	0.03
652	⅓	s_c/s_m	***0.52***	***0.49***	***0.80***	***0.29***	***0.74***	0.92	0.86
		$\|s_c-s_m\|$	***0.10***	***0.10***	0.04	***0.13***	0.07	0.07	0.09
	½	s_c/s_m	***0.60***	***0.59***	0.91	***0.41***	***0.77***	***0.49***	***0.65***
		$\|s_c-s_m\|$	***0.11***	***0.12***	0.03	***0.17***	0.06	***0.14***	***0.10***
666	⅓	s_c/s_m	***0.52***	***0.49***	***0.86***	***0.29***	***0.74***	0.92	0.86
		$\|s_c-s_m\|$	0.08	0.09	0.02	0.12	0.05	0.01	0.02
	½	s_c/s_m	***0.43***	***0.40***	***0.71***	***0.24***	***0.60***	***0.50***	***0.71***
		$\|s_c-s_m\|$	***0.18***	***0.19***	0.09	***0.25***	***0.13***	***0.16***	0.09

† Outliers are bold-faced and italicized

The following factors are investigated for the outliers: 1) soil layering, 2) total length (L), 3) diameter (D), 4) L/D ratio, and 5) stiffness (A_pE_p/L, where A_p is cross-sectional area and E_p is Young's modulus of pile).

Relevant information from the FinalCT database for the load tests, including soil layering along the length of the pile, is presented in Table 5.6. The first pile (LTN: 413) was driven into a soil profile with three layers of sand constituting 8% of the side area of the pile and 9% of the total capacity. Three of the four piles were driven through a larger casing at the top.

The distribution of the pile diameter versus s_c/s_m is presented for predictions made using Poulos' (1989) correlation, which exemplifies the outcome of all correlations and of the other three parameters considered (Figure 5.8). The range of values for all piles

driven in cohesive soils is compared to that for outliers in Table 5.7. None of the investigated parameters provides a clear explanation for the outliers.

Table 5.6 Details of pile load tests that have been investigated further.

LTN	Type	Sect.	C/T	L	DR	AE/L	W	D	Q_f	S_{fail}	Setup	Layer	Soil	h	c_u/N
413	STLP	CIRC	T	75.5	1.04	1184	9.5	24	455	1.48	14	1	Clay	4	0.3
												2	Clay	15	1.77
												3	Sand	3	29
												4	Clay	25	3.15
												5	Sand	2	23
												6	Clay	4	2.54
												7	Sand	1	20
												8	Clay	12.5	3.81
LTN	**Type**	**Sect.**	**C/T**	**L**	**DR**	**AE/L**	**W**	**D**	**Q_f**	**S_{fail}**	**Setup**	**Layer**	**Soil**	**h**	**c_u/N**
448	STLP	CIRC	T	92.7	0.12	1324	40.7	24	203	0.87	35	1	Clay	4.3	0.9
												2	Clay	5	0.63
												3	Clay	5	0.51
												4	Clay	5	0.74
												5	Clay	15	0.53
												6	Clay	10	0.58
												7	Clay	25	0.81
												8	Clay	9.7	0.87
LTN	**Type**	**Sect.**	**C/T**	**L**	**DR**	**AE/L**	**W**	**D**	**Q_f**	**S_{fail}**	**Setup**	**Layer**	**Soil**	**h**	**c_u/N**
652	CONC	SQRE	C	105.5	1	674	22.3	14	272	0.72	N/A	1	Clay	25	0.65
												2	Clay	40	1.5
												3	Clay	15	1
												4	Clay	5.5	2
LTN	**Type**	**Sect.**	**C/T**	**L**	**DR**	**AE/L**	**W**	**D**	**Q_f**	**S_{fail}**	**Setup**	**Layer**	**Soil**	**h**	**c_u/N**
666	STLP	CIRC	C	85	0.12	693	9.2	16	323	1.67	1553	1	Clay	82.1	0.33
												2	Clay	2.9	1.5

LTN : Load test number (arbitrary number identifying the test)
Type : Pile type (CONC: concrete, STLP: steel pipe pile, HPIL: H-pile etc.)
Sect. : Pile cross-section (SQRE: square, CIRC: circular etc.)
C/T : Pile load test direction: tension (T) or compression (C)
L : Length of pile penetrated in soil (feet)
DR : Displacement ratio (1 for solid pile, >1 for oversized cover plates)
AE/L : Pile spring constant, stiffness (kips/inch)
W : Weight of pile submerged in soil (kips)
D : Pile diameter (inch)
Q_f : Plunging failure load (kips)
S_{fail} : Displacement at plunging load (inch)
Setup : Set up time, time from end of driving to start of test, N/A if not known (days)

Layer : The number of soil layer along the length of the pile
Soil : Type of soil described by four letters: e.g. Clay, Sand, etc.
h : Layer height (feet)
c_u/N : Undrained shear strength for Clay (ksf); standard penetration blow count for Sand (bpf)

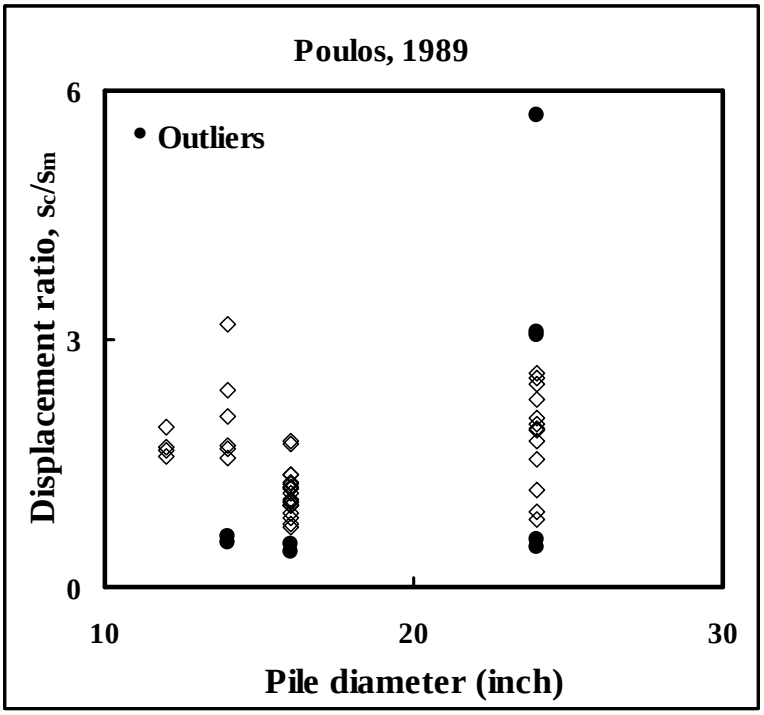

Figure 5.8 Pile diameter versus displacement ratio for outliers.

Table 5.7 Range of parameters for all pile load tests in clay compared to those for outliers.

Parameter	Range from All Tests in Clay (min – max)	Values for outliers			
		413	448	652	666
Pile length, L (ft)	51.2 – 110.8	75.5	100	105.5	110.2
Pile diameter, D (inch)	49.3 – 90.8	66.5	79	85.5	90.2
L/D	34.5 – 90.9	37.8	50	90.4	82.7
Pile stiffness, AE/L (kips/inch)	674 – 1559	1184	1324	674	693

5.3 COHESIONLESS SOILS

Thirty-four load tests driven into cohesionless soils were investigated (see Chapter 4 for details).

5.3.1 Magnitude of Displacements

For load ratios up to a half, all of the measured displacements are less than 0.5 inches (Figure 5.9).

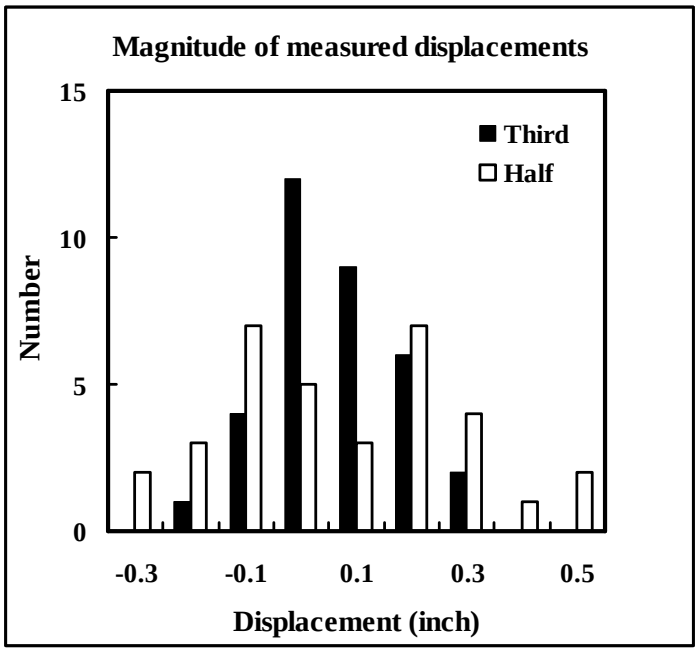

Figure 5.9 The magnitude of measured displacements for load ratios up to a half.

The s_m/D ratios are presented in Figure 5.10 for load ratios of a third and a half. For a load ratio of a third, all but one of the measurements are less than 1.5% of the pile diameter. However, for a load ratio of a half, approximately 25% of the measurements are larger than 1.5% of the pile diameter.

Direct estimation of displacements of a pile by a percentage of its diameter has a higher variability for piles in sandy soils than for piles in clayey soils. Thus, for piles driven into sandy soils, the s_m/D ratio of 1.5% may be used as an upper limit of predicted displacements for load ratios up to a third, whereas the same ratio is valid up to a load ratio of a half for piles in clayey soils. The larger s_m/D ratio for piles in cohesionless soils may be due to differences in how pile responds to increased loading; piles in sandy soils typically require larger displacements to develop tip capacity.

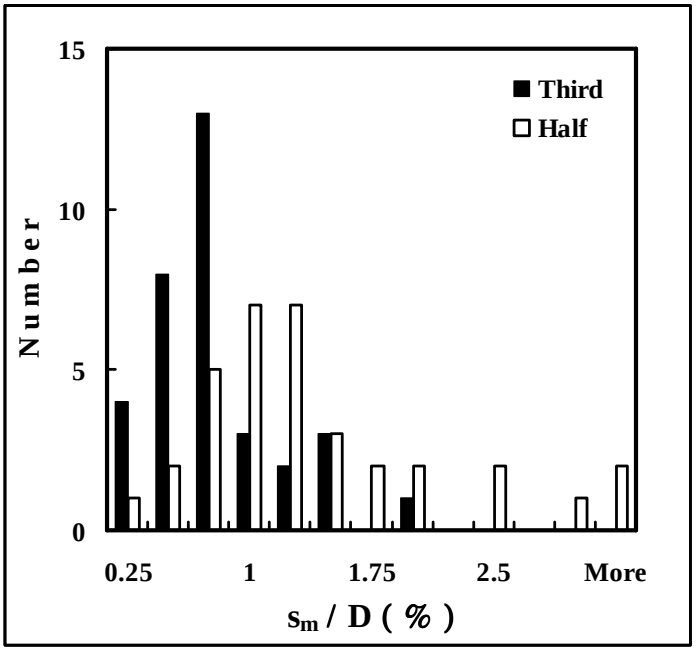

Figure 5.10 Measured displacements over pile diameter for piles in cohesionless soils.

5.3.2 Correlations

The correlations utilized for predicting displacements in cohesionless soils are listed in Table 5.8 and shown in Figure 5.11.

There is a wide range of values for Young's modulus correlated with SPT blow count. Part of the variability lies in the fact that there are many sources of error in standard penetration testing as outlined in Section 3.7.2. Some of the suggested correlations were developed by directly relating blow counts from SPT's to the value of Young's modulus, or shear modulus, determined from pressuremeters, screw-plates or geophysical measurements. The relationship can not be perfect especially when Young's modulus converted from a shear modulus at small strain is correlated with the N value from a standard penetration test at large strains.

Table 5.8 Correlations for Young's modulus, E_s with SPT blow count (N in bpf).

Pile Install.	E_s (ksf)[†]	Reference	Notes/Method
Driven	4N[‡]	Komornik (1974)*	Israeli experience, derived from pressuremeter results and correlating them with SPT N obtained at the same sites.
	(2.5-2.8)N	Shioi & Fukui (1982)*	Japanese railway and bridge standards
	(2.5[†]±0.5)N	Decourt et al. (1989)*	Pile-soil interface, Brazilian experience
All	$150\sqrt{N}$	Denver (1982)	Average of pressuremeter and screw-plate tests and correlated to SPT N obtained at the sites.
All	400+16N	D'Appolonia et al. (1970)	Normally consolidated (NC) sand, case studies involving structural displacements
All	750+20N	D'Appolonia et al. (1970)*	Preloaded, i.e., overconsolidated (OC) sand, case study
Driven	150N-1900	Christoulas (1988)	N>15, valid for piles that are not tapered.
Driven	25N+375	Yamashita et al. (1987)*	Cast-in-place concrete, side
Driven	0.4N (625 ksf max)	Yamashita et al. (1987)*	Cast-in-place concrete, tip
Driven	$1250+65N_s$	Kurkur (1986)*	N_s: average N along pile shaft. Valid at 50% of failure load.

[*] Used for mixed profiles
[†] Some correlations originally given in MPa, converted by the writer
[‡] N values not corrected for the effective stress increases with depth or the applied hammer energy

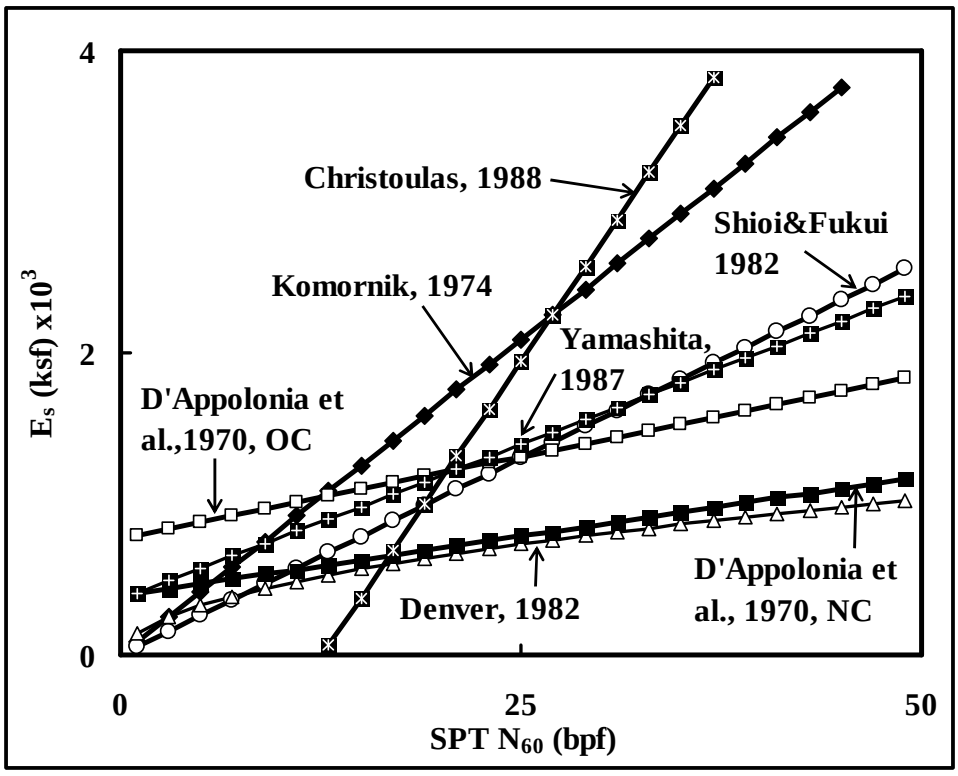

Figure 5.11 Correlations of SPT blow count with Young's modulus of soil.

5.3.3 Predictions versus Measurement

A comparison of measured displacements with those predicted using Komornik's (1974) correlation, for a load ratio up to a half, are shown in Figure 5.12. Overall, the measured and calculated displacements agree well with each other and are, for the most part, similar to the outcome obtained from the other correlations that were investigated.

The absolute values of the displacements are less than 0.5 inches. The direction of the pile loading does not seem to have an effect on the predicted displacements in terms of the errors observed. Displacements estimated at a load ratio of a third conform better to the measured displacements than those at a load ratio of a half. There is an overall tendency to predict smaller displacements than those measured in pile load tests. The

only exception is obtained from the elastic column approach, which generally suggests higher displacements than the measured ones.

Only the outliers for a load ratio of a half are marked in Figure 5.12 to avoid clutter. Further discussion of these pile load tests is provided in section 5.3.6.

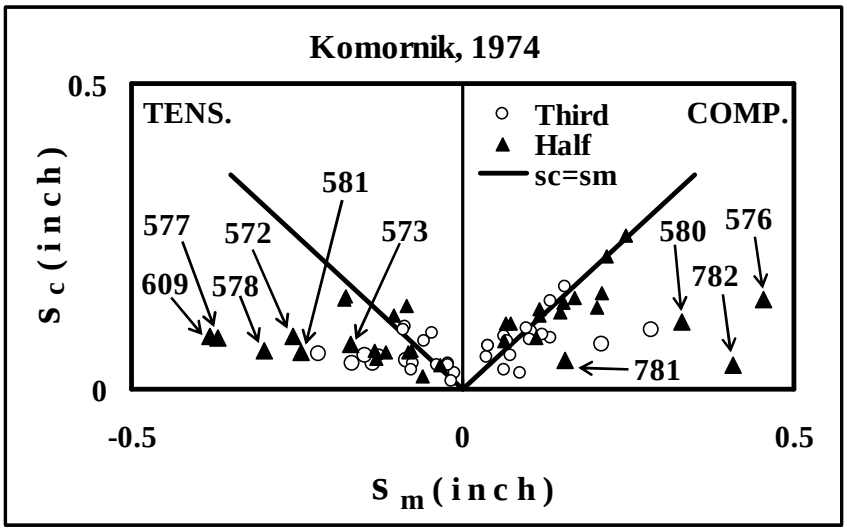

Figure 5.12 Measured and predicted displacements for piles in sandy soils.

5.3.4 Displacement Ratio, s_c/s_m

The mean and standard deviation of the displacement ratio for all investigated correlations loaded up to a load ratio of a half are listed in Table 5.9 and shown in Figure 5.13.

Predictions using the correlation suggested by Christoulas (1988) have *a* high mean with a large scatter. Therefore, his method is excluded from further comparisons.

Unlike the correlations for clayey soils, the ranking of correlations for sandy soils does not point toward a specific correlation that works for load ratios of a third and a half (Table 5.10). For example, the predictions using Komornik's correlation are most

accurate for the load ratio of a third. However, its ranking drops to sixth when a load ratio of a half is considered.

Kurkur's predictions have the smallest standard deviation for both load ratios, which may be due to the single averaged value of SPT N utilized for all soil layers, based on their thicknesses, which prevents errors that may occur when the properties of layers vary significantly.

Table 5.9 Mean and standard deviation for correlations (N = 34).

Load Ratio	Value	Komor-nik, 1974	Shioi/ Fukui, 1982; Decourt, 1989	Den-ver, 1982	D'Appo-lonia et al., 1970 (NC)	D'Appo-lonia et al., 1970 (OC)	Chris-toulas, 1988	Yamas-hita et al., 1987	Kur-kur, 1986	Frank, 1985	Elastic column
⅓	Mean, $\overline{x}$	0.97	1.26	1.86	1.62	1.19	18.19	1.16	0.79	2.74	1.24
	St. Dev., s_x	0.58	0.80	1.23	1.16	0.75	91.96	0.71	0.48	2.88	0.62
½	Mean, $\overline{x}$	0.74	0.96	1.43	1.26	0.90	16.92	0.88	0.62	0.94	0.93
	St. Dev., s_x	0.42	0.61	0.91	0.75	0.50	87.24	0.49	0.35	1.19	0.42

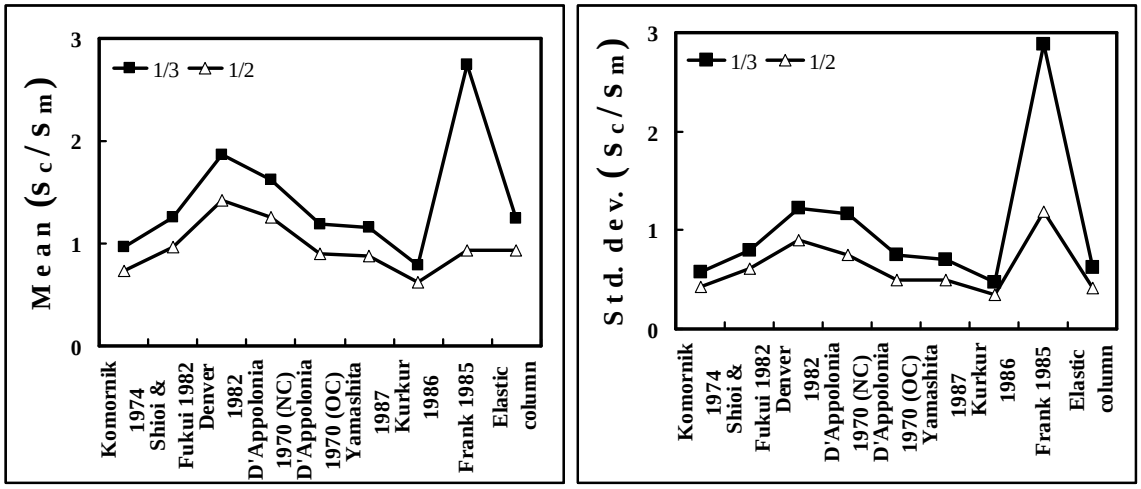

Figure 5.13 Comparison of correlations based on mean and standard deviation of displacement ratio (s_c/s_m).

Table 5.10 Rankings corresponding to each correlation.

Load Ratio	Value	Komor-nik, 1974	Shioi/ Fukui, 1982; Decourt, 1989	Den-ver, 1982	D'Appo-lonia et al., 1970 (NC)	D'Appo-lonia et al., 1970 (OC)	Yamas-hita et al., 1987	Kur-kur, 1986	Frank, 1985	Elastic column
⅓	Mean, $\overline{x}$	1	6	8	7	3	2	4	9	5
	St. Dev., s_x	2	6	8	7	5	4	1	9	3
½	Mean, $\overline{x}$	7	1	9	6	3	4	8	5	2
	St. Dev., s_x	3	6	9	7	5	4	1	8	2

5.3.5 Displacement Difference, s_c-s_m

The mean and standard deviation of displacement differences for all of the investigated methods vary within a narrow margin at load ratios of a third and a half (Table 5.11 and Figure 5.14).

Seven out of nine methods have positive displacement differences, i.e., the calculated displacements are higher than the ones that are measured. Although the scatter increases when a load ratio of a half is considered, displacement differences remain approximately constant. The ranking of displacement differences is of little value because the outcomes are similar.

The correlations produce acceptable results as far as the differences between predicted and measured displacements at working loads are concerned.

Table 5.11 The statistics of displacement difference (s_c-s_m) for comparison with correlations in cohesionless soils (N = 34).

Load Ratio	Value (inch)	Komor-nik, 1974	Shioi/ Fukui, 1982; Decourt, 1989	Den-ver, 1982	D'Appo-lonia et al., 1970 (NC)	D'Appo-lonia et al., 1970 (OC)	Yamas-hita et al., 1987	Kur-kur, 1986	Frank, 1985	Elastic column
⅓	Mean, $\overline{x}$	0.00	0.01	0.02	0.02	0.01	0.01	0.00	-0.02	-0.01
	St. Dev., s_x	0.06	0.06	0.07	0.07	0.06	0.06	0.07	0.09	0.06
½	Mean, $\overline{x}$	0.01	0.02	0.05	0.04	0.02	0.02	0.01	-0.02	-0.01
	St. Dev., s_x	0.14	0.13	0.15	0.13	0.13	0.13	0.14	0.11	0.10

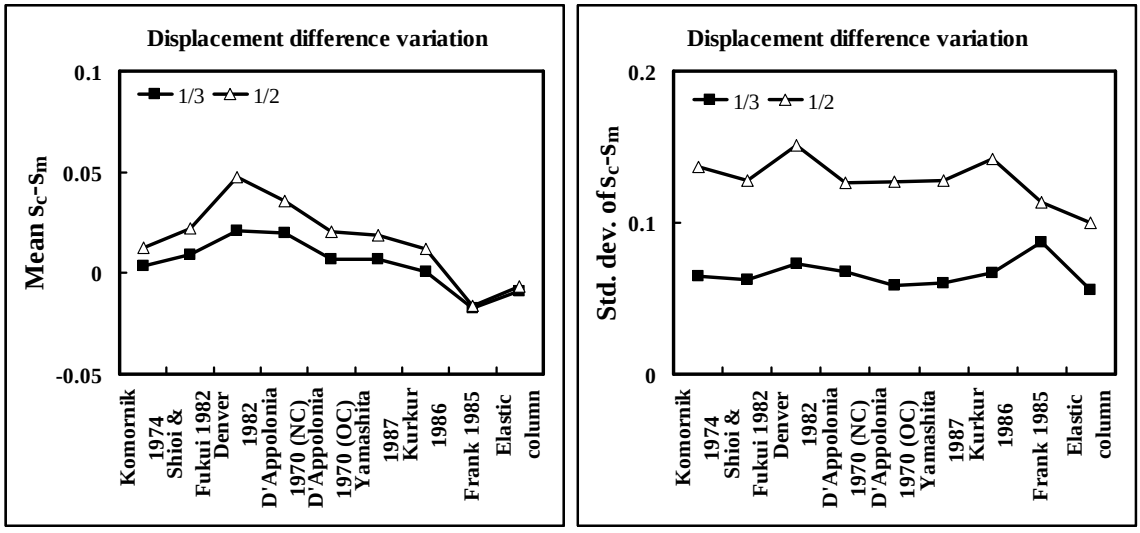

Figure 5.14 Comparison of predictions based on mean and standard deviation of displacement difference (s_c-s_m).

5.3.6 Outliers

Ten pile load tests (six tension and four compression) out of 34 are outside the criteria established for cohesive soils in section 5.2.6 and may benefit from a closer

investigation (Table 5.12). Other relevant information for each pile load test, including the soil layering, is presented in Table 5.13.

Table 5.12 Displacement ratio and difference for outliers.

Load Test Number (LTN)	Load Ratio	Displ. Ratio or Diff. (inch)	Komor-nik, 1974	Shioi/ Fukui, 1982; Decourt, 1989	Den-ver, 1982	D'Appo-lonia et al., 1970 (NC)	D'Appo-lonia et al., 1970 (OC)	Yamas-hita et al., 1987	Kur-kur, 1986	Frank, 1985	Elastic column
572	⅓	s_c/s_m	***0.45***†	***0.56***	***0.81***	***0.75***	***0.57***	***0.54***	***0.41***	***1.27***	***2.13***
		$\lvert s_c-s_m\rvert$	0.07	0.06	0.02	0.03	0.05	0.06	0.07	-0.03	***-0.14***
	½	s_c/s_m	***0.33***	***0.41***	***0.60***	***0.55***	***0.42***	***0.40***	***0.30***	***0.62***	***1.56***
		$\lvert s_c-s_m\rvert$	***0.17***	***0.15***	***0.10***	***0.12***	***0.15***	***0.15***	***0.18***	***0.10***	***-0.14***
573	⅓	s_c/s_m	***0.57***	***0.71***	1.00	0.92	***0.70***	***0.68***	***0.53***	***1.67***	***2.76***
		$\lvert s_c-s_m\rvert$	0.04	0.02	0.00	0.01	0.02	0.03	0.04	-0.06	***-0.15***
	½	s_c/s_m	***0.43***	***0.53***	***0.74***	***0.68***	***0.52***	***0.50***	***0.40***	0.82	***2.05***
		$\lvert s_c-s_m\rvert$	***0.10***	0.08	0.04	0.05	0.08	0.08	***0.10***	0.03	***-0.18***
576	⅓	s_c/s_m	***0.34***	***0.40***	***0.61***	***0.55***	***0.43***	***0.40***	***0.32***	***0.56***	***1.41***
		$\lvert s_c-s_m\rvert$	***-0.19***	***-0.17***	***-0.11***	***-0.13***	***-0.16***	***-0.17***	***-0.20***	***-0.13***	***0.12***
	½	s_c/s_m	***0.32***	***0.38***	***0.58***	***0.52***	***0.41***	***0.38***	***0.32***	***0.35***	***1.33***
		$\lvert s_c-s_m\rvert$	***-0.31***	***-0.28***	***-0.19***	***-0.22***	***-0.27***	***-0.28***	***-0.31***	***-0.30***	***0.15***
577	⅓	s_c/s_m	***0.26***	***0.31***	***0.47***	***0.43***	***0.33***	***0.31***	***0.24***	***0.74***	1.09
		$\lvert s_c-s_m\rvert$	***0.16***	***0.15***	***0.12***	***0.12***	***0.15***	***0.15***	***0.17***	0.06	-0.02
	½	s_c/s_m	***0.23***	***0.27***	***0.41***	***0.37***	***0.29***	***0.27***	***0.22***	***0.43***	0.96
		$\lvert s_c-s_m\rvert$	***0.28***	***0.27***	***0.22***	***0.23***	***0.26***	***0.27***	***0.29***	***0.21***	0.02
578	⅓	s_c/s_m	***0.25***	***0.32***	***0.50***	***0.45***	***0.32***	***0.31***	***0.20***	0.97	***1.71***
		$\lvert s_c-s_m\rvert$	***0.12***	***0.11***	0.08	0.09	***0.11***	***0.11***	***0.13***	0.01	***-0.12***
	½	s_c/s_m	***0.21***	***0.27***	***0.42***	***0.38***	***0.27***	***0.26***	***0.18***	***0.53***	***1.42***
		$\lvert s_c-s_m\rvert$	***0.24***	***0.22***	***0.18***	***0.19***	***0.22***	***0.22***	***0.25***	***0.14***	***-0.13***
580	⅓	s_c/s_m	***0.35***	***0.42***	***0.61***	***0.57***	***0.43***	***0.41***	***0.31***	***0.67***	***1.38***
		$\lvert s_c-s_m\rvert$	***-0.14***	***-0.12***	-0.08	-0.09	***-0.12***	***-0.12***	***-0.15***	-0.07	0.08
	½	s_c/s_m	***0.33***	***0.40***	***0.58***	***0.54***	***0.41***	***0.39***	***0.31***	***0.42***	***1.31***
		$\lvert s_c-s_m\rvert$	***-0.22***	***-0.20***	***-0.14***	***-0.15***	***-0.19***	***-0.20***	***-0.23***	***-0.19***	***0.10***
581	⅓	s_c/s_m	***0.30***	***0.36***	***0.53***	***0.49***	***0.38***	***0.36***	***0.26***	1.04	***1.20***
		$\lvert s_c-s_m\rvert$	0.09	0.09	0.06	0.07	0.08	0.09	***0.10***	-0.01	-0.03
	½	s_c/s_m	***0.25***	***0.30***	***0.44***	***0.41***	***0.31***	***0.30***	***0.23***	***0.58***	0.99
		$\lvert s_c-s_m\rvert$	***0.18***	***0.17***	***0.14***	***0.14***	***0.17***	***0.17***	***0.19***	***0.10***	0.00
609	⅓	s_c/s_m	***0.38***	***0.44***	***0.73***	***0.64***	***0.46***	***0.45***	***0.27***	***1.26***	***0.59***
		$\lvert s_c-s_m\rvert$	0.09	0.08	0.04	0.05	0.08	0.08	***0.11***	-0.04	0.06
	½	s_c/s_m	***0.23***	***0.27***	***0.43***	***0.38***	***0.28***	***0.27***	***0.18***	***0.49***	***0.34***
		$\lvert s_c-s_m\rvert$	***0.29***	***0.28***	***0.22***	***0.24***	***0.27***	***0.28***	***0.31***	***0.19***	***0.25***
781	⅓	s_c/s_m	***0.51***	***0.74***	1.04	0.93	***0.59***	***0.63***	***0.38***	***1.93***	0.87
		$\lvert s_c-s_m\rvert$	-0.03	-0.02	0.00	0.00	-0.03	-0.02	-0.04	0.06	-0.01

Load Test Number (LTN)	Load Ratio	Displ. Ratio or Diff. (inch)	Komor-nik, 1974	Shioi/ Fukui, 1982; Decourt, 1989	Den-ver, 1982	D'Appo-lonia et al., 1970 (NC)	D'Appo-lonia et al., 1970 (OC)	Yamas-hita et al., 1987	Kur-kur, 1986	Frank, 1985	Elastic column
	½	s_c/s_m	***0.31***	***0.45***	***0.63***	***0.56***	***0.36***	***0.38***	***0.23***	***0.78***	***0.52***
		$\|s_c-s_m\|$	***-0.11***	-0.09	-0.06	-0.07	***-0.10***	***-0.10***	***-0.12***	-0.03	-0.07
782	⅓	s_c/s_m	***0.30***	***0.44***	***0.62***	***0.55***	***0.35***	***0.37***	***0.23***	***1.37***	***0.50***
		$\|s_c-s_m\|$	-0.06	-0.05	-0.03	-0.04	-0.06	-0.06	-0.07	0.03	-0.04
	½	s_c/s_m	***0.10***	***0.14***	***0.20***	***0.18***	***0.11***	***0.12***	***0.07***	***0.29***	***0.16***
		$\|s_c-s_m\|$	***-0.37***	***-0.35***	***-0.33***	***-0.33***	***-0.36***	***-0.36***	***-0.38***	***-0.29***	***-0.34***

† Outliers are given in bold and italics.

Table 5.13 Properties and soil layering for outlying pile load tests.

LTN	Type	Sect.	C/T	L	DR	AE/L	W	D	Q_f	S_{fail}	Setup	Layer	Soil	h	N
572	STLP	CIRC	T	91.1	0.12	610	12.8	16	476	1.32	6	1	SaSi	6.5	25
												2	SaSi	15	15
												3	Sand	5	20
												4	Sand	21.5	8
												5	Sand	6.5	8
												6	Sand	8	14
												7	Sand	11	24
												8	Sand	7	18
												9	Sand	5	34
												10	Sand	5.6	55
LTN	**Type**	**Sect.**	**C/T**	**L**	**DR**	**AE/L**	**W**	**D**	**Q_f**	**S_{fail}**	**Setup**	**Layer**	**Soil**	**h**	**N**
573	STLP	CIRC	T	85.0	0.12	499	7.6	14	341	1.62	7	1	SaSi	6.5	25
												2	SaSi	15	15
												3	Sand	5	20
												4	Sand	21.5	8
												5	Sand	6.5	8
												6	Sand	8	14
												7	Sand	11	24
												8	Sand	7	18
												9	Sand	4.5	34
LTN	**Type**	**Sect.**	**C/T**	**L**	**DR**	**AE/L**	**W**	**D**	**Q_f**	**S_{fail}**	**Setup**	**Layer**	**Soil**	**h**	**N**
576	STLP	CIRC	C	48.5	0.12	583	13.8	16	720	1.85	4	1	Sand	6	16
												2	Sand	7	8
												3	SaSi	7	14
												4	SaSi	5	27
												5	SaSi	5	32

												6	SaSi	10	69
												7	SaSi	6	42
												8	SaSi	2.5	68
LTN	**Type**	**Sect.**	**C/T**	**L**	**DR**	**AE/L**	**W**	**D**	**Q_f**	**S_{fail}**	**Setup**	**Layer**	**Soil**	**h**	**N**
577	STLP	CIRC	T	48.5	0.12	583	13.8	16	398	1.50	4	1	Sand	6	16
												2	Sand	7	8
												3	SaSi	7	14
												4	SaSi	5	27
												5	SaSi	5	32
												6	SaSi	10	69
												7	SaSi	6	42
												8	SaSi	2.5	68
LTN	**Type**	**Sect.**	**C/T**	**L**	**DR**	**AE/L**	**W**	**D**	**Q_f**	**S_{fail}**	**Setup**	**Layer**	**Soil**	**h**	**N**
578	STLP	CIRC	T	92.5	0.12	583	13.9	16	483	0.98	2	1	SiSa	13	20
												2	SiSa	4	19
												3	SiSa	5	6
												4	SiSa	6	14
												5	Grav	5	46
												6	SiSa	6	32
												7	SiSa	6	12
												8	SiSa	8	16
												9	SiSa	7	8
												10	SiSa	7	14
												11	SiSa	5	27
												12	SiSa	5	32
												13	SiSa	10	69
												14	SiSa	5.5	42
LTN	**Type**	**Sect.**	**C/T**	**L**	**DR**	**AE/L**	**W**	**D**	**Q_f**	**S_{fail}**	**Setup**	**Layer**	**Soil**	**h**	**N**
580	STLP	CIRC	C	43.0	0.12	475	9.7	14	421	1.67	8	1	Sand	6.5	16
												2	Sand	7	8
												3	Sand	7	14
												4	Sand	5	27
												5	Sand	5	32
												6	Sand	10	69
												7	Sand	2.5	42
LTN	**Type**	**Sect.**	**C/T**	**L**	**DR**	**AE/L**	**W**	**D**	**Q_f**	**S_{fail}**	**Setup**	**Layer**	**Soil**	**h**	**N**
581	STLP	CIRC	T	43.0	0.12	475	9.7	14	220	1.70	8	1	Sand	6.5	16
												2	Sand	7	8
												3	Sand	7	14
												4	Sand	5	27

												5	Sand	5	32
												6	Sand	10	69
												7	Sand	2.5	42
LTN	**Type**	**Sect.**	**C/T**	**L**	**DR**	**AE/L**	**W**	**D**	**Q_f**	**S_{fail}**	**Setup**	**Layer**	**Soil**	**h**	**N**
609	HPIL	SQRE	T	18.0	0.16	1160	2.0	10.11	300	2.38	25	1	GvSa	4	24
												2	SaGv	2	59
												3	SaGv	4	50
												4	SaGv	5	27
												5	Grav	3	175
LTN	**Type**	**Sect.**	**C/T**	**L**	**DR**	**AE/L**	**W**	**D**	**Q_f**	**S_{fail}**	**Setup**	**Layer**	**Soil**	**h**	**N**
781	STLP	CIRC	C	39.9	1.04	1117	2.4	12	150	1.56	7	1	SaSi	6.3	13
												2	SaSi	17	12
												3	SaSi	5	24
												4	SaSi	11.6	8
LTN	**Type**	**Sect.**	**C/T**	**L**	**DR**	**AE/L**	**W**	**D**	**Q_f**	**S_{fail}**	**Setup**	**No.**	**Soil**	**h**	**N**
782	STLP	CIRC	C	39.1	1.04	1117	2.4	12	150	1.56	7	1	SaSi	6.3	13
												2	SaSi	17	12
												3	SaSi	5	24
												4	SaSi	10.8	8

LTN : Load test number (arbitrary number identifying the test)
Type : Pile type (CONC: concrete, STLP: steel pipe pile, HPIL: H-pile etc.)
Sect. : Pile cross-section (SQRE: square, CIRC: circular etc.)
C/T : Pile load test direction: tension (T) or compression (C)
L : Length of pile penetrated in soil (feet)
DR : Displacement ratio (1 for solid pile, >1 for oversized cover plates, <1 for open-ended or H-piles)
AE/L : Pile spring constant, stiffness (kips/inch)
W : Weight of pile submerged in soil (kips)
D : Pile diameter (inch)
Q_f : Plunging failure load (kips)
S_{fail} : Displacement at plunging load (inch)
Setup : Set up time, time from end of driving to start of test, N/A if not known (days)
Layer : The number of soil layer along the length of the pile
Soil : Type of soil described by four letters: e.g. Sand, SiSa (silty sand), SaGr (sandy gravel), GvSa (gravelly sand), Grav (gravel), etc.
h : Layer height (feet)
N : Standard penetration blow count (bpf)

Seven out of the ten piles, for which the displacements are outside the established criteria, are open-ended pipes. The rest are a single H-pile and two closed-ended pipe piles.

In Figure 5.15, displacements from Komornik's correlation are used for comparing pile diameter for outliers. These results are typical of those for other investigated correlations and factors.

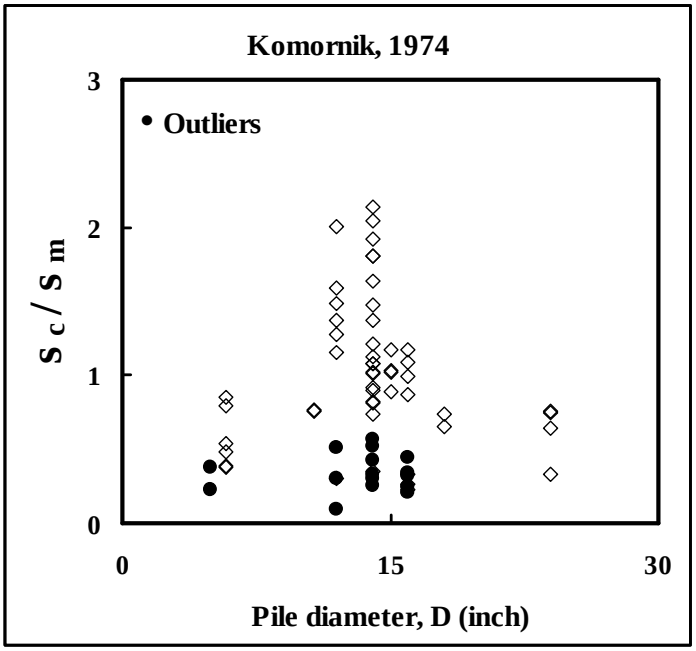

Figure 5.15 Pile diameter and displacement ratio for all tests and outliers.

The only factor investigated which is typical for all of the outliers is pile stiffness, i.e., AE/L, which remains at less than 1200 kips/inch for all of the identified outliers (Figure 5.16). Small pile stiffness produces larger observed displacements of piles that have a large exposed section, which may explain the discrepancy between predicted and measured displacements. None of the other factors indicates any significant effect on the outcome of estimations (Table 5.14).

Table 5.14 Range of parameters for all pile load tests in sand versus that for outliers.

Parameter	Range from All Tests in Sand (max - min)	Load Test Number (LTN)									
		572	573	576	577	578	580	581	609	781	782
Pile length, L (ft)	96.5 - 24	91.1	90.5	95.5	95.5	92.5	89.5	89.5	33	44.9	44.1
Pile diameter, D (inch)	24 – 4.9	16	14	16	16	16	14	14	4.9	12	12
L/D	116.7 - 20	68.3	77.6	71.6	71.6	69.4	76.7	76.7	80.7	44.9	44.1
Pile stiffness, AE/L (kips/inch)	4324 - 475	610	499	583	583	583	475	475	1160	1094	1117

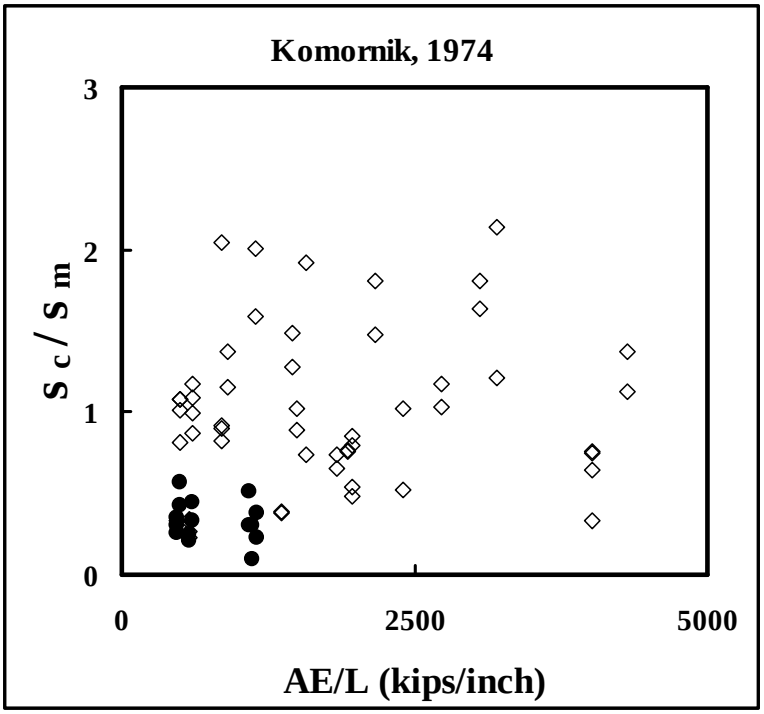

Figure 5.16 The pile stiffness and displacement ratio for all tests and outliers.

The predicted displacements of the outlying pile load tests are almost always less than the measured displacements, i.e., $s_c/s_m < 0.8$ in accordance with the previously

established criteria. A few predictions using Frank's correlation and elastic column are exceptions. Contrary to the tests in cohesive soils, the erroneous estimations may be attributed to one or many of the following factors:

– All but three (LTN's: 572, 573 and 578) of the piles are driven through a larger casing or excavation through the top layers. At Site 2 of I5/I8 Indicator Pile Test Program (LTN's from 576 through 581), the casing depth reached 47 feet. Cased portions of a pile are considered in the Tapile program by assuming that these sections are part of the exposed length of the pile. Therefore, cased sections do not provide any load carrying capacity and displace as a free-standing column. The elastic compression or tension of the exposed pile column is then simply added to the movement of the lower sections of the pile that are in contact with soil. However, the effect of the displacements from the upper sections to the lower sections in is disregarded, which possibly may lead to lower predicted displacements than those measured in pile load tests.

– No borings were conducted at or near the location of the pile load test (LTN: 572, 573 and 609). Consequently, soil profiles and SPT blow counts had to be estimated from pile driving records, for which the accuracy is questionable.

5.4 MIXED PROFILES

FinalCT database contains 83 pile load tests that are driven into mixed profiles.

Displacements of piles driven into mixed soils are predicted using the correlations denoted with (*) in Tables 5.1 and 5.8. Twelve predictions are made for each pile load test at load ratios up to a half.

5.4.1 Magnitude of Displacements

All of the measured displacements are less than |0.35| inches (Figure 5.17). The magnitude of displacements is within a smaller range in mixed profiles than those in clayey or sandy soils.

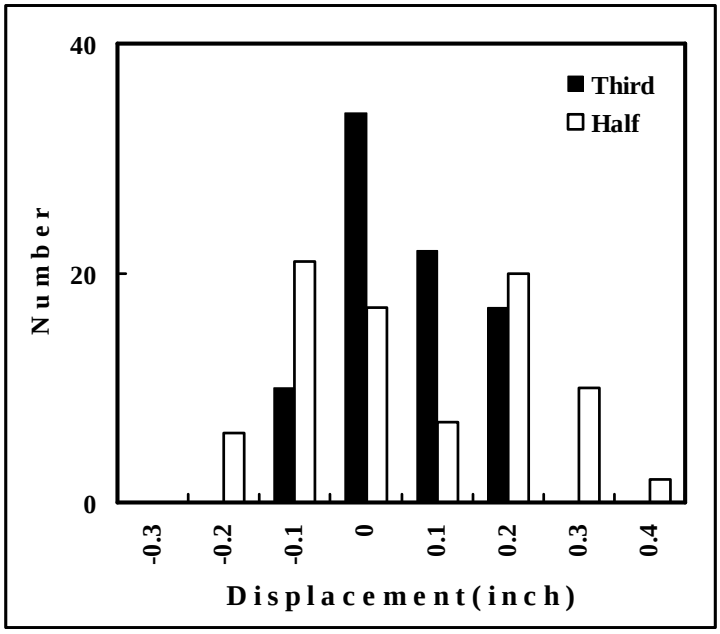

Figure 5.17 Magnitudes of measured displacements.

The s_m/D for axial loads up to half of peak applied load is shown in Figure 5.18. For a load ratio of a third, all but three of the tests had an upper limit of s_m/D = 1%. The upper limit reaches s_m/D = 2% at a load ratio of a half.

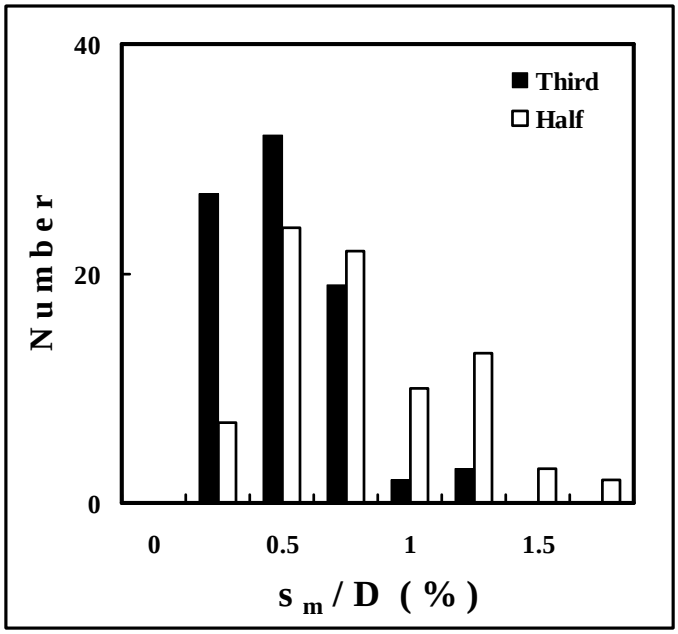

Figure 5.18 Absolute value of measured displacements, s_m, divided by pile diameter, D.

5.4.2 Measured versus Predicted Displacements

A typical example of the comparison between estimated and measured displacements up to a load ratio of a half is given in Figure 5.19, where Komornik's correlation for cohesionless soils is combined with Aschenbrener's and Poulos' suggestions for cohesive soils. Displacements are approximately less than |0.30| inches with little variability between correlations. The predicted displacements are less than the measured values in most cases, especially when Aschenbrener's equation for cohesive soils is used with any of the correlations for cohesionless soils.

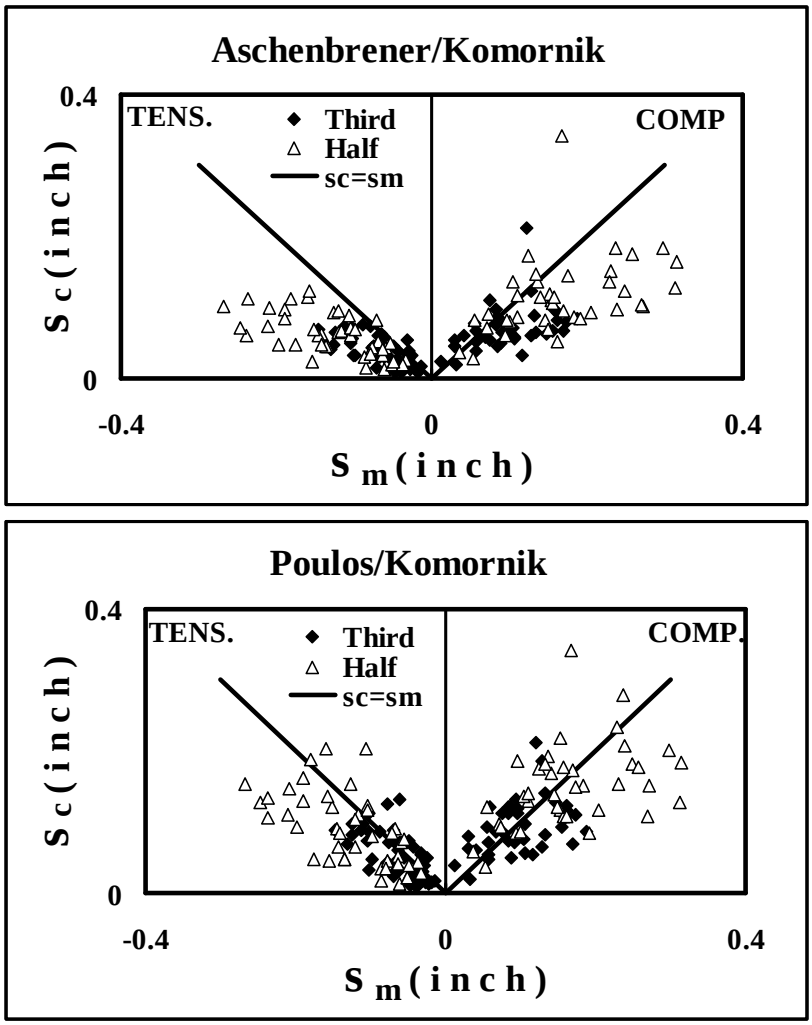

Figure 5.19 Comparison of displacements for piles driven into mixed profiles (N = 83).

A comparison of the displacements indicates a larger dispersion as the applied load is increased from a third to a half although the error remains small, reinforcing the idea that the elastic method is applicable for load ratios up to a half.

Overall the values of calculated displacements are similar between predictions if they are grouped according to the correlation employed for cohesive soil layers. For example, all of the displacements calculated with Aschenbrener's correlation for Young's

modulus in cohesive layers result in almost the same spread and dispersion data irrespective of the correlation employed for cohesionless layers.

Use of Frank's method generally led to overprediction of displacements (Figure 5.20). The formulation is intended as an upper-limit value for displacements at a load equal to half of the pile capacity. Although most of the estimations are too large to be accurate, the method may provide a reasonable first guess of expected displacements at low load ratios. Predictions based on the elastic column vary within a narrow band although they tend to be larger than measurements in most cases (Figure 5.21). The elastic column provides a simple and quick approach to predict displacements simply and quickly.

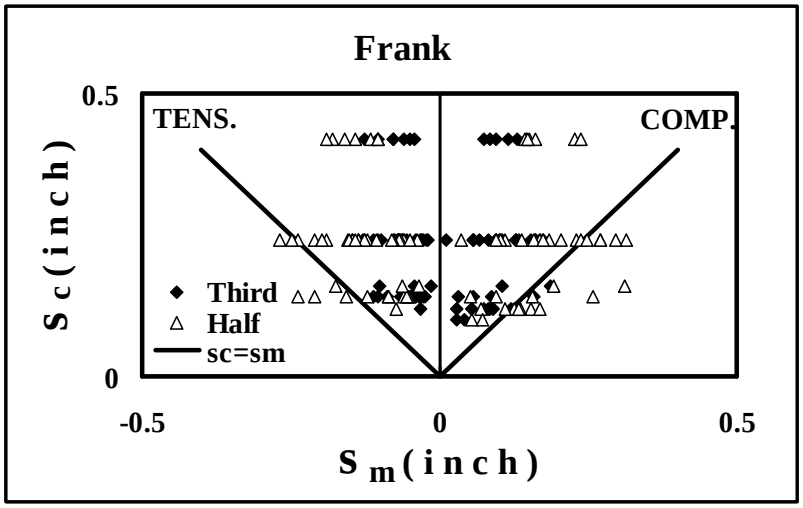

Figure 5.20 Comparison of displacements predicted using Frank's correlation.

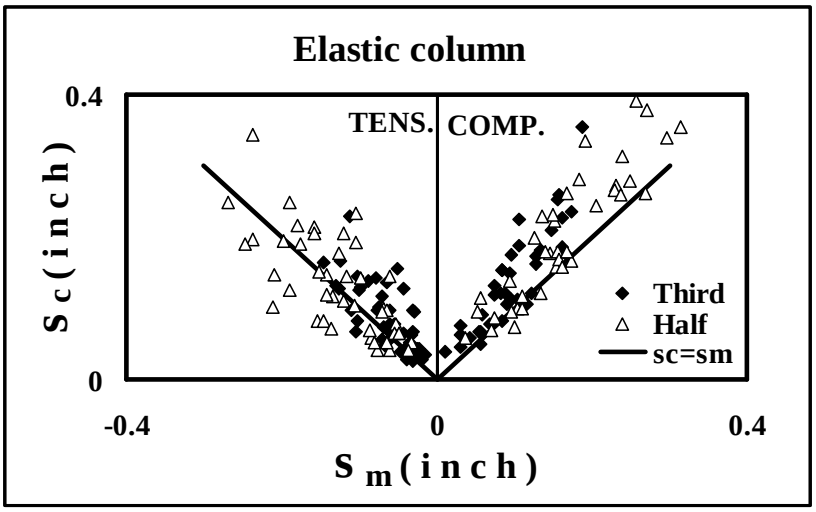

Figure 5.21 Predictions utilizing the elastic column approach in mixed profiles.

5.4.3 Displacement Ratio, s_c/s_m

The predicted displacements are in-large-part less than those measured in pile load tests. The majority (varying from 68% to 85%) of the displacement ratios obtained by pairing Aschenbrener's correlation with those recommended for cohesionless soils are between 0.2 and 1, thus further attesting to the underestimation of actual displacements. In contrast, the same range of displacement ratios obtained by combining the same correlations with Poulos varies from 41% to 64%. The scatter is over wider displacement ratios utilizing Poulos' correlation for cohesive soil layers than the spread for the same correlations with Aschenbrener, whereas the scatter was similar for predictions for cohesive soils only.

Frank's correlation leads to larger predicted displacements than those measured in pile load tests for about 85% of the comparisons with 68% of the predictions resulting in displacement ratios in excess of 1.6. Large displacement ratios, up to 24.7, indicate the low reliability of this correlation.

The predictions with the elastic column approach are larger than the measurements 65% of the time. Although large s_c/s_m values occur, the range of displacement ratios is similar to those obtained from other correlations.

Displacement ratios are summarized and correlations are ranked in Tables 5.15 and 5.16. For a load ratio, the mean as well as standard deviation of all estimates vary within a narrow range when grouped according to the correlation employed for cohesive layers (Aschenbrener or Poulos). On the average, for each corresponding correlation, the calculated displacements involving Aschenbrener are about 20 to 30% smaller than those paired with Poulos, which is less than 50 to 60% observed for the same correlations in cohesive soils only.

Table 5.15 Mean and standard deviation of displacement ratio (s_c/s_m) for correlations.

Load Ratio	Parameter	CLAY: Aschenbrener, 1984					Frank, 1985
		Komor-nik, 1974	Shioi/Fukui, 1982; Decourt, 1989	D'Appolonia, et al., 1970	Yamashita, et al., 1987	Kurkur, 1986	
⅓	Mean, $\overline{x}$	0.75	0.90	1.00	0.92	0.75	4.13
	Stand. Dev., s_x	0.41	0.46	0.52	0.46	0.41	3.86
½	Mean, $\overline{x}$	0.63	0.76	0.85	0.77	0.65	2.03
	Stand. Dev., s_x	0.32	0.38	0.48	0.39	0.39	1.37
Load Ratio	**Parameter**	**CLAY: Poulos, 1989**					**Elastic column**
		Komor-nik, 1974	**Shioi/Fukui, 1982; Decourt, 1989**	**D'Appolonia, et al., 1970**	**Yamashita, et al., 1987**	**Kurkur, 1986**	
⅓	Mean, $\overline{x}$	1.02	1.21	1.33	1.21	1.00	1.50
	Stand. Dev., s_x	0.56	0.61	0.66	0.61	0.56	0.58
½	Mean, $\overline{x}$	0.88	1.02	1.11	1.02	0.88	1.19
	Stand. Dev., s_x	0.43	0.45	0.52	0.45	0.47	0.39

Table 5.16 Rankings for correlations based on the statistics of s_c/s_m.

Load Ratio	Parameter	CLAY: Aschenbrener, 1984					Frank, 1985
		Komor-nik, 1974	Shioi/Fukui, 1982; Decourt, 1989	D'Appolonia, et al., 1970	Yamashita, et al., 1987	Kurkur, 1986	
⅓	Mean, $\overline{x}$	9	5	2	4	8	12
	Stand. Dev., s_x	1	3	5	4	2	12
½	Mean, $\overline{x}$	11	9	6	8	10	12
	Stand. Dev., s_x	1	2	10	3	5	12
Load Ratio	**Parameter**	**CLAY: Poulos, 1989**					**Elastic column**
		Komor-nik, 1974	**Shioi/Fukui, 1982; Decourt, 1989**	**D'Appolonia, et al., 1970**	**Yamashita, et al., 1987**	**Kurkur, 1986**	
⅓	Mean, $\overline{x}$	3	6	10	7	1	11
	Stand. Dev., s_x	7	10	11	9	6	8
½	Mean, $\overline{x}$	5	1	3	2	4	7
	Stand. Dev., s_x	6	7	11	8	9	4

When averages are considered, overall results are better if the correlation by Poulos (1989) is used for cohesive soils. However, the standard deviations obtained from predictions involving Aschenbrener's equation are smaller, although in general the predicted displacements of piles are less than those measured in load tests.

Displacement ratios obtained in mixed soils are closer to measured values with smaller standard deviation and coefficient of variation than those in a single type of soil. The outcome for some of the predicted displacements is almost equal. While displacements calculated via Komornik and Kurkur are similar, the results from Shioi/Fukui and Decourt are like those from Yamashita et al.. Although the mean and standard deviation obtained utilizing D'Appolonia's correlation are higher than the rest, they do not differ by a large amount. Thus, it can be concluded that specific combination

of correlations for Young's modulus does not have a significant impact on the estimated displacements in mixed profiles when load ratios are equal to or less than a half. Within the context of this dissertation, any combination of the correlations for cohesive soils with those for cohesionless soil will result in similar outcomes. The use of elastic method is likely the main reason for such a conclusion.

5.4.4 Displacement Difference, s_c-s_m

All of the displacement differences obtained from predictive methods, with the exception of those from Frank, result in similar outcomes regardless of the correlation used for cohesive and cohesionless layers. Over 90% of the displacement differences are less than $|0.1|$ inch of the measured values. The range of displacement differences, corresponding average and standard deviation values for each load ratio are positive and almost the same (Table 5.17).

Table 5.17 Summary of the mean and standard deviation for displacement differences (all in inches).

Load Ratio	Parameter	CLAY: Aschenbrener, 1984					Frank, 1985
		Komor-nik, 1974	Shioi/ Fukui, 1982; Decourt, 1989	D'Appolonia, et al., 1970	Yamashita, et al., 1987	Kurkur, 1986	
⅓	Mean, $\overline{x}$	0.00	0.00	0.01	0.00	0.00	-0.04
	Stand. Dev., s_x	0.04	0.04	0.04	0.04	0.04	0.19
½	Mean, $\overline{x}$	0.01	0.02	0.03	0.02	0.02	-0.04
	Stand. Dev., s_x	0.08	0.07	0.08	0.07	0.08	0.15
Load Ratio	Parameter	CLAY: Poulos, 1989					Elastic column
		Komor-nik, 1974	Shioi/Fukui, 1982; Decourt, 1989	D'Appolonia, et al., 1970	Yamashita, et al., 1987	Kurkur, 1986	
⅓	Mean, $\overline{x}$	0.00	0.01	0.01	0.01	0.00	0.01
	Stand. Dev., s_x	0.04	0.04	0.04	0.04	0.04	0.05
½	Mean, $\overline{x}$	0.01	0.02	0.03	0.02	0.02	0.02
	Stand. Dev., s_x	0.07	0.06	0.07	0.06	0.07	0.06

5.4.5 Outliers

Out of 83 pile load tests, there is only one (1.2%) for which all but one (LTN: 789) of the predictive methods results in overestimation of measured displacements. The load-displacement curve for this particular test is almost linear without any break to indicate the capacity because the pile load testing had to be terminated prematurely due to equipment failure. Therefore, the measured loads as well as displacements are significantly less than what would be observed if the testing had been successful. Another factor that could lead to larger displacements is the small shear strength values from laboratory tests. Interestingly, for this pile load test, the only prediction that is close to the measurements is obtained by the elastic column approach. The outcome may provide an example for the effect of a load test that was terminated before reaching failure.

5.5 CONCLUSIONS

In this study, correlations from the literature are used for load ratios up to a half to predict displacements, which are compared with the measurements from pile load tests.

5.5.1 Piles in Cohesive Soils (N = 26)

All of the measured displacements are less than an absolute value of 0.25 inches up to a load ratio of a half, where a displacement to pile diameter ratio, ρ/D, of 1.5% is determined to be a reasonable first estimate. A direct comparison of predicted and measured displacements provides good overall agreement, although their scatter increases with increasing load ratio. For all of the predictive methods, the loading direction does not appear to affect the outcome. The mean and standard deviation of the displacement ratio (s_c/s_m) and displacement difference (s_c-s_m) for each load ratio are presented in Tables 5.18 and 5.19.

Table 5.18 The statistics for the displacement ratios (s_c/s_m) in cohesive soils.

Load Ratio	Value	Poulos (1989)	Poulos (1972) (driven)	Poulos (1972) (bored)	Aschenbrener (1984)	Callanan/ Kulhawy 1985; Johnson 1986	Frank 1985	Elastic column
⅓	Mean, $\bar{x}$	1.76	1.81	3.09	1.15	2.44	3.25	1.63
	Stand. Dev., s_x	1.14	1.33	2.70	1.18	1.68	2.54	0.64
½	Mean, $\bar{x}$	1.42	1.46	2.49	0.89	1.97	1.77	1.36
	Stand. Dev., s_x	0.67	0.80	1.69	0.61	1.00	1.22	0.41

Table 5.19 Mean and standard deviation of displacement differences (s_c-s_m).

Load Ratio	Value (inch)	Poulos, (1989)	Poulos, (1972) (driven)	Poulos, (1972) (bored)	Aschenbrener, (1984)	Callanan/ Kulhawy 1985; Johnson 1986	Frank, 1985	Elastic column
⅓	Mean, $\bar{x}$	-0.01	-0.01	-0.01	-0.02	-0.01	0.00	0.00
	Stand. Dev., s_x	0.05	0.06	0.12	0.05	0.08	0.13	0.05
½	Mean, $\bar{x}$	0.02	0.02	0.06	0.02	0.04	0.06	0.03
	Stand. Dev., s_x	0.04	0.05	0.09	0.05	0.06	0.09	0.04

The correlations can be ranked starting from the best as: elastic column, Aschenbrener (1984), Poulos (1989), and Poulos (1972, driven piles). These findings coincide with the conclusions reached visually from a direct comparison of the displacements.

The mean values of displacement differences for each prediction are not large and the standard deviation does not change significantly with increased loading.

Three out of seven predictive methods utilized result in predictions that have a large mean and standard deviation for s_c/s_m: Callanan and Kulhawy (1985)/Johnson (1986), Poulos (1972, bored pile), and Frank (1985).

Four pile load tests are consistently identified as outliers for all the predictions. However, none of the investigated parameters explain this outcome.

5.5.2 Piles in Cohesionless Soils (N = 34)

For load ratios up to a half, the absolute values of all of the measured displacements are less than 0.5 inches and have ρ/D=2.5%. The pile loading direction does not affect the predicted displacements. Displacements estimated at the load ratio of a third conform better to the measured displacements than those at a half. The calculated displacement ratios and differences are summarized in Tables 5.20 and 5.21.

Table 5.20 Mean and standard deviation of the displacement ratio for predictive methods in cohesionless soils.

Load Ratio	Value	Komornik, 1974	Shioi/ Fukui, 1982; Decourt, 1989	Denver, 1982	D'Appolonia et al., 1970 (NC)	D'Appolonia et al., 1970 (OC)	Christoulas, 1988	Yamashita et al., 1987	Kurkur, 1986	Frank, 1985	Elastic column
⅓	Mean, $\bar{x}$	0.97	1.26	1.86	1.62	1.19	18.19	1.16	0.79	2.74	1.24
	St. Dev., s_x	0.58	0.80	1.23	1.16	0.75	91.96	0.71	0.48	2.88	0.62
½	Mean, $\bar{x}$	0.74	0.96	1.43	1.26	0.90	16.92	0.88	0.62	0.94	0.93
	St. Dev., s_x	0.42	0.61	0.91	0.75	0.50	87.24	0.49	0.35	1.19	0.42

Table 5.21 The statistics of displacement difference (s_c-s_m) for predictive methods in cohesionless soils.

Load Ratio	Value (inch)	Komornik, 1974	Shioi/ Fukui, 1982; Decourt, 1989	Denver, 1982	D'Appolonia et al., 1970 (NC)	D'Appolonia et al., 1970 (OC)	Yamashita et al., 1987	Kurkur, 1986	Frank, 1985	Elastic column
⅓	Mean, $\bar{x}$	0.00	0.01	0.02	0.02	0.01	0.01	0.00	-0.02	-0.01
	St. Dev., s_x	0.06	0.06	0.07	0.07	0.06	0.06	0.07	0.09	0.06
½	Mean, $\bar{x}$	0.01	0.02	0.05	0.04	0.02	0.02	0.01	-0.02	-0.01
	St. Dev., s_x	0.14	0.13	0.15	0.13	0.13	0.13	0.14	0.11	0.10

Predictions using Young's modulus as suggested by Komornik are the best at a load ratio of a third, despite having a slightly increased standard deviation. The elastic column approach is the best overall estimator at or near a load ratio of a half.

The correlations by Denver (1982), D'Appolonia et al. (1970a, normally consolidated), Christoulas (1988), and Frank (1985) result in estimates for displacement that can vary significantly from those measured in pile load tests.

For ten out of 34 pile load tests, the predicted displacements are much lower than the measured displacements. The only investigated factor, which may explain the underestimation of displacements for pile load tests is pile stiffness, i.e., AE/L, which remains at less than 1200 kips/inch for all the identified outliers.

5.5.3 Piles in Mixed Profiles (N = 83)

Up to a load ratio of a half, all of the measured displacements are less than a half inch, of which 92% are less than a quarter inch. All of the measured displacements are scattered within 1% and 1.5% of the pile diameter at a load ratio of a third and a half, respectively. Tension or compression loading does not have a significant impact on the predicted displacements. On the average, correlations for cohesionless material that are paired with Poulos' equation for cohesive soils produce 20% to 30% lower displacements than those paired with Aschenbrener, although the standard deviation also increases. The results of comparing predictions and measurements are summarized in Tables 5.22 and 5.23.

Within the bounds of the predictive methods investigated in this study, any combinations of two correlations, –one for cohesive and another for cohesionless layers, result in similar outcomes.

Table 5.22 Statistics of displacement ratio (s_c/s_m) for predictions in mixed profiles.

Load Ratio		CLAY: Aschenbrener, 1984					Frank, 1985
		Komornik, 1974	Shioi/Fukui, 1982; Decourt, 1989	D'Appolonia, et al., 1970	Yamashita, et al., 1987	Kurkur, 1986	
⅓	Mean	0.75	0.90	1.00	0.92	0.75	4.13
	Stand. Dev.	0.41	0.46	0.52	0.46	0.41	3.86
½	Mean	0.63	0.76	0.85	0.77	0.65	2.03
	Stand. Dev	0.32	0.38	0.48	0.39	0.39	1.37
Load Ratio		**CLAY: Poulos, 1989**					
		Komornik, 1974	**Shioi/Fukui, 1982; Decourt, 1989**	**D'Appolonia, et al., 1970**	**Yamashita, et al., 1987**	**Kurkur, 1986**	**Elastic column**
⅓	Mean	1.02	1.21	1.33	1.21	1.00	1.50
	Stand. Dev.	0.56	0.61	0.66	0.61	0.56	0.58
½	Mean	0.88	1.02	1.11	1.02	0.88	1.19
	Stand. Dev.	0.43	0.45	0.52	0.45	0.47	0.39

Table 5.23 Summary of mean and standard deviation for displacement differences of predictions with measurements.

Load Ratio	(all in inches)	CLAY: Aschenbrener, 1984					Frank, 1985
		Komor-nik, 1974	Shioi/Fukui, 1982; Decourt, 1989	D'Appolonia, et al., 1970	Yamashita, et al., 1987	Kurkur, 1986	
⅓	Mean, $\overline{x}$	0.00	0.00	0.01	0.00	0.00	-0.04
	Stand. Dev., s_x	0.04	0.04	0.04	0.04	0.04	0.19
½	Mean, $\overline{x}$	0.01	0.02	0.03	0.02	0.02	-0.04
	Stand. Dev., s_x	0.08	0.07	0.08	0.07	0.08	0.15
Load Ratio	**(all in inches)**	**CLAY: Poulos, 1989**					
		Komor-nik, 1974	**Shioi/Fukui, 1982; Decourt, 1989**	**D'Appolonia, et al., 1970**	**Yamashita, et al., 1987**	**Kurkur, 1986**	**Elastic column**
⅓	Mean, $\overline{x}$	0.00	0.01	0.01	0.01	0.00	0.01
	Stand. Dev., s_x	0.04	0.04	0.04	0.04	0.04	0.05
½	Mean, $\overline{x}$	0.01	0.02	0.03	0.02	0.02	0.02
	Stand. Dev., s_x	0.07	0.06	0.07	0.06	0.07	0.06

5.6 SUMMARY

In this chapter, direct predictive methods of displacements along with routinely employed correlations for soil Young's modulus are introduced and utilized in

conjunction with the elastic method for predicting displacements within half of the peak applied loads or “working loads” for which the correlations are proposed.

These correlations (five for cohesive soils, ten for piles in cohesionless and mixed profiles) involve triaxial undrained shear strength, c_u, and standard penetration blow count, N, for cohesive and cohesionless soil layers, respectively.

Separate comparisons are made for cohesive, cohesionless and mixed profiles. The relative magnitudes of estimated and measured displacements up to a load ratio of a half are established in terms of their absolute values as well as their percentage of the pile diameter. Estimated displacements are then compared graphically and statistically with those measured from pile load tests included in the Caltrans database. Results that vary significantly from others in terms of displacement ratio (s_c/s_m) and displacement difference (s_c-s_m) are identified. Various factors affecting these results are further examined in an attempt to determine their respective influences. The selected correlations are then ranked based on the outcome of these analyses.

Chapter 6: Proposed Method of Predicting Displacements

6.1 INTRODUCTION

Young's modulus of soil decreases with increasing applied loads on a pile comparable to a secant modulus from a stress-strain curve. Young's modulus values calculated at varying loads may then be used to construct the load-displacement curve for an axially loaded pile.

A new predictive method based on data from pile load tests provided by Caltrans is proposed to calculate displacements at various applied loads. The aim is to develop a more accurate and reliable method for determining the displacement of axially loaded piles in compression as well as in tension. The proposed correlations are developed using data from piles in cohesive soils and separately for piles in cohesionless soils and are then applied to piles in mixed profiles as independent measures of validity.

The analytical approach to determine Young's moduli used in the following sections are outlined in Chapter 4.

6.2 COHESIVE SOILS

The changes of Young's modulus, E_s, with undrained shear strength are presented in Figure 6.1 separately for each load test direction and load ratio (⅓, ½, and ⅔). Some trends can be observed:

- Young's modulus increases with increasing c_u. The scatter of points from the mean is substantial.
- Tension and compression tests seem to yield the same values of E_s at any c_u.

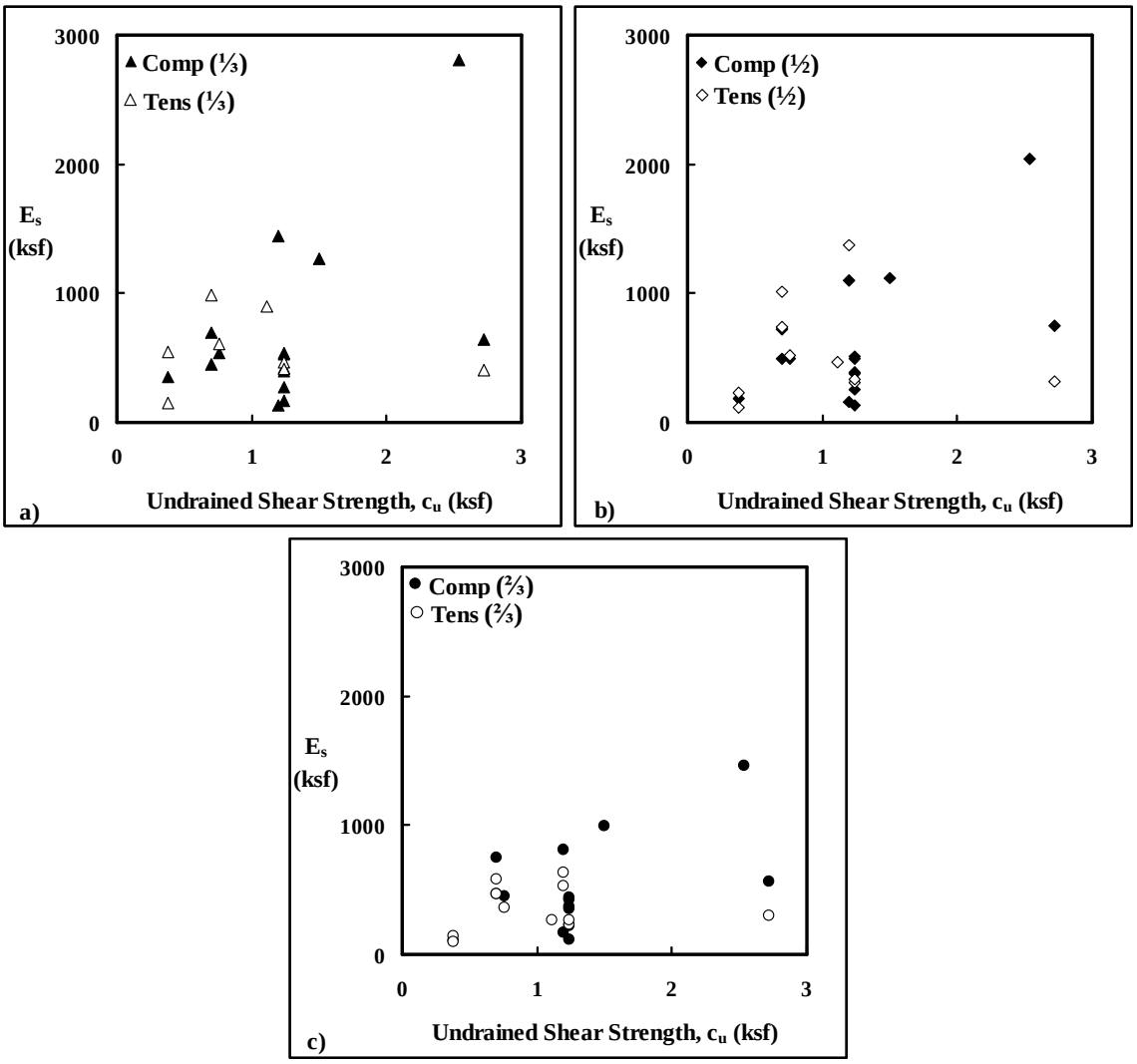

Figure 6.1 Young's modulus versus undrained shear strength for each load ratio (N=26).

Low values of undrained shear strength can be seen better when the E_s-c_u relation is depicted on a logarithmic scale (Figure 6.2a and b). The outcome for load ratios of a third and a half are similar and are shown together. The suggested linear correlation for the E_s-c_u relationship is also given, which was obtained by minimizing the differences in the suggested and calculated Young's moduli. The correlation factor between E_s and c_u is given to only one significant figure to reflect the substantial scatter.

Young's modulus decreases as the load ratios increase because of the curvature of the load-displacement curves.

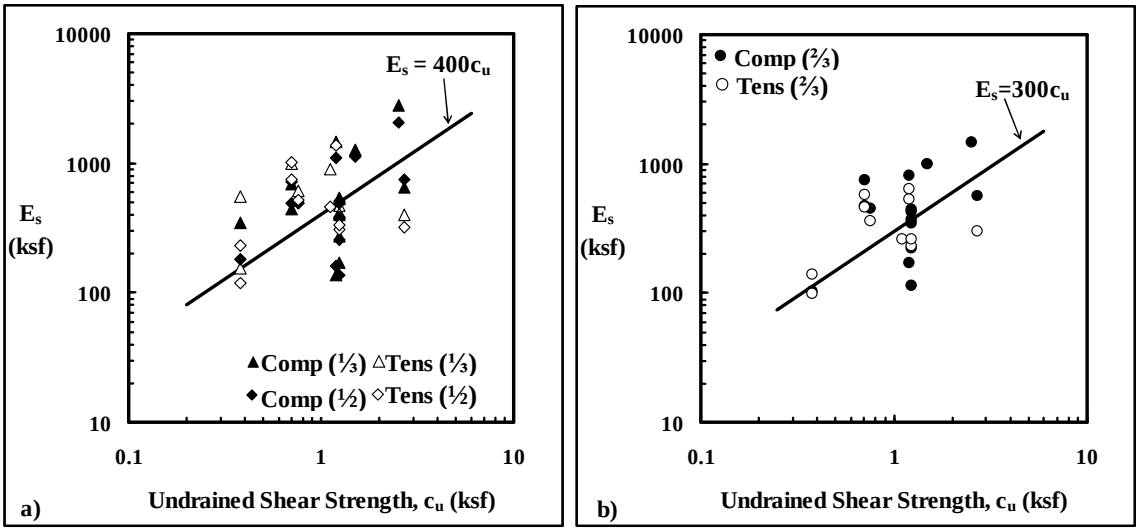

Figure 6.2 Change of Young's modulus with undrained shear strength and fitted correlations.

Overall, the calculated displacements compare well with the measured displacements in pile load tests (Figure 6.3 and Table 6.1). However, the mean values of s_c/s_m are higher than one for all load ratios although s_c-s_m values remain small. Larger ratios can be expected when such small displacements are involved.

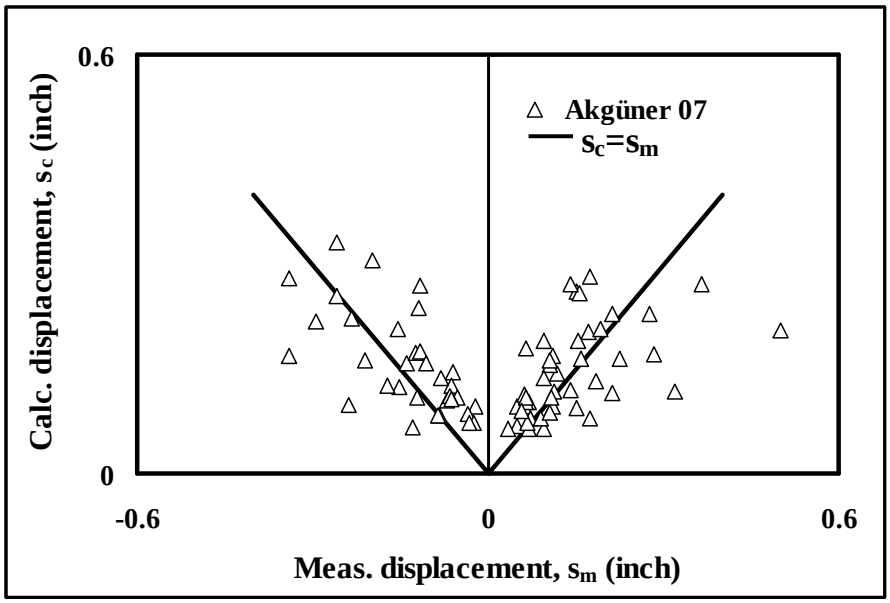

Figure 6.3 Calculated and measured displacements using suggested correlations.

Table 6.1 Summary statistics for (s_c/s_m) and (s_c-s_m) employing the proposed method (N=26).

Statistics for (s_c/s_m)	Third	Half	Two-Third
Mean, $\bar{x}$	1.49	1.21	1.19
Standard Dev., s_x	1.09	0.62	0.53
cov (%)	72.9	51.6	45.0
Maximum	5.92	3.17	2.68
Minimum	0.44	0.36	0.38
Statistics for (s_c-s_m)	**Third**	**Half**	**Two-Third**
Mean, $\bar{x}$ (inch)	-0.01	-0.01	0.00
Standard Dev., s_x (inch)	0.05	0.07	0.10
Maximum	0.07	0.14	0.19
Minimum	-0.11	-0.21	-0.31

The averages for s_c/s_m are higher than one because the E_s-c_u correlation was developed to minimize the difference between the suggested and observed E_s. For small displacements as measured for load ratios less than approximately half to two-thirds, small variations in displacements affect the outcome of s_c/s_m significantly. Therefore, the

least squares of the displacement differences are selected to establish the proposed correlations.

Young's moduli calculated with the suggested correlations are within the range of values obtained from other researchers, except Aschenbrener (Figure 6.4). Young's moduli for the load ratio of two-thirds and Poulos (1989) are almost identical although the latter correlation was suggested for working loads, which could lead to predicting excessive displacements for smaller loads.

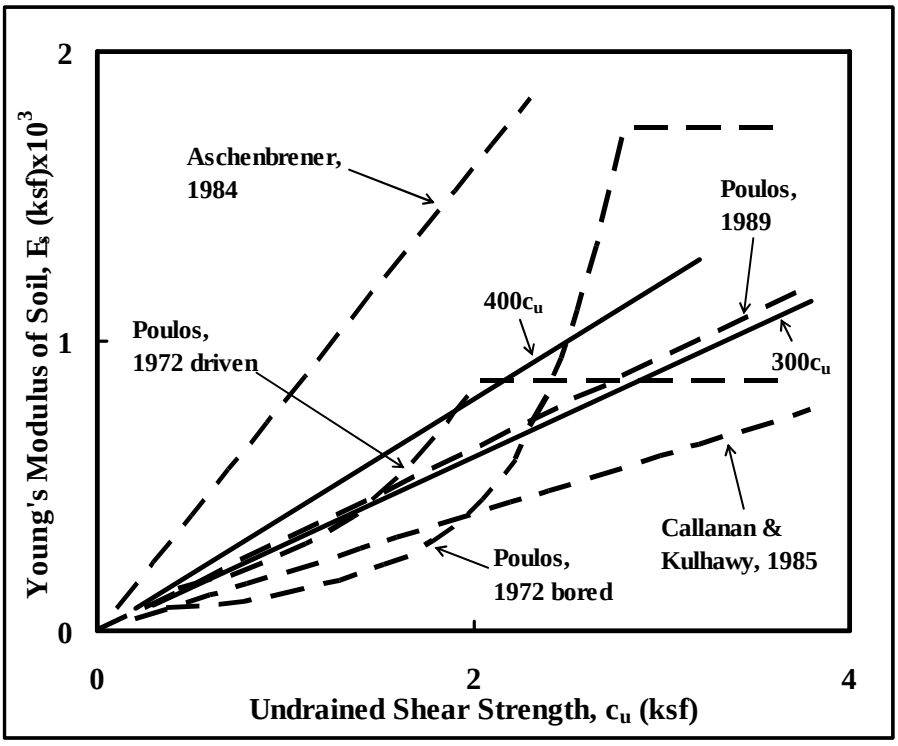

Figure 6.4 Comparison of proposed E_s correlations with others from literature.

In this investigation, the minimum and maximum values of undrained shear strength are approximately 0.4 and 3 ksf, respectively. The suggested correlations may not be applicable outside this range of c_u values. Calculated Young's modulus values are

compared with those from the proposed approach for each pile type in Figures 6.5 through 6.7.

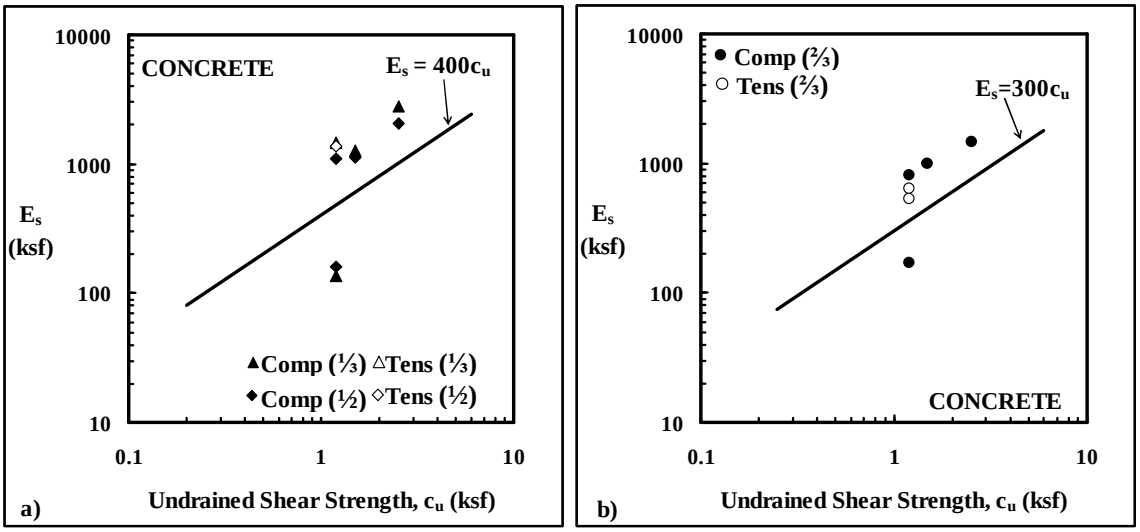

Figure 6.5 Suggested correlations and data for concrete piles (N=6).

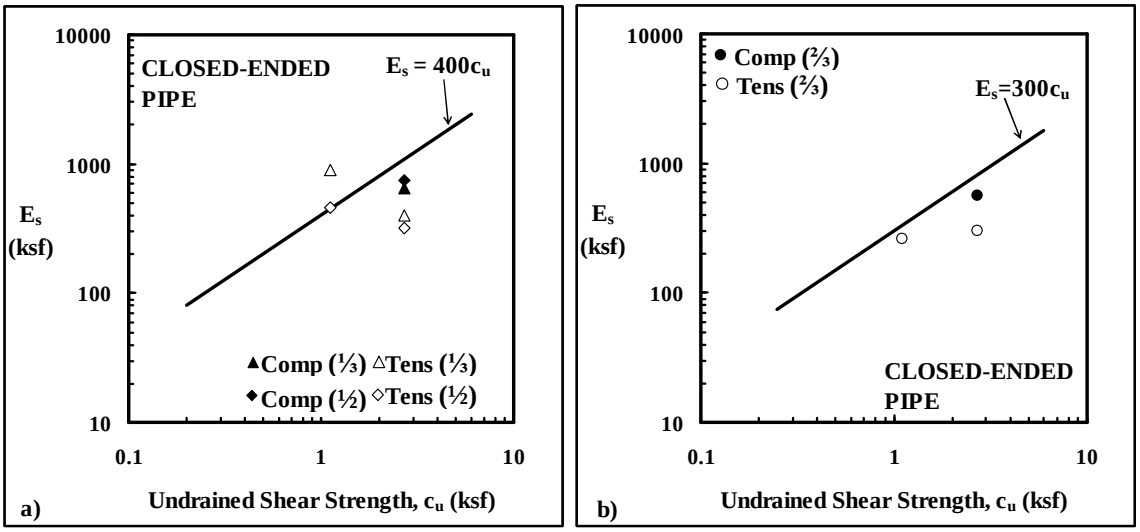

Figure 6.6 Suggested correlations and available data for closed-ended pipe piles (N=3).

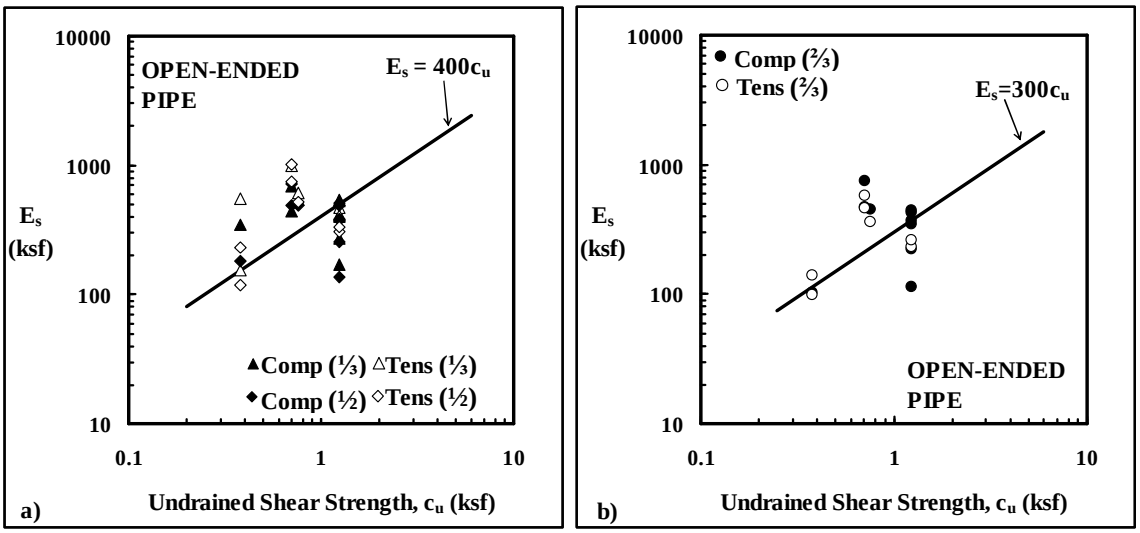

Figure 6.7 Calculated Young's moduli from pile load tests and suggested correlations for open-ended pipe piles (N=17).

6.3 COHESIONLESS SOILS

The Young's modulus for all of the investigated pile load tests are presented in relation to standard penetration test blow counts, *N*, in Figure 6.8.

Although the values of Young's modulus vary widely, a few trends can be observed:

- Most data are concentrated between SPT blow counts of 10 to about 25, and Young's modulus of 200 and 3000 ksf,
- Overall, the Young's moduli are larger for pile load tests in compression than in tension, which differs from the outcome in cohesive soils,
- There is more scatter for values of E_s for piles in tension than for piles in compression,
- The observed Young's moduli increase with increasing SPT blow count.

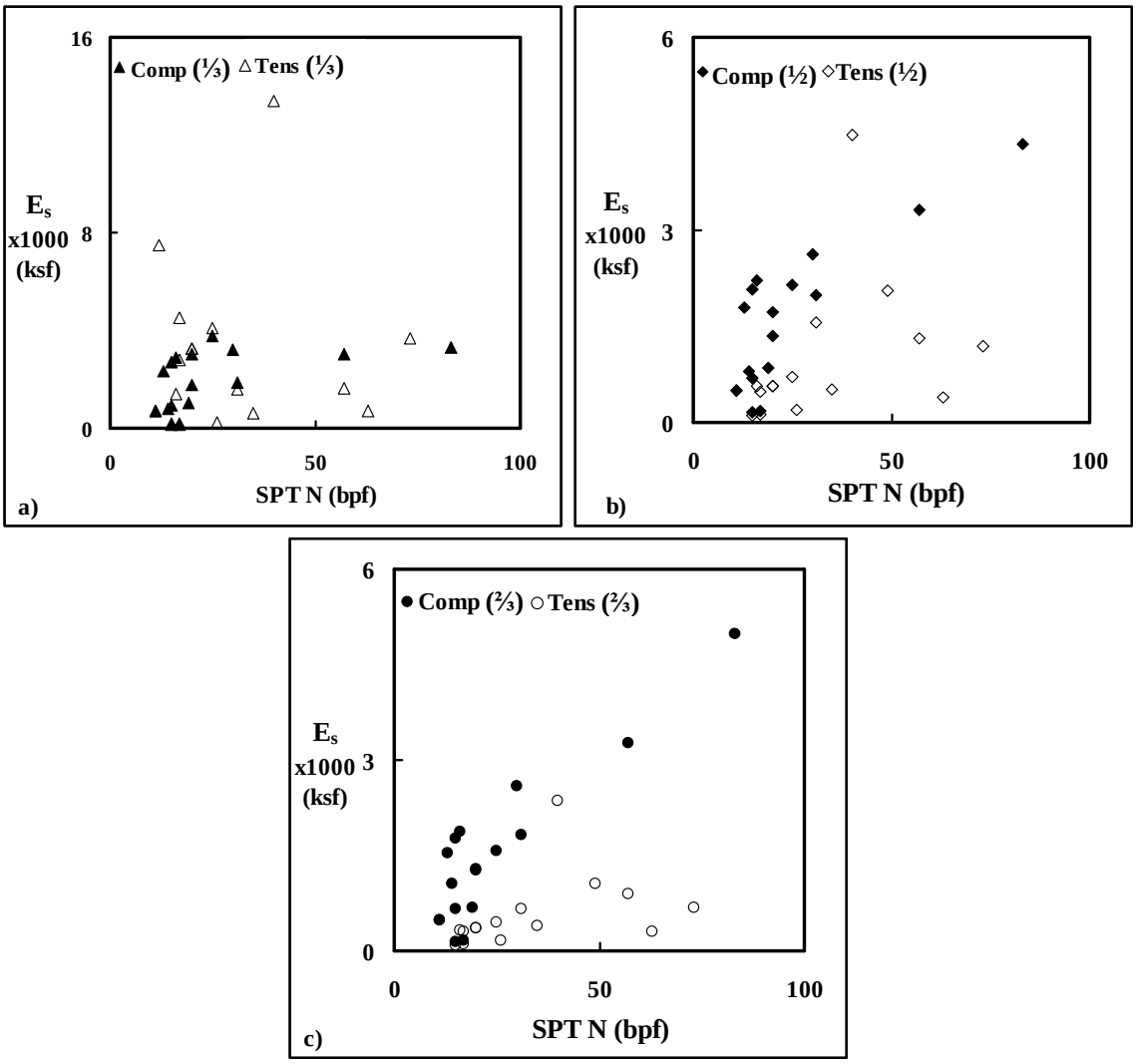

Figure 6.8 Variations of Young's modulus with SPT blow count (N=34).

A reasonable linear relationship between Young's modulus and SPT blow counts cannot be established. Therefore, a logarithmic fit to the calculated Young's moduli for each load ratio has been adopted in order to provide an approximation (Figure 6.9), which minimizes the difference between the suggested Young's moduli and those obtained from pile load tests. The values of Young's moduli are depicted against log(N) to develop an equation of the form (also shown in Figure 6.9):

$E_s = a + b \times \log_e(N)$ .....(6.1),

The range of SPT blow counts used for the suggested correlations varies from eleven to 83.

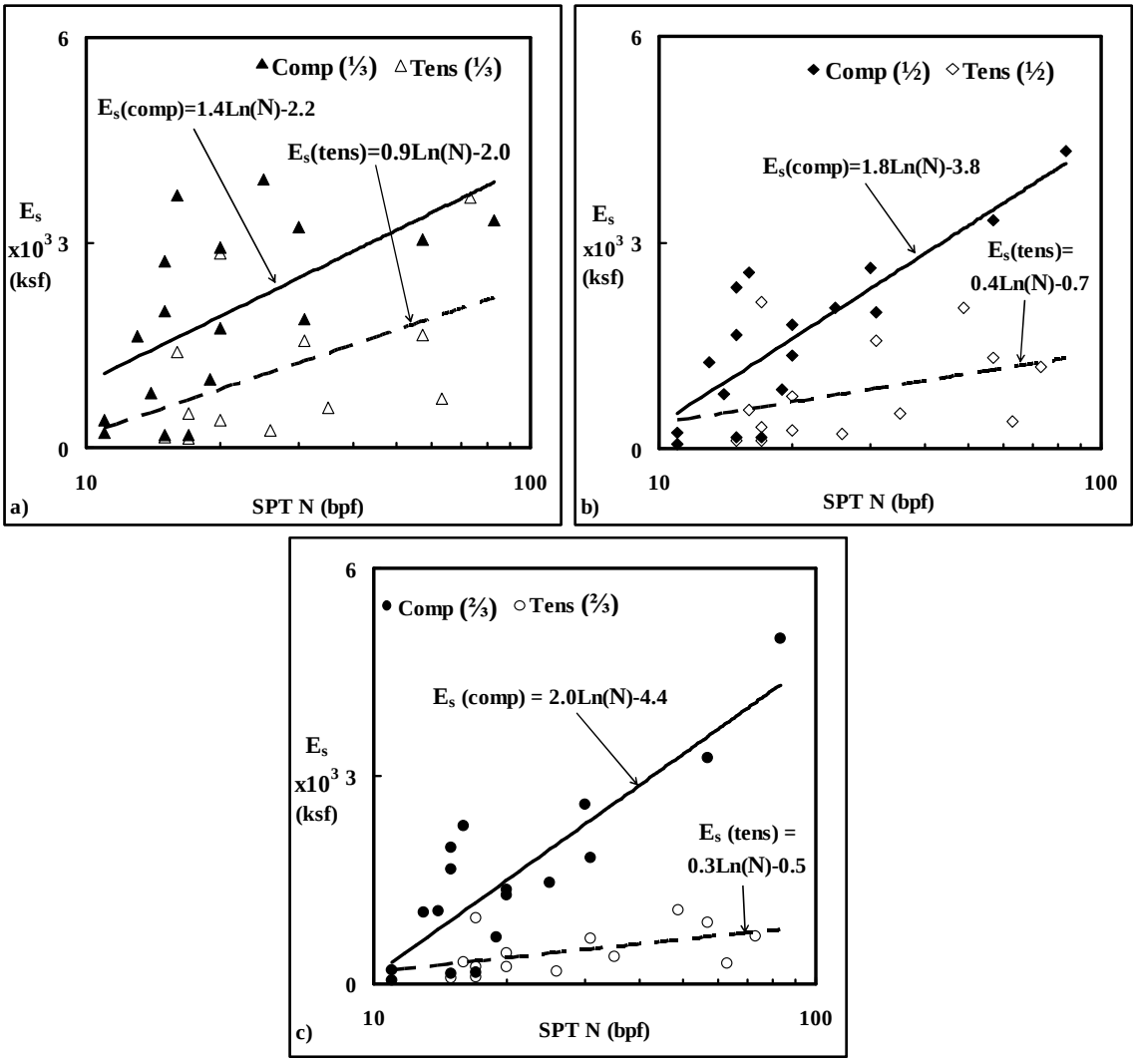

Figure 6.9 Young's modulus versus blow count in logarithmic axes given along with fitted curves (N=31).

Three of the load tests (LTNs: 495, 571 and 752) were excluded in developing the fitted curves. Load testing for one of the piles (14-inch concrete, LTN: 495) was terminated early at a displacement of 0.5 inch before an actual failure load could be reached. Therefore, the measured displacements are smaller and in turn the calculated Young's modulus larger than the rest of the load tests. The second pile (16x0.5 inch open-ended pipe, LTN: 571) had about 40 feet from the tip of the pile which was plugged, which is significant for a pile that has penetrated 43 feet into the ground and also unusual for non-displacement piles. The site characterization for the third excluded pile (12-inch concrete, LTN: 752) was based on a boring that was over 100 feet away; therefore, the soil layering and properties may not correspond to the conditions at the location of the pile.

With respect to the three rejected tests, the question arose as to whether it was likely that incorrect N values or errors in measuring settlements could be the cause of the variation between measured and computed settlements. Analyses demonstrated that unreasonably high values of *N* were required to bring data from the three rejected tests into the scatter band of the other tests so that explanation of their outlier status seems unlikely. Alternatively, small errors in the measured settlement could cause large errors in s_c/s_m. The measured displacements at the on-set of a pile load test are typically small and prone to equipment or personnel errors. The values of Young's modulus for the excluded tests are considerably higher than the rest of the results. The measured displacements are increased between 0.005 and 0.01 inches to decrease the observed values of Young's modulus (Figure 6.10). Such small variations have an important impact on the outcome.

All of the correlations for all load ratios are shown together in Figure 6.11. The correlations for piles tested in compression have approximately the same increasing trend for the Young's modulus, which for all practical purposes can be replaced by a single relationship applicable to all load ratios.

Fitted curves are compared with other correlations recommended in the literature (Figure 6.12).

Predicted displacements are larger than the measured displacements (Figure 6.13) although the differences remain small. The statistical values of the displacement ratio and displacement differences are provided in Table 6.2.

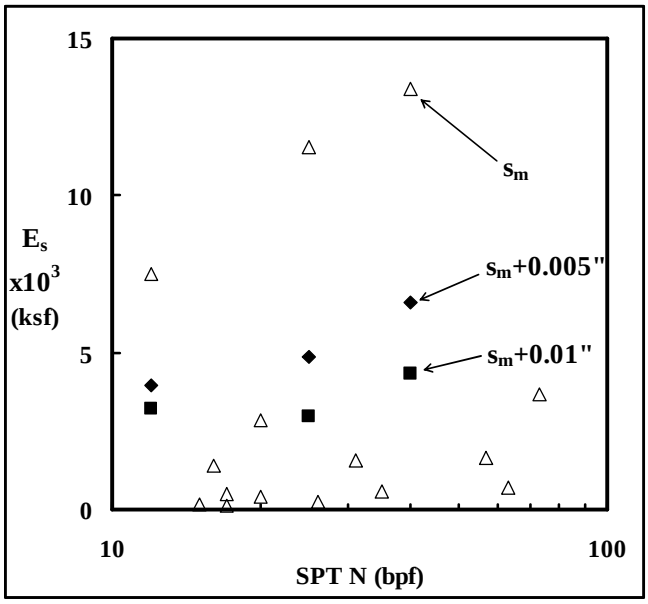

Figure 6.10 The effect of varying displacements on the values of Young's modulus.

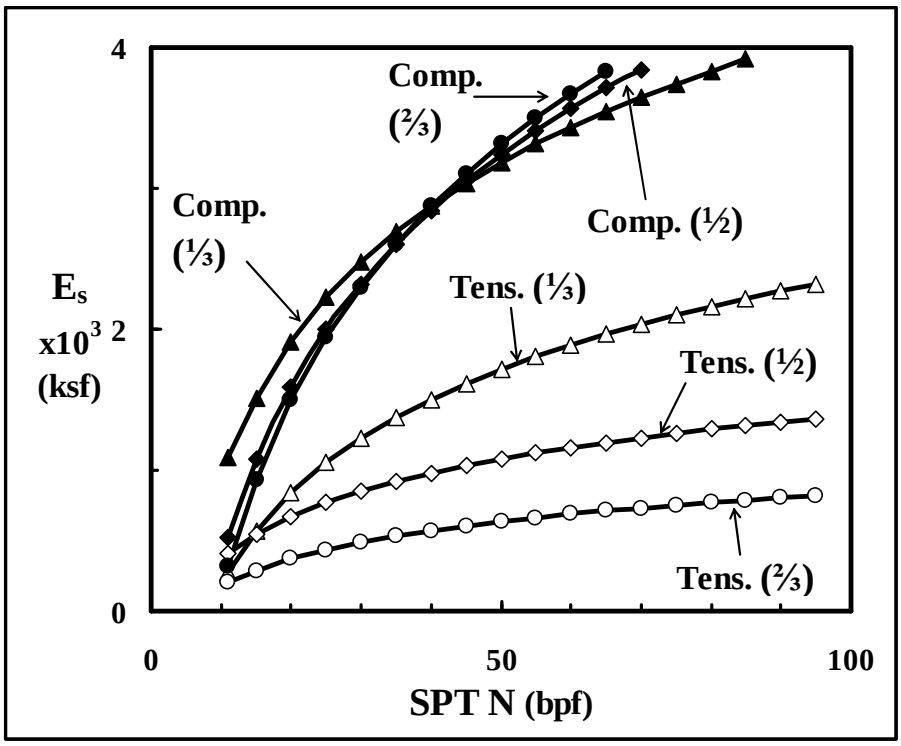

Figure 6.11 Comparison of fitted curves to Young's modulus versus blow count results at each load ratio.

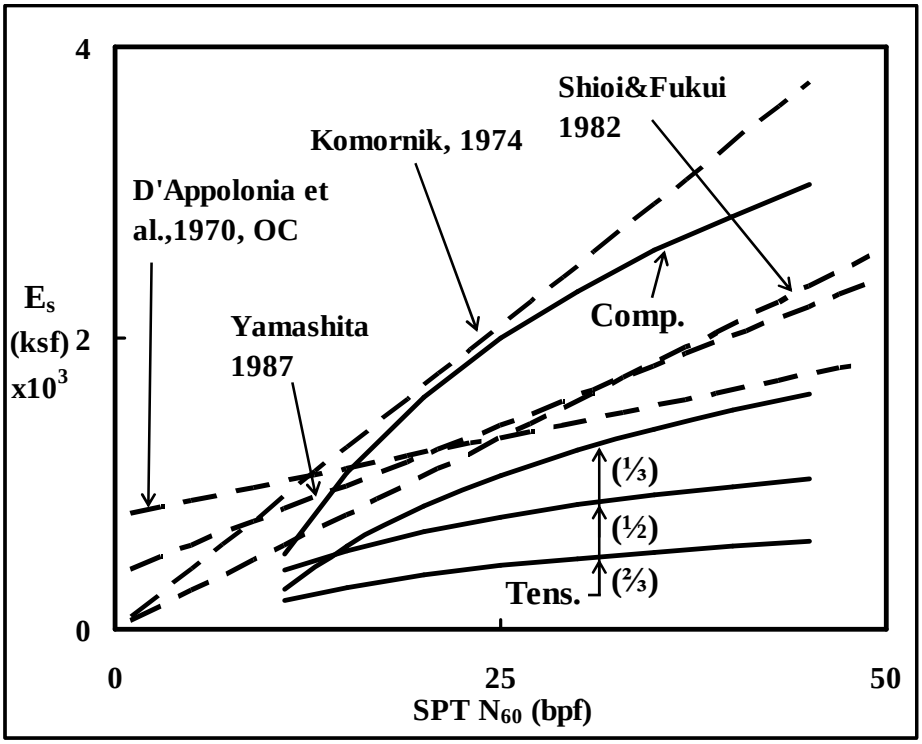

Figure 6.12 Fitted curves in relation to other recommended correlations for cohesionless soils.

Table 6.2 Statistical values for displacement ratios and differences in cohesionless soils (N=34).

Statistics (s_c/s_m)	Third	Half	Two-Thirds
Mean, $\bar{x}$	1.16	1.10	1.24
Standard Dev., s_x	0.68	0.54	0.63
cov (%)	58.1	48.9	51.0
Statistics (s_c-s_m)	Third	Half	Two-Thirds
Mean, $\bar{x}$ (inch)	0.01	0.00	0.00
Standard Dev., s_x (inch)	0.06	0.13	0.19

Calculated Young's moduli are given in Figures 6.14 through 6.18 for all load ratios and loading directions, although no correlations have been deduced based on pile

type. Most of the Young's moduli for concrete piles are higher than those suggested by the fitted curves. Four of the six concrete piles are from the same location and have a high stiffness ranging from 2200 to 4300 kips/inch.

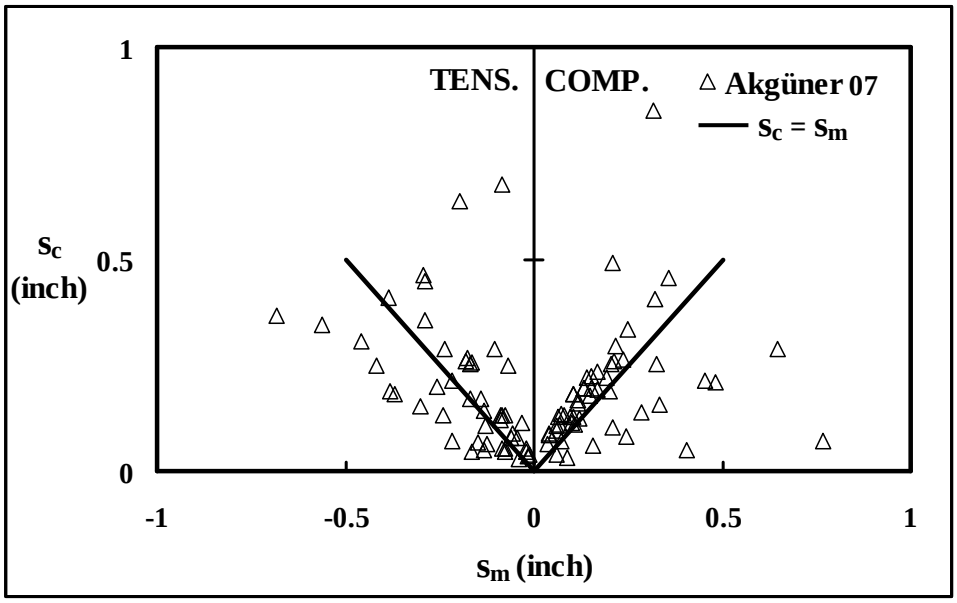

Figure 6.13 Displacements calculated for piles in cohesionless soils using correlations derived from Caltrans database.

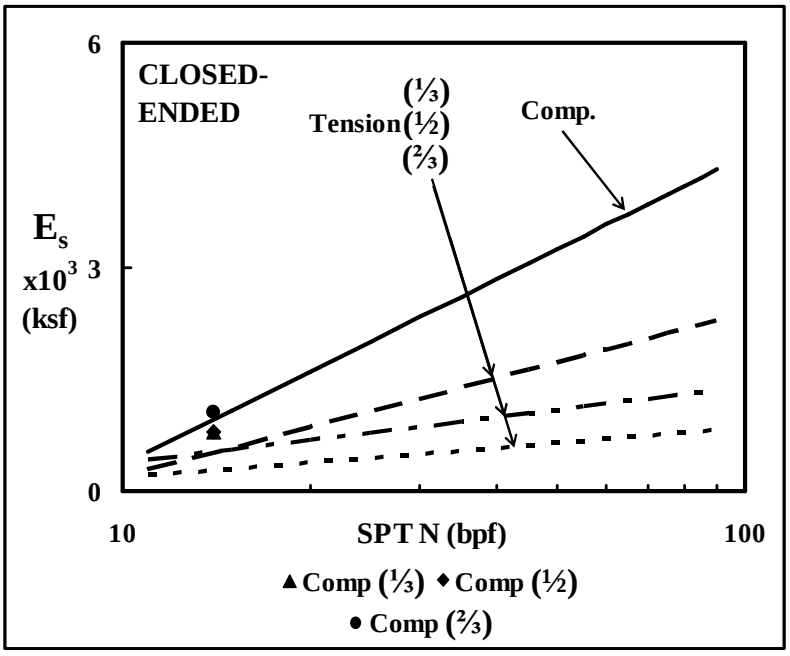

Figure 6.14 Values of Young's modulus obtained for the closed-ended pipe pile (N=1).

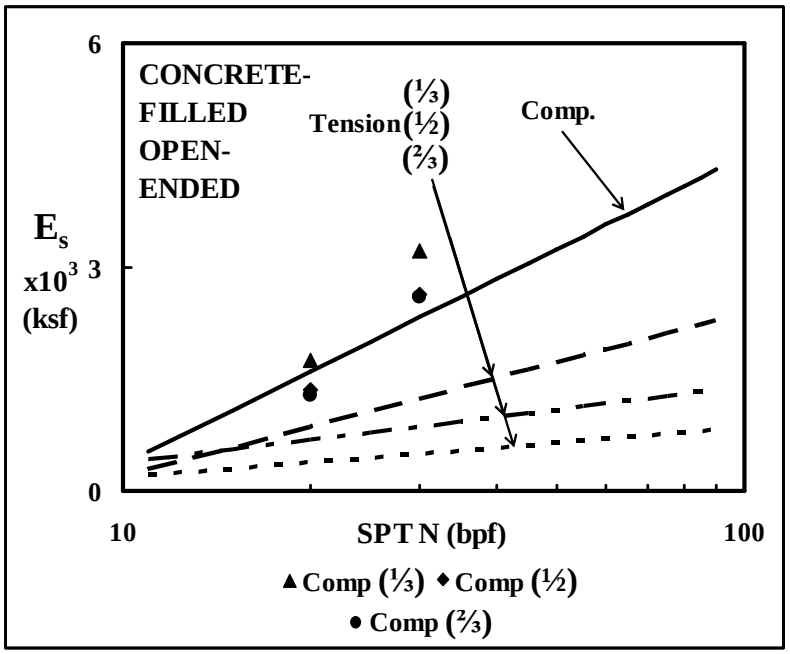

Figure 6.15 Calculated Young's modulus for concrete-filled pipe piles (N=2).

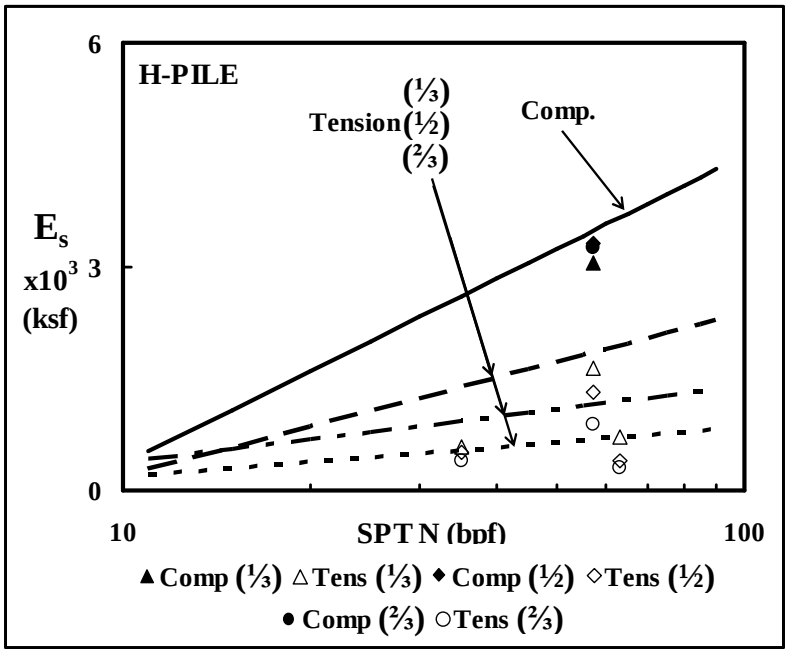

Figure 6.16 Young's modulus values calculated from H-piles in Caltrans pile load tests (N=4).

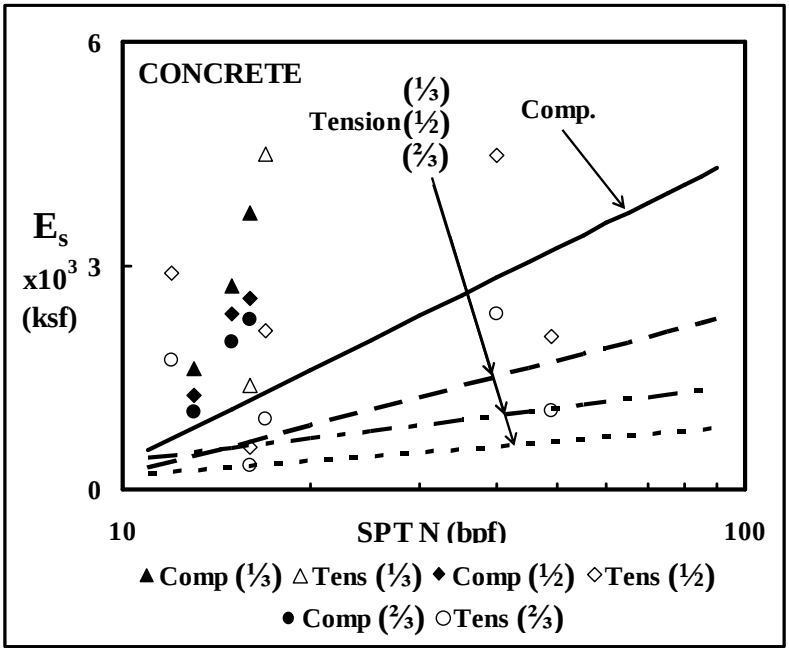

Figure 6.17 Variation of E_s and N for concrete piles (N=6).

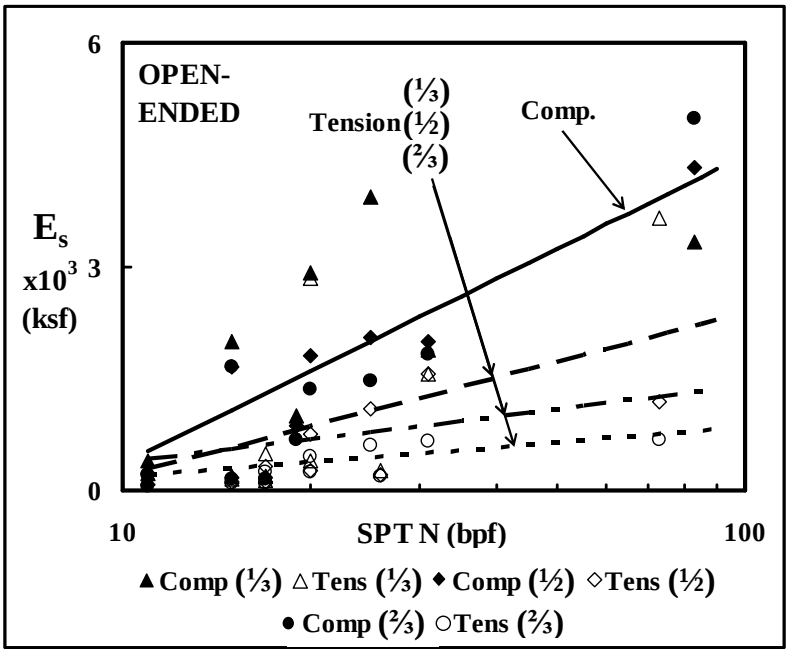

Figure 6.18 Young's modulus versus SPT N for open-ended pipe piles (N=18).

6.4 PROPOSED METHOD APPLIED TO PILES IN MIXED PROFILES

The database of piles in mixed profiles provides an independent means of verifying the proposed method because these piles were not included in deriving the predictive approach. The proposed equations are utilized to predict the displacements of the piles driven in mixed profiles (Figure 6.19). The statistical outcome of the comparison is presented in Table 6.3.

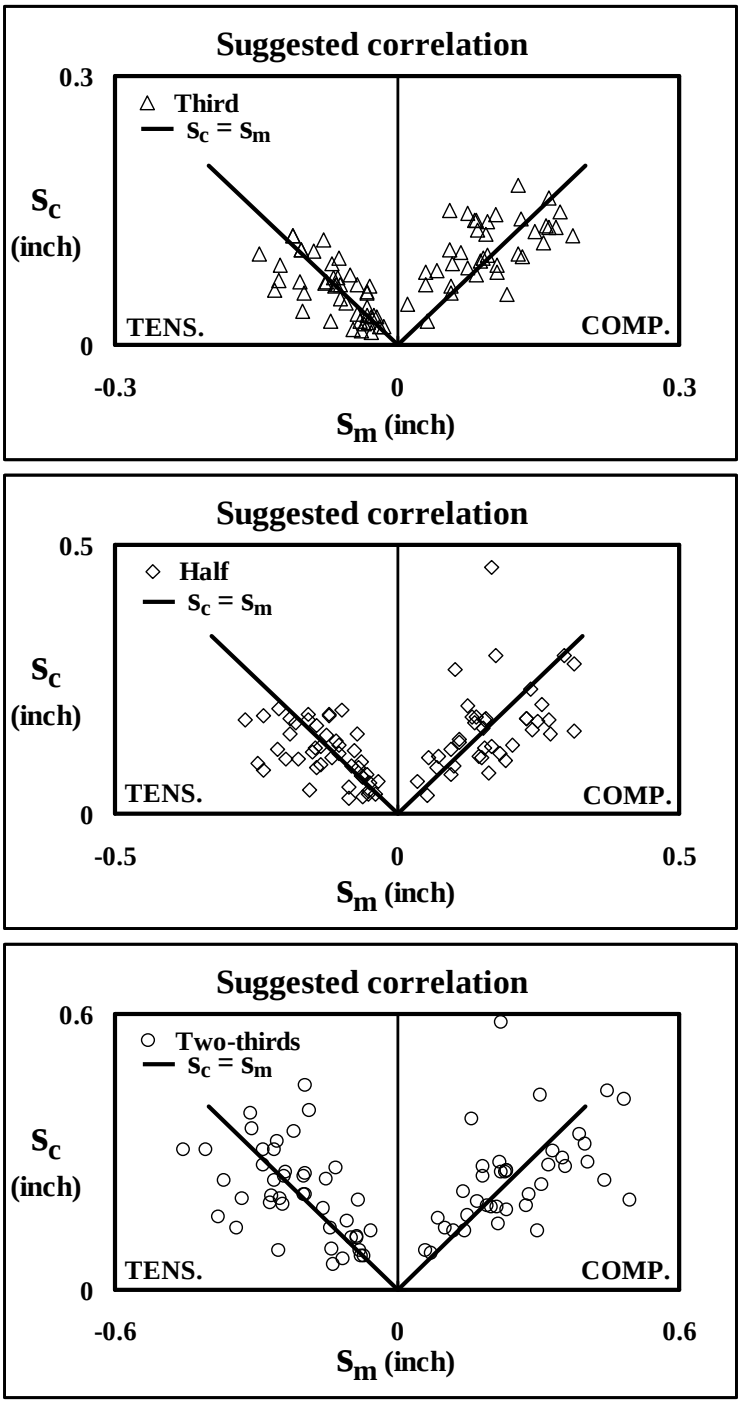

Figure 6.19 Predicted and measured displacements of piles in mixed profiles (N=83).

Table 6.3 Statistics for settlement ratio (s_c/s_m) and displacement difference (s_c-s_m) (N=83).

Statistics (s_c/s_m)	**Third**	**Half**	**Two-Thirds**
Mean, $\bar{x}$	1.18	1.02	1.08
Standard Dev., s_x	0.60	0.47	0.48
Statistics (s_c-s_m) (inch)	**Third**	**Half**	**Two-Thirds**
Mean, $\bar{x}$	0.01	0.00	-0.01
Standard Dev., s_x	0.04	0.07	0.10

6.5 SUMMARY

In this chapter, the steps in developing an improved method to predict axial pile displacements are shown. Caltrans pile load tests provide the basis for this approach.

Measured displacements obtained from the load-displacement curves are matched at load ratios of a third, a half, and two-thirds. Soil Young's moduli for each load ratio are correlated to either undrained shear strength, c_u, for cohesive soils or SPT blow count, N, for cohesionless soils. Graphical as well as statistical evaluations of the calculated displacements from resulting correlations are made and summarized. The proposed method is also applied to piles driven in mixed profiles. Findings are evaluated against recommendations from the literature. All of the pile load tests within each soil type (cohesive, cohesionless and mixed profiles) are evaluated together without separating them in groups according to the pile type to increase the number of tests that can be used for correlations.

The proposed correlation predicts the increases in displacements within reasonable accuracy when applied loads are larger than a half of the pile capacity, i.e., outside of the conventional range of applicability of the elastic method.

Chapter 7: Conclusions

The elastic method presents one of the most commonly used algorithms to estimate displacements of foundations. It is based on Mindlin's solution (1936) for stresses and displacements due to a single vertical point load within a homogeneous, isotropic half space. The objective of this dissertation research is to develop an improved approach to predict the displacements of axially loaded single piles using the *elastic method*. Poisson's ratio, which has little effect on outcome, and Young's modulus are the two unknown parameters in this approach. An attempt is made to develop a straightforward Young's modulus correlation based on routinely available or obtained parameters relying on a database containing pile load tests supplied by California Department of Transportation (Caltrans), i.e., the FinalCT database. Separate analyses are conducted on subsets of this database for each soil type, all of which are dominated by open-ended pipe piles:

- twenty-six load tests on piles driven in primarily cohesive soils,
- thirty-four pile load tests founded in cohesionless soils,
- eighty-three tests in mixed profiles.

Within the context of this dissertation, almost all of the pile displacements that are investigated are less than 0.5 inch exhibiting approximately a linear increase up to a load of about two-thirds of the failure load. Non-linear behavior is observed when the loading on the pile is in excess of 67% of the pile capacity. Therefore, it may be justified to employ the elastic method for load ratios only up to a half, similar to the findings and recommendations by other researchers.

In this research, the focus is on predicting immediate or short-term displacements of driven piles. The first step in predicting pile displacements is to determine the pile

capacity, which in this dissertation is assumed to be estimated with an acceptable accuracy utilizing available parameters.

The changes in displacements due to sustained loading (creep, consolidation), and the distribution of loads and displacements along the length of the pile are not considered because the database utilized in this research does not include such information.

In the following paragraphs, conclusions are drawn on various aspects of this research. Also suggestions for future work are specified.

7.1 PUBLISHED METHODS TO PREDICT AXIAL DISPLACEMENTS

Many correlations are suggested in the literature to predict pile displacements under axial loading. As part of this dissertation, five correlations for cohesive soils and ten correlations for cohesionless soils are utilized to predict displacements of piles in the Caltrans database. For mixed profiles consisting of multiple layers of differing soil types, combinations of two correlations for cohesive soils and five correlations for cohesionless soils are utilized. Each predictive method is suggested to be applicable within working loads. Graphical and statistical comparisons are made with displacements measured in pile load tests to assess their accuracy.

7.1.1 Cohesive Soils

The predictive methods can be ranked starting from the best as: elastic column, Aschenbrener (1984), Poulos (1989), and Poulos (1972, driven piles). These findings coincide with the conclusions reached visually from a direct comparison of the displacements.

The mean value of displacement differences, (the absolute value of the difference between measured and computed displacements, s_c-s_m) for each prediction is less than 0.1

inches. The standard deviation of s_c-s_m does not change significantly with increasing applied loads.

Three out of seven predictive methods utilized result in predictions that have a large mean and standard deviation for the displacement ratio, s_c/s_m: Callanan and Kulhawy (1985)/Johnson (1986), Poulos (1972, bored pile), and Frank (1985). These three correlations are not recommended for predicting displacements of driven piles.

7.1.2 Cohesionless Soils

Predictions using the Young's modulus suggested by Komornik are the best at a load ratio of a third, despite having a slightly increased standard deviation. The elastic column approach is the best overall estimator at or near a load ratio of a half.

The correlations by Denver (1982), D'Appolonia et al. (1970a, normally consolidated), Christoulas (1988), and Frank (1985) estimate displacements that can vary significantly from those measured in pile load test at both extremes in over- and underestimation.

7.1.3 Mixed Profiles

On the average, correlations for cohesionless material that are paired with Poulos' equation for cohesive soils produce 20% to 30% lower displacements than those paired with Aschenbrener, although the standard deviation also increases.

Regardless of the combination of the correlations utilized for cohesive and cohesionless layers, the predicted displacements in mixed profiles are similar to each other.

7.1.4 Recommendations for Future Work

Multiple approaches and various correlations may be used in estimating parameters for elastic analyses or indirectly predicting pile displacements without the

need for a pile load test. A few that are deemed to have the greatest potential are cited in Appendix B.

Recent correlations developed from the cone penetrometer test (CPT) and the pressuremeter (PMT) as well as seismic testing methods (the last one especially for granular material which cannot be sampled without disturbance) can be used to estimate displacements.

7.2 SUGGESTED CORRELATIONS

Caltrans pile load tests were used to develop Young's modulus correlations for cohesive and cohesionless soils. The variation of Young's modulus with loading direction and with loading amount in relation to the failure load is investigated. Each analysis involves manually adjusting the Young's moduli of the soil, E_s, along the side and at the tip of the pile to match the measured displacements. For example, if at a load the calculated displacement is greater than the measured displacement, then E_s is increased so that the soil behavior is stiffer against displacement until the calculated and measured displacements are successfully matched.

7.2.1 Conclusions on Methodology

For cohesive soils, Young's modulus seems to vary linearly with undrained shearing strength, c_u, but more complex relationships are observed for E_s as a function of SPT blow count, N, in cohesionless soils. A single linear or simplified correlation for Young's modulus is not sufficient to model the variability of the load-displacement behavior from pile load test. The load ratio at which the fitting is being made needs to be specified in order to reduce the variability between the measured and calculated displacements. Soil Young's modulus used in calculations with elastic analyses decreases as the load ratio increases; i.e., soil interacting with pile becomes softer, therefore causing

a larger displacement of a loaded pile. In general, obtaining a Young's modulus correlation from a smaller load ratio and then applying it to calculate the displacements for a pile under a larger load would lead to an underestimation of the displacement.

7.2.1.1 *Cohesive Soils*

Young's moduli, E_s, are obtained at various load ratios. The ensuing E_s-c_u relationship provides the following observations:

- Young's modulus increases with increasing c_u. The scatter of points from the mean is substantial.
- Tension and compression tests seem to yield the same values of E_s at any c_u.

The suggested parameters based on the aforementioned findings and the linear approximation of the E_s versus c_u variation is summarized in Table 7.1. The correlations are obtained by minimizing the square of the difference between the E_s predicted with the correlations and the observed E_s from pile load tests, i.e., the least squares method.

Table 7.1 Multiplication factors at loading increments ($^{\dagger}K_1 = E_s/c_u$).

Load ratio	**⅓ and ½**	**⅔**
$K_1^{\dagger}$ (dimensionless)	400	300

It may be reasonable to interpolate multiplication factors for intermediate load ratios up to two-thirds although the accuracy of such an approach has not been investigated as part of this dissertation.

The mean and standard deviation of s_c-s_m using the above parameters are -0.01 inch and 0.07 inch, respectively for 26 tests from the Caltrans database. The standard deviation is large, a likely effect of linear approximation of results as well as other factors such as scatter in c_u due to sampling disturbance or laboratory testing, possible pile damage during driving, errors in taking readings, the presence of casings, etc.

All of the recommended correlations from the literature utilized in this dissertation are for a load ratio of a half or less. The correlation of Young's modulus ($E_s = 400c_u$) recommended by this study indicates a lower predicted displacement, i.e., stiffer behavior, than the other correlations at working loads (except for Aschenbrener, 1984).

7.2.1.2 *Cohesionless Soils*

The following observations can be made when variations of Young's modulus are graphed against SPT blow count:

- Most data are concentrated between SPT blow counts of 10 to about 25, and Young's modulus of 200 and 3000 ksf,
- Overall, the Young's moduli are larger for pile load tests in compression than in tension, which differs from the outcome in cohesive soils,
- More scatter for values of E_s is observed for piles in tension than for piles in compression,
- The back-calculated Young's moduli increase with increasing SPT blow count.

Unlike piles driven in cohesive soils, no clear correlation is observed from variations of Young's modulus in relation to blow counts. Thus a logarithmic fit for each load ratio and loading direction is established as an indication of a general trend in the form of the equation $E_s = A + B \log_e (N)$ by using the least squares method (Table 7.2).

Table 7.2 Values for logarithmic fitting conducted for piles in cohesionless soils.

Load Ratio	Compression		Tension	
	A	B	A	B
⅓	-2.2	1.4	-2.0	0.9
½	-3.8	1.8	-0.7	0.4
⅔	-4.4	2.0	-0.5	0.3

When the factors listed above are utilized for the 34 load tests in the Caltrans database, the mean value of s_c-s_m is zero while the standard deviation is 0.13 inches. In addition to the errors in conducting the pile load test, the variability of SPT blow counts due to applied hammer energy can also be a significant source of error.

7.2.1.3 *Suggested Correlations Applied to Piles in Mixed Profiles*

Displacements are predicted for 83 piles in the Caltrans database, which are driven into soils with mixed profiles, using the proposed correlations. None of these piles was included in the derivation of the suggested correlations. Therefore, these piles provide an independent means of investigating the applicability of the correlations. The results indicate a satisfactory outcome for all load ratios (Table 6.3).

Table 7.3 Statistics for settlement ratio (s_c/s_m) and displacement difference (s_c-s_m) (N=83).

Statistics (s_c/s_m)	**Third**	**Half**	**Two-Thirds**
Mean, $\bar{x}$	1.18	1.02	1.08
Standard Dev., s_x	0.60	0.47	0.48
Statistics (s_c-s_m) (inch)	**Third**	**Half**	**Two-Thirds**
Mean, $\bar{x}$	0.01	0.00	-0.01
Standard Dev., s_x	0.04	0.07	0.10

7.2.2 Recommendations for Future Work

Cone penetration testing (CPT) has been gaining in popularity for purposes of site characterization and design. Research based on CPT seems to be improving its use for characterizing soils in the field with the exception of dense sandy and/or gravelly layers. Thus, CPT can be utilized to analyze the data collected as part of the Caltrans project.

A natural extension of any developed method for a single pile is towards pile groups because piles used for support of structures on land (as opposed to offshore)

typically are in groups. Unfortunately, none of the Caltrans pile load tests was conducted on groups of piles although most of the piles were a part of a group.

In areas with gravel and cobbles, often the cone penetrometer cannot be pushed to the desired depth and SPT blow counts reach refusal as well. For such cases, geophysical methods such as the Oyo suspension logger or spectral analysis of shear waves (SASW) would be very useful. To the best of the author's knowledge, there is a lack of correlations for estimating displacements of piles in coarse materials, especially gravels and cobbles.

An integral approach to pile design combining pile capacity with displacement would bridge the gap in design of piled foundations, where emphasis is usually given to the capacity.

7.3 OTHER RECOMMENDATIONS

Other analyses methods can be considered:

- Analyses with t-z curves are widely used and may be especially useful for cases in which load shedding is significant. Moreover, a realistic incorporation of the effects of residual stresses due to pile driving (Alyahyai, 1987) into the analyses would be a step towards a more comprehensive explanation of all aspects of pile displacement.

- Numerical approaches such as neural networks and finite element methods with non-linear models of soil-pile interaction might well be further investigated with positive results for predicting pile displacement. These might well help characterize the non-linear behavior of load-displacement curves as failure loads are approached.

Appendix A: Pile Load Test Information

Appendix A.1 Coupling of bridge numbers, site names, load test numbers, and other descriptive terms.

Bridge	Name	City	Inter. Route	Bent	Pile	CTID	LTN
04-0017	Van Duzen River Bridge	Fortuna	101	Pier 2	72	001-01	384
				Pier 3	108	001-02	385
20-0172	Central Cloverdale Underpass	Cloverdale	101	3	14	004-02	390
20-0251	Central Cloverdale Undercrossing	Cloverdale	101	Abutment 2R	28	004-01	389
20-0254	Russian River Bridge	Guerneville	116	Pier 3	14 (#1)	006a-01	397
						006a-02	398
					14 (#2)	006a-03	399
						006a-04	400
					10	006a-05	401
					14 (#3)	006b-01	402
					27	006b-02	403
22-0032	Sacramento River Bypass	Bryte	16	Pier 37	2	124L-01	735
22-0062	Mullen Overhead	Woodland	113	2R	21	122L-01	736
28-0009	San Joaquin River Bridge	Antioch	84	19	15	007-01	404
28-0056	Railroad Ave. Overhead	Richmond	17	5L	10	118L-01	788
28-0249	West Connector Overcrossing	Concord	4/242	4	3	002-01	386
				8	20	002a-01	387
28-0292	Harbor Way Overcrossing	Richmond	580	Abut. 3	10	003-01	388
29-0013	Stanislaus River - Ripon	Modesto	99	22	3	120L-01	790
				6	1	120L-02	762
33-0025	San Francisco-Oakland Bay Bridge	Oakland	80	E28L	17	085-01	675
						085-02	676
				E31R	1	086-01	677
						086-02	678
33-0393	West Grand Avenue Viaduct	Oakland	880	3F	27	011-01	455
						011-02	456
33-0611	East Bay Viaduct	Oakland	880	13L	8	009-01	408
						009-02	409
				17R (LT)	17	009-03	410

Bridge	Name	City	Inter. Route	Bent	Pile	CTID	LTN
						009-04	411
				29R	23	009-05	412
						009-06	413
33-0612	Port of Oakland Connector Viaduct	Oakland	880/80	10NCI	3	012-05	461
						012-06	462
				17NCI(LT)	6	012-03	459
						012-04	460
				27NC(RT)	9	012-01	457
						012-02	458
				31NC(LT)	9	010-01	417
						010-02	418
I-880 IPTP	I-880 Replacement Project IPTP	Oakland	880	Site 1	1B	040-01	559
					1C	040-02	560
					1J	040-03	561
						040-04	562
						040-05	563
					1M	040-06	564
						040-07	565
					1R	040-08	566
						040-09	567
					1U	040-10	568
						040-11	569
				Site 2	2-H	029-01	501
						029-02	502
					2-L	029-03	503
						029-04	504
					2-P	029-05	505
						029-06	506
					2-T	029-07	507
						029-08	508
					2-W	029-09	509
						029-10	510
				Site 3	3-C	030-01	511
						030-02	512
					1M	030-03	513
						030-04	514
				Site 4	4-B	031-01	515
					4-C	031-02	516
					4-H	031-03	517

Bridge	Name	City	Inter. Route	Bent	Pile	CTID	LTN
						031-04	518
					4-L	031-05	519
						031-06	520
					4-P	031-07	521
						031-08	522
					4-T	031-09	523
						031-10	524
					4-W	031-11	525
						031-12	526
34-0046	Southern Freeway Viaduct	San Francisco	280	28R	12	077-03	638
					12	077-04	639
				34R	17	083-01	673
				43AL	13	077-01	636
				45AR	13	077-02	637
				52C	21	081-02	670
						082-01	671
				52R	15	082-02	672
				B-88	D	072-01	631
				SE-68	11	073-01	632
				SE-71	4	071-01	630
				Tension Pile Test Site	48	079-07	663
						079-08	664
						079-09	665
						079-10	666
						079-11	667
					49	079-01	657
						079-02	658
						079-03	659
						079-04	660
						079-05	661
						079-06	662
					50	078-11	650
						078-12	651
					51	078-13	652
						078-14	653
34-0070	280/101 Retrofit	San Francisco	101/280	WU-28	19	070-01	629
34-0088	Bayshore Freeway Viaduct	San Francisco	80	Site A	1	094-01	429
						094-02	430
					2	094-03	431

Bridge	Name	City	Inter. Route	Bent	Pile	CTID	LTN
						094-04	432
					3	094-05	433
						094-06	434
				Site B	1	095-01	435
						095-02	436
					2	095-03	437
						095-04	438
				Site C	1	096-01	439
						096-02	440
					2	096-03	441
						096-04	442
				Site D	1	097-01	443
						097-02	444
					2	097-03	445
						097-04	446
				Site E	1	098-01	447
						098-02	448
					2	098-03	449
						098-04	450
				Site F	1	099-01	451
						099-02	452
					2	099-03	453
						099-04	454
				Site G	5	100-01	771
						100-02	772
34-0100	China Basin Viaduct	San Francisco	280	20	14	021-01	478
				22, Column 4	4	014-03	470
				23, Column 4	5	014-02	469
				29, Column 2	19	014-01	468
				29, Column 3	4	015-01	471
				Site 2	2	019-01	476
				Site 3	3	018-01	475
					3C	017-01	474
				Site 4	4	013-01	463
				Site 5	6	013-02	464
					7	013-03	465
				Site 6	8	013-04	466
				Site 7	10	013-05	467
35-0038	Dumbarton Bridge	Fremont/ Newark/	84	Pier 04	33	135-01	421
				Pier 16	29	138-02	425

Bridge	Name	City	Inter. Route	Bent	Pile	CTID	LTN
		Menlo Park			41	138-01	424
				Pier 18	3	137-01	423
				Pier 20	8	139-01	426
					8	139-02	427
					8	139-03	428
				Pier 23	9	136-01	422
				Pier 31	24	130-01	715
					24	130-02	716
					36	130-03	717
				Pier 36	24	132-01	414
					24	132-02	415
					26B	132-03	416
					34	133-01	419
					35	134-01	420
					36	131-01	718
35-0284	Mariner's Island Boulevard Overhead	Foster City	97	8B	3	119L-01	789
37-0011	Bassett Street Overhead	San Jose	87	4	8	127L-01	711
37-0270	Three Connector Viaduct	San Jose	87/280	14, Line GC-4	25	022-08	486
						022-09	487
				06, Line GD-2	22 (#1)	022-01	479
						022-02	480
					22 (#2)	022-03	481
						022-04	482
				14, Line GD-2	22	022-10	488
				03, Line GD-4	22	022-05	483
						022-06	484
						022-07	485
				11, Line GD-4	39	022-11	489
37-0279	First Street Separation	San Jose	101/280	2L-2	21	129L-01	713
						129L-02	714
				3R-2	1	023-01	490
				6L-2	11	023-02	491
37-0353	South Connector Overcrossing	San Jose	280/680	8	5	104L-01	773
37-0410	Guadalupe Connector Viaduct	San Jose	87	3	34	128L-01	712
44-0002	Salinas River Bridge Replacement	San Ardo	101	Test Group	Test Pile (#1)	025-01	493

Bridge	Name	City	Inter. Route	Bent	Pile	CTID	LTN
					Test Pile (#2)	025-02	494
44-0030	San Lorenzo Creek Bridge	King City	198	Pier 2	13	027-01	496
				Pier 2	13	027-02	497
				Pier 3	13	027-03	498
44-0216	Salinas River Bridge	Marina/ Castroville	1	Test Group	Test Pile	093-01	699
						093-02	700
46-0252	Linwood Street Bridge	Visalia	198	2	Test Pile	112-01	779
46-0254	Demaree Street Bridge	Visalia	198	2	Test Pile	113-01	780
46-0255	County Center Bridge	Visalia	198	2	Test Pile	111-01	778
49-0133	Tefft Street Overcrossing	Nipomo	101	2, Column 1	11	026-01	495
					31	117L-01	787
51-0273	Garden Street Seal Slab	Santa Barbara	101	Station 16+67	1	116L-02	785
51-0273	Garden Street Seal Slab	Santa Barbara		Station 20+04	Test Pile	116L-01	755
						116L-03	753
				Station 20+12	A	116L-04	786
				Station 22+58	2	102L-01	752
51-0276	State Street Seal Slab	Santa Barbara	101	Abutment 1	3	115L-01	757
				Abutment 2	Test Pile	115L-04	759
				5	907	115L-02	756
					909	115L-03	758
52-0118	Santa Clara River Bridge	Fillmore	23	Pier 02	25	065-01	622
						065-02	623
				Pier 11	406	066-01	624
						066-02	625
52-0178	Ventura Underpass	Ventura	2	Abutment 1	69	114L-04	784
				Abutment 3	113	114L-02	782
					123	114L-01	781
				3	200	114L-03	783
52-0202	Rose Road Overcrossing	Ventura	2	4	15	110L-01	777
52-0217	Chestnut Street Overrail Overhead	Ventura	2	6	101	123L-01	791
52-0271	Nyeland Acres Overcrossing	Ventura	2	3	24	109L-01	776
52-0331	Arroyo Simi Bridge and Overhead	Moorpark	23/118	5R	Test Pile	064-01	621

Bridge	Name	City	Inter. Route	Bent	Pile	CTID	LTN
53-0527	Route 2/5 Separation	Los Angeles	5	10, Ramp 7	31	063-01	620
					35	062-01	619
				04, Ramp 8	27	061-01	618
53-1144	Vermont Avenue Overcrossing	Los Angeles	405	5	7	058-01	610
						058-02	611
53-1181	Griffith Park Off-Ramp Overcrossing	Los Angeles	5	5	25	057-01	609
53-1193	Los Coyotes Diagonal Undercrossing	Long Beach	405	6	5	056-01	608
53-1261	182nd Street Bridge	Los Angeles	110	2	8	055-01	607
53-1397	Route 5/60 Separation	Los Angeles	5	5	14	051-01	598
53-1424	Elysian Viaduct	Los Angeles	5/110	5	3	103L-02	770
				5, Ramp 18	8	103L-01	769
53-1790	Los Angeles River Bridge and Overhead	Los Angeles/ Glendale	134	C-5	6	052-02	600
				D-3	6	052-04	602
				D-5	10	052-03	601
				D-8	10	052-01	599
53-1851	Route 90/405 Separation (Retrofit)	Culver City	90/405	21, Footing A	2	050-01	597
53-2518	Dominquez Channel Bridge	Inglewood	105	Abutment 1	4	047-01	593
				Abutment 2	220	047-04	594
53-2598	Yukon Avenue Undercrossing	Inglewood	105	Abutment 1	31	046-01	592
53-2653	Imperial Highway On-Ramp	Hawthorne	105	7	10	048-01	595
53-2733	HOV Viaduct No. 1	Los Angeles	110/5	2	36	044-01	589
					38	044-02	590
				20	Test Pile	045-01	591
53-2791	LaCienega-Venice Separation	Los Angeles	10	5	71	088-01	683
55-0422	West Connector Overcrossing	Costa Mesa	55/405	2	5	032-01	527
55-0438	Northeast Connector Overcrossing	Costa Mesa	55/405	9	22	032-02	528
55-0642	Southbound Off Ramp Overcrossing	Tustin	5/55	6	18	108L-02	732
					21	108L-01	731
55-0680	57/5 Separation (WB Conn.)	Orange	57/5	5	2C	126L-03	799
					3C	126L-02	798
					4S	126L-01	795
55-0681	Route 57/5	Orange	5/57	5	1C	125L-05	764

Bridge	Name	City	Inter. Route	Bent	Pile	CTID	LTN
	Separation				2C	125L-01	792
					3C	125L-04	794
					4S	125L-03	763
					6C	125L-02	793
55-0682	57/5 Southbound Connector	Orange/ Santa Ana	5/57	4	7	140-07	707
					29R	140-10	710
					38	140-09	709
55-0689	HOV Connector Viaduct	Tustin	5/55	4	20	106L-02	734
					21	106L-01	733
				16	16	105L-01	765
					21	105L-02	766
				44	2	033-02	530
					3	033-01	529
				47	15	107L-01	774
					19	107L-02	775
55-0794	WS Connector Overcrossing	Yorba Linda	231/91	8	23	060-01	613
						060-03	615
					47	060-02	614
						060-05	617
					48	060-04	616
54-0823	Colton Interchange (NW Conn. Overcrossing)	Ontario	10/215	Smooth Pile Group	#1-2	090b-01	691
					#1-4	090a-01	690
						090b-02	692
54-0967	Southeast Connector Separation	Fontana/ Rancho Cucamo	15/30	2	Test Pile	042-01	582
						042-02	583
				9	Test Pile	042-03	584
						042-04	585
				13	Test Pile	042-05	586
						042-06	587
57-0488	San Diequito River Bridge	San Diego	5/55	Test Group	Test Pile	035-01	533
						035-02	534
57-0720	Mission Valley Viaduct	San Diego	8/805	Control Location 01	5	036-01	535
					5	036-02	536
				Control Location 02	5	036-03	537
					5	036-04	538
				Control Location 03	5	036-05	539
					5	036-06	540
				Control Location 06	5	036-07	541
					5	036-08	542

Bridge	Name	City	Inter. Route	Bent	Pile	CTID	LTN
				Control Location 07	5	036-09	543
					5	036-10	544
				Control Location 08	5	036-11	545
					5	036-12	546
				Control Location 09	5	036-13	547
					5	036-14	548
				Control Location 10	5	036-15	549
				03R	4	036-16	550
				11, Ramp 3	7	036-19	553
				11, Ramp 5	2	036-18	552
				17, Ramp 6	3	036-17	551
				19, Ramp 7	7	036-20	554
57-0783	Northeast Connector Overcrossing	San Diego	5	5	18	038-01	557
57-0982	Spring Canyon Road Undercrossing	San Diego	52	Pier 2L	48	039a-01	558
57-0989	Route 5/56 Separation	San Diego	5/56	4L	8	037-01	555
						037-02	556
57-0990	Carmel Valley Creek Connector	San Diego	5/56	2	17	034-01	531
						034-02	532
57-1017	Mission Avenue Viaduct	Oceanside	76	Abutment 7R	5	087-03	681
				2L	5	087-01	679
					5	087-02	680
				Retaining Wall 179	5	087-04	682
I-5/I-8 IPTP	I-5/I-8 Interchange IPTP	San Diego	5/8	Site 1	1C	041-01	570
						041-02	571
					1D	041-03	572
					1E	041-04	573
					1F	041-05	574
						041-06	575
				Site 2	2C	041-07	576
						041-08	577
					2D	041-09	578
					2E	041-10	579
					2F	041-11	580
						041-12	581

1. "Bridge" is a unique number assigned by Caltrans to each bridge
2. "Bridge Num" is a unique number we assigned to each bridge as we received data for that structure. It is used as shorthand notation in large tables.
3. "Site" is an abbreviation that brings to mind a site without having to enter a site description, e.g., Oak is a site in Oakland. The site numbers were assigned for convenience in this report.
4. "Name" is a more general description of the site and structure.
5. "City" is the name of the city within whose borders the site is located. In some cases it is the name of a nearby city.
6. "County" is the name of the country.
7. "Inter. Route" is the name of an intersecting highway.
8. "Bent" may be an actual bridge bent number or it may be a special term, e.g., identification of an abutment.
9. "Pile" is the pile number from the plans for this structure. It is not used further in this report.
10. "LTN is a load test number assigned by us and used in later tables.

Appendix B: Correlations for Young's Modulus

Appendix B.1 Correlations with Standard Penetration Test (SPT) Blowcount, N.

SPT				
Soil Type	Pile/Found. Type	E_s (MPa)	Reference	Notes/Method
ALL				
Clays and Sands	All	$1.58+0.316N$	Webb (1970)	
All soil		$35N^{0.8}$	Ohsaki and Iwasaki (1973)	
Clays and sands	All	$39.5N^{0.68}$ (initial tangent modulus)	Imai & Tonouchi (1982)	Eq. given for G, assumed υ=0.4 (Japanese practice)
All		$(2.5\text{-}2.8)N$	Shioi & Fukui (1982)	Japanese railway and bridge standards
Clays and Sands		$(2.5\pm0.5)N$	Decourt et al. (1989)	Pile-soil interface

SPT				
Soil Type	Pile / Found. Type	E_s (MPa)	Reference	Notes/Method
COHESIVE/ CLAY				
Clays	All	$(0.5\pm0.2)N$	Stroud (1974)	Below pile tip
Clays		$(0.5\pm0.2)N$	Stroud (1974)	Modulus well-below pile tips, E_s(MPa)
Clays, bored piles		$(0.5\text{-}0.7)M$ M =constrained modulus	Stroud (1974)	Modulus well-below pile tips, E_s(MPa)
Clays	All	$1.5N$	Decourt (1978)	
Clays	Driven	$3(1+0.16z)$ / $1.5N$	Yamashita et al. (1987)	Cast-in-place concrete, side, use the larger value
Clays	Driven	$3(1+0.16z)$	Yamashita et al. (1987)	Cast-in-place concrete, tip
Clays	Driven	$(15\pm5)c_u$	Poulos (1989)	
Clays	All	$14N$	Hirayama (1991)	Small strain

SPT				
Soil Type	Pile/Found. Type	E_s (MPa)	Reference	Notes/Method
SAND				
Sand	All	$7.46+0.517N$	Schultze & Menzenbach (1960)	
Sand		$E_s = 7.5(1-\nu^2)N$ tons/ft^2 ν=Poisson's ratio	Farrent (1963)	Terzaghi and Peck load settlement curves
Dry sand		$\nu*\sigma^{0.522}$ $\nu = 246.2\log_{10}(N)-253.4p_o+375.6+57.6$ $0<p_o<1.2$kg/cm^2 p_o=effective overburden pressure σ =applied stress (kg/cm^2)` $E=246.2\log_{10}(N)+300$	Schultze and Melzer (1965)	E=kg/cm^2 =100kPa =0.1MPa For calculated E, assume p_o=30kPa =0.3kg/cm^2 σ =100kPa =1.0kg/cm^2
Saturated sand		$5(N+15)$	Webb (1969)	E=kg/cm^2 =100kPa =0.1MPa
Sand	All	$36.79+1.043N$	D'Appolonia (1970)	Preloaded
Sand	All	$7.17+0.478N$	Webb (1970)	Saturated
Soil modulus for driven piles in sand	Driven	$2.8N$ (MPa)	Parry (1971, 1977)	
Silica sands		$16.9N^{0.9}$	Ohsaki and Kawasaki (1973)	Small strain modulus, E_{si} (MPa)
Sand	Driven	$4N$	Komornik (1974)	
Dry sand		$500\log_{10}(N)$	Trofimenkov (1974)	E=kg/cm^2 =100 kPa =0.1 MPa
Soil modulus for driven piles in sand	Driven	$(0.6-3)N$ Upper bound	Burland et al. (1977)	
Sand	All	$3N$	Decourt (1978)	
Silts, sandy		$8N_1$, N_1=Standard	Bowles	E_s=(ksf)

SPT				
Soil Type	Pile/Found. Type	E_s (MPa)	Reference	Notes/Method
SAND				
silts, slightly cohesive mixtures Clean fine to medium sands and slightly silty sands Coarse sands and sands with little gravel		Penetration Test (SPT) resistance $14N_1$, N_1=Standard Penetration Test (SPT) resistance $20N_1$, N_1=Standard Penetration Test (SPT) resistance	(1982) and U.S. Department of the Navy (1982)	
Sand	All	$7\sqrt{N}$	Denver (1982)	Average of pressuremeter and screw-plate tests
Silica sands		$7N^{0.5}$	Denver (1982)	Modulus well-below pile tips, E_s(MPa)
Silica sands, driven piles		$53q_c^{0.61}$	Imai and Tonouchi (1982)	Small strain modulus, E_{si} (MPa)
Partially saturated sand		$2.22N^{0.888}$	Wrench and Nowatzki (1985)	E=kg/cm^2 =100kPa =0.1MPa
Sand	Driven	$60+3.2N_s$	Kurkur (1986)	N_s: average N along shaft. Valid at 50% of failure load.
Sand	Driven	$6[N/5+3]$	Yamashita et al. (1987)	Cast-in-place concrete, side
Sand	Driven	$0.4N$ (30 MPa max.)	Yamashita et al. (1987)	Cast-in-place concrete, tip
Sand		$500(N+15)$	Bowles	kPa (1

SPT				
Soil Type	Pile/Found. Type	E_s (MPa)	Reference	Notes/Method
SAND				
(normally consolidated) Sand (over-consolidated) Clayey sand Silty sand		(15000-22000)ln$N$ 18000+750N $E_{sOCR} = E_{sNC}(OCR)^{0.5}$ 320(N+15) 300(N+6)	(1988)	tsf=100kPa)
Sand	Driven	7.5N-94.5	Christoulas (1988)	Valid for piles that are not tapered

SPT				
Soil Type	Pile/Foundation Type	E_s (MPa)	Reference	Notes/Method
GRAVEL				
Gravel		15N	Schmertmann (1970) Schmertmann (1978)	Under axisymmetric loading E=kg/cm^2 =100kPa =0.1MPa
Gravel		2.22$N^{0.888}$	Wrench & Nowatzki (1986)	Horizontal plate load test

SPT				
Soil Type	Pile/Foundation Type	E_s (MPa)	Reference	Notes/Method
COHESIONLESS Sand to Gravel				
Sands and gravel	All	18.75+0.756*N*	D'Appolonia (1970)	Normally consolidated sand
Gravel with sand		12(*N*+6) *N*<15 40+12(*N*-6) *N*>15	Begemann (1974)	E=kg/cm^2 =100kPa =0.1MPa
Silt with sand to gravel with sand		$E_s = 40 + C(N - 6)$ kg/cm^2 *N*>15 $Es = C(N + 6)$ kg/cm^2 *C*= 3 (silt with sand) to 12 (gravel with sand)	Begemann (1974)	Used in Greece
Sand and gravel Silty sand		$S = p\sqrt{B}/2N$ $S = p\sqrt{B}/N$ inches p in tons/ft^2, *B* in inches	Meyerhof (1974)	Analysis of field data of Schultze and Sherif (1973) Conservative estimate of maximum settlement of shallow foundations
Sandy gravel and gravels		24N_1, N_1=Standard Penetration Test (SPT) resistance	Bowles (1982) and U.S. Department of the Navy (1982)	Es=(ksf)
Gravelly sand and gravel		600(*N*+6) $N \leq 15$ 600(*N*+6)+2000 *N*>15	Bowles (1988)	kPa (1 tsf=100kPa)

Appendix B.2 Correlations based on cone penetration test (CPT) data

Soil Type	Pile/Foun-dation Type	E_s (MPa)	Reference	Notes/Method
ALL				
All		$1.5q_c$	Buisman (1940)	Very conservative
Pure sand Silty sand Clayey sand Soft clay		$E_s = \alpha q_c$ $\alpha = 0.8 - 0.9$ $\alpha = 1.3 - 1.9$ $\alpha = 3.8 - 5.7$ $\alpha = 7.7$	Bachelier and Parez (1965)	
All		$C = 1.9q_c / p_o$	Meyerhof (1965)	Based on back-calculated settlement records
All		E_s=$2q_c$	Schmertmann (1970)	Screw plate tests used to measure E
Clayey sand		2.4+1.67q_c	Webb (1970)	Saturated
All		E= function of both cone resistance and overburden pressure	Folque (1974)	
All		$E = m_p \sqrt{q_{net} q_a}$ q_a=ref stress =100 kPa q_{net} =net cone resistance	Janbu (1974)	m_p is determined from N_q value
All		$E = 1.141q_c + 33.129$ (E in kg/cm^2)	Schultze (1974)	Based on laboratory tests
Sands Clays		$E_s = 3q_c$ $E_s = 7q_c$	Trofimenkov (1974)	U.S.S.R. practice
All		αq_c, $3 < \alpha < 10$	Veismanis (1974)	Txl tests and penetration tests in small chamber
Unspecified		$E_{st} = \alpha q_c$ $E_s = 10.8 + 6.6q_c$	Holeyman (1985) Verbrugge (1982)	α =24-30 Dynamic modulus value E_s and q_c in

Soil Type	Pile/Foun-dation Type	E_s (MPa)	Reference	Notes/Method
ALL				
				MN/m^2 (for q_c >0.4MN/m^2)
Clays and sands	All	$21.066q_c^{1.091}$	Christoulas (1988)	
Silica sands, driven piles Clays, driven piles		$(7.5 \pm 2.5)q_c$ $(7.5 \pm 2.5)q_c$	Poulos (1989) Stroud (1974)	Near-shaft modulus, E_s (MPa) Modulus well-below pile tips, E_s(MPa)

Soil Type	Pile/Foundation Type	E_s (MPa)	Reference	Notes/Method
CLAY				
Clays, driven piles		$(500 \pm 5)q_c$	Callanan and Kulhawy (1985)	Near-shaft modulus, E_s (MPa)
Clays		(150-225)c_u 200	Johnson (1986)	
Clays		(3-8)q_c	Johnson (1986)	
Clay and silts		$E_s^* = 21.0q_c^{1.09}$ $E_s = 15\,q_c$	Christoulas (1988) Poulos (1988c)	Various pile types E_s and q_c in MN/m^2 E_s^* = secant Young's modulus
Clays, bored piles		$10q_c$	Christoulas and Frank (1991)	Near-shaft modulus, E_s (MPa)
Clays, driven piles		$49.4q_c^{0.695}e_0^{-1.13}$	Mayne and Rix (1993)	Small strain modulus, E_{si} (MPa)

Soil Type	E_s (MPa)	Reference	Notes/Method
SAND			
Sands	$E_s = 1.5q_c$	Buisman (1940)	Overpredicts settlements by a factor of about two
NC Sands	$1.5q_c$	De Beer & Martens (1957)	
Sand	$E_s = 2.5qc$ $E_s = 100 + 5q_c$	Trofimenkov (1964)	Lower limit Average
Sand	$1.9q_c$	Meyerhof (1965)	
Dry sand	$E = \frac{1}{mv} = v\sigma^{-.552}$ $v = 301.1 \log q_c - 382.3\gamma +$ $60.3 \pm 50.3 log/cm^2$	Shultze and Melzer (1965)	Compacted in 3m diameter test pit
Sand	$E = 2(1 + D_r^{\ 2})q_c$, D_r=rel. density	Vesic (1965)	Pile load tests in sand
Sand	$E_s = 1.5q_c$	De Beer (1967)	Overpredicts settlements by a factor of two
Overconsolidated sand	$A = C(A_{oed} / C_{oed})$	De Beer (1967)	C from field tests A_{oed} and C_{oed} from lab oedometer tests $C_{oed} = 2.3(1+e)/C_c$ $A_{oed} = 2.3(1+e)/C_s$
Normally consolidated sands	$E_s = \alpha q_c$ $\alpha = 3 - 12$	Thomas (1968)	Based on penetration and compression tests in large chambers Lower values of α at higher values of q_c; attributed to grain crushing
Sands	$E = 2.5q_c + 75 ton/ft^2$	Webb (1969)	Plate load tests on sands. E values checked with observed settlements
Sands	$2q_c$	Schmertmann	Based on screw plate

Soil Type	E_s (MPa)	Reference	Notes/Method
SAND			
		(1970)	tests $\triangle\sigma = 2tsf$
Sand	$E_s = 2(1+D_R{}^2)q_c$ D_R =relative density	Vesic (1970)	Based on pile load tests and assumptions concerning state of stress
Sand	$7.17+2.5q_c$	Webb (1970)	Saturated
Sands, sandy gravels Silty saturated sands Clayey silts with silty sand and silty saturated sands with silt	$E_s = \alpha q_c$ $q_c > 40kg/cm^2 \quad \alpha = 1.5$ $20 < q_c < 40 \quad \alpha = 1.5-1.8$ $10 < q_c < 20$ $\alpha = 1.8-2.5$ $5 < q_c < 10 \quad \alpha = 2.5-3.0$	Bogdanovic (1973)	Based on analysis of silo settlements over a period of 10 years
NC and OC sands	$E = \alpha q_c$ $1 < \alpha < 4$	Dalhberg (1974)	E_s back-calculated from screw plate settlement using Buisman-DeBeer and Schmertmann methods; α increases with increasing q_c
NC sands NC sands	$E_s = 2.5q_c$ $E_s = 3.5q_c$	Schmertmann (1974a)	*L/B*=1 to 2 axisymmetric $L/B \geq 10$ plane strain
NC sands OC sands Sand Sand Sand	$C > \frac{3}{2}\frac{q_c}{\sigma_o}$ $A > \varepsilon\frac{3}{2}\frac{q_c}{\sigma_o}$ $E_s = 1.6q_c - 8$ $E_s = 1.5q_c$, q_c>30kg/cm^2 $E_s = 3q_c$, q_c<30kg/cm^2 $E_s > 3/2q_c$ or $E_s = 2q_c$	De Beer (1974b)	Belgian practice $3 < \varepsilon < 10$, Belgian practice Bulgarian practice Greek practice Italian practice

Soil Type	E_s (MPa)	Reference	Notes/Method
SAND			
Sand Fine to medium sand Clayey sands, PI<15% Sands	$E_s = 1.9q_c$ $E_s = \frac{5}{2}(q_c + 3200) kN/m^2$ $E_s = \frac{5}{3}(q_c + 1600) kN/m^2$ $E_s = \alpha q_c$, $1.5 < \alpha < 2$		South African practice U.K. practice
Sands	$2.5q_c$	Schmertmann (1978)	Modified, axisymmetrical footing
Sands	$8\sqrt{q_c / q_0}$	Denver (1982)	q_0 = 1 MPa, $q_{CPT}/q_{Dutchcone} = 1.3$
Silica Sands	$E_s = \alpha q_c$ $E_{st}^{\dagger} = 53 q_c^{0.61}$	Milovic and Stevanovic (1982) Poulos (1988c) Imai and Tonouchi (1982)	α =20-40 α =5 (normally-consolidated sands) α =7.5 (over-consolidated sands) E_{st} and q_c in MN/m^2 Dynamic modulus value $E_{st}^{\dagger}$ =initial tangent Young's modulus
Sandy soils	$4\,q_c$	Bowles (1982) and U.S. Department of the Navy (1982)	q_c =Cone penetration resistance (ksf)
Sand (normally	$2 - 4\,q_c$	Bowles	kPa (1 tsf=100kPa)

Soil Type	E_s (MPa)	Reference	Notes/Method
SAND			
consolidated) Sand (over-consolidated) Clayey sand Silty sand Soft clay	$(1+D_r^2)q_c$ 6-30 q_c 3-6q_c 1-2q_c 3-8q_c	(1988)	
Silica sands, driven piles	$(7\pm4)q_c$	Jamiolkowski et al. (1988)	Modulus well-below pile tips, E_s(MPa)
Silica, bored piles	$(3\pm0.5)q_c$	Poulos (1993)	Near-shaft modulus, E_s (MPa)

Soil Type	Pile/Foundation Type	E_s (MPa)	Reference	Notes/Method
COHESIONLESS Sand to Gravel				
Cohesionless soil		$S = pB/2q_c$ in consistent units *S*=settlement	Meyerhof (1974)	Conservative estimate, based on analysis of vertical strain

Appendix B.3 Correlations based on Undrained Shear Strength, s_u

Clays, bored piles		$(150 \pm 50)s_u$	Stroud (1974)	Modulus well-below pile tips, E_s(MPa)
Clays, bored piles		$(150 - 400)s_u$	Poulos and Davis (1980)	Near-shaft modulus, E_s (MPa)
Soft sensitive clay Medium stiff to stiff clay Very stiff clay		$400s_u$-$1000s_u$ $1500s_u$-$2400s_u$ $3000\ s_u$-$4000s_u$	Bowles (1982) and U.S. Department of the Navy (1982)	s_u=undrained shear strength (ksf)
Clay		$I_p > 30$ or organic Es= 100-500s_u $I_p < 30$ or stiff Es= 500-1500s_u $E_{sOCR} = E_{sNC}(OCR)^{0.5}$	Bowles (1988)	Expressed in terms of undrained shear strength, s_u; and in same pressure units as s_u Unit of E_s is in kPa.
Clays, driven piles		$1500s_u$	Hirayama (1991)	Small strain modulus, E_{si} (MPa)

Appendix C: Tapile Input and Output Files

Appendix C.1 Example Input File

```
**********************************************************************
*                                                                    *
*                    Data File from Program TAPILE                   *
*                                                                    *
**********************************************************************

Title
=====
657.dat 34-0046 SouthFW Via. TensPTS Pile 49 110.8' 16x0.5 OP Tens.

Exposed Pile Data
=================
 25.1          Exposed pile length (feet).....(ExpLen)
 24.35         Exposed cross sectional area (sq.in.).....(ExpArea)
 29000          Youngs modulus of exposed pile section.....(ExpMod)

Data for Pile Below Ground Surface
==================================
 105            Pile penetration (feet).....(LEN)
 11.2          Diameter of the base (inches).....(DB)
 12             Number of shaft elements.....(NS)
 1              Number of base elements.....(NB)
 0              1 for uniform pile, 0 if nonuniform.....(UNIPIL)
 0.4           Poissons ratio.....(PR)

              LE(I)          DIA(I)          AR(I)          EP(I)
 I            feet           inches          sq.In.         ksi
 1              10             16             98.57          29000
 2              10             16             98.57          29000
 3              2.5            16             98.57          29000
 4              10             16             98.57          29000
 5              10             16             98.57          29000
 6              10             16             98.57          29000
 7              10             16             98.57          29000
 8              10             16             98.57          29000
 9              10             16             98.57          29000
 10             10             16             98.57          29000
 11             10             16             98.57          29000
 12             2.5            16             98.57          29000
```

Data for Soil
==========

0	0 for nonuniform soil,1 for uniform soil.....(IUNIF)

Layer	Youngs Modulus (ksf)
1	0.001
2	0.001
3	394
4	636
5	636
6	636
7	636
8	636
9	636
10	636
11	636
12	636
13	636

1212	Youngs modulus of soil below the pile tip(ksf)..(EBase)
115	Thickness of soil (feet).....(SoilH)

Side Shear Stresses at Failure in Compression
==========

0.001	side shear at failure in compression (ksf).....[TA(1)]
0.001	side shear at failure in compression (ksf).....[TA(2)]
0.858	side shear at failure in compression (ksf).....[TA(3)]
0.904	side shear at failure in compression (ksf).....[TA(4)]
0.904	side shear at failure in compression (ksf).....[TA(5)]
0.904	side shear at failure in compression (ksf).....[TA(6)]
0.904	side shear at failure in compression (ksf).....[TA(7)]
0.904	side shear at failure in compression (ksf).....[TA(8)]
0.904	side shear at failure in compression (ksf).....[TA(9)]
0.904	side shear at failure in compression (ksf).....[TA(10)]
0.904	side shear at failure in compression (ksf).....[TA(11)]
0.904	side shear at failure in compression (ksf).....[TA(12)]

End Bearing Stresses in Compression
==========

9.436	tip failure stress in compression (ksf).....[TA(13)]

Side Shear Stresses at Failure in Tension
==========

0.001	side shear at failure in tension (ksf).....[TAUP(1)]
0.001	side shear at failure in tension (ksf).....[TAUP(2)]

```
 0.807          side shear at failure in tension (ksf).....[TAUP(3)]
 0.85           side shear at failure in tension (ksf).....[TAUP(4)]
 0.85           side shear at failure in tension (ksf).....[TAUP(5)]
 0.85           side shear at failure in tension (ksf).....[TAUP(6)]
 0.85           side shear at failure in tension (ksf).....[TAUP(7)]
 0.85           side shear at failure in tension (ksf).....[TAUP(8)]
 0.85           side shear at failure in tension (ksf).....[TAUP(9)]
 0.85           side shear at failure in tension (ksf).....[TAUP(10)]
 0.85           side shear at failure in tension (ksf).....[TAUP(11)]
 0.85           side shear at failure in tension (ksf).....[TAUP(12)]

Tip Tensile Stresses at Failure
==============================
 0.001          tip failure stress in tension (ksf).....[TAUP(13)]

Loads
=====
 16              Number of loads.....(Loads)
-20              Total applied load (kips).....[PSum(1)]
-40              Total applied load (kips).....[PSum(2)]
-60              Total applied load (kips).....[PSum(3)]
-80              Total applied load (kips).....[PSum(4)]
-100.77          Total applied load (kips).....[PSum(5)]
-120             Total applied load (kips).....[PSum(6)]
-140             Total applied load (kips).....[PSum(7)]
-151.16          Total applied load (kips).....[PSum(8)]
-160             Total applied load (kips).....[PSum(9)]
-180             Total applied load (kips).....[PSum(10)]
-201.55          Total applied load (kips).....[PSum(11)]
-220             Total applied load (kips).....[PSum(12)]
-240             Total applied load (kips).....[PSum(13)]
-260             Total applied load (kips).....[PSum(14)]
-280             Total applied load (kips).....[PSum(15)]
-302.22          Total applied load (kips).....[PSum(16)]

Data for Measured Load-Settlement Curve
=======================================
 0                =number of points on measured Q-S curve (MeasPts)
```

Appendix C.2 Example Output File

```
**********************************************************************
*                                                                    *
*                    Output from Program TAPILE                      *
*                                                                    *
**********************************************************************

Analysis performed on    7/ 3/2006 at 22:46

Title
=====
657.dat 34-0046 SouthFW Via. TensPTS Pile 49 110.8' 16x0.5 OP Tens.

Input Data
==========
Exposed Length.....(ExpLen)       25.10 feet
Exposed Area.....(ExpArea)         24.4 sq.in.
Exposed Modulus.....(ExpMod)      29000. ksi
Pile Penetration.....(LEN)      105.00 feet
Base Diameter.....(DB)        11.20 inches
Pile Poissons Ratio.....(PR)         0.40
Number of Side Elements.....(NS)           12
Number of Base Elements.....(NB)            1
Number of Discontinuities.....(ND)          0
```

Element Num.	Length feet	Diameter inches	Pile Modulus ksi	Section Area sq.in.
1	10.00	16.00	29000.	98.57
2	10.00	16.00	29000.	98.57
3	2.50	16.00	29000.	98.57
4	10.00	16.00	29000.	98.57
5	10.00	16.00	29000.	98.57
6	10.00	16.00	29000.	98.57
7	10.00	16.00	29000.	98.57
8	10.00	16.00	29000.	98.57
9	10.00	16.00	29000.	98.57
10	10.00	16.00	29000.	98.57
11	10.00	16.00	29000.	98.57
12	2.50	16.00	29000.	98.57

Element Num.	Soil Modulus ksf
1	0.
2	0.
3	394.

4	636.
5	636.
6	636.
7	636.
8	636.
9	636.
10	636.
11	636.
12	636.
13	636.

Total Depth of Soil (feet)..... 115.00 feet
Modulus of Sublayer..... 1212.00 ksf
Ultimate Load in Compression..... 327.92 kips
Ultimate Load in Tension..... 302.27 kips

Side Shearing Stresses

Element Num	Compression ksf	Tension ksf
1	0.001	0.001
2	0.001	0.001
3	0.858	0.807
4	0.904	0.850
5	0.904	0.850
6	0.904	0.850
7	0.904	0.850
8	0.904	0.850
9	0.904	0.850
10	0.904	0.850
11	0.904	0.850
12	0.904	0.850

Tip Stresses

Element Num	Compression ksf	Tension ksf
13	9.44	0.00

Tip Stresses for Discontinuities

Element Num	Compression ksf	Tension ksf

****

Load Number 1
Load Increment..... -20.00
Total Load..... -20.00

Element No.	Side Shearing Stress, ksf	Movement inch
1	0.0000	-0.0115
2	0.0000	-0.0106
3	-0.0695	-0.0101
4	-0.0758	-0.0096
5	-0.0598	-0.0089
6	-0.0539	-0.0084
7	-0.0503	-0.0079
8	-0.0481	-0.0075
9	-0.0469	-0.0072
10	-0.0478	-0.0070
11	-0.0528	-0.0069
12	-0.0978	-0.0068
13	-0.0010	-0.0068

Compression of exposed pile -0.0085 inch
Compression of immersed pile -0.0119 inch

Depth feet	Load kips
0.00	-20.00
10.00	-20.00
20.00	-20.00
22.50	-19.27
32.50	-16.09
42.50	-13.59
52.50	-11.33
62.50	-9.22
72.50	-7.21
82.50	-5.24
92.50	-3.24
102.50	-1.03
105.00	0.00

****

Load Number 2
Load Increment..... -20.00
Total Load..... -40.00

Element No.	Side Shearing Stress, ksf	Movement inch
1	0.0000	-0.0229
2	0.0000	-0.0213

3	-0.1390	-0.0202
4	-0.1517	-0.0193
5	-0.1196	-0.0179
6	-0.1079	-0.0167
7	-0.1006	-0.0158
8	-0.0963	-0.0150
9	-0.0938	-0.0144
10	-0.0957	-0.0140
11	-0.1056	-0.0137
12	-0.1957	-0.0136
13	-0.0010	-0.0136

Compression of exposed pile -0.0085 inch
Compression of immersed pile -0.0323 inch

Depth feet	Load kips
0.00	-40.00
10.00	-40.00
20.00	-40.00
22.50	-38.54
32.50	-32.19
42.50	-27.18
52.50	-22.66
62.50	-18.45
72.50	-14.41
82.50	-10.48
92.50	-6.47
102.50	-2.05
105.00	0.00

****

Load Number 3
Load Increment..... -20.00
Total Load..... -60.00

Element No.	Side Shearing Stress, ksf	Movement inch
1	0.0000	-0.0344
2	0.0000	-0.0319
3	-0.2086	-0.0303
4	-0.2276	-0.0289
5	-0.1795	-0.0268
6	-0.1618	-0.0251
7	-0.1509	-0.0237

8	-0.1445	-0.0225
9	-0.1407	-0.0216
10	-0.1435	-0.0210
11	-0.1584	-0.0206
12	-0.2936	-0.0204
13	-0.0010	-0.0204

Compression of exposed pile -0.0085 inch
Compression of immersed pile -0.0527 inch

Depth feet	Load kips
0.00	-60.00
10.00	-60.00
20.00	-60.00
22.50	-57.82
32.50	-48.28
42.50	-40.77
52.50	-33.99
62.50	-27.67
72.50	-21.62
82.50	-15.72
92.50	-9.71
102.50	-3.08
105.00	0.00

****

Load Number 4
Load Increment..... -20.00
Total Load..... -80.00

Element No.	Side Shearing Stress, ksf	Movement inch
1	0.0000	-0.0459
2	0.0000	-0.0425
3	-0.2781	-0.0404
4	-0.3034	-0.0385
5	-0.2393	-0.0358
6	-0.2158	-0.0335
7	-0.2012	-0.0316
8	-0.1926	-0.0300
9	-0.1876	-0.0288
10	-0.1913	-0.0279
11	-0.2112	-0.0274
12	-0.3915	-0.0272

13	-0.0010	-0.0272

Compression of exposed pile -0.0085 inch
Compression of immersed pile -0.0731 inch

Depth feet	Load kips
0.00	-80.00
10.00	-80.00
20.00	-80.00
22.50	-77.09
32.50	-64.38
42.50	-54.36
52.50	-45.32
62.50	-36.89
72.50	-28.82
82.50	-20.96
92.50	-12.95
102.50	-4.10
105.00	0.00

****

Load Number 5
Load Increment..... -20.77
Total Load..... -100.77

Element No.	Side Shearing Stress, ksf	Movement inch
1	0.0000	-0.0578
2	0.0000	-0.0535
3	-0.3503	-0.0509
4	-0.3822	-0.0485
5	-0.3014	-0.0451
6	-0.2718	-0.0422
7	-0.2534	-0.0398
8	-0.2426	-0.0378
9	-0.2364	-0.0363
10	-0.2410	-0.0352
11	-0.2661	-0.0345
12	-0.4931	-0.0343
13	-0.0010	-0.0343

Compression of exposed pile -0.0089 inch
Compression of immersed pile -0.0940 inch

Depth feet	Load kips
0.00	-100.77
10.00	-100.77
20.00	-100.77
22.50	-97.10
32.50	-81.09
42.50	-68.47
52.50	-57.08
62.50	-46.47
72.50	-36.31
82.50	-26.41
92.50	-16.31
102.50	-5.16
105.00	0.00

****

Load Number 6
Load Increment..... -19.23
Total Load..... -120.00

Element No.	Side Shearing Stress, ksf	Movement inch
1	0.0000	-0.0688
2	0.0000	-0.0638
3	-0.4171	-0.0606
4	-0.4551	-0.0578
5	-0.3589	-0.0537
6	-0.3237	-0.0502
7	-0.3018	-0.0474
8	-0.2889	-0.0450
9	-0.2815	-0.0432
10	-0.2870	-0.0419
11	-0.3169	-0.0411
12	-0.5872	-0.0408
13	-0.0010	-0.0408

Compression of exposed pile -0.0082 inch
Compression of immersed pile -0.1143 inch

Depth feet	Load kips
0.00	-120.00
10.00	-120.00
20.00	-120.00

22.50	-115.63
32.50	-96.57
42.50	-81.53
52.50	-67.98
62.50	-55.34
72.50	-43.23
82.50	-31.44
92.50	-19.42
102.50	-6.15
105.00	0.00

****

Load Number 7
Load Increment..... -20.00
Total Load..... -140.00

Element No.	Side Shearing Stress, ksf	Movement inch
1	0.0000	-0.0803
2	0.0000	-0.0744
3	-0.4867	-0.0707
4	-0.5310	-0.0674
5	-0.4187	-0.0626
6	-0.3776	-0.0586
7	-0.3520	-0.0553
8	-0.3371	-0.0526
9	-0.3284	-0.0504
10	-0.3348	-0.0489
11	-0.3697	-0.0480
12	-0.6851	-0.0476
13	-0.0010	-0.0476

Compression of exposed pile -0.0085 inch
Compression of immersed pile -0.1344 inch

Depth feet	Load kips
0.00	-140.00
10.00	-140.00
20.00	-140.00
22.50	-134.90
32.50	-112.66
42.50	-95.12
52.50	-79.30
62.50	-64.56

72.50	-50.44
82.50	-36.69
92.50	-22.66
102.50	-7.18
105.00	0.00

****

Load Number 8
Load Increment..... -11.16
Total Load..... -151.16

Element No.	Side Shearing Stress, ksf	Movement inch
1	0.0000	-0.0867
2	0.0000	-0.0803
3	-0.5255	-0.0764
4	-0.5733	-0.0728
5	-0.4521	-0.0676
6	-0.4078	-0.0633
7	-0.3801	-0.0597
8	-0.3639	-0.0567
9	-0.3545	-0.0544
10	-0.3615	-0.0528
11	-0.3991	-0.0518
12	-0.7397	-0.0514
13	-0.0010	-0.0514

Compression of exposed pile -0.0048 inch
Compression of immersed pile -0.1495 inch

Depth feet	Load kips
0.00	-151.16
10.00	-151.16
20.00	-151.16
22.50	-145.66
32.50	-121.64
42.50	-102.71
52.50	-85.63
62.50	-69.70
72.50	-54.46
82.50	-39.61
92.50	-24.47
102.50	-7.75
105.00	0.00

****

Load Number 9
Load Increment..... -8.84
Total Load..... -160.00

Element No.	Side Shearing Stress, ksf	Movement inch
1	0.0000	-0.0917
2	0.0000	-0.0850
3	-0.5562	-0.0808
4	-0.6068	-0.0770
5	-0.4785	-0.0716
6	-0.4316	-0.0670
7	-0.4023	-0.0632
8	-0.3852	-0.0601
9	-0.3753	-0.0576
10	-0.3826	-0.0559
11	-0.4225	-0.0548
12	-0.7830	-0.0544
13	-0.0010	-0.0544

Compression of exposed pile -0.0038 inch
Compression of immersed pile -0.1596 inch

Depth feet	Load kips
0.00	-160.00
10.00	-160.00
20.00	-160.00
22.50	-154.18
32.50	-128.76
42.50	-108.71
52.50	-90.63
62.50	-73.78
72.50	-57.65
82.50	-41.93
92.50	-25.90
102.50	-8.20
105.00	0.00

****

Load Number 10
Load Increment..... -20.00
Total Load..... -180.00

Element No.	Side Shearing Stress, ksf	Movement inch
1	0.0000	-0.1033
2	0.0000	-0.0957
3	-0.6258	-0.0910
4	-0.6832	-0.0868
5	-0.5388	-0.0806
6	-0.4861	-0.0755
7	-0.4532	-0.0712
8	-0.4338	-0.0677
9	-0.4229	-0.0650
10	-0.4314	-0.0630
11	-0.4787	-0.0618
12	-0.8500	-0.0614
13	-0.0010	-0.0613

Compression of exposed pile -0.0085 inch
Compression of immersed pile -0.1753 inch

Depth feet	Load kips
0.00	-180.00
10.00	-180.00
20.00	-180.00
22.50	-173.45
32.50	-144.83
42.50	-122.26
52.50	-101.90
62.50	-82.92
72.50	-64.74
82.50	-47.03
92.50	-28.96
102.50	-8.90
105.00	0.00

****

Load Number 11
Load Increment..... -21.55
Total Load..... -201.55

Element No.	Side Shearing Stress, ksf	Movement inch
1	0.0000	-0.1160
2	0.0000	-0.1075

3	-0.7011	-0.1022
4	-0.7668	-0.0975
5	-0.6049	-0.0906
6	-0.5459	-0.0848
7	-0.5093	-0.0800
8	-0.4874	-0.0761
9	-0.4760	-0.0731
10	-0.4862	-0.0709
11	-0.5474	-0.0696
12	-0.8500	-0.0692
13	-0.0010	-0.0691

Compression of exposed pile -0.0092 inch
Compression of immersed pile -0.1970 inch

Depth feet	Load kips
0.00	-201.55
10.00	-201.55
20.00	-201.55
22.50	-194.21
32.50	-162.09
42.50	-136.75
52.50	-113.88
62.50	-92.55
72.50	-72.13
82.50	-52.20
92.50	-31.83
102.50	-8.90
105.00	0.00

****

Load Number 12
Load Increment..... -18.45
Total Load..... -220.00

Element No.	Side Shearing Stress, ksf	Movement inch
1	0.0000	-0.1268
2	0.0000	-0.1176
3	-0.7656	-0.1119
4	-0.8385	-0.1066
5	-0.6614	-0.0991
6	-0.5971	-0.0928
7	-0.5573	-0.0876

8	-0.5333	-0.0834
9	-0.5214	-0.0801
10	-0.5330	-0.0777
11	-0.6062	-0.0763
12	-0.8500	-0.0758
13	-0.0010	-0.0758

Compression of exposed pile -0.0079 inch
Compression of immersed pile -0.2174 inch

Depth feet	Load kips
0.00	-220.00
10.00	-220.00
20.00	-220.00
22.50	-211.98
32.50	-176.86
42.50	-149.16
52.50	-124.14
62.50	-100.80
72.50	-78.46
82.50	-56.62
92.50	-34.29
102.50	-8.90
105.00	0.00

****

Load Number 13
Load Increment..... -20.00
Total Load..... -240.00

Element No.	Side Shearing Stress, ksf	Movement inch
1	0.0000	-0.1397
2	0.0000	-0.1297
3	-0.8070	-0.1234
4	-0.8500	-0.1177
5	-0.7488	-0.1094
6	-0.6634	-0.1025
7	-0.6177	-0.0967
8	-0.5900	-0.0920
9	-0.5775	-0.0884
10	-0.5900	-0.0858
11	-0.6780	-0.0843
12	-0.8500	-0.0838

13	-0.0010	-0.0837

Compression of exposed pile -0.0085 inch
Compression of immersed pile -0.2386 inch

Depth feet	Load kips
0.00	-240.00
10.00	-240.00
20.00	-240.00
22.50	-231.55
32.50	-195.94
42.50	-164.58
52.50	-136.79
62.50	-110.92
72.50	-86.20
82.50	-62.01
92.50	-37.30
102.50	-8.90
105.00	0.00

****

Load Number 14
Load Increment..... -20.00
Total Load..... -260.00

Element No.	Side Shearing Stress, ksf	Movement inch
1	0.0000	-0.1530
2	0.0000	-0.1421
3	-0.8070	-0.1353
4	-0.8500	-0.1290
5	-0.8435	-0.1200
6	-0.7331	-0.1123
7	-0.6807	-0.1060
8	-0.6489	-0.1009
9	-0.6356	-0.0970
10	-0.6488	-0.0941
11	-0.7522	-0.0925
12	-0.8500	-0.0919
13	-0.0010	-0.0919

Compression of exposed pile -0.0085 inch
Compression of immersed pile -0.2608 inch

Depth feet	Load kips
0.00	-260.00
10.00	-260.00
20.00	-260.00
22.50	-251.55
32.50	-215.94
42.50	-180.61
52.50	-149.90
62.50	-121.39
72.50	-94.21
82.50	-67.59
92.50	-40.41
102.50	-8.90
105.00	0.00

****

Load Number 15
Load Increment..... -20.00
Total Load..... -280.00

Element No.	Side Shearing Stress, ksf	Movement inch
1	0.0000	-0.1677
2	0.0000	-0.1560
3	-0.8070	-0.1487
4	-0.8500	-0.1419
5	-0.8500	-0.1320
6	-0.8356	-0.1236
7	-0.7574	-0.1166
8	-0.7192	-0.1110
9	-0.7037	-0.1066
10	-0.7170	-0.1035
11	-0.8374	-0.1017
12	-0.8500	-0.1011
13	-0.0010	-0.1011

Compression of exposed pile -0.0085 inch
Compression of immersed pile -0.2845 inch

Depth feet	Load kips
0.00	-280.00
10.00	-280.00
20.00	-280.00

22.50	-271.55
32.50	-235.94
42.50	-200.34
52.50	-165.34
62.50	-133.61
72.50	-103.49
82.50	-74.01
92.50	-43.98
102.50	-8.90
105.00	0.00

****

Load Number 16
Load Increment..... -22.22
Total Load..... -302.22

Element No.	Side Shearing Stress, ksf	Movement inch
1	0.0000	-0.1912
2	0.0000	-0.1785
3	-0.8070	-0.1706
4	-0.8500	-0.1632
5	-0.8500	-0.1524
6	-0.8500	-0.1430
7	-0.8500	-0.1352
8	-0.8500	-0.1288
9	-0.8507	-0.1240
10	-0.8500	-0.1206
11	-0.8500	-0.1187
12	-0.8500	-0.1182
13	-0.0010	-0.1181

Compression of exposed pile -0.0095 inch
Compression of immersed pile -0.3169 inch

Depth feet	Load kips
0.00	-302.22
10.00	-302.22
20.00	-302.22
22.50	-293.77
32.50	-258.16
42.50	-222.56
52.50	-186.95
62.50	-151.35

72.50	-115.75
82.50	-80.11
92.50	-44.51
102.50	-8.90
105.00	0.00

FINAL TABLE OF RESULTS

Load kips	Settlement inch
-20.00	-0.0204
-40.00	-0.0408
-60.00	-0.0612
-80.00	-0.0817
-100.77	-0.1029
-120.00	-0.1225
-140.00	-0.1429
-151.16	-0.1543
-160.00	-0.1633
-180.00	-0.1838
-201.55	-0.2062
-220.00	-0.2253
-240.00	-0.2471
-260.00	-0.2694
-280.00	-0.2930
-302.22	-0.3264

References

Abe, S.K. and Teferra, W. (1998), "SPT Energy Measurements, Sonoma Valley CSD, Reclamation Ponds R1 and R2, Sonoma County, California", *Report No. 988031*, Goble Rausche Likins and Associates, Inc.

Alyahyai, K.S. (1987), *Use of Case Histories in Prediction of Load-Settlement Behavior of Steel Pipe Piles in Sand*, M.S. thesis, University of Texas at Austin, 161 pages.

American Petroleum Institute (1993), "Recommended Practice for Planning, Designing and Constructing Fixed Offshore Platforms – Working Stress Design: API Recommended Practice 2A-WSD (RP 2A-WSD)", Washington, DC.

Arman, A. and McManis, K.L. (1976), "Effects of Storage and Extrusion on Sample Properties", *Soil Specimen Preparation for Laboratory Testing*, ASTM Special Technical Publication No. 599, Philadelphia, 66-87.

Aschenbrener, T.B. (1984), *The Settlement Behavior of Single Piles in Clay*, M.S. thesis, University of Texas at Austin, 184 pages.

Aschenbrener, T.B. and Olson, R.E. (1984), "Prediction of Settlement of Single Piles in Clay", *Proceedings*, Analysis and Design of Pile Foundations, San Francisco, California, 41-58.

Atkinson, J.H. (2000), "Non-linear soil stiffness in routine design", *Géotechnique*, Vol. 50, No. 5, 487 – 508.

Azizi, F. (2000), *Applied Analyses in Geotechnics*, E&FN Spon, New York.

Baguelin, F., Jézéquel, J.-F. and Shields, D.H. (1978) *The Pressuremeter and Foundation Engineering*, TransTech Publications, Clausthal, Germany.

Barbour, S.L. and Krahn, J. (2004), "Numerical modeling - prediction or process?", *Geotechnical News*, BiTech Publishers, Richmond, British Columbia, 44-52.

Basile, F. (1999), "Non-linear analysis of pile groups", *Proceedings of the Institution of Civil Engineering: Geotechnical Engineering*, Vol. 137, No. 2, 105-115.

Basile, F. (2002), "Integrated form of singular Mindlin's solution", *Proceedings of 10th Annual Conference of the* Association for Computational Mechanics in Engineering *(ACME)-United Kingdom*, Swansea, 191-194.

Bazaraa, A.R. and Kurkur, M.M. (1986), "N-Values Used to Predict Settlements of Piles in Egypt", *Use of In Situ Tests in Geotechnical Engineering*, Proceedings, In Situ '86, Virginia Tech, Blacksburg, Virginia, 462-474.

Bond, A.J. and Jardine, R.J. (1995), "Shaft Capacity of Displacement Piles in a High OCR Clay", *Geotechnique*, Vol. 45, No. 1, 3-23.

Brettmann, T. (1995), "Computer Methods for Settlement Analyses of Piles", *Computing in Civil Engineering*, Proceedings of the Second Congress held in conjunction with A/E/C Systems '95, Atlanta, Georgia, 907-914.

Briaud, J.L. and Tucker, L.M. (1988), "Measured and Predicted Axial Response of 98 Piles", *Journal of Geotechnical Engineering*, Vol.114, No.9, 984-1001.

Briaud, J-L. and Miran, J. (1992), *The Cone Penetrometer Test*, Report FHWA-SA-91-043, U.S. Federal Highway Administration, Washington, DC.

Briaud, J-L., Tucker L. and Olsen, R. (1985), *Cone Penetrometer and Foundation Design*, short course notes, Texas A&M University.

Brown, D.A. and Vinson, J. (1998), "Comparison of Strength and Stiffness Parameters for a Piedmont Residual Soil", in *Geotechnical Site Characterization*, Robertson and Mayne (Eds.), Balkema, Rotterdam, 1229-1234.

Brown, R.E. (1977), "Drill Rod Influence on Standard Penetration Test", *Journal of the Geotechnical Engineering Division*, ASCE, Vol. 103, No. 11, 1332-1336.

Brown, R.P. (2001), *Predicting the Ultimate Axial Resistance of Single Driven Piles*, PhD dissertation, The University of Texas at Austin, 220 pages.

Butterfield, R. and Abdrabbo, F.M. (1983), "Static Working Load Tests on Small Scale Pile Groups in Clay", *Developments in Soil Mechanics and Foundation Engineering, Vol. 1: Model Studies*, Banerjee, P.K. and Butterfield, R. (eds.), 111-168.

Butterfield, R. and Banerjee, P.K. (1971), "The Elastic Analysis of Compressible Piles and Pile Groups", *Géotechnique*, Vol. 21, No. 1, pp. 43-60.

California Foundation Manual, State of California Department of Transportation, Engineering Service Center, Division of Structures, Office of Structure Construction, July 1997.

Callanan, J.F. and Kulhawy, F.H. (1985), *Evaluation of Procedures for Predicting Foundation Uplift Movements*, Electric Power Research Institute EL-4107 Project 1493-4 Final Report, Cornell University, Ithaca, New York.

Campanella, R.G. and Robertson, P.K. (1988), "Current Status of the Piezocone Test", *Proceedings*, First International Symposium on Penetration Testing (ISOPT-1), Orlando, de Ruiter (ed.), Vol. 1, 93-116.

Chapman, G.A. (1980), *The Interpretation of Friction Cone Penetrometer Tests in Sand*, PhD dissertation, Monash University, Melbourne.

Chin, F.K. (1970), "Evaluation of the Ultimate Load of Piles from Tests Not Carried to Failure", *Proceedings*, 2nd Southeast Asian Conference on Soil Engineering, Singapore, 81-90.

Christoulas, S. (1988), "Dimensionnement de Pieux: Quelques Experiences et Recherches en Grece", *Bulletin de Liaison des Laboratoires des Ponts et Chaussees*, No. 154, 5-10.

Christoulas, S. and Pachakis, M. (1987), "Pile Settlement Prediction Based on SPT Results", *Bulletin of the Research Center of Public Works Department of Greece*, Vol. 3, 221-226.

Clayton, C. R. I., Matthews, M. C. & Simons, N. E. (1995), *Site Investigation*, 2nd Edition. Blackwell, Oxford, (accessible at geotechnique.info).

Coyle, H.M. and Reese, L.C. (1966), "Load Transfer for Axially Loaded Piles in Clay", *Journal of the Geotechnical Engineering Division*, ASCE, Vol. 92, SM2, 1-26.

Coyle, H.M. and Sulaiman, I.H. (1967), "Skin Friction for Steel Pipe Piles in Sand", *Journal of the Geotechnical Engineering Division*, ASCE, Vol. 93, SM6, 261-278.

D'Appolonia, D.J., D'Appolonia, E. and Brisette, R.F. (1970), "Closure to Discussion of Settlement of Spread Footings on Sand", *Journal of the Geotechnical Engineering Division*, ASCE, Vol. 96, SM2, 754-761.

D'Appolonia, E. and Romualdi, J.P. (1963), "Load Transfer in End Bearing Steel H-Piles", *Journal of the Geotechnical Engineering Division*, ASCE, Vol. 89, SM2, 1-25.

Daniel, C.R., Howie, J. A. and Sy, A. (2003), "A method for correlating large penetration test (LPT) to standard penetration test (SPT) blow counts", *Canadian Geotechnical Journal*, Vol. 40, 66-77.

Davisson, M.T. (1972), "High Capacity Piles", *Proceedings*, Lecture Series on Innovations in Foundation Construction, Illinois Section, ASCE, Chicago, 81-112.

De Nicola, A. and Randolph, M.F. (1999), "Centrifuge Modeling of Pipe Piles in Sand under Axial Loads", *Geotechnique*, Vol. 49, No. 3, 295-318.

De Ruiter, J. and Beringen, F.L. (1979), "Pile Foundations for Large North Sea Structures", *Marine Geotechnology*, Vol. 3, No. 3, 267-314.

Decourt, L. (1982), "Prediction of the Bearing Capacity of Piles Based Exclusively on *N* Values of the SPT", *Proceedings*, Second European Symposium of Penetration Testing (ESOPT II), Amsterdam, Netherlands, Vol. 1, 29-34.

Deep Foundations Institute (1981), *Glossary of Foundations Terms*, edited by A.G. MacKinnon and H. W. Hunt.

Dennis, N.D. (1982), *Development of Correlations to Improve the Prediction of Axial Pile Capacity*, PhD dissertation, The University of Texas at Austin, 297 pages.

Dennis, N.D. and Olson, R.E. (1983a), "Axial Capacity of Steel Pipe Piles in Clay", *Proceedings*, Geotechnical Practice in Offshore Engineering, ASCE, Austin, Texas, 370-388.

Dennis, N.D. and Olson, R.E. (1983b), "Axial Capacity of Steel Pipe Piles in Sand", *Proceedings*, Geotechnical Practice in Offshore Engineering, ASCE, Austin, Texas, 389-402.

Denver, H. (1982), "Modulus of Elasticity Determined by SPT and CPT", *Proceedings*, Second European Symposium of Penetration Testing (ESOPT II), Amsterdam, Netherlands, Vol. 1, 35-40.

DiMillio, A.F. (1999), "A Quarter Century of Geotechnical Research", Federal Highway Administration, Report No. FHWA-RD-98-139, 151 pages. Also through (accessed 06/2007): http://www.fhwa.dot.gov/engineering/geotech/pubs/century/.

Djoenaidi, W. J. (1985), *A Compendium of Soil Properties and Correlations*, M. Eng. Sc. Thesis, University of Sydney, Sydney, Australia. 836 pages.

Douglas, B.J. and Olsen, R.S. (1981), "Soil Classification Using Electric Cone Penetrometer", *Cone Penetration Testing and Experience*, proceedings, ASCE National Convention, St. Louis, 209-227.

Eslami, A. and Fellenius, B.H. (1997), "Pile Capacity by Direct CPT and CPTu Methods Applied to 102 Case Histories", *Canadian Geotechnical Journal*, Vol. 34, No. 6, 886-904.

Fahey, M. (1999), "Determining the Parameters of a Non-linear Elastic Model for Prediction of Ground Deformation", *Australian Geomechanics*, Vol. 34, No. 1, 39-59.

Federal Highway Administration (FHWA) (2006), *Design and Construction of Driven Pile Foundations – Reference Manual*, Vol. 1, Publication No. FHWA NHI-05-042, April.

Fellenius, B.H. (1995), "Computer-Assisted Design of Piles and Pile Groups for Capacity, Settlement, and Negative Skin Friction", *Computing in Civil Engineering*, Proceedings of the Second Congress held in conjunction with A/E/C Systems '95, Atlanta, Georgia, 919-926.

Fellenius, B.H. (1996), *Basics of Foundation Design*, BiTech, Richmond, BC, Canada.

Fleming, W.G.K. (1992), "A New Method for Single Pile Settlement Prediction and Analysis", *Géotechnique*, Vol. 42, No. 3, 411-425.

Frank, R. (1985), "Recent Developments in the Prediction of Pile Behaviour from Pressuremeter Results", *Proceedings*, From Theory to Practice on Deep Foundations, Porto Alegre, Brazil, Vol. 1, 69-99.

Frank, R. (1995), *Fondations Profondes*, Collection Technique de L'Ingénieur, C248.

Frank, R., Kalteziotis, N., Bustamante, M., Cristoulas, S. and Zervogiannis, H. (1991), "Evaluation of Performance of Two Piles Using Pressuremeter Method", *ASCE Journal of Geotechnical Engineering*, Vol.117, No.5, 695-713.

Frost, J.D. (1992), "Evaluation of Repeatability and Efficiency of Energy Delivered with a Diedrich Automatic SPT Hammer System", unpublished report prepared for Diedrich Drill, Inc.

Gambin, M.P. and Rousseau, J. (1988), "The Menard pressuremeter: interpretation and application of pressuremeter test results to foundation design", ISSMFE Technical Committee on Pressuremeter and Dilatometer Testing, General Memorandum, Sols Soils No. 26, 50 pages.

Guo, W.D. (2001), "Pile capacity in nonhomogeneous softening soil", *Soils and Foundations*, Vol. 41, No. 2, pp. 111-120.

Hannigan, P.J., Goble, G.G., Thendean, G., Likins, G.E. and Rausche, F. (1997), "Design and Construction of Driven Pile Foundations", Vol. 1, *Report FHWA-HI-97-013*, U.S. Federal Highway Administration, Washington, DC.

Hunter, A.H. and Davisson, M.T. (1969), "Measurements of Pile Load Transfer", Performance of Deep Foundations, ASTM, STP No. 444, 106-117.

Imai, T. and Tonouchi, K. (1982), "Correlation of N Value with S-wave Velocity and Shear Modulus", *Proceedings*, Second European Symposium of Penetration Testing (ESOPT II), Amsterdam, Netherlands, Vol. 1, 67-72.

Jardine, R.J. and Chow, F.C. (1996), "New Design Methods for Offshore Piles", *Report No. 96-103*, Marine Technology Directorate, Ltd., London.

Jefferies, M.G. and Davies, M.P. (1991), "Soil Classification by the Cone Penetration Test", discussion, *Canadian Geotechnical Journal*, Vol. 28, No. 1, 173-176.

Jefferies, M.G. and Davies, M.P. (1993). "Use of CPT to Estimate Equivalent SPT N_{60}", *ASTM Geotechnical Testing Journal*, Vol. 16, No. 4, 458-468.

Johnson, L.D. (1986), "Correlation of Soil Parameters From In Situ and Laboratory Tests for Building 333", *Use of In Situ Tests in Geotechnical Engineering*, proceedings, In Situ '86, Virginia Tech, Blacksburg, Virginia, 635-648.

Kiousis, P.D. and Elansary, A.S. (1987), "Load Settlement Relation For Axially Loaded Piles", *Journal of Geotechnical Engineering*, Vol.113, No.6, 655-661.

Komornik, A. (1974), "Penetration Testing in Israel: State-of-the-Art Report", *Proceedings*, First European Symposium of Penetration Testing (ESOPT I), Stockholm, Sweden, 185-192.

Kondner, R.L. (1963), "Hyperbolic Stress-Strain Response: Cohesive Soils". *Journal of the Soil Mechanics and Foundations Division*, ASCE, Vol. 89, No. 4, 241-242.

Kraft, L.M., Focht, J.A. and Amerasinghe, S.F. (1981), "Friction Capacity of Piles Driven into Clay", *Journal of the Geotechnical Engineering Division*, ASCE, Vol. 107, No. 11, 1521-1541.

Kulhawy, F.H. and Mayne, P.W. (1990), *Manual on Estimating Soil Properties for Foundation Design*, Report No. EL-6800, Electric Power Research Institute, Palo Alto, CA, August, 306 pages.

Ladd, C.C., Foott, R., Ishihara, K., Schlosser, F. and Poulos, H.G. (1977), "Stress Deformation and Strength Characteristics", *Proceedings*, 9th International Conference on Soil Mechanics and Foundation Engineering, Tokyo, Vol. 2, 421-494.

Lake, L.M. (1974), ""Discussion on Granular Materials", *Proceedings*, Conference on Settlement of Structures, Cambridge, 663.

Lehane, B.M. and Jardine, R.J. (1994), "Displacement-Pile Behavior in a Soft Marine Clay", *Canadian Geotechnical Journal*, Vol. 31, No. 2, 181-191.

Lehane, B.M., Jardine, R.J., Bond, A.J. and Frank, R. (1993), "Mechanisms of Shaft Friction in Sand from Instrumented Pile Tests", *Journal of the Geotechnical Engineering Division*, ASCE, Vol. 119, No. 1, 19-35.

Liebich, B.A. (2003), "High Capacity Piles: Confirming the Viability of Cost-Efficient Bridge Designs", *Transportation Research News (TR News)*, Transportation Research Board, No. 228, September-October, 42-43.

Lunne, T., Robertson, P.K. and Powell, J.J.M. (1997), *Cone Penetration Testing in Geotechnical Practice*, Blackie, New York.

Martin, R.E. (1987), "Settlement of Residual Soils", *Foundations and Excavations in Decomposed Rock of the Piedmont Province*, Proceedings of a Session Sponsored by the Geotechnical Engineering Division of the ASCE in conjunction with the ASCE Convention in Atlantic City, New Jersey, edited by Smith, R.E., ASCE, New York, 1-14.

Matsumoto, K. and Matsubara, M. (1982), "Effects of Rod Diameter in the Standard Penetration Test", *Proceedings*, 2nd European Symposium on Penetration Testing, ESOPT-II, Amsterdam, Vol. 1, 107-122.

Mattes, N.S. and H.G. Poulos (1969), "Settlement of Single Compressible Pile", *Journal of the Geotechnical Engineering Division*, ASCE, Vol. 95, SM1, 189-207.

Meigh, A.C., (1987), *Cone Penetration Testing - Methods and Interpretation*, CIRIA, Butterworth, London.

Ménard, L. (1957), "Mesure In-Situ des Propriétés Physiques des Sols", *Annales des ponts et chaussées*, No. 14, pp. 357–377.

Meyerhof, G.G. (1959), "Compaction of Sands and Bearing Capacity of Piles", *Journal of the Geotechnical Engineering Division*, ASCE, Vol. 85, No. 6, 1-29.

Meyerhof, G.G. (1976), "Bearing Capacity and Settlement of Pile Foundations", *Journal of the Geotechnical Engineering Division*, ASCE, Vol. 102, No. 3, 195-228.

Mindlin, R.D. (1936), "Force at a Point in the Interior of a Semi-Infinite Solid", *Physics*, Vol. 7, 195-202.

Murff, J.D. (1980), "Pile capacity in a softening soil", *International Journal for Numerical and Analytical Methods in Geomechanics*, Vol. 4, No. 2, 185-189.

Nevels, J.B. and Snethen, D.R. (1994), "Comparison of Settlement Predictions for Single Piles in Sand Based on Penetration Test Results", *Proceedings*, Vertical and Horizontal Deformations of Foundations and Embankments, Geotechnical Special Publication No. 40, College Station, Texas, Vol. 2, 1028-1038.

Nordlund, R.L. (1963), "Bearing Capacity of Piles in Cohesionless Soils", *Journal of the Soil Mechanics and Foundations Division*, ASCE, Vol. 89, No. 3, 1-35.

Nordlund, R.L. and Deere, D.U. (1970), "Collapse of Fargo Grain Elevator", *Journal of the Soil Mechanics and Foundations Division*, Vol. 96, No. 2, 585-607.

O'Neill, M.W. and Raines, R.D. (1991), "Load Transfer for Pipe Pile in Highly Pressurized Dense Sand", *Journal of the Geotechnical Engineering Division*, ASCE, Vol. 117, No. 8, 1208-1226.

O'Neill, M.W., Vipulanandan, C. and Wong, D. (1990), "Laboratory Modeling of Vibro-Driven Piles", *Journal of the Geotechnical Engineering Division*, ASCE, Vol. 116, No. 8, 1190-1209.

Ohsaki, Y. and Iwasaki, R. (1973), "On Dynamic Shear Moduli and Poisson's Ratios of Soil Deposits", *Soils and Foundations*, Vol.13, No.4, 61-73.

Olson, R.E. (1990), "Axial Load Capacity of Steel Pipe Pile in Sand", *Proceedings*, Offshore Technology Conference, Houston, OTC Paper No. 6419, Vol. 4, 17-24.

Olson, R.E. (2005), Personal communication.

Olson, R.E. and Dennis, N.D. (1982), "Review and Compilation of Pile Test Results, Axial Capacity", *Report GR83-4*, Geotechnical Engineering Center, The University of Texas at Austin.

Peck, R.B., Hanson, W.E. and Thornburn, T.H. (1974), *Foundation Engineering*, 2nd ed., John Wiley and Sons, New York.

Pelletier, J.H., Murff, J.D. and Young, A.C. (1993), "Historical Development and Assessment of the Current API Design Methods for Axially Loaded Pipes", *Proceedings*, Offshore Technology Conference, Houston, OTC Paper No. 7517, Vol. 2, 253-282.

Poulos, H.G. (1972), "Load-Settlement Prediction For Piles and Piers", *Journal of the Soil Mechanics and Foundations Division*, Proceedings of the American Society of Civil Engineers, Vol.98, No. SM9, 879-897.

Poulos, H.G. (1979), "Settlement of Single Piles in Non-Homogeneous Soil", *Journal of the Geotechnical Engineering Division*, ASCE, Vol. 105, GT5, 627-641.

Poulos, H.G. (1989), "Pile Behaviour-Theory and Application", *Géotechnique*, Vol. 39, No. 3, 365-415.

Poulos, H.G. (1994), "Settlement Prediction for Driven Piles and Pile Groups", *Proceedings*, Vertical and Horizontal Deformations of Foundations and Embankments, Geotechnical Special Publication No. 40, College Station, Texas, Vol. 2, 1629-1649.

Poulos, H.G. (2001), "Pile Foundations", in Rowe, R. K. (Ed.), *Geotechnical and Geoenvironmental Engineering Handbook*, Kluwer Academic Publishers, Norwell, Massachusetts, 261-304.

Poulos, H.G. and Davis, E.H. (1968), "The Settlement Behavior of Single Axially-Loaded Incompressible Piles and Piers", *Géotechnique*, Vol. 18, No. 3, 351-371.

Poulos, H.G. and Davis, E.H. (1974), *Elastic Solutions for Soil and Rock Mechanics*, New York: John Wiley and Sons, Inc.

Poulos, H.G. and Davis, E.H. (1980), *Pile Foundation Analysis and Design*, John Wiley and Sons, New York.

Poulos, H.G. and Mattes, N.S. (1969), "The Behavior of Axially-Loaded End-Bearing Piles", *Géotechnique*, Vol. 19, No. 2, 285-300.

Randolph, M.F. (1983), "Design Considerations for Offshore Piles", *Proceedings*, Conference on Geotechnical Practice in Offshore Engineering, Austin, pp. 422-439.

Randolph, M.F. and Murphy, B.S. (1985), "Shaft Capacity of Driven Piles in Clay", *Proceedings*, Offshore Technology Conference, Houston, Vol. 1, 371-378.

Richman, R.L. and Speer, D. (1989), "Comparison of Measured Pile Capacity to Pile Capacity Predictions Made using Electronic Cone Penetration Data." *Report No. FHWA/CA/TL-89/16*, Division of New Technology, Materials and Research, Office of Transportation Materials and Research, California Department of Transportation, Sacramento, California.

Sanglerat, G. and Sanglerat, T.R.A. (1982), "Pitfalls of the SPT", *Proceedings*, 2nd European Symposium on Penetration Testing, ESOPT-II, Amsterdam, Vol. 1, 143-145.

Schmertmann, J.H. (1970), "Suggested Method for Screw-Plate Load Test", *Special Procedures for Testing Soil and Rock for Engineering Purposes: Fifth Edition*, ASTM Special Technical Publication No: 479, pp. 81-85.

Schmertmann, J.H. (1978), "Guidelines for Cone Penetration Test: Performance and Design", *Report FHWA-TS-78-209*, U.S. Federal Highway Administration, Washington, DC.

Schmertmann, J.H. and Palacios, A. (1979), "Energy Dynamics of SPT", *Journal of the Geotechnical Engineering Division*, ASCE, Vol. 105, No. 8, 909-926.

Seed, H.B. and Reese, L.C. (1957), "The Action of Soft Clay along Friction Piles", *Transactions*, ASCE, Vol. 122, 731-764.

Shen, W.Y., Chow, Y.K. and Yong, K.Y. (2000), "Practical Method for Settlement Analysis of Pile Groups", *Journal of Geotechnical and Geoenvironmental Engineering*, Vol.126, No.10, 890-897.

Shioi, Y. and Fukui, J. (1982), "Application of N-value to Design of Foundations in Japan", *Proceedings*, Second European Symposium of Penetration Testing (ESOPT II), Amsterdam, Netherlands, Vol. 1, 159-164.

Skaug, T.M. (1998), "CPT/SPT Site-Specific Correlation and Calibration Program", *Report No. 1P2/598/159*, Taber Consultants.

Skempton, A.W. (1986), "Standard Penetration Test Procedures and the Effects in Sands of Overburden Pressure, Relative Density, Particle Size, Ageing and Overconsolidation", *Geotechnique*, Vol. 36, No. 3, 425-447.

Steinbrenner, W. (1934), "Tafeln zur Setzenberechnung", *Die Strasse*, Vol. 1, 221.

Sterpi, D. (1999), "An Analysis of Geotechnical Problems Involving Strain Softening Effects", *International Journal for Numerical and Analytical Methods in Geomechanics*, Vol. 23, No. 13, 1427-1454.

Stokoe, K.H. and Santamarina, J.C. (2000), "Seismic-wave-bases testing in geotechnical engineering", *GeoEng 2000, International Conference on Geotechnical and Geological Engineering*, Melbourne, Vol. 1, 1490-1536.

Stroud, M. A. (1989), "Standard Penetration Test: Its Application and Interpretation", *Institution of Civil Engineering, Penetration Testing, Proceedings of the Geotechnology Conference Organized by the Institution of Civil Engineers and held in Birmingham on 6-8 July 1988*, 29-51.

Sy, A. (1997), "Twentieth Canadian Geotechnical Colloqium: Recent developments in the Becker penetration test: 1986-1996", *Canadian Geotechnical Journal*, Vol. 34, 952-973.

Takesue, K., Sasao, H. and Matsumoto, T. (1998), "Correlation between Ultimate Pile Skin Friction and CPT Data", *Geotechnical Site Characterization*, proceedings, ISC'98, Atlanta, Vol. 2, 1177-1182.

Thurman, A.G. (1964), *Computed Load Capacity and Movement of Friction and End-Bearing Piles Embedded in Uniform and Stratified Soil*, Ph.D. dissertation, Carnegie Institute of Technology.

Tomlinson, M.J. (1957), "The Adhesion of Piles in Clay Soils", *Proceedings*, 4th International Conference on Soil Mechanics and Foundation Engineering, London, Vol. 2, 66-71.

Tomlinson, M.J. (1971), "Some Effects of Pile Driving on Skin Friction", *Proceedings*, Conference on Behavior of Piles, Institution of Civil Engineers, London, 107-114, 149-152.

Toolan, F.E., Lings, M.L. and Mirza, U.A. (1990), "An Appraisal of API RP2A Recommendations for Determining Skin Friction of Piles in Sand", *Proceedings*, Offshore Technology Conference, Houston, OTC Paper No. 6422, Vol. 4, 33-42.

Tumay, M.T. and Fakhroo, M. (1981), "Pile Capacity in Soft Clays using QCPT Data", *Proceedings, Cone Penetration Testing and Experience*, ASCE National Convention, St. Louis, 434-455.

Vallabhan, C.V.G. and Mustafa, G. (1996), "A New Model for the Analysis of Settlement of Drilled Piers", *International Journal for Numerical and Analytical Methods in Geomechanics*, Vol. 20, No. 2, 143-152.

Valle-Molina, C. (2006), *Measurements of V_p and V_s in Dry, Unsaturated and Saturated Sand Specimens with Piezoelectric Transducers*, PhD dissertation, The University of Texas at Austin.

Vesic, A.S. (1970), "Tests on Instrumented Piles, Ogeechee River Site", *Journal of the Soil Mechanics and Foundations Division*, Vol.96, No. SM2, 561-584.

Vesic, A.S. (1977), "Design of Pile Foundations", *NCHRP Synthesis 42*, Transportation Research Board, National Academy of Sciences, Washington, DC.

Vijayvergiya, V.N. and Focht, J.A. (1972), "A New Way to Predict the Capacity of Piles in Clay", *Proceedings, Offshore Technology Conference*, Houston, Vol. 2, 865-874.

Weiher, B. and Davis, R. (2004), "Correlation of Elastic Constants with Penetration Resistance in Sandy Soils", *International Journal of Geomechanics*, Vol. 4, No. 4, 319-329.

Wrench, B.P., Nowatzki, E.A. (1986), "A Relationship Between Deformation Modulus and SPT N for Gravels", *Proceedings, Use of In Situ Tests in Geotechnical Engineering*, In Situ '86, ASCE/Virginia Tech, Blacksburg, Virginia. 1163-1177.

Yamashita, K., Tomono, M. and Kakurai, M. (1987), "A Method for Estimating Immediate Settlement of Piles and Pile Groups", *Soils and Foundations*, Vol. 27, No. 1, 61-76.

Vita

Cem Akgüner was born in Washington, D.C., on May 26, 1970, the son of Mary and Tayfun Akgüner. He graduated from İstanbul (Erkek) High School, Turkey, in 1988 and entered İstanbul Technical University, where he graduated with a Bachelor of Science Degree in Civil Engineering in 1992. After completing a Master of Science in Geotechnical Engineering at the Bosphorus University, İstanbul (1995), Akgüner started working as a teaching assistant in the Geotechnical Division of Yıldız Technical University, İstanbul. In 1996, he began his doctoral studies in the geotechnical engineering program of the Department of Civil, Architectural and Environmental Engineering at The University of Texas at Austin. He is a member of the American Society of Civil Engineers (ASCE), ASCE Geo-Institute, Turkish Chamber of Civil Engineers (İMO), and Turkish Clay Minerals Society.

Permanent address: Türkbeyi Sok. No. 48-50 D.4, 34375, ŞİŞLİ/İSTANBUL/TURKEY

This dissertation was typed by Cem Akgüner.